Protein quality control in the cytoplasm of yeast cells: Substrate diversity and pathway selection

Von der Fakultät Energie-, Verfahrens- und Biotechnik der Universität Stuttgart zur Erlangung der Würde eines Doktors der Naturwissenschaften (Dr. rer. nat.) genehmigte Abhandlung

Vorgelegt von

Dipl. Biologe (t.o.) Ingo Amm

aus Fellbach

Hauptberichter:	Prof. Dr. Dieter H. Wolf
Mitberichter:	Priv. Doz. Dr. Hans Rudolph
	Prof. Dr. Albert Jeltsch

Tag der mündlichen Prüfung: 6. August 2015

Institut für Biochemie der Universität Stuttgart

2015

Eidesstattliche Erklärung

Hiermit versichere ich, dass ich diese Arbeit selbst verfasst und dabei keine anderen als die angegebenen Quellen und Hilfsmittel verwendet habe.

Fellbach, den 11. Mai 2015

Ingo Amm

TABLE OF CONTENTS

I. LIST OF ABBREVIATIONS

(in alphabetical order)

ADP	Adenosine diphosphate
Amp	Ampicillin
APS	Ammonium persulphate
Arg	Arginine
ATP	Adenosine triphosphate
Bq	Becquerel
BSA	Bovine serum albumin
CHX	Cycloheximide
CM	Complete medium
CPY	Carboxypeptidase Y
ddH_2O	Ultrapure water
DMSO	Dimethyl sulphoxide
DNA	Deoxyribonucleic acid
DTT	Dithiothreitol
dNTP	Deoxyribonucleotide
E. coli	*Escherichia Coli*
EDTA	Ethylendiaminetetraacetic acid
ER	Endoplasmic reticulum
ERAD	Endoplasmic reticulum-associated degradation
Fig.	Figure
GFP	Green fluorescent protein
HA	Hemagglutinin
HECT	Homologous to E6-AP Carboxyl Terminus
Hsp	Heat shock protein
Ile	Isoleucine
IP	Immunoprecipitation
IPOD	Insoluble protein deposit
JUNQ	Juxtanuclear quality control compartment
kb	Kilobase
kDa	Kilodalton
LB	Lysogeny broth medium
Leu	Leucine
M	Molar
MDa	Megadalton
Min	Minute(s)
mM	Milimolar

NAD^+	Nicotinamide adenine dinucleotide
NES	Nuclear export signal
NLS	Nuclear localization signal
OD_{600}	Optical density measured at 600 nm
ON	Overnight
PAGE	Polyacrylamide gel electrophoresis
PBS	Phosphate-buffered saline
PCR	Polymerase chain reaction
PEG	Polyethylene glycol
PGK	3-Phosphoglycerate kinase
Phe	Phenylalanine
PP_i	Pyrophosphate
RING	Really interesting new gene
RNA	Ribonucleic acid
Rpm	Revolutions per minute
RT	Room temperature
S	Svedberg unit
S. cerevisiae	*Saccharomyces cerevisiae*
SDS	Sodium dodecyl sulphate
SOC	Salt-optimized plus carbon
ssDNA	Single-stranded DNA
Tab.	Table
TAP	Tandem affinity purification
TAE	Tris acetate EDTA
TCA	Trichloroacetic acid
TE	Tris EDTA
TEMED	N,N,N'N'-Tetramethylethylendiamine
Tris	Tris(hydroxymethyl)aminomethane
Trp	Tryptophan
Tyr	Tyrosine
U	Unit
v/v	Volume per volume
WT	Wild type
w/o	Without
w/v	Weight per volume
YPD	Yeast peptone dextrose medium

II. LIST OF FIGURES

III. LIST OF TABLES

IV. SUMMARY

Protein misfolding occurs constantly in living cells. It occurs already at the stage of protein biosynthesis when polypeptides emerge from translating ribosomes. Misfolded proteins may disturb cellular functions and cause severe neurological and other diseases in mammals. Therefore, the cell has evolved protein quality control pathways for specific recognition and degradation of misfolded proteins. Protein folding is supported by different sets of chaperones which prevent unwanted intramolecular or intermolecular protein interactions. Furthermore, specific chaperones recognize irreversibly damaged proteins for subsequent elimination from the cellular environment. For proteins of the secretory pathway the protein quality control system is rather well understood. This study concentrates on the characterization of the cytoplasmic protein quality control mechanisms and pathways by using a variety of terminally misfolded proteins as model substrates. As model organism for these studies the yeast *S. cerevisiae* was chosen.

In previous studies, the degradation of the cytosolic model substrate ΔssCPY*Leu2myc (ΔssCL*myc) which is based on the irreversibly misfolded carboxypeptidase Y (CPY*) had been shown to be dependent on the ubiquitin ligase Ubr1 (Eisele and Wolf, 2008). The enzyme ubiquitinates the substrate leading to subsequent recognition and degradation by the proteasome. In this work, additional cytosolic chaperones acting in the protein quality control process of the misfolded substrate ΔssCL*myc were uncovered. The Hsp31 chaperone family was found to be involved in controlling the steady state level of ΔssCL*myc in the stationary growth phase of cells. It was shown via epistasis analyses that the Hsp31 chaperones act in a pathway overlapping with Ubr1-mediated protein degradation.

Using truncations of the model substrate ΔssCL*myc revealed that the nuclear ubiquitin ligase San1 is also involved in the protein quality control of some of these cytosolic misfolded proteins. They are obviously directed into the nucleus prior to degradation. Experiments with the model substrates of different sizes indicate that the molecular mass is a determinant of the nuclear San1-dependency of substrate degradation. The degradation of small substrates shows an increased dependency on San1.

A further set of cytosolic model substrates was generated consisting of firefly luciferase. A chemoluminescence assay for quantitative determination of corresponding substrates in yeast cells was established. This test is supposed to be very suitable for high throughput screening.

Not only artificial terminally misfolded cytosolic model substrates are targets of Ubr1-dependent proteasomal degradation. Also an orphan subunit of the cytosolic fatty acid synthase (FAS) complex, Fas2, is a target of Ubr1-dependent proteasomal degradation if its binding partner Fas1 is missing (Scazzari, 2013). This study revealed that the Hsp70 chaperone Ssa1 is essential for keeping orphan Fas2 in a soluble state for subsequent ubiquitination by the ubiquitin ligase Ubr1. The Cdc48 machinery was found to act downstream of the ubiquitination process mediated by Ubr1 and it may be responsible for dissociation of ubiquitinated oligomeric orphan Fas2 complex into monomers, an essential step for subsequent proteasomal degradation.

Publications:

Amm I, Sommer T, Wolf DH (2014) Protein quality control and elimination of protein waste: The role of the ubiquitin-proteasome system. *Biochim Biophys Acta* **1843:** 182-196

Scazzari M *, Amm I *, Wolf DH (2015) Quality Control of a Cytoplasmic Protein Complex: CHAPERONE MOTORS AND THE UBIQUITIN-PROTEASOME SYSTEM GOVERN THE FATE OF ORPHAN FATTY ACID SYNTHASE SUBUNIT Fas2 OF YEAST. *J Biol Chem* **290:** 4677-4687
* These authors contributed equally

Amm I, Norell D, Wolf DH (2015) Absence of the yeast Hsp31 chaperones of the DJ-1 superfamily perturbs cytoplasmic protein quality control in late growth phase. *PlosOne.* (Accepted)

Further publication in progress:

Amm I, Wolf DH (2015) Molecular mass as a determinant for nuclear San1-dependent targeting of misfolded cytoplasmic proteins to proteasomal degradation.

V. ZUSAMMENFASSUNG

In lebenden Zellen findet ständig Fehlfaltung von Proteinen statt. Dies geschieht bereits während der Proteinbiosynthese, wenn Polypeptide an translatierenden Ribosomen entstehen. Fehlgefaltete Proteine können die Zellfunktionen massiv stören und schwere neurologische und andere Krankheiten in Säugetieren auslösen. Daher hat die Zelle Mechanismen und Wege entwickelt, den Faltungsprozess von Proteinen zu überprüfen und fehlgefaltete Proteine spezifisch zu erkennen und abzubauen. Einerseits wird die Proteinfaltung durch verschiedene Klassen von Chaperonen unterstützt, die nicht gewollte intra- oder intermolekulare Proteininteraktionen verhindern. Andererseits werden irreversibel fehlgefaltete Proteine durch bestimmte Chaperone erkannt und anschließend aus der zellulären Umgebung entfernt. Für Proteine des sekretorischen Weges ist diese Proteinqualitätskontrolle bereits recht gut verstanden. Diese Arbeit konzentriert sich auf die Charakterisierung der Mechanismen und Wege der zytoplasmatischen Proteinqualitätskontrolle im Modellorganismus *Saccharomyces cerevisiae* durch Verwendung einer Vielzahl irreversibel fehlgefalteter Proteine als Modellsubstrate.

In vorangegangenen Studien wurde gefunden, dass der Abbau des zytosolischen Modellsubstrates ΔssCPY*Leu2myc (ΔssCL*myc), das auf endgültig fehlgefalteter Carboxypeptidase Y (CPY*) basiert, abhängig von der Ubiquitin-Ligase Ubr1 ist (Eisele and Wolf, 2008). Ubr1 ubiquitiniert das Substrat, so dass es vom Proteasom erkannt und abgebaut werden kann. In dieser Arbeit wurde gezeigt, dass für die Proteinqualitätskontrolle von ΔssCL*myc zusätzlich noch nicht näher charakterisierte zytosolische Chaperone benötigt werden. In der stationären Phase ist die Hsp31 Chaperonfamilie an der Kontrolle der Proteinmenge von ΔssCL*myc beteiligt. Epistaseanalysen zeigten eine Funktion der Hsp31 Chaperone auf einem Weg parallel zum Ubr1-abhängigen Proteinabbau.

Durch Untersuchung verkürzter Varianten des Modellsubstrats ΔssCL*myc wurde gefunden, dass auch die Zellkern-lokalisierte Ubiquitin-Ligase San1 an der Proteinqualitätskontrolle einiger zytosolischer Proteine beteiligt ist, die vor ihrem Abbau in den Zellkern transportiert werden. Die Verwendung zytosolischer Modellsubstrate unterschiedlicher molekularer Masse deutet darauf hin, dass die molekulare Masse ein Kriterium für die San1-Abhängigkeit des Substratabbaus ist. Kleinere Substrate zeigten eine stärkere San1-Abhängigkeit des Abbaus.

Basierend auf dem in Glühwürmchen produzierten Enzym Luciferase wurden weitere zytosolische Modellsubstrate hergestellt. Mit Hilfe der Chemolumineszenz wurde ein

einfacher Test für die quantitative Bestimmung entsprechender Substrate in Hefezellen etabliert. Dieser Test sollte für Hochdurchsatzscreening-Experimente geeignet sein.
Nicht nur künstlich hergestellte, endgültig fehlgefaltete zytosolische Modellsubstrate sind Ziele des Ubr1-abhängigen proteasomalen Abbaus sondern auch „orphan proteins“ wie die β-Untereinheit des Fettsäuresynthasekomplexes (FAS), Fas2, wenn dessen Bindungspartner Fas1 fehlt (Orphan Fas2), (Scazzari, 2013). Diese Arbeit deckte auf, dass das Hsp70 Chaperon Ssa1 essentiell für die Löslichkeit von Orphan Fas2, sowie für die darauffolgende Ubiquitinierung durch die Ubiquitin-Ligase Ubr1 ist. Es wurde ferner gefunden, dass die Cdc48-Maschinerie nach dem Ubiquitinierungsprozess benötigt wird. Sie bewirkt sehr wahrscheinlich die Dissoziation von ubiquitiniertem oligomeren Orphan Fas2 aus einem Komplex in Fas2 Monomere, ein Prozess, der essentiell für den darauffolgenden proteasomalen Abbau ist.

Veröffentlichungen:

Amm I, Sommer T, Wolf DH (2014) Protein quality control and elimination of protein waste: The role of the ubiquitin-proteasome system. *Biochim Biophys Acta* **1843:** 182-196

Scazzari M *, Amm I *, Wolf DH (2015) Quality Control of a Cytoplasmic Protein Complex: CHAPERONE MOTORS AND THE UBIQUITIN-PROTEASOME SYSTEM GOVERN THE FATE OF ORPHAN FATTY ACID SYNTHASE SUBUNIT Fas2 OF YEAST. *J Biol Chem* **290:** 4677-4687
***** Diese Autoren sind in gleichem Maße beteiligt

Amm I, Norell D, Wolf DH (2015) Absence of the yeast Hsp31 chaperones of the DJ-1 superfamily perturbs cytoplasmic protein quality control in late growth phase. *PlosOne.* (Akzeptiert)

Weitere in Arbeit befindliche Veröffentlichung:

Amm I, Wolf DH (2015) Molecular mass as a determinant for nuclear San1-dependent targeting of misfolded cytoplasmic proteins to proteasomal degradation.

1. INTRODUCTION

1.1 Protein folding and misfolding

1.1.1 Principles of protein folding

Protein folding defines the process in which proteins adopt their three dimensional structure. Only if proteins are folded correctly into their native conformation they can fulfil their biological functions. How this can be achieved in a short time scale and in an accurate way is a not well-understood phenomenon until now. More than 40 years ago pioneering work from Anfinsen and co-workers using the protein ribonuclease A brought the amino acid sequence of the protein in correlation with its biological active conformation. They showed that the protein's three-dimensional structure is determined by its primary sequence only. They denatured the biological active ribonuclease A using urea and β-mercaptoethanol. After removing both chemicals via dialysis and allowing reshuffling of the disulphide bonds they observed a refolding of the enzyme into the native state and a recovery of enzymatic activity of the enzyme (Anfinsen, 1973; Anfinsen *et al*, 1961). However, the detailed folding mechanism is still largely unknown. To illustrate the complexity of protein folding Levinthal formulated a paradox which shows the combinational problem of the folding process. The amount of possible conformations of a protein increases exponentially with the length of the amino acid chain. He argued that if each amino acid can only adopt two folding states and a change of one conformation would take 10^{-13} seconds, the folding of a protein of 150 amino acids in length would take 2^{150} x 10^{-13} s which amounts to more than 10^{24} years. Therefore, there must be a mechanism which favours the folding process towards the native state of a protein. This mechanism must be characterized by a continuous decrease in free energy towards the folded state. As the number of conformational states and therefore also the conformational entropy of the chain decreases on the way to the folded state causing an increase in free energy, there must be a compensating effect decreasing the total free energy of folding. This is achieved by an increase in entropy caused by the hydrophobic effect. In principle water molecules that surround a hydrophobic molecule are restricted in their

conformational flexibility by this possessing low entropy. Proteins consist of approximately 50 % hydrophilic and 50 % hydrophobic amino acids. Upon folding the hydrophobic chains become shielded from the water environment. The entropy of the previously ordered water molecules more and more increases and therefore the free energy decreases (Chandler, 2005). But the relatively weak hydrophobic effect alone cannot explain the total decrease in free energy of folding. There are also enthalpic contributions to the total free energy coming from hydrogen bond formation, van der Waals interactions or ion-ion interactions. Both the entropic and enthalpic contributions to the total free energy are described through the Gibbs-Helmholtz equation $\Delta G = \Delta H - T\Delta S$, named after Josiah Willard Gibbs and Hermann von Helmholtz (Stryer *et al*, 2013), (Fig. 1.1).

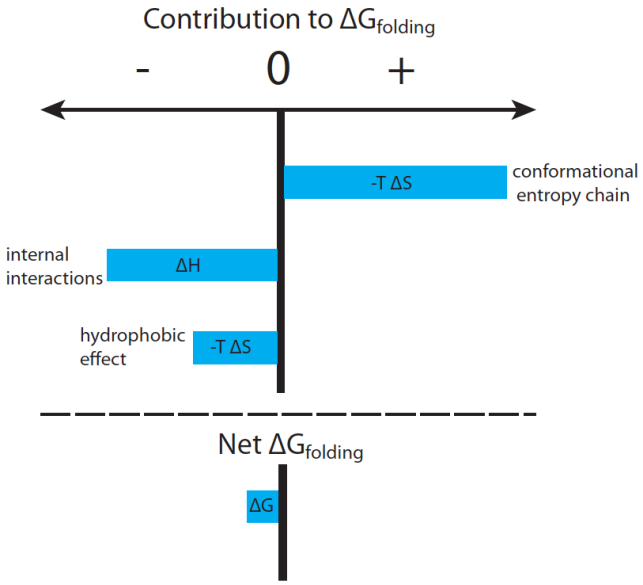

Figure 1.1: Negative and positive contributions to the total free energy of the folding process according to the Gibbs-Helmholtz equation. Formation of intramolecular interactions and the hydrophobic effect favour the folding whereas the increasing order of the protein in the folding process increases ΔG.

The current model of protein folding is described by the folding funnel hypothesis which is based on the thermodynamic concept of minimizing free energy (Dill and Chan, 1997; Dobson *et al*, 1998; Jahn and Radford, 2005; Onuchic and Wolynes, 2004). In this model the folding energy landscape is funnel-shaped where the unfolded proteins on the top have both high entropy corresponding to the large numbers of possible conformations and high free energy which is reasoned by the high flexibility of the unfolded species. On the way down to

the native state the width of the funnel decreases which represents the number of available conformational states of the folding protein. Particularly the folding of large proteins does not directly result in the native state but first in folding intermediates, partly folded states, which are represented in the model by local minima in the folding funnel surface. Also, misfolded conformations which have to be reorganized prior to further productive folding, are represented by local minima. These conformations are metastable and therefore decelerate the time of folding. Misfolded states often have the tendency to aggregate because of exposed hydrophobic patches on their surface. These aggregates are often even more stable than the native state and are therefore represented in the model by large free energy minima even lower than the folded state (Fig. 1.2), (Kim *et al*, 2013). Aggregates can either be amorphous or highly organized in fibrillar aggregates called amyloids. Amyloid formation of misfolded proteins is the reason for several neurodegenerative diseases like Parkinson's disease.

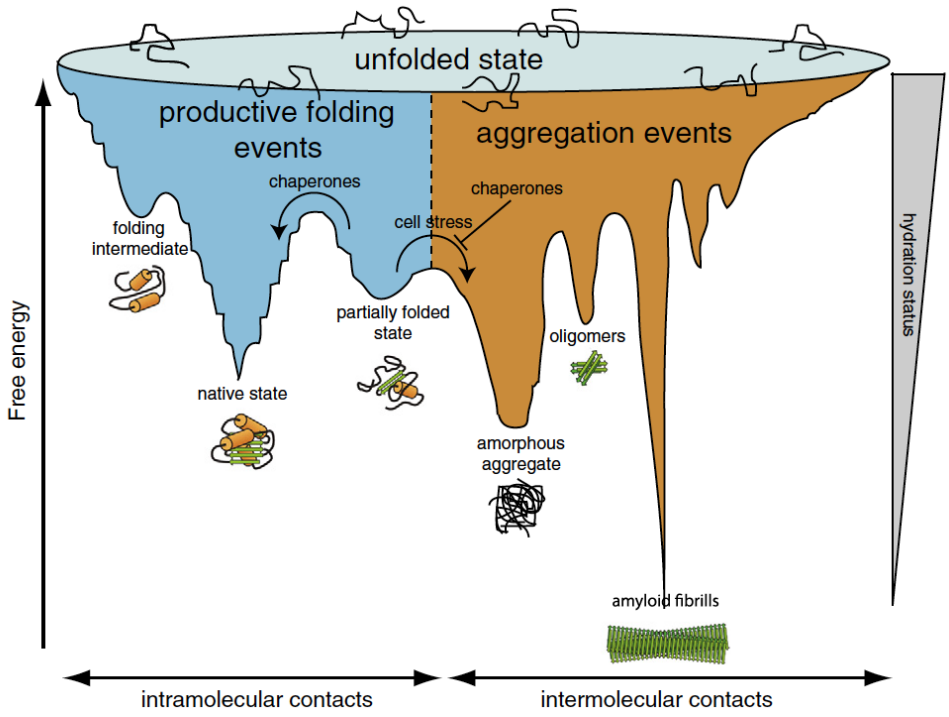

Figure 1.2: Schematic funnel-shaped energy landscape of protein folding to the native state. The polypeptide chains traverse local minima of free energy representing metastable protein conformations towards the native state. Partially folded protein species and non-native conformations respectively are often prone to aggregation leading to aggregates or even highly ordered fibrils characterized by very low free energy values. Chaperones (described in the next chapter) may prevent formation of non-native intermolecular interactions and assist the polypeptide in adopting its native state. Figure: (Amm *et al*, 2014).

1.1.2 Chaperones in protein folding

The interior of living cells is highly crowded consisting of up to 400 mg/ml of macromolecules (Ellis, 2001). This molecular crowding can either accelerate the productive protein folding because folded proteins need less space and occupy less solvent volume respectively, or promote aggregation of proteins by increasing the interaction of partly folded or misfolded domains (Ellis and Minton, 2006; van den Berg *et al*, 1999; van den Berg *et al*, 2000). For this reason the cell possesses a machinery of specialized proteins called chaperones, which are proteins enhancing the efficiency of productive protein folding. Chaperones can either prevent formation of non-native intermolecular interactions, or are involved in recognition and subsequent proteolytic degradation of terminally misfolded proteins or even actively dissociate already formed protein aggregates (Fig. 1.2). Conditions promoting misfolding like heat or oxidative stress induce the expression of chaperones which then handle these protein species for refolding or chaperone mediated degradation (Bukau *et al*, 2006; Hartl *et al*, 2011) Chaperones are classified in different groups according to their molecular mass. These are the Hsp40, Hsp60, Hsp70, Hsp90, Hsp100 classes and in addition the small heat shock proteins (sHsps) which are all described in the following chapters.

1.1.2.1 The Hsp70 chaperone system

Hsp70 chaperones are a highly conserved and ubiquitously expressed family of heat shock proteins. Members of this family have diverse functions including *de novo* folding of newly synthesized proteins, membrane translocation, recognition and delivery of misfolded proteins to the proteasome and even refolding of stress denatured proteins (Becker *et al*, 1996; Craig *et al*, 2003; Glover and Lindquist, 1998; McClellan *et al*, 2005; Park *et al*, 2007; Preissler and Deuerling, 2012). All these diverse functions of the Hsp70 chaperones are based on their ability to bind hydrophobic peptide segments in proteins. The binding and release of substrates is controlled in an ATP-dependent manner (Fig. 1.3).

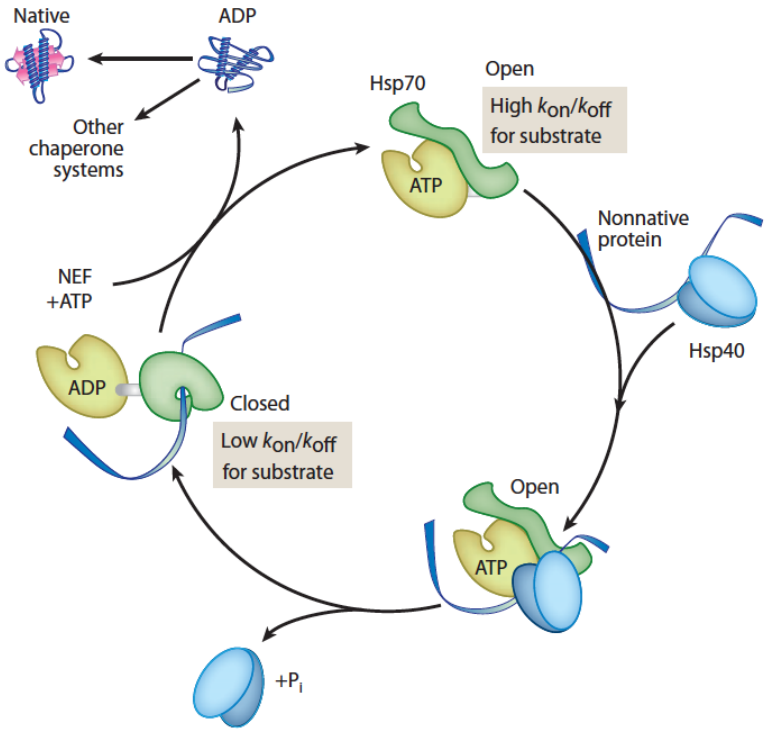

Figure 1.3: ATP-dependent reaction cycle of the Hsp70 system. Non-native proteins are delivered to ATP-bound Hsp70 with open conformation by the J-domain-containing Hsp40 proteins. After ATP hydrolysis, Hsp40 dissociates and Hsp70 changes to a closed conformation the client protein undergoes conformational changes towards the native state. The nuclear exchange factors (NEFs) finally promote the ADP/ATP exchange necessary for the next round of the reaction cycle. Figure: (Kim *et al*, 2013).

The substrate binding domain is localized to the C-terminus and can be further divided into a substrate binding subdomain and a C-terminal subdomain which acts as a lid for the substrate binding pocket (Lund, 2001). The N-terminal domain of Hsp70 can bind ATP and provides ATPase activity (Mayer and Bukau, 2005). The ATP/ADP exchange results in a conformational change in the substrate-binding domain. In the ATP-bound state the substrate binding domain has an open conformation and low affinity for substrates, therefore dissociation is favoured over tight binding of the substrate in the binding pocket (Mayer *et al*, 2001). After ATP hydrolysis which is the rate-limiting step in the reaction cycle the binding domain switches to a closed conformation characterized by a high substrate affinity. Because of the weak ATPase activity of the Hsp70 chaperones co-chaperones of the Hsp40 family and nucleotide exchange factors (NEFs) are necessary for facilitating the ATP/ADP-dependent substrate binding and release. The members of the Hsp40 chaperone family are very diverse in length, sequence and structure. They all have a J-domain (described first for the *E. coli*

Hsp70 co-chaperone DnaJ) in common which is essential for stimulating the ATPase activity of the Hsp70 chaperones (Jiang *et al*, 2007). The diversity of the J-domain provides the specificity of Hsp70-Hsp40 interaction (Hennessy *et al*, 2005). The C-terminus varies dramatically among the Hsp40 members. The C-terminal part plays an essential role in substrate binding and subsequent recruitment to the Hsp70 chaperones. The high diversity is thought to provide substrate specificity of the Hsp70 system (Kampinga and Craig, 2010). The other important cofactors of the Hsp70 system, the nucleotide exchange factors or NEFs, promote the replacement of ADP with ATP, therefore resulting in substrate release. This way the next round of a folding cycle can begin (Alberti *et al*, 2003).

1.1.2.2 The Hsp90 chaperone system

The Hsp90 chaperone system acts downstream of the Hsp70 system. It is not involved in nascent chain binding and folding respectively, but assists folding of substrates which are in a near native state. Hsp90 represents one of the most abundant protein classes in cell, both under stressed and unstressed conditions (Li *et al*, 2012; Wandinger *et al*, 2008). The Hsp90 chaperones differ from other chaperones in that the substrates are mainly signalling molecules like transcription factors or protein kinases that have to be converted from an inactive to an active conformation. Therefore, the Hsp90 family has an important role in cell regulation (Picard, 2002). Because of its function in maturation of many proteins involved in cell signalling, the Hsp90 system is a promising target in cancer therapy (Trepel *et al*, 2010; Whitesell and Lindquist, 2005). An Hsp90 protein consists of three functional domains: the N-terminal domain containing the ATP binding pocket, the middle domain (M-domain) and the C-terminal dimerization domain. As in Hsp70, the ATP binding pocket is closed by a lid in the ATP-bound state (Ali *et al*, 2006; Dollins *et al*, 2007). The M-domain is involved in ATP-hydrolysis providing important catalytic residues and in addition in binding of the client protein and some co-chaperones (Fig. 1.4).

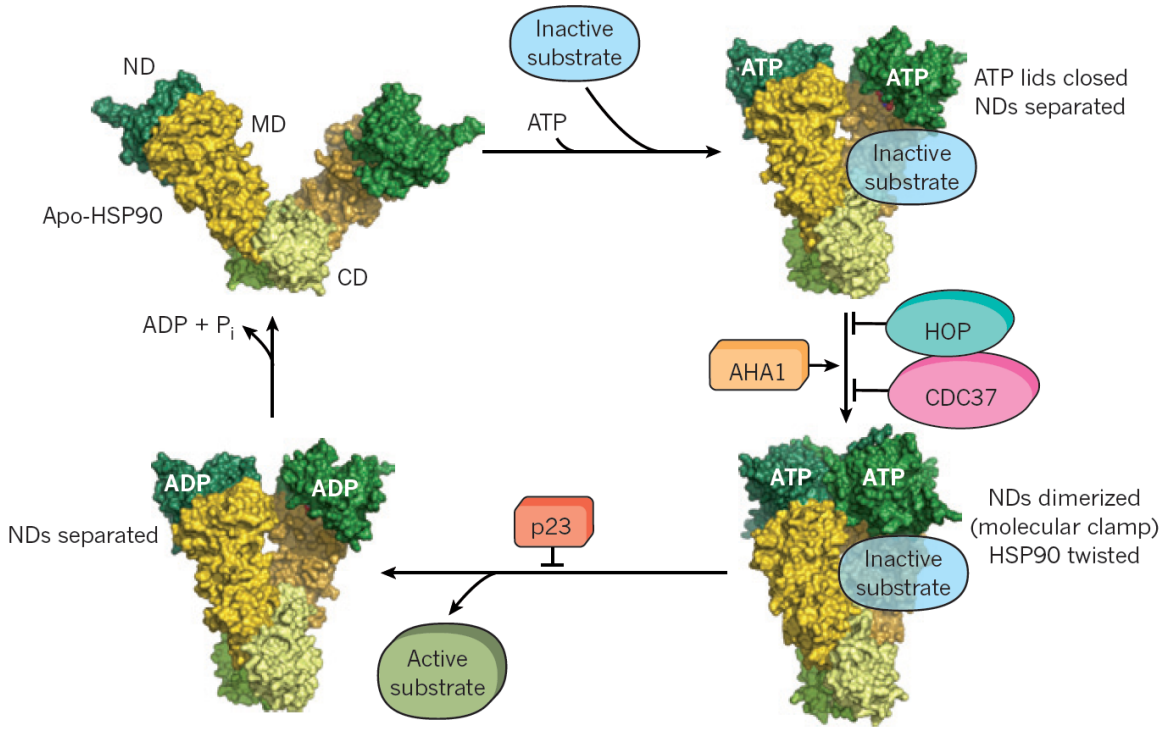

Figure 1.4: The Hsp90 reaction cycle. Client proteins are transferred to Hsp90 with the help of Hop1/Sti1 and Cdc37 which stabilize the open conformation and decrease the rate of ATP hydrolysis. After ATP binding the N-terminal domains (NDs) dimerize causing a tight substrate binding. Aha1 promotes ATP hydrolysis whereas p23 stabilizes the closed state of Hsp90 therefore enhancing the substrate-bound state. Figure: (Hartl *et al*, 2011).

The C-terminal domain is necessary for formation of the Hsp90 homodimer which is essential for Hsp90 function (Harris *et al*, 2004) and also mediates the interaction with co-chaperones containing TPR (tetratricopeptide) domains (Scheufler *et al*, 2000). The Hsp90 reaction cycle comprises drastic conformational changes within the protein (Krukenberg *et al*, 2008; Li *et al*, 2012). In the open form (apo-Hsp90) ATP and afterwards the corresponding client protein is bound. After these binding events Hsp90 undergoes conformational changes resulting in a closed conformation characterized by dimerization of the N-terminal domains. ATP hydrolysis then causes dissociation of the N-terminal domains allowing release of the activated client protein. For an efficient ATP cycle and regulation of the Hsp90 dependent substrate maturation several co-chaperones are bound to the Hsp90. As mentioned above, the Hsp70 system is involved in early folding of proteins. For final maturation, protein substrates like kinases are recruited to the Hsp90 machinery in an Hsp70-bound state via the co-chaperone Hop1/Sti1 which connects both chaperone systems (Chen and Smith, 1998; Johnson *et al*, 1998). The substrates mostly bind to the middle domain (MD) of Hsp90. In

addition Hop1/Sti1 inhibits the N-terminal dimerization process of Hsp90. Cdc37 represents another co-chaperone which inhibits the ATPase activity of Hsp90. Both co-chaperones therefore facilitate substrate binding (Roe *et al*, 2004; Vaughan *et al*, 2006). Further regulation of the Hsp90 system occurs via the action of the co-chaperone p23/Sba1 which stabilizes the ATP-bound state and the closed conformation respectively (Ali *et al*, 2006; Richter *et al*, 2004). This slows down the substrate release providing more time for substrate maturation. ATP hydrolysis which is a very slow process is stimulated by the activator protein Aha1 through binding to the M-domain of Hsp90 (Panaretou *et al*, 2002).

1.1.2.3 The Hsp100 chaperone system

The Hsp100 chaperones (ClpB/Hsp104) belong to the AAA+ ATPase family (ATPases associated with various cellular activities) possessing main functions in protein remodelling, protein disaggregation and protein degradation (Diamant *et al*, 2000; Doyle and Wickner, 2009; Glover and Lindquist, 1998; Lindquist and Kim, 1996). The common structural property of AAA+ ATPases is their organization in oligomeric rings (usually a six-fold symmetry) (Ogura and Wilkinson, 2001). These molecular machines receive their energy for disassembly of protein complexes or aggregates from ATP hydrolysis (Fig. 1.5). For ATP hydrolysis all members of the Hsp100 chaperone family possess at least one nucleotide-binding domain (NBD). Yeast Hsp104 possesses two NBD domains. NBD2 of Hsp104 mediates formation of the active hexamer and the NBD1 domain provides energy for threading the aggregated protein through the hexameric ring for disaggregation (Hattendorf and Lindquist, 2002). The N-terminal domain of Hsp104 is involved in binding of the protein aggregates (Shorter and Lindquist, 2006).

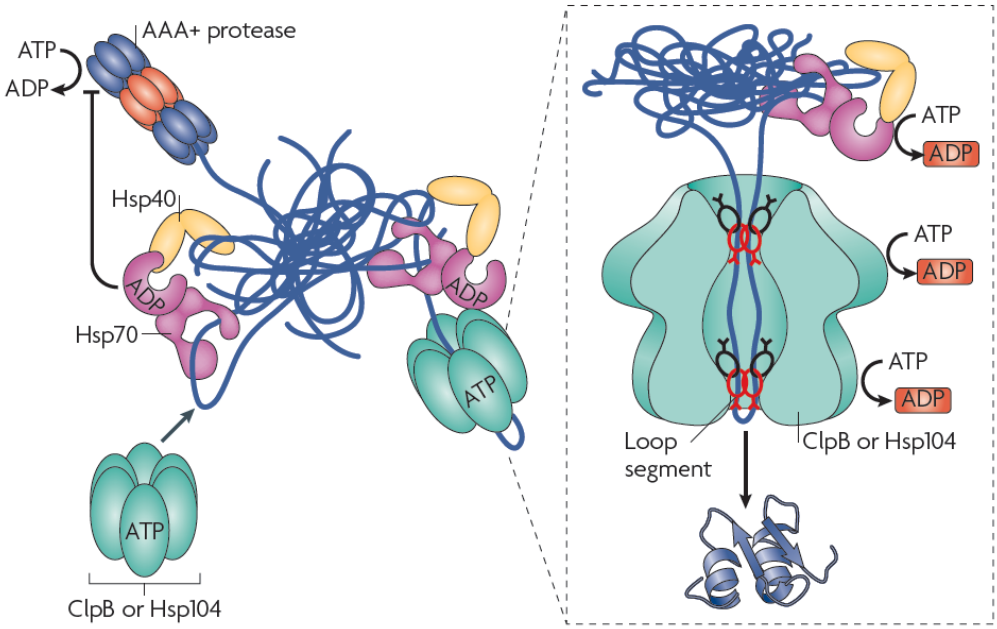

Figure 1.5: Disaggregation process of aggregated proteins mediated by the Hsp100 chaperone family (ClpB/Hsp104). The Hsp70 system acts upstream of the Hsp100 chaperones. The Hsp70 system is involved in targeting the aggregates to the disaggregase machinery. In sequential ATP-consuming steps the substrate is threaded through the pore. Figure: (Tyedmers *et al*, 2010).

The Hsp100-mediated disaggregation has to be assisted in most cases by the Hsp70 chaperone system which targets the substrates to Hsp100 (Glover and Lindquist, 1998; Goloubinoff *et al*, 1999; Winkler *et al*, 2012). Another important function of the Hsp70 system in the disaggregation process is to restrict the access of proteases to the aggregated protein, thereby directing the protein´s fate from degradation to disaggregation and reactivation respectively (Haslberger *et al*, 2007; Haslberger *et al*, 2008). Once the substrate has been transferred to the disaggregase, it is threaded into the hexameric channel in an ATP-consuming manner (Lum *et al*, 2004). Aromatic residues in mobile loop-segments at the inner surface of the pore mediate the threading process through the channel (Fig. 1.5), (Lum *et al*, 2004; Schlieker *et al*, 2004). Besides the upstream activity of the Hsp70 system in Hsp100 function, the Hsp70 system is also needed for assisting folding of the released polypeptide from the Hsp100 channel (Tyedmers *et al*, 2010).

1.1.2.4 Small heat shock proteins (sHsps)

The group of the small heat shock proteins (sHsps) is very diverse and consists of proteins from 16 kD up to 43 kD in size. The common feature of the sHsps is their ATP-independent mode of action and their ability to form oligomeric structures. Their main function consists of binding to unfolded proteins for preventing their aggregation (Haslbeck *et al*, 2004; Haslbeck *et al*, 2005; Jakob *et al*, 1993). One sHsp complex has the ability to bind more than one polypeptide chain. The extensively studied yeast sHsps Hsp26 and Hsp42 are organized in barrel-shaped oligomers. Stress-induced Hsp26 can promote Hsp104-mediated disaggregation (Cashikar *et al*, 2005; Haslbeck *et al*, 2004) whereas Hsp42 is involved in targeting of excess of misfolded proteins to large peripheral aggregate deposits (Specht *et al*, 2011). Hsp31, Hsp32, Hsp33 and Hsp34 belong to the DJ-1/ThiJ/PfpI superfamily which, as most prominent member, includes the human protein DJ-1 (PARK7). Dysfunctions of DJ-1 caused by mutations are linked to Parkinson's disease representing one of the major neurodegenerative diseases in humans (Abou-Sleiman *et al*, 2003; Bonifati *et al*, 2003; Hague *et al*, 2003). The Hsp31 family represents a class of small chaperones which are localized to yeast cytosol and expressed under conditions of nutrient limitation and oxidative stress (Skoneczna *et al*, 2007). It has also been shown that the Hsp31 family is required for the diauxic shift of yeast cells characterized by glucose limitation and the entering of the cells into stationary phase (Miller-Fleming *et al*, 2014). Additionally, it has been shown that Hsp31 and Hsp32 are localized to stress granules and processing bodies (P-bodies). Both represent storage compartments for translationally silenced mRNAs, formed during cell stress (Buchan *et al*, 2008; Buchan and Parker, 2009; Miller-Fleming *et al*, 2014).

1.1.2.5 The Hsp60 (chaperonin) system

The chaperonin family of molecular chaperones represents a group of specialized folding machines that is involved in folding of proteins with complex topologies. The chaperonins are divided into two classes. Type I chaperonins are found in the bacterial cytoplasm (GroEL), mitochondria (Hsp60) and chloroplasts (Rubisco-binding protein). Type II chaperonins reside in the archaebacterial and eukaryotic cytosol (Horwich *et al*, 2007; Stoldt *et al*, 1996). The

CCT/TRiC type II chaperonin of the eukaryotic cytosol mediates folding of approximately 10 % of newly translated proteins including the cytoskeletal components actin, α-and β-tubulin (Gao *et al*, 1992; Gomez-Puertas *et al*, 2004; Yaffe *et al*, 1992). Binding of some TRiC substrates occurs cotranslationally and requires either the action of chaperones including the Hsp70 family chaperones Ssb1/2 (Frydman *et al*, 1994; Melville *et al*, 2003) or in case of newly synthesized actin or tubulin the co-chaperone GimC/prefoldin (Siegers *et al*, 2003). Another feature of TRiC substrates is that they are often part of major protein complexes. TRiC can prevent the release of these substrates in the absence of their partner proteins (Camasses *et al*, 2003; Feldman *et al*, 1999; Gao *et al*, 1993). CCT/TRiC is a high molecular complex consisting of two stacked rings, each containing 8 subunits, which surround a central cavity (Kalisman *et al*, 2012; Leitner *et al*, 2012). Apical protrusions of CCT/TRiC function as a built-in lid in order to close the reaction chamber which is essential for the folding process (Douglas *et al*, 2011). The type II chaperonins cycle between an open and closed state in an ATP-dependent manner (Fig. 1.6). The switch to the closed state is promoted by ATP hydrolysis (Douglas *et al*, 2011; Meyer *et al*, 2003; Spiess *et al*, 2004).

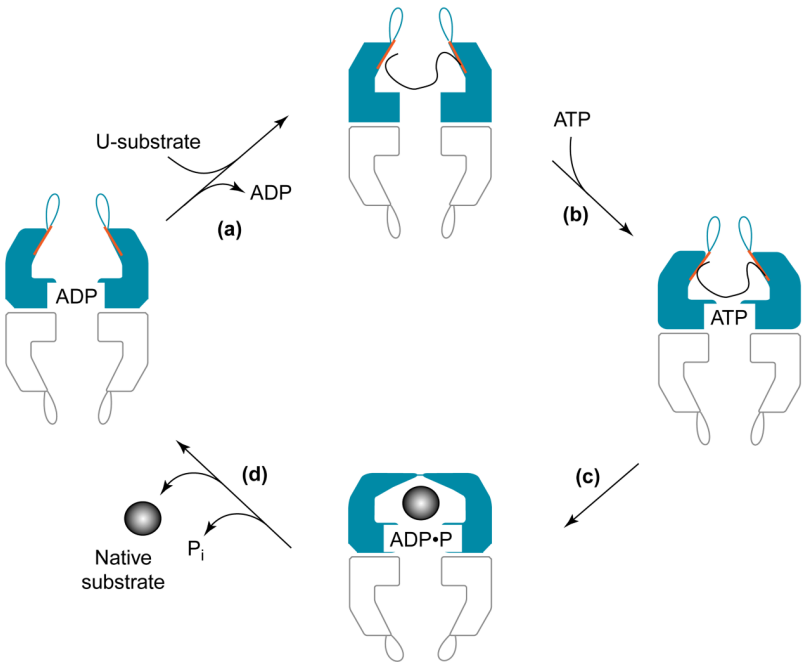

Figure 1.6: Model of the ATP-dependent reaction cycle of eukaryotic class II chaperonin. Substrates are bound by the chaperonin in the absence of bound nucleotides resulting in an open conformation (a). Closure of the lid is caused by both ATP binding and subsequent hydrolysis (b, c). Reopening of the lid and substrate release is driven by dissociation of inorganic phosphate (d) Figure: (Spiess *et al*, 2004).

1.2 Protein degradation mechanisms

1.2.1 The ubiquitin-proteasome system (UPS)

The ubiquitin-proteasome system which is found only in eukaryotic cells is responsible for the selective degradation of short-lived and misfolded proteins. Among the short-lived substrates are mainly regulatory proteins involved in many processes in the cell like cell cycle control (Fig. 1.7), (Koepp *et al*, 1999), apoptosis (Wojcik, 2002) or metabolism (Schork *et al*, 1994). Even in the immune system the proteasome function is essential. It generates peptide fragments from cytosolic proteins which are subsequently displayed via MHC class I proteins to cytotoxic T cells (Wang and Maldonado, 2006). Playing such a crucial role in many pathways, it is not surprising that defects in proteasomal functions can cause severe diseases.

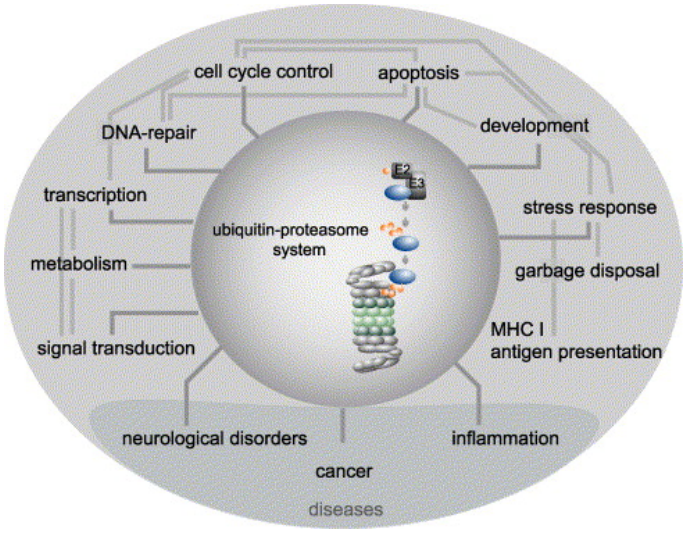

Figure 1.7: Cellular functions of the ubiquitin-proteasome system. The UPS plays a role in many regulatory pathways in eukaryotic cells. Dysfunction of this important proteolytic system causes a multitude of disorders and diseases. Figure: (Wolf and Hilt, 2004).

For providing selectivity of substrate recognition almost all substrates to be degraded are covalently tagged with ubiquitin chains serving as degradation signals. Ubiquitin is a small protein of 76 amino acid residues. It is highly conserved and present in all eukaryotic cells. Ubiquitin is attached to the substrates by the sequential action of three enzymes in an ATP-consuming manner. In a first step ubiquitin has to be activated. This is achieved by the action of ubiquitin-activating enzymes (E1), which under consumption of ATP, form an energy-rich thioester bond between the C-terminal glycine residue of ubiquitin and the cysteine residue of the active site of the E1 enzyme. Afterwards, ubiquitin is transferred to an active site cysteine residue of an ubiquitin-conjugating enzyme (E2). With the help of ubiquitin ligases (E3), ubiquitin is transferred from the E2 enzyme to corresponding substrates resulting in the formation of an isopeptide bond between the C-terminal glycine of ubiquitin and the ε amino group of mainly lysine residues of substrates (Fig. 1.8), (Hershko *et al*, 1979; Hershko *et al*, 1983). Also the N-terminus of proteins as well as cysteine, serine and threonine residues can serve as ubiquitin acceptor sites in substrates (Ciechanover and Stanhill, 2014; Kravtsova-Ivantsiv *et al*, 2013). In eukaryotes multiple E3 enzymes are present, each of them having the ability of binding different sets of substrates, therefore providing substrate specificity to this process (Glickman and Ciechanover, 2002). The E3 ligases are divided into two main classes, the RING (Really Interesting New Gene) and HECT (Homologous to E6AP Carboxy Terminus) type E3 ligases. While E3 RING ligases only mediate the transfer of ubiquitin from E2 enzymes to the substrates (Deshaies and Joazeiro, 2009; Metzger *et al*, 2014), HECT-type E3 ligases covalently bind the ubiquitin before transferring it to the substrate (Huibregtse *et al*, 1995; Scheffner and Kumar, 2014; Scheffner *et al*, 1995).

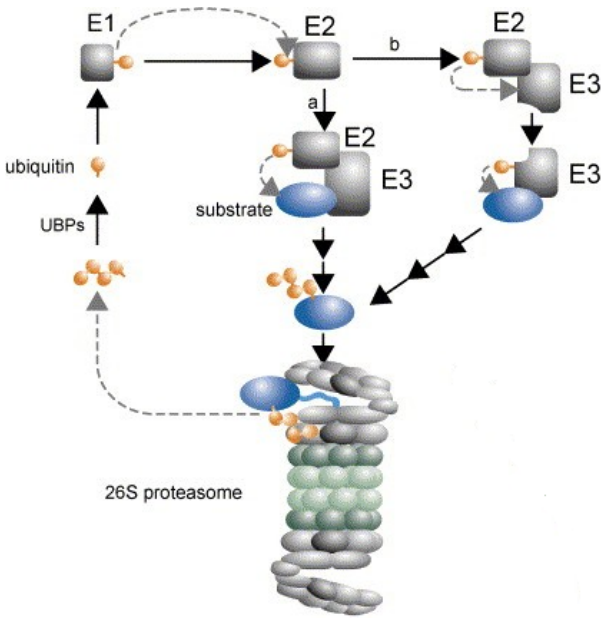

Figure 1.8: Ubiquitination process of substrates for proteasomal degradation. A coordinated action of three enzymes is necessary for tagging proteins with ubiquitin. A ubiquitin-activating enzyme (E1), a ubiquitin conjugating enzyme (E2) and a ubiquitin ligase (E3) which finally transfers the ubiquitin to the substrate are essential in this process. After substrate binding to the proteasome for degradation the ubiquitin chain is cut off by ubiquitin proteases (UBPs) and recycled for further rounds of reactions of ubiquitin attachment leading to polyubiquitination. Figure: (Wolf and Hilt, 2004).

Ubiquitin contains 7 internal lysine residues; therefore different linkages within the polyubiquitin chain can be formed. The K48 residue is the most important residue for formation of polyubiquitin chains as signal for proteasomal targeting. These kinds of polyubiquitin chains serve as signals for proteasomal degradation of corresponding substrates (Chau *et al*, 1989; Ciechanover and Stanhill, 2014; Thrower *et al*, 2000). In contrast, K63-linked ubiquitin chains are involved in DNA repair, endocytosis or lysosomal (vacuolar) degradation (Barriere *et al*, 2007; Ikeda and Dikic, 2008). If the length of an ubiquitin chain is not sufficient for efficient proteasomal degradation, E4 enzymes (Ubiquitin elongases) elongate already attached ubiquitin chains on substrates (Koegl *et al*, 1999). Interestingly, there are also examples of substrates which are degraded by the proteasome in an ubiquitin-independent manner of which the substrate ornithine decarboxylase is the most prominent example (Coffino, 2001; Erales and Coffino, 2014).

Elimination of ubiquitinated substrates occurs via the 26S proteasome, a 2.5 MDa large protease complex found in the eukaryotic nucleus and cytosol. It consists of a barrel-shaped 20S core particle providing the catalytic activities for proteolysis and two 19S regulatory

particles which mediate substrate recognition, unfolding and translocation into the catalytic chamber of the 20S core particle in an ATP-consuming manner (Fig. 1.9), (Wolf and Hilt, 2004). Substrates can directly bind to the regulatory particle of the proteasome (Deveraux *et al*, 1994; Elsasser *et al*, 2004; Husnjak *et al*, 2008) or they are transferred to the proteasome by shuttle proteins like yeast Rad23 or Dsk2 containing UBA domains for binding polyubiquitin chains and UBL domains for binding to the proteasome (Elsasser *et al*, 2004; Elsasser *et al*, 2002; Hartmann-Petersen and Gordon, 2004a; Hartmann-Petersen and Gordon, 2004b; Hartmann-Petersen and Gordon, 2004c; Hartmann-Petersen *et al*, 2003; Medicherla *et al*, 2004).

The 20S core particle consists of 4 heptameric rings (α7β7β7α7) based on 7 different α and β subunits of which only the two middle rings (β) contain the catalytic activities for proteolysis. Three different proteolytic activities are located in each β ring. The β1 subunit exhibits a peptidyl-glutamyl-peptide-hydrolyzing activity cleaving after acidic and small hydrophobic amino acid residues, the β3 subunit has a trypsin-like activity cleaving after basic and small hydrophobic residues and the β5 subunit possesses chymotrypsin-like activity cleaving generally after hydrophobic residues. The gate to the 20S catalytic chamber is formed by the two outer α-rings of the 20S core particle which serve as docking sites for the 19S particle and prevent unregulated access to the 20S catalytic core (Tomko and Hochstrasser, 2013; Wolf and Hilt, 2004).

The 19S regulatory particle can be divided into two subcomplexes, the lid and the base which are linked together via the 19S subunit Rpn10. Rpn10 is also able to bind ubiquitin chains via its ubiquitin-interacting (UIM) motif (Fig. 1.9). The lid is composed of subunits without any ATPase activity. The lid also functions in the deubiquitination of proteins during their translocation into the catalytic chamber of the 20S core particle, therefore being responsible for recycling of ubiquitin (Amerik *et al*, 1997; Lander *et al*, 2013; Park *et al*, 1997), (Fig. 1.9). The base contains a 6-fold ATPase ring providing the energy for unfolding of substrates, for gate opening and for translocation of the substrates into the 20S core particle (Tomko and Hochstrasser, 2013; Wolf and Hilt, 2004). The 20S core particle alone, separated from the 19S regulatory particles under conditions of oxidative stress, is able to degrade oxidatively damaged proteins in an ubiquitin- and ATP-independent manner providing the possibility of a more effective removal of irreparably damaged proteins (Davies, 2001; Kastle *et al*, 2012; Pickering *et al*, 2010).

Degradation of proteins by the proteasome finally generates oligopeptides which can be further processed into single amino acids by the action of endopeptidases and

aminopeptidases. The resulting free amino acids can then serve as building blocks for the synthesis of new proteins (Saric *et al*, 2004).

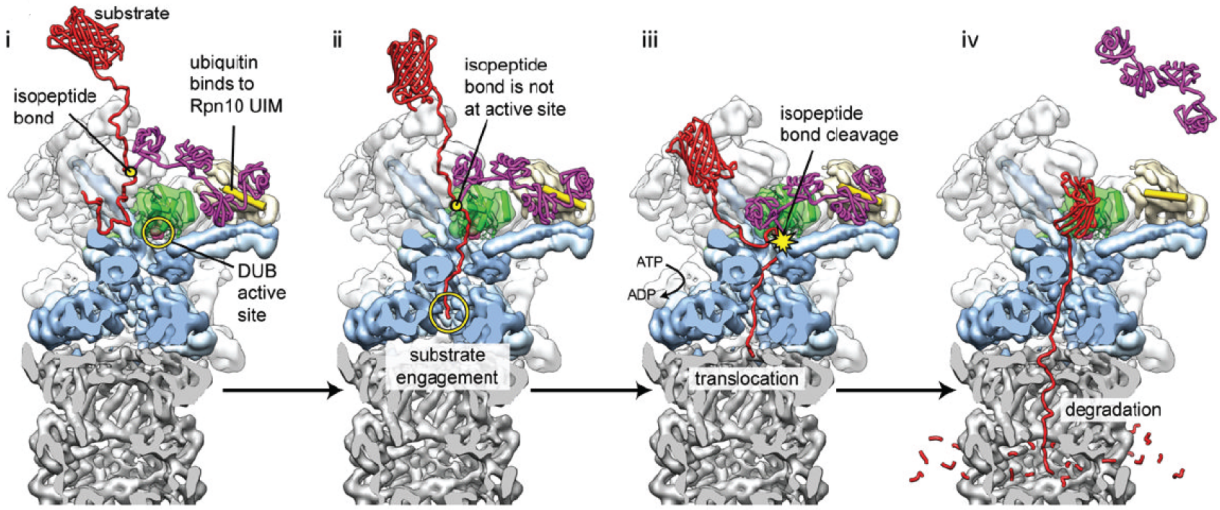

Figure 1.9: Model of substrate recognition by the 19S regulatory particle. (i) The ubiquitin chain (purple) of the ubiquitinated substrate binds to the ubiquitin-interacting motif (UIM) of Rpn10 (yellow). (ii) The unfolded tail of the substrate is then threaded through the pore consisting of ATPase domains (blue). (iii) The isopeptide bond between substrate and tetraubiquitin is in proximity to the 19S subunit Rpn11 (green) which catalyses the isopeptide bond cleavage. The translocation through the pore occurs in an ATP-consuming manner. (iv) The tetraubiquitin dissociates from the 19S regulatory particle followed by translocation of the substrate into the catalytic chamber of the 20S core particle prior to proteolytic cleavage. Figure: (Lander *et al*, 2013).

1.2.2 The lysosome (vacuole) system

Besides the ubiquitin-proteasome system for selective proteolysis of misfolded and short-lived proteins there exists an additional proteolytic mechanism in eukaryotic cells called autophagy. Autophagy handles long-lived, membrane-associated proteins, whole ribosomes or mitochondria. During autophagy the substrates are sequestered into double-membrane vesicles called autophagosomes which finally fuse with the lysosome (vacuole in yeast) for proteolytic degradation (Fig. 1.10), (Achstetter *et al*, 1984; He and Klionsky, 2009; Nakatogawa *et al*, 2009; Stolz *et al*, 2014). The lysosome (vacuole) is an organelle containing

a wide spectrum of unspecific hydrolytic enzymes not only responsible for protein degradation but also for breaking down nucleic acids, carbohydrates and lipids (Yorimitsu and Klionsky, 2005). In addition to its function in degradation of different biomolecules, the lysosome plays an important role as storage compartment for amino acids, different ions, polyphosphates or carbohydrates. There are different forms of autophagy differing in their substrate specificity. Macroautophagy becomes relevant if the cell is subjected to starvation conditions like in stationary growth phase (Takeshige *et al*, 1992). Macroautophagy provides the cell with important nutrients in the form of different metabolites (Cuervo, 2004). In this process substrates like proteins or even whole organelles are degraded in a rather non-selective manner. A selective form of macroautophagy includes the clearance of protein aggregates in the mammalian cytosol which can complement the ubiquitin-proteasome system in clearance of aggregates consisting of α-synuclein or mutant huntingtin known to be involved in neurodegenerative disease (Iwata *et al*, 2005; Kirkin *et al*, 2009; Nakatogawa *et al*, 2009; Rubinsztein, 2006; Webb *et al*, 2003). Other selective autophagy pathways include pexophagy or mitophagy where peroxisomes and mitochondria respectively are degraded in a more specific manner (Leao-Helder *et al*, 2004). These two processes are important when the physiological conditions in a cell change in a way that mitochondria or peroxisomes are not needed any more in high concentrations. Also damaged mitochondria are degraded by mitophagy (Dunn *et al*, 2005; Kundu and Thompson, 2005; Stolz *et al*, 2014).

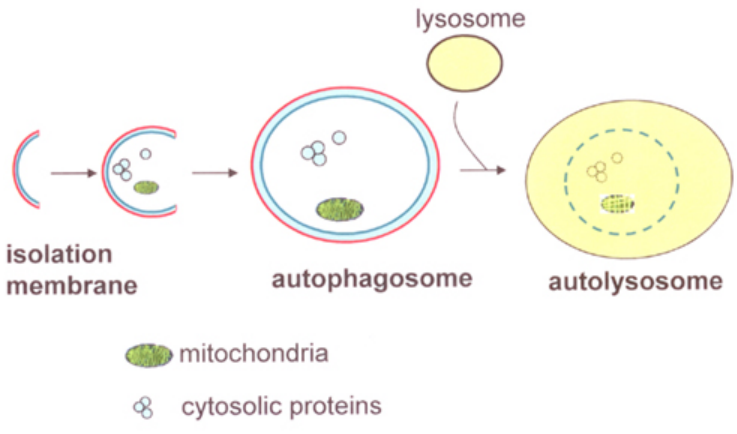

Figure 1.10: Schematic illustration of lysosomal (vacuolar) substrate recruitment. Organelles or macromolecular complexes to be degraded are sequestered into double membrane autophagosomes. These cargo-containing autophagosomes finally fuse to the lysosomes (vacuoles) for substrate delivery and subsequent degradation. Figure: (Zeng and Kinsella, 2011).

1.3 Cellular protein quality control systems

1.3.1 Protein quality control: principles and mechanisms

To maintain the integrity of the proteome the cell has evolved protein quality control mechanisms which detect misfolded proteins and target them to three different processes respectively: refolding, degradation or sequestration to specialized quality control compartments (Fig. 1.11), (Frydman, 2001; Hartl and Hayer-Hartl, 2009) (for details see chapter 1.3.3). In all three quality control pathways chaperones are of immense value because they recognize misfolded stretches on proteins and direct them, - dependent on their probability to aggregate, their localization in cell or the degree of misfolding -, to one of these three pathways (Hartl and Hayer-Hartl, 2002). Each decision a cell has made towards one pathway poses potential dangers, therefore a tight regulation of these three processes and the expression of proteins involved in protein quality control respectively, has to be ensured. The following chapters focus on the different branches of the cellular protein quality control system highlighted for the model organism yeast

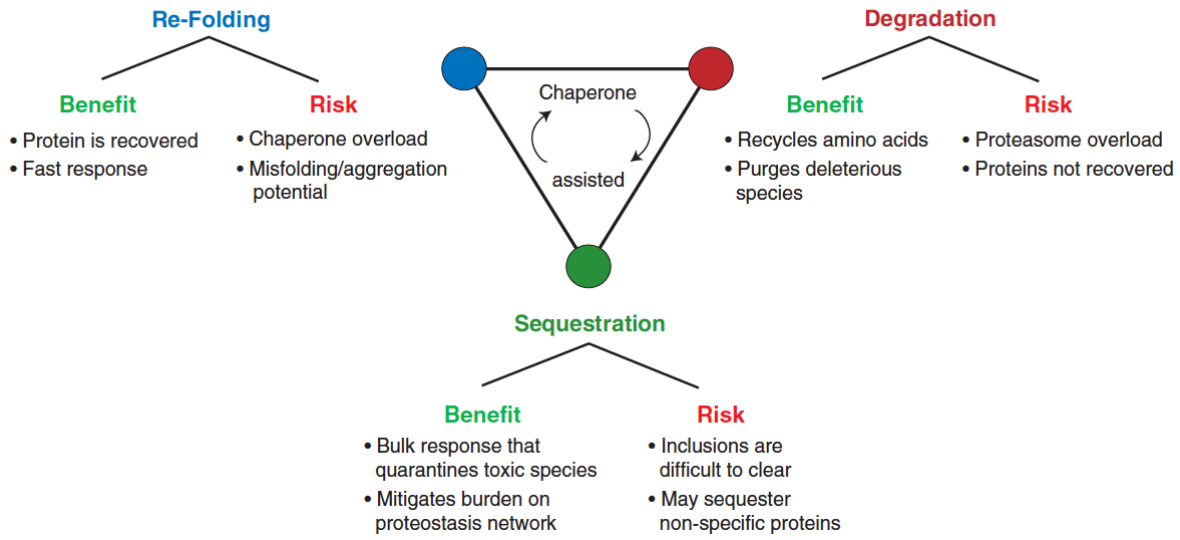

Figure 1.11: Schematic overview of the main pathways for maintenance of protein homeostasis. Misfolded proteins in the cell can have three destinies including degradation by proteolytic pathways like the ubiquitin-proteasome system, reactivation and refolding respectively and sequestration into specialized protein quality compartments. A functional chaperone system is essential for each of the three strategies for handling misfolded protein species. Figure: (Chen *et al*, 2011).

1.3.2 The cytoplasmic protein quality control

Proteins are synthesized at ribosomes in a process called translation where mRNA is used as template for production of polypeptide chains. Already at this early stage the cell possesses a protein quality control mechanism dealing with aberrant proteins emerging on the ribosome exit channel. Defective nascent proteins are often the consequence of non-stop mRNA caused by DNA mutations or transcriptional mistakes (Akimitsu, 2008; Ito-Harashima *et al*, 2007). Non-stop mRNA finally results in C-terminal poly-lysine tracts in corresponding proteins (Dimitrova *et al*, 2009). The main E3 ligase involved in recognition and ubiquitination of such, still ribosome bound aberrant proteins, is Ltn1 (Alamgir *et al*, 2010; Brandman *et al*, 2012; Braun *et al*, 2007). After ubiquitination corresponding substrates are extracted from the ribosome via the Cdc48 machinery which uses its intrinsic ATPase activity for generation of the force necessary for this extraction process (Brandman *et al*, 2012; Stolz *et al*, 2011). Afterwards, the ubiquitinated substrates are degraded by the proteasome. In general, during folding of proteins emerging from ribosomes it is important to prevent the formation of incorrect interactions. This is achieved by the heterodimeric NAC complex (nascent–polypeptide-associated complex) which binds to nascent polypeptides (Rospert *et al*, 2002). The NAC complex works together with a ribosome-associated Hsp70/Hsp40 chaperone system composed of the RAC complex (Hsp70 chaperone Ssz1 and Hsp40 chaperone Zuo1) and the Hsp70 chaperone Ssb1 (Conz *et al*, 2007; Craig *et al*, 2003; Huang *et al*, 2005; Preissler and Deuerling, 2012).

Proteins released from the ribosome and fulfilling functions in the cytosol are subjected to further protein quality control including binding of the Hsp70 chaperones of the Ssa type (Ssa1-Ssa4 in yeast) which can prevent aggregation of proteins by shielding their hydrophobic surfaces against the solvent (for details see chapter 1.1.2.1). Small aggregates which have already built up can be dissolved by the Hsp100 chaperone Hsp104 which uses its ATPase activity for the disaggregation process. For larger aggregates Hsp104 acts in concert with the Hsp70 system (for details see chapter 1.1.2.3). The next level of protein quality control includes the Hsp90 chaperones which act downstream of the Hsp70 system and are involved in maturation and refolding processes of selected substrates like signalling proteins (for details see chapter 1.1.2.2).

Irreversibly misfolded cytosolic proteins are mainly targeted for proteasomal degradation via the action of the E3 ligase Ubr1 (Eisele and Wolf, 2008; Heck *et al*, 2010; Nillegoda *et al*,

2010). Ubr1 was discovered as E3 ligase of the N-end rule pathway targeting substrates containing N-terminal degradation signals (N-degrons) for ubiquitination. An N-degron is composed of an N-terminal type 1 destabilizing amino acid residue (Arg, Lys, His) or type 2 destabilizing residue (Leu, Phe, Trp, Tyr or Ile) respectively, which are both recognized by two different specific binding pockets in Ubr1. Additionally, the corresponding N-end rule substrates possess unstructured N-termini and internal lysine residues for Ubr1 binding and ubiquitin attachment respectively (Bartel *et al*, 1990; Choi *et al*, 2010; Varshavsky, 2011; Xia *et al*, 2008). The Ubr1-dependent ubiquitination of misfolded proteins seems to work independently of the classical N-end rule pathway (Heck *et al*, 2010; Nillegoda *et al*, 2010). The Hsp70 chaperones and the Hsp110 chaperone Sse1 which acts as nucleotide exchange factor for Hsp70 are necessary for the targeting process to Ubr1 *in vivo* (Heck *et al*, 2010; Nillegoda *et al*, 2010). The E2 enzymes involved in the Ubr1-dependent ubiquitination process of misfolded cytoplasmic proteins are Ubc2 (Rad6) which also mediates the Ubr1 dependent ubiquitination in the N-end rule pathway and the stress inducible E2 enzymes Ubc4 and Ubc5 (Byrd *et al*, 1998; Nillegoda *et al*, 2010; Park *et al*, 2007). In recent studies the E3 ligase San1 (Dasgupta *et al*, 2004) which is localized to the nucleus was also discovered to be involved in the ubiquitination process of misfolded cytoplasmic substrates (Heck *et al*, 2010; Khosrow-Khavar *et al*, 2012; Prasad *et al*, 2010). San1 was originally discovered only for being involved in proteasomal targeting of misfolded nuclear proteins (Gardner *et al*, 2005). In contrast to Ubr1, San1 possesses large disordered regions outside of its RING domain providing San1 with a high flexibility to bind different client substrates (Fredrickson *et al*, 2011; Rosenbaum *et al*, 2011). This property, also known from some small chaperones (Jaya *et al*, 2009), might explain why San1 can ubiquitinate substrates independently of any help of chaperones. The involvement of nuclear San1 in cytoplasmic quality control implies a shuttling process of corresponding substrates into the nuclear lumen (Heck *et al*, 2010; Khosrow-Khavar *et al*, 2012; Prasad *et al*, 2010). It has been shown that effective shuttling into the nucleus requires the Hsp70 chaperone family of the Ssa type and the Hsp110 chaperone Sse1 (Heck *et al*, 2010). In addition, the Hsp40 chaperone Sis1 was discovered to be essential for the shuttling into the nucleus (Park *et al*, 2013).

Another branch of the cytoplasmic protein quality control includes the E3 ligase Doa10 which is localized in the ER membrane and is involved in ubiquitination of substrates localized in the ER membrane exposing a misfolded domain in the cytosol (ERAD-C substrates) (for details see chapter 1.3.2). It has also been reported that some fully cytoplasmically localized

substrates are ubiquitinated by this E3 ligase with help of the Hsp70 system and the Cdc48 machinery (Gilon *et al*, 1998; Gilon *et al*, 2000; Metzger *et al*, 2008).

Once ubiquitinated, either by Ubr1, San1 or Doa10, the substrates are delivered to the proteasome for subsequent degradation. Hul5, representing a 19S proteasome-associated E3/E4 enzyme can further enhance the processivity of the proteasome by elongating the ubiquitin chains built onto the substrates (Fig. 1.12), (Aviram and Kornitzer, 2010; Koegl *et al*, 1999; Kohlmann *et al*, 2008).

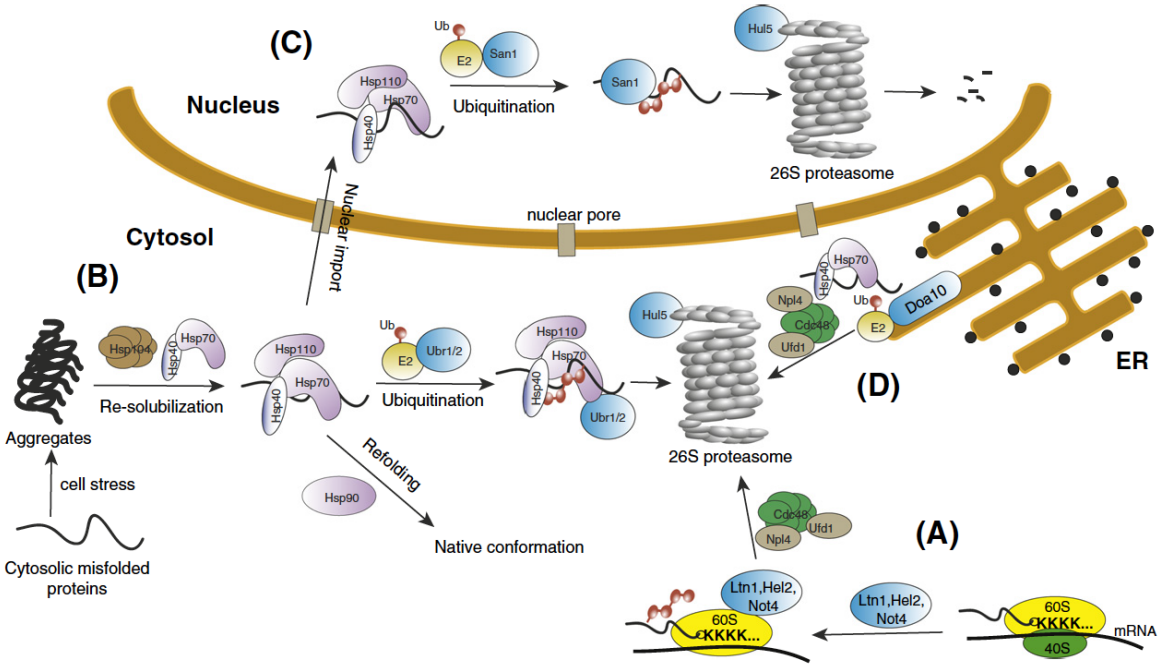

Figure 1.12: Cytoplasmic protein quality control and degradation. Ubiquitination of misfolded cytoplasmic proteins is carried out by different E3 ligases depending on the localization within the cell. (A) Nascent polypeptides translated from defective mRNA are ubiquitinated mainly by Ltn1 and extracted from the ribosome via the Cdc48 machinery for final proteasomal degradation. (B) The main portion of cytoplasmically localized misfolded proteins is ubiquitinated by the E3 ligase Ubr1 with help of the Hsp70 chaperone family. Already aggregated proteins can be resolubilized by Hsp104 and Hsp70. (C) Some cytosolic substrates are shuttled into the nucleus for San1-dependent proteasomal degradation. (D) The ER membrane-localized E3 ligase Doa10 together with other ERAD-components are also able to ubiquitinate some cytosolic substrates. Figure: (Amm *et al*, 2014).

1.3.3 Endoplasmic reticulum-associated protein degradation (ERAD)

About one third of all synthesized proteins enter the secretory pathway for folding and delivery to their sites of function including the endoplasmic reticulum (ER), the Golgi apparatus, the lysosome, the plasma membrane and the exterior of the cell. The entry site into the secretory pathway is the ER into which the secretory proteins are imported either cotranslationally or posttranslationally (Araki and Nagata, 2011; Haigh and Johnson, 2002; Rapoport, 2007). The ER contains a complex folding and folding surveillance machinery consisting of chaperones, oxido-reductases, glycan-modifying enzymes and lectins (Aebi *et al*, 2010; Freedman *et al*, 1994; Pearse and Hebert, 2010; van Anken and Braakman, 2005). Proteins which cannot be folded correctly due to mutations or cell stress are retained in the ER and cause the induction of the unfolded protein response (UPR). In yeast the UPR causes transcriptional upregulation of proteins involved in ER folding and protein degradation (Kimmig *et al*, 2012; Korennykh and Walter, 2012; Walter and Ron, 2011). Misfolded proteins in the ER are specifically modified with a unique glycosylation pattern (Clerc *et al*, 2009; Gauss *et al*, 2011; Jakob *et al*, 1998; Knop *et al*, 1996b; Quan *et al*, 2008) directing corresponding proteins to retrograde transport out of the ER and degradation by the cytosolic ubiquitin-proteasome system (Hiller *et al*, 1996; Kostova and Wolf, 2003). Misfolded proteins of the ER are classified into three main groups depending on their topology: Misfolded ER-lumenal proteins (ERAD-L substrates), misfolded ER membrane proteins (ERAD-M) and ER membrane proteins containing a misfolded cytosolic domain (ERAD-C) (Carvalho *et al*, 2006; Vashist and Ng, 2004). After retrotranslocation through the ER membrane to the cytosolic side of the ER, a process still under extensive debate (Hampton and Sommer, 2012), the substrates are ubiquitinated by two main E3 ligases. ERAD-L substrates like the misfolded carboxypeptidase Y (CPY*) (Finger *et al*, 1993; Wolf and Fink, 1975) and ERAD-M substrates require the E3 ligase Hrd1/Der3 (Bays *et al*, 2001; Deak and Wolf, 2001) whereas ERAD-C substrates use the E3 ligase Doa10 (Swanson *et al*, 2001) for ubiquitination. Recent studies revealed the cytosolic E3 ligase Ubr1 as being involved in ubiquitination of ERAD-C substrates under stress conditions or when the canonical ER ligase Doa10 and Hrd1/Der3 are absent (Stolz *et al*, 2013). As for misfolded cytosolic substrates, ERAD-C substrates require the cytosolic Hsp70 machinery of the Ssa class for recognition of the misfolded domain (Huyer *et al*, 2004; Nakatsukasa *et al*, 2008; Taxis *et al*, 2003). The extraction of ERAD substrates from the ER membrane is managed by the Cdc48 machinery

consisting of a hexameric Cdc48 ring providing the mechanical force for the extraction process, the two cofactors Ufd1 and Npl4 (Stolz *et al*, 2011; Wolf and Stolz, 2012) and Ubx2. Ubx2 which is anchored in the ER membrane is responsible for recruitment of the Cdc48 machinery (Neuber *et al*, 2005; Schuberth and Buchberger, 2005). Downstream of the Cdc48 machinery, the two shuttle proteins Dsk2 and Rad23 containing UBA domains for binding of ubiquitin chains and UBL domains able to bind the 26S proteasome finally transfer the substrates to the 26S proteasome for subsequent degradation (Fig. 1.13), (Hartmann-Petersen and Gordon, 2004a; Hartmann-Petersen *et al*, 2003; Medicherla *et al*, 2004; Raasi and Wolf, 2007; Richly *et al*, 2005).

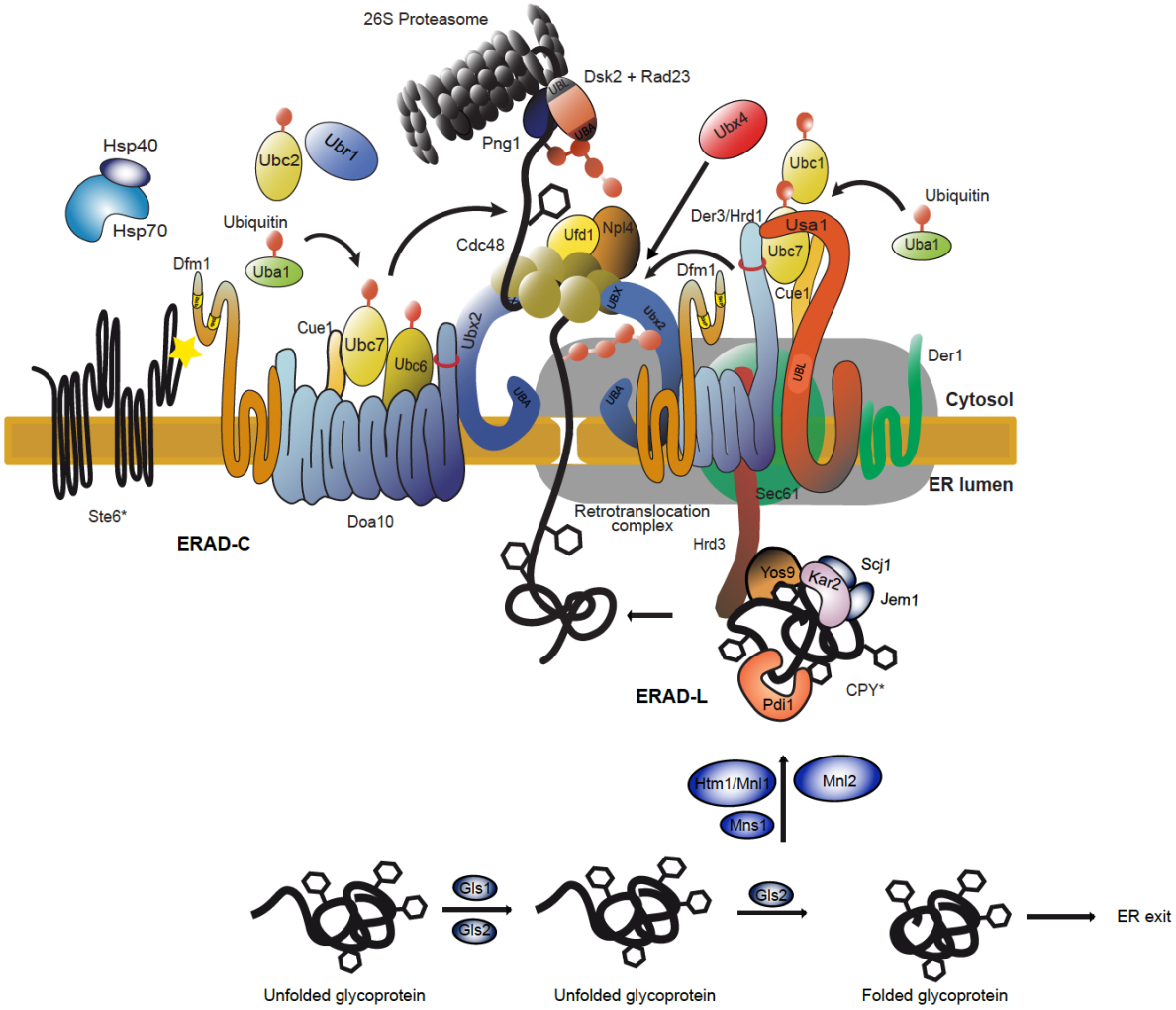

Figure 1.13: Endoplasmic reticulum-associated protein degradation (ERAD). Misfolded proteins of the secretory pathway are retrotranslocated for ubiquitination and proteasomal degradation. Depending on the topology of ERAD substrates several branches exist for substrate ubiquitination. The ERAD-L pathway targets lumenal misfolded proteins to proteasomal degradation involving the ER membrane localized E3 ligase Der3/Hrd1. ERAD-C substrates are characterized by misfolded cytosolic domains and are ubiquitinated by the E3 ligase Doa10. After ubiquitination, all types of ERAD substrates are extracted out of the ER by the Cdc48 machinery. Figure: Modified from (Amm *et al*, 2014).

1.3.4 Spatial organization of cellular protein quality control

The quality control system is not only characterized by different sets of chaperones or components of the protein degradation machinery, but also a spatial organization in separated protein quality control compartments was observed in eukaryotic cells (Kaganovich *et al*, 2008). It was found found that misfolded proteins which cannot be refolded can be deposited into two distinct protein quality control compartments, JUNQ and IPOD. JUNQ (juxtanuclear quality control compartment) is termed a compartment which is localized to the cytosolic side of the ER. It is formed in stressed cells and contains mainly soluble misfolded proteins which are still ubiquitinated, therefore representing a storage pool for proteasomal degradation (Kaganovich *et al*, 2008). Sequestration into JUNQ avoids overloading of the ubiquitin-proteasome system by shielding the proteins from the cellular environment. IPOD (insoluble protein deposit) represents a perivacuolar storage compartments for insoluble protein aggregates which are often toxic for cells. These aggregates are built up of misfolded and amyloid-forming proteins and are delivered to IPOD in a mostly non-ubiquitinated form (Fig. 1.14), (Kaganovich *et al*, 2008). IPOD colocalizes with Atg8 which is a ubiquitin-like adaptor protein essential for autophagic vacuole delivery (Kuma *et al*, 2007; Yorimitsu and Klionsky, 2005). Therefore the vacuole plays a main role in clearance of protein deposited in the IPOD. The cytoskeleton is important for sequestration of aggregates to both quality control compartments. Impairment or inhibition of the ubiquitin-proteasome system lead to transfer of JUNQ proteins to the IPOD (Kaganovich *et al*, 2008). Recent results redefined JUNQ as an intranuclear compartment termed INQ (Miller *et al*, 2015a; Miller *et al*, 2015b) to which misfolded cytosolic proteins are delivered in a Sis1-dependent manner (Park *et al*, 2013), (chapter 1.3.2).

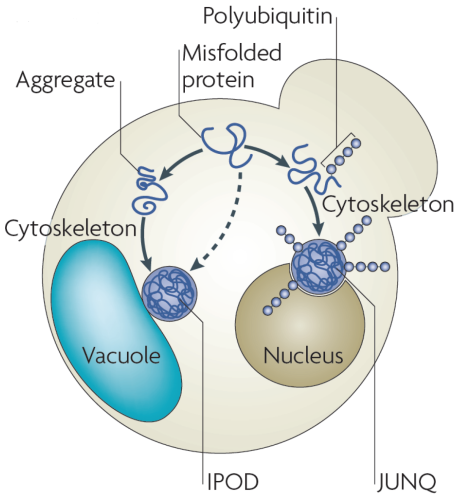

Figure 1.14: Protein quality control compartments in yeast. At 2008, it was shown that *Saccharomyces cerevisiae* possesses two distinct protein quality control compartments: JUNQ (juxtanuclear quality-control compartment) is localized at the ER and contains misfolded ubiquitinated proteins. IPOD (insoluble protein deposit) is localized near the vacuole and contains terminally aggregated proteins in a mainly non-ubiquitinated state. Figure: (Tyedmers *et al*, 2010). Recent studies revealed the JUNQ compartment as being localized in the nucleus therefore redefined this compartment as intranuclear quality control compartment (INQ), (Miller *et al*, 2015a; Miller *et al*, 2015b).

1.3.5 Aims of the study

The entire study was undertaken to shed light on cytoplasmic protein quality control mechanisms and elimination of misfolded proteins in the eukaryotic model organism *Saccharomyces cerevisiae*. Terminally misfolded substrates based on cytoplasmic permanently misfolded CPY* were used for unravelling new components of the cytoplasmic protein quality control system and to further characterize the involvement of the nucleus in the clearance of cytosolic misfolded proteins. For prospective screening experiments new model substrates based on firefly luciferase were established.

An obvious question was whether there are differences in components of the protein quality control system and the mechanism of degradation when instead of the fate of a permanently misfolded protein the fate of an orphan protein is followed. For this purpose the control pathway of the fatty acid synthase complex subunit Fas2 lacking its partner Fas1 was further analysed.

2. MATERIAL AND METHODS

2.1 Material

2.1.1 Instruments

Table 2.1: Instruments used in this study.

Instrument	Manufacturer
Cell Disruptor Genie® Digital	Scientific Industries
Centrifuge 5417C	Bio-Rad Labaratories
Centrifuge 5415C	Bio-Rad Labaratories
Centrifuge Hermle Z 320 K	Eppendorf
Centrifuge Biofuge fresco	Heraeus
Centrifuge Pico 21	Heraeus
Chemiluminescence Imaging System Fusion	Peqlab
DNA Electrophoresis System Mini-Sub® Cell GT	Bio-Rad Labaratories
Film Developing machine Optimax Type TR	MS Laborgeräte
Gel Imaging System Quantum	Peqlab
Microscope Axioskop	Zeiss
Microwave 6160-13	Neff
Multimode Plate Reader Enspire®	Perkin Elmer
PCR Thermocycler T Professional Basic Gradient	Biometra
pH Measuring System CG 832	Schott
PhosphorImager Storm 860	Molecular Dynamics
Photometer Novospec II	Pharmacia
Photometer Gene Quant 1300	GE Healthcare
Pipets Pipetman P10/P20/P200/P1000	Gilson
Power Supply Power Pac® Basic	Bio-Rad Laboratories
SDS Gel Electrophoresis System Mini-Protean® Tetra Cell	Bio-Rad Laboratories
Thermomixer Pro	Cell Media
Thermomixer 5437	Eppendorf

Vacuum gel dryer	Fröbel
Vacuum pump	Vaccubrand
Vortexer VF1	Janke und Kunkel –Labortechnik
Vortexer Eurolab	Merck
Wet Tank Western blot System Mini-Trans-Blot®	Bio-Rad Laboratories

2.1.2 Consumables

Table 2.2: List of consumables used in this study.

Material	**Manufacturer**
Chemiluminescence films Hyperfilm™ ECR	GE Healthcare
Chemiluminescence films Bio Max MR	Kodak
Falcon tubes Cellstar® 15ml/50ml	Greiner Bio-One
Glass beads, acid-washed, 425-600 µm	Sigma-Aldrich
Gloves Rotiprotect Latex	Roth
Micro tubes 1,5ml/2.0 ml	Sarstedt
Nitrocellulose membranes BioTrace™ MT	Pall Life Sciences
PCR Thermo tubes 0.2 ml	Sarstedt
Petri dishes 94/16	Greiner Bio-One
Pipet tips (all sizes)	Sarstedt
Scalpels	Braun
Screw cap micro tubes 1.5 ml	Sarstedt
Semi-micro cuvettes	Sarstedt
Syringes 5 ml, 10 ml, 20 ml	Braun
Syringe filter Rotilabo® 0.45 µm	Roth
Whatman paper	Sartorius
Whatman filter No. 5	Sigma-Aldrich
96 well plate Lumitrac 600	Greiner Bio-One
96 well plates	Sarstedt

2.1.3 Chemicals

Table 2.3: List of chemicals used in this study.

Chemical	Manufacturer
Acetone	Fisher Chemicals
Acetic acid	Applichem
Ampicillin	Roth
Acrylamide (Rotiphorese® Gel 30)	Roth
Adenine	Roth
Ammonium persulphate	Roth
ATP (Adenosine triphosphate)	Roth
Bacto™ Peptone	Becton Dickinson
Bacto™ Agar	Becton Dickinson
Bacto™ Tryptone	Becton Dickinson
Bromophenol blue	Roth
BSA (Bovine serum albumine)	Roth
Coomassie brilliant blue G-250	Serva
Complete Protease Inhibitor Cocktail	Roche
Cycloheximide	Sigma Aldrich
D-Galactose	Roth
D-Glucose	Roth
D-Luciferin sodium salt	Roth
Dipotassium hydrogen orthophosphate	Roth
Disodium hydrogen phosphate	Genaxxon
DMF (Dimethyl formamide)	Acros Organics
DMSO (Dimethyl sulphoxide)	Acros Organics
DTT (Dithiothreitol)	Roth
EDTA (Ethylendiaminetetraacetic acid)	Roth
Ethanol	VWR
GelRed®	Genaxxon
Geldanamycin	Invivogen
GenAgaroseLE	Genaxxon
Glycerol	Roth
Glycine	Roth
Urea	Roth
Isopropanol	Acros Organics

Pepstatin A	Sigma Aldrich
Potassium chloride	Roth
Potassium dihydrogen phosphate	Roth
L-Alanine	Sigma Aldrich
L-Arginine	Sigma Aldrich
L.Asparagine	Sigma Aldrich
L-Aspartic acid	Sigma Aldrich
L-Cysteine	Sigma Aldrich
L-Glutamic acid	Sigma Aldrich
L-Glutamine	Sigma Aldrich
L-Histidine	Sigma Aldrich
L-Isoleucine	Sigma Aldrich
Lithium acetate	Sigma Aldrich
L-Leucine	Sigma Aldrich
L-Lysine	Sigma Aldrich
L-Methionine	Sigma Aldrich
L-Methionine ^{35}S labelled, 0.37 MBq/µl	Hartmann Analytics
L-Phenylalanine	Sigma Aldrich
L-Proline	Sigma Aldrich
L-Serine	Sigma Aldrich
L-Sorbitole	Sigma Aldrich
L-Threonine	Sigma Aldrich
L-Typtophane	Sigma Aldrich
L-Tyrosine	Sigma Aldrich
L-Valine	Sigma Aldrich
Magnesium acetate	Roth
Methanol	VWR
MG-132	Selleckchem
Milk powder	Roth
Myristic acid	Sigma Aldrich
NAD^+	Roth
Ni-NTA agarose	Qiagen
Phosphoric acid	Sigma
Rapamycin	Calbiochem
Sodium azide	Roth
Sodium chloride	Roth
Sodium dihydrogen phosphate	Roth
SDS	Roth
Sodium hydroxide	Roth

Nonidet® P-40	Sigma Aldrich
PageRuler™Prestained Protein ladder	Thermo Scientific
PEG 3350	Sigma Aldrich
Pepstatin A	Sigma Aldrich
Protein A Sepharose™ CL-4B	GE Healthcare
TEMED (N,N,N'N'-Tetramethyletylendiamine)	Merck
TCA (Trichloroacetic acid)	Roth
Tris (Tris(hydroxymethyl)aminomethane)	Roth
Triton X-100	Roth
Tween 20	Roth
Tween 40	Roth
Uracil	Roth
X-Gal	Roth
Yeast Nitrogen Base w/o amino acids	Becton Dickinson
Yeast Nitrogen Base w/o ammonium sulphate and w/o amino acids	Becton Dickinson

2.1.4 Buffers and solutions

Table 2.4: List of buffers and solutions used in this study.

Buffer/solution	**Composition**
SDS running buffer	25 mM Tris 192 mM Glycine 0.1 % (m/v) SDS
Blotting buffer	12 mM Tris 96 mM Glycine 20 % (v/v) Methanol 0.02 % (m/v) SDS
PBS-T buffer	140 mM NaCl 2.7 mM KCl 10 mM Na_2HPO_4 1.8 mM KH_2PO_4 0.1 % (v/v) Tween 20
TAE buffer	40 mM Tris/acetate (pH 7.5)

	2 mM EDTA
TE buffer	10 mM Tris/HCl (pH 7.5) 1 mM EDTA (pH 8.0)
SDS urea loading buffer	200 mM Tris/HCl (pH 6.8) 8 M Urea 5 % (m/v) SDS 100 mM EDTA 200 µg/ml Bromophenol blue 1 % (v/v) β-mercaptoethanol
Sorbitol buffer	0.7 M Sorbitol 50 mM Tris-HCl (pH 7.5)
6 x DNA loading buffer	40 mM Tris/acetate (pH 7.5) 2 mM EDTA 30 % (v/v) Glycerol 200 µg/ml Bromophenol blue
Bradford solution	100 mg/l Coomassie brilliant blue G-250 4.8 % (v/v) Ethanol 8.5 % (v/v) Phosphoric acid
IP buffer (Pulse Chase analysis)	50 mm Tris/HCl (pH 7.5) 190 mM NaCl 1.25 (v/v) Triton X-100 6 mM EDTA
BB1 buffer (Pulse Chase analysis)	50 mM Tris/HCl (pH 7.5) 6 M Urea 1 % (w/v) SDS 1 mM EDTA (pH 8.0)
Z-buffer (β-galactosidase filter assay)	16.1 g/l Na_2HPO_4 x $7H_2O$ 5.5 g/l NaH_2PO_4 x H_2O 0.75 g/l KCl 0.25 g/l $MgSO_4$ x 7 H_2O pH 7.0
X-Gal solution (β-galactosidase filter assay)	20 mg/ml X-Gal in DMF

2.1.5 Commercial Kits

Table 2.5: List of commercial kits used in this study.

Kit	Manufacturer
NucleoSpin® Gel and PCR Clean-up	Macherey-Nagel
GeneJET™ Plasmid Miniprep Kit	Thermo Scientific
Pierce® ECL Western blotting substrate	Thermo Scientific
Rapid DNA Ligation Kit	Thermo Scientific

2.1.6 Enzymes

Table 2.6. List of enzymes used in this study.

Enzyme	Manufacturer
Phusion High-Fidelity DNA Polymerase	Thermo Scientific
Velocity™ DNA Polymerase	Bioline
Taq DNA Ligase	NEB
Taq DNA Polymerase	Genaxxon
Shrimp alkaline phosphatase	Thermo Scientific
BamHI, EcoRI, EcoRV, SalI, SphI, SpeI, HpaI, NotI, DpnI, XhoI, XbaI, NheI with corresponding reaction buffers	NEB
Zymolyase-100T	MP Biomedicals

2.1.7 Oligonucleotides

Table 2.7. List of oligonucleotides used in this study.

Primer name	Sequence (5´ to 3´)	Description
p31xhopr.FP	GATGCTCGAGAGTTCAGTTTGTCATATAATTATGTTT	Amplification of XhoI-*HSP31*-EcoRI fragment including promoter and terminator.
P31ecoterm.RP	GATGGAATTCAGCTCACTAAGATGCAAATAAC	Amplification of XhoI-*HSP31*-EcoRI fragment including promoter and terminator.
FP NLS	ATTCGCATGCATGATCCCAAAAAAGAAGCGTAAAGTTATCTCATTGCAAAGACCGTTGG	N-terminal insertion of NLS sequence into pIA1 and pIA3.
FP NES	ATTCGCATGCATGATCAATATTAATGAATTGGCTTTGAAATTTGCTGGTTTGGATTTGATCTCATTGCAAAGACCGTTGG	N-terminal insertion of NES sequence into pIA1 and pIA3.
Rp NES/NLS	TTGTAGGATTTGACTTCACCAGC	N-terminal insertion of NLS/ NES sequences into pIA1 and pIA3.
termHpaIFP	ACTGTTAACTAAACTACTGAATTCGCGCCACTTCT	Amplification of HpaI-*CPY*Term.-SpeI for generating pIA19.
SpeFPTerm	GCTGCATACTAGTGAATTCGCGCCACTTCTAA	Amplification of SpeI-*CPY*Ter.-SpeI for generating pIA20-21.
SpeRPTerm	GCTGCATACTAGTGGATCCCCCGGGCT	Amplification of HpaI/SpeI-*CPY*Term.-SpeI for generating pIA19-21.
CPYHpaFP	GACTGTTAACATGATCTCATTGCAAAGACCG	Amplification of *ΔssCPY** for generating pIA19-21.
CPYSpeRP	GACTACTAGTTTAATTAACCATACTTAAGGCGTTTTC	Amplification of *ΔssCPY** for generating pIA20-21.
CPYHpaRP	GACTGTTAACATTAACCATACTTAAGGCGTTTTC	Amplification of *ΔssCPY** for generating pIA19-21.
Mut NLS1	PO_4-GACGAATATGAAGATGAAGTTGATTCAACTAAAGCATGCTCTGCTACTGATTCTGAAAATGAGGAGGAATCTGAAGGAAC	Mutagenesis of part 1 of NLS of San1.
Mut NLS2	PO_4-TTCTGAAAATGAGGAGGAATCTGAAGGAACTAGTCAATCTAAGGATAATGAAGGTGCGCCCC	Mutagenesis of part 2 of NLS of San1.

	TACGCACAACC	
San1 C257S Mut	PO_4 - CTCACCAATCAAGTTACCTTCTGGCCACATTTTTGGGAGG	Mutagenesis of RING domain of San1.
FP ubarg	AGACATGCATGCATGCAGATTTTCGTCAAGAC	Generation of ΔssCL*myc N-terminally fused to UbArg.
Rpubarg	AGACATGCATGCTCTACCACCTCTTAGCCTTAG	Generation of ΔssCL*myc N-terminally fused to UbArg.
UbIlepFE15	PO_4 - GTGCTAAGGCTAAGAGGTGGTATCGCATGCATGATCTCATTGCAAAG	Substitution of Arg by Ile using plasmid pIA11.
FpdelYap1	TTGCCACCCAAAACGTTTAAAGAAGGAAAAGTTGTTTCTTAAACCCAGCTGAAGCTTCGTACGC	Deletion of gene *YAP1*.
RPdelYap1	AGAAAAAGTTCTTTCGGTTACCCAGTTTTCCATAAAGTTCCCGCTGCATAGGCCACTAGTGGATCTG	Deletion of gene *YAP1*.
A Yap1	TCTTCGCATAAAACGCATG	Control primer for checking *YAP1* deletion.
B yap1	ATTTGGTGAAGGTAATTGTTTC	Control primer for checking *YAP1* deletion.
GD PRA1 pUG6 FW	CTAGTATTTAATCCAAATAAAATTCAAACAAAAACCAAAACTAACCAGCTGAAGCTTCGTACGC	Deletion of gene *PEP4*.
GD PRA1 pUG6 Re	TAGATGGCAGAAAAGGATAGGGCGGAGAAGTAAGAAAAGTTTAGCGCATAGGCCACTAGTGGATCTG	Deletion of *PEP4*.
DisPep4 checkA	GTAATTCGCTGCTATTTA	Control primer for checking *PEP4* deletion.
Dis Pep4 checkB	GGAGTACCCAAAGTAATG	Control primer for checking *PEP4* deletion.
Forw UBR1 dis	TCCCTAATCTTTACAGGTCACACAAATTACATAGAACATTCCAATCAGCTGAAGCTTCGTACGC	Deletion of gene *UBR1*.
Rev UBR1 dis	TATATACAAATATGTCAACTATAAAACATAGTAGAGGGCTTGAATGCATAGGCCACTAGTGGATCTG	Deletion of gene *UBR1*.
UBR1 B Verific	GCACACAAGTATCATCGCAACC	Control primer for checking *UBR1* deletion.
UBR1 A	ACCATAAGGCAACTACCCAG	Control primer for checking *UBR1*

		deletion.
PD1forw (J. Jureschke**)**	CCGTCTAGACGGTCTGCCCCTAAGAAGATC	Amplification of XbaI-*LEU2mycCPY*Term.-SalI for generating pIA13.
RpTerLeumyc	TCGCGTCGACGGATCCCCCGGGCTG	Amplification of XbaI-*LEU2mycCPY*Term.-SalI for generating pIA13.
XbaPrCPYFP	ATGATCTCTAGAATCGATTTCCGTATATGATG ATAC	Amplification of XbaI-*CPY*Prom.-XbaI for generating pIA13.
XbaPrRP	ATGATCTCTAGACATGCATGCAGCGTATG	Amplification of XbaI-*CPY*Prom.-XbaI for generating pIA13.
Ubr1C1220S	PO_4 - TGAATCGGAGGATTTTACCAGTGCACTATGT CAAGATTCCAGTTCG	Mutagenesis of the RING domain of Ubr1.

2.1.8 Plasmids

Table 2.8: List of plasmids used in this study.

Name	Marker gene	Description/genotype	Source/reference
pRS316	*URA3*	Empty CEN plasmid	(Sikorski and Hieter, 1989)
pRS313	*HIS3*	Empty CEN plasmid	(Sikorski and Hieter, 1989)
pRS424	*TRP1*	Empty 2µ plasmid	(Christianson *et al*, 1992)
pRS426	*URA3*	Empty 2µ plasmid	(Christianson *et al*, 1992)
YEPlac181	*LEU2*	Empty 2µ plasmid	(Gietz and Sugino, 1988)
pFE15	*URA3*	pRS316-*ΔssCPY*LEU2myc*	(Eisele and Wolf, 2008)
pSK007	*URA3*	pRS316-*GAL4-CTL*myc*	(Kohlmann *et al*, 2008)
pRBUBR1	*LEU2*	YEPlac181-*ADH1-UBR1HA*	(Xia *et al*, 2008)
pRB208 IMI	*LEU2*	YEPlac181-*ADH1-UBR1HA(D176E)*	(Xia *et al*, 2008)
pRB208IIMI	*LEU2*	YEPlac181-*ADH1-UBR1HA(P406E)*	(Xia *et al*, 2008)
pIA5	*LEU2*	YEPlac181-*ADH1-UBR1HA(D176E, P406S)*	This study
pIA7	*TRP1*	pRS424-*ADH1-*	This study

		UBR1HA(D176E)	
pIA8	*TRP1*	pRS424-*ADH1-UBR1HA (P406S)*	This study
pIA9	*TRP1*	pRS424-*ADH1-UBR1HA (D176S, P406S)*	This study
pIA6	*TRP1*	pRS424-*ADH1UBR1HA*	This study
pIA10	*TRP1*	pRS424-*ADH1-UBR1HA(C1220S)*	This study
pIA11	*URA3*	pRS316-*UbArg ΔssCL*myc*	This study
pIA12	*URA3*	pRS316-*UbIle ΔssCL*myc*	This study
pBARUPR	*TRP1*	pRS314-*CUP1-DHFR-HA-Ub-Arg-URA3HA*	(Xia *et al*, 2008)
pUB23-R	*URA3*	Yep24-*GAL1-Ub-Arg-βGal*	(Bachmair *et al*, 1986)
pIA1	*HIS3*	pRS313- *ΔssCL*myc*	This study
pIA13	*URA3*	pRS316-*LEU2myc*	This study
pIA14	*URA3*	pRS316-*GAL1-LUC-LEUmyc*	Mona Kavan (Bachelor thesis 2012)
pIA15	*URA3*	pRS316-*GAL1-LUCDM-LEUmyc*	Mona Kavan (Bachelor thesis 2012)
pIA2	*URA3*	pRS316-*ΔssCPY*LEU2myc (Δ16-204)*; (F1 ΔssCPY*LEU2myc)	Marc Harjung (Bachelor thesis 2011)
pIA3	*URA3*	pRS316-*ΔssCPYLEU2myc (Δ16-398*); (F2 ΔssCPY*LEU2myc)	Marc Harjung (Bachelor thesis 2011)
pIA4	*URA3*	pRS316-*ΔssCPY*LEU2myc (Δ16-585)*; (F3 ΔssCPY*LEU2myc)	Marc Harjung (Bachelor thesis 2011)
pSK146	*URA3*	pRS316-*GAL1-SAN1V5*	(Prasad *et al*, 2010)
pIA16	*URA3*	pRS316-*GAL1-SAN1V5(-NLS)*	This study
pIA17	*URA3*	pRS316-*GAL1-SAN1V5(-NLS) (C257S)*	This study
pIA26	*URA3*	pRS316-*GAL1-SAN1V5(C257S)*	This study
pIA19	*URA3*	pRS316-*ΔssCPY**	This study
pIA20	*URA3*	pRS316- *ΔssCPY* x2*	This study
pIA21	*URA3*	pRS316- *ΔssCPY* x 3*	This study
pIA22	*HIS3*	pRS313- *NLS-ΔssCl*myc*	This study
pIA23	*HIS3*	pRS313-*NES-ΔssCL*myc*	This study

pIA24	*HIS3*	pRS313-*NLS-F2ΔssCl*myc*	This study
pIA25	*HIS3*	pRS313-*NES-F2ΔssCL*myc*	This study
pIA30	*URA3*	pRS426-*HSP31*	This study
pUG6	*KANMX*	Insert*: loxP-KANMX-loxP*	(Gueldener *et al*, 2002)
pUG27	*his5+*	Insert*: loxP-his5+-loxP*	(Gueldener *et al*, 2002)
pSH47	*URA3*	Insert*: GAL1-Cre*	(Gueldener *et al*, 2002)
pSH63	*TRP1*	Insert*: GAL1-Cre*	(Gueldener *et al*, 2002)
pJD421	*LEU2*	YEplac181-*His6-Ub*	(Dohmen *et al*, 1995)
pIA18	*URA3*	YEplac195-*His6-Ub*	Derrick Norell (Diploma thesis 2011)

2.1.9 Antibodies

Table 2.9: List of antibodies used in this study.

Antibody	Used dilution	Details	Source/manufacturer
Mouse anti-c-Myc	1.5000	Monoclonal, Clone 9E10, sc-40, IgG_1	Santa Cruz
Mouse anti-HA	1:2500	Monoclonal, clone 16B12, IgG_1	Covance
Mouse anti-V5	1:10000	Monoclonal, clone E10/V4RR, IgG_1	Thermo Scientific
Mouse anti-CPY	1:10000	Monoclonal, clone 10A5, IgG_1	Invitrogen
Rabbit anti-CPY	1:5000	polyclonal	Rockland
Rabbit anti-Fas	1:10000	polyclonal	(Egner *et al*, 1993)
Mouse anti-His_5	1:2000	Monoclonal, IgG_1	Qiagen
Mouse anti-PGK	1.10000	Monoclonal, clone 22C5	Molecular Probes
Mouse anti-rabbit	1.10000	Secondary antibody, monoclonal, clone RG-96, HRPO-conjugated	Sigma Aldrich
Goat anti-mouse	1:10000	Secondary antibody, AffiniPur Goat Anti-	Jackson Immuno Research Laboratories

		mouse IgG (H+L), HRPO conjugated	

2.1.10 Growth media

All the different media described in Tab. 2.10 were prepared using ultra pure water and were afterwards autoclaved.

For plasmid selection in *E. coli* the LB medium was supplemented with 100 µg/ml ampicillin. Depending on the yeast selection conditions the CM medium prepared as described in Tab. 2.10 has to be supplemented with 0.3 mM L-histidine, 1.7 mM L-leucine, 1 mM L-lysine, 0.4 mM L-tryptophan, 0.3 mM adenine and 0.2 mM uracil. The YPD medium was supplemented with 200 µg/ml G418 (Geneticin) for selection for the *KANMX* marker gene. For growth of yeast strains defective in the *FAS1* and/or the *FAS2* gene(s) the used media (YPD, CM) were supplemented with 0.03 % myristic acid and 1 % Tween 40.

Solid medium contained in addition 2 % (m/v) Bacto® agar.

Table 2.10: List of the growth media used in this study.

Medium	Description	Composition
LB	Complete medium for bacteria	5 g/l NaCl 10 g/l Bacto®tryptone 5 g/l Bacto®Yeast extract
YPD	Complete medium for yeast	20 g/l Bacto® peptone 10 g/l Bacto®Yeast extract 2 % (m/v) D-Glucose
SOC	Complete medium for bacteria (for stressed cells)	10 g/l Bacto®tryptone 5 g/l Bacto®Yeast extract 4 g/l D-Glucose 10 mM NaCl 10 mm $MgCl_2$ 10 mM $MgSO_4$
CM	Complete minimal medium for yeast (selection medium)	0.67 % (w/v) Yeast nitrogen base w/o amino acids

		20 g/l D-Glucose 0.0117 % (w/v) L-Alanine, L-Arginine, L-Asparagine, L-Asparatic acid, L-Glutamic acid, L-Lysine, L-Methionine, L-Phenylalanine, L-Serine, L-Threonine, L-Tyrosine, L-Valine, myo-Inositole 0.00117 % 4-Aminobenzoic acid
Labelling medium	Selection medium without L-Methionine for Pulse Chase experiments	1.7 g/l Yeast nitrogen base w/o Ammonium sulphate and w/o amino acids 1 g/l D-Glucose 20 mg/l L-Adenine, L Tryptophan, L-Histidine 30 mg/l L-Arginine, L-Tyrosine, L-Lysine 50 mg/l L-Phenylalanine 100 mg/l L-Glutamic acid, L-Asparatic acid 150 mg/l L-Valine 200 mg/l L-Threonine 400 mg/l L-Serine
Chase medium	Like Labelling medium but with L-Methionine	See Labelling medium plus: 6 g/l L-Methionine 2 g/l BSA

2.1.11 *S. cerevisiae* strains

Table 2.11: List of yeast strains used in this study.

Name	Genotype	Source/reference
W303-1Ca	*Mat a ade2-1 ura3-1 his3-11,15 leu2-3,112 trp1-1 can1-100 prc1-1*	(Knop *et al*, 1996a)

W303-1B	*Mat α ade2-1 ura3-1 his3-11,15 leu2-3,112 trp1-1 can1-100*	(Chiang and Schekman, 1991)
W303ΔC	*Mat α ade2-1 ura3-1 his3-11,15 leu2-3,112 trp1-1 can1-100 Δprc1::LEU2*	(Plemper *et al*, 1999)
YPH499	*Mat α ade2-101 ura3-5 his3-Δ20 leu2-Δ1 trp1Δ lys2-801*	(Ghislain *et al*, 1993)
Δubr1	W303-1Ca *Δubr1::loxP*	Frederik Eisele
Δsan1	W303-1Ca *Δsan1::KANMX*	Frederik Eisele
Δubr1Δsan1	W303-1Ca *Δubr1::HIS5 Δsan1::KANMX*	Frederik Eisele
Δubc2/rad6	W303-1Ca *Δubc2::KANMX*	This study
Δyap1	W303-1Ca *Δyap1::HIS5*	This study
Δubr1Δyap1	W303-1Ca *Δubr1::loxP Δyap1::HIS5*	This study
Δhsp32	W303-1Ca *Δhsp32::HIS5*	This study/ Derrick Norell
Δhsp32Δhsp33	W303-1Ca *Δhsp32::loxP Δhsp33::loxP*	This study/ Derrick Norell
***Δhsp31Δhsp32Δhsp33* (*Δhsp31-33*)**	W303-1Ca *Δhsp31::loxP Δhsp32::loxP Δhsp33::loxP*	This study/ Derrick Norell
***Δubr1 Δhsp31Δhsp32Δhsp33* (*Δubr1Δhsp31-33*)**	W303-1Ca *Δhsp31::loxP Δhsp32::loxP Δhsp33::loxP Δubr1::loxP*	This study
Δyap1 Δhsp31Δhsp32Δhsp33	W303-1Ca *Δhsp31::loxP Δhsp32::loxP Δhsp33::loxP Δyap1::HIS5*	This study
Δpep4 Δhsp31Δhsp32Δhsp33	W303-1Ca *Δhsp31::loxP Δhsp32::loxP Δhsp33::loxP Δpep4;;HIS5*	This study
Δpep4	W303-1Ca *Δpep4::HIS5*	This study
Δubr1Δpep4	W303-1Ca *Δubr1::loxP Δpep4:: HIS5*	Frederik Eisele
Δubr1Δhsp31Δhsp32Δhsp33 Δpep4	W303-1Ca *Δhsp31::loxP Δhsp32::loxP Δhsp33::loxP Δubr1::loxP Δpep4::HIS5*	This study
Δder3/hrd1	W303-1B *Δprc1::LEU2 Δder3/hrd1::HIS3*	Sonja Kohlmann
SSA1Δssa2Δssa3Δssa4	W303-1Ca *Δprc1-1::loxP Δssa2::loxp Δssa3::loxP Δssa4::loxP*	Frederik Eisele

ssa1-45^{ts} Δssa2Δssa3Δssa4	W303-1Ca *ssa1-45^{ts} Δprc1-1::loxP Δssa2::loxp Δssa3::loxP Δssa4::loxP*	Frederik Eisele
Δubr1 ssa1-45^{ts} Δssa2Δssa3Δssa4	W303-1Ca *ssa1-45^{ts} Δprc1-1::loxP Δssa2::loxp Δssa3::loxP Δssa4::loxP Δubr1::loxP*	This study
Δfas1	W303-1B *Δfas1::HIS5*	(Scazzari *et al*, 2015)
Δubr1Δfas1	W303-1Ca *Δubr1::loxP Δfas1::HIS5*	(Scazzari *et al*, 2015)
Δfas1 FAS2-TAP	W303-1B *Δfas1::HIS5 FAS2-TAP-TRP1*	(Scazzari *et al*, 2015)
FAS2-TAP	W303-1B *FAS2-TAP-TRP1*	(Scazzari *et al*, 2015)
cdc48ts (T413) Δfas1	W303-1B *cdc48^{ts} Δfas1::HIS5*	(Scazzari *et al*, 2015)
SSA1Δfas1	W303-1A *Δssa2::loxp Δssa3::loxP (1-1126) Δssa4::loxP Δprc1::LEU2 Δfas1::HIS5*	(Scazzari *et al*, 2015)
ssa1-45^{ts} Δfas1	W303-1A *ssa1-45^{ts} Δssa2::loxp Δssa3::loxP (1-1126) Δssa4::loxP Δprc1::LEU2 Δfas1::HIS5*	(Scazzari *et al*, 2015)
CIM3Δfas1	YPH499 *Δfas1::HIS5*	(Scazzari *et al*, 2015)
cim3-1Δfas1	YPH499 *cim3-1 Δfas1:HIS5*	(Scazzari *et al*, 2015)
Δfas1Δfas2	W303-1B *Δfas1::loxP Δfas2::HIS5*	(Scazzari, 2013)
uba1-204	W303-1B *UBA1::KANMX* [pRS313-*uba1-204-HIS*]	(Ghaboosi and Deshaies, 2007)
UBA1	W303-1B *UBA1::KANMX* [pRS313-*UBA1-HIS*]	(Ghaboosi and Deshaies, 2007)

2.1.12 *E. coli* strains

Table 2.12. List of *E. coli* strains used in this study.

Name	Genotype	Source/reference
***Escherichia Coli* DH5α**	F$^-$ ϕ80*lac*ZΔM15 Δ(*lac*ZYA-*arg*F)U169 *rec*A1 *end*A1 *hsd*R17 (r_{k^-}, m_{k^+}) *pho*A *sup*E44 *thi*-1	Invitrogen

	*gyr*A96 *rel*A1 λ$^-$	

2.2 Methods

2.2.1 Cell culture and cell biological methods

2.2.1.1 Growth conditions for *S. cerevisiae* cells

All *S. cerevisiae* strains were grown at 30 °C either in liquid medium in Erlenmeyer flasks or on agar plates except temperature-sensitive yeast strains which were grown for restrictive conditions at 37 °C. The growth of *S. cerevisiae* was monitored by photometric measurement at 600 nm (OD_{600}). An OD_{600} value of 1.0 corresponds to a cell density of approximately 2 x 10^7 cells/ml. For long time storage of yeast strains, the cells were kept in 15 % glycerol at -80 °C.

2.2.1.2 Growth conditions for *E. coli* cells

E. coli cells were generally grown at 37 °C in LB medium. Cells transformed with plasmids were grown in LB medium supplemented with ampicillin for plasmid selection. The growth was also monitored by photometric measurement at 600 nm. For long time storage, bacterial cells were kept in 60 % glycerol at -80 °C.

2.2.1.3 Growth tests on agar plates

For monitoring the viability of yeast strains on certain conditions or monitoring the steady state levels of proteins fused to an auxotrophic marker and expressed in yeast, growth tests on agar plates were performed. 5 ml of yeast cultures were prepared and grown overnight. After measuring the OD_{600} values, each strain was diluted with ddH_20 to an OD_{600} of 1.0. According to Fig. 2.1 a 1:5 serial dilution row of each cell solution was prepared and pipetted into a 96 well plate. Equal amounts of the dilutions of the different strains were spotted on corresponding agar plates using a metal stamp. The plates were afterwards incubated at defined conditions for 2 to 5 days. If not otherwise indicated all the agar plates used in this study contained glucose as carbon source.

Each growth test experiment in this study was performed at least three times.

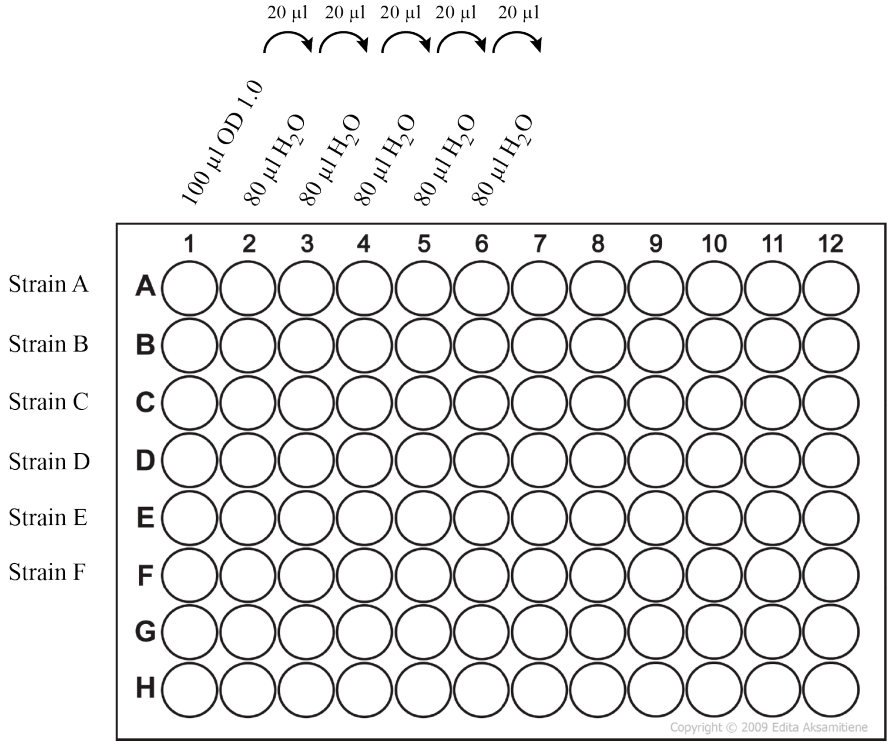

Figure 2.1: Pipetting instructions for growth tests using 96 well plates. Overnight cultures of the strains of interest were diluted to an OD_{600} of 1.0 with ddH_2O and pipetted in the first column of a 96 well plate (#1). Serial 1:5 dilutions were prepared in the columns #2 to #6 using ddH_2O. Equal amounts of the different dilutions were spotted onto agar plates using a metal stamp.

2.2.2 Molecular biological methods

2.2.2.1 Agarose gel electrophoresis

Agarose gel electrophoresis is a method for separation of DNA by size. The separation is achieved by migration of the negatively charged DNA through an agarose matrix in an applied electric field. Smaller DNA fragments migrate faster.
For preparation of a 1 % (m/v) agarose gel, 1 g agarose was dissolved in 100 ml TAE buffer. For staining the DNA GelRed® was added to the buffer in a dilution of 1:40,000. The electrophoresis was conducted at constant voltage (120 V) and run for 30 min. TAE buffer was used as running buffer. For size estimation of the separated DNA 1 µl of a 1 kb ladder (Roth) was pipetted into one pocket of the gel. DNA samples were prepared by adding DNA loading buffer containing glycerol and bromophenol blue. After separation of the DNA fragments the bands were visualized using the Gel Imaging System Quantum (Peqlab).

2.2.2.2 Plasmid isolation from *E. coli*

For plasmid isolation, 5 ml LB (+Amp) medium were inoculated with the plasmid containing *E. coli* strain. After approximately 16 h of growth at 37 °C the plasmid DNA was isolated using the GeneJET™ Plasmid Miniprep kit according to the instructions of the manufacturer.

2.2.2.3 Extraction of DNA fragments from agarose gels

For DNA gel extraction the commercial kit NucleoSpin® Gel and PCR Clean-up (Macherey-Nagel) was used according the manufacturer's protocol.

2.2.2.4 Polymerase chain reaction (PCR)

Polymerase chain reaction is a technique for amplification of defined stretches of DNA. The PCR needs several components listed in Tab.2.13.

Tab. 2.13: Description of the standard components of a PCR reaction.

PCR component	Function
Template	Original DNA which contains the DNA stretch to be amplified.
Primer	Two short oligonucleotides which define the beginning and the end of the DNA stretch to be amplified.
DNA polymerase	Heat stable enzyme which assembles a new DNA strand by using nucleotides as DNA-building blocks and single-stranded DNA as template.
Deoxynucleoside triphosphates (dNTPs)	The 4 dNTPs (dATP, dTTP, DGTP, dCTP) serve as DNA-building blocks.
Mg^{2+} ions	Essential for proper DNA-Polymerase function.

A typical PCR program consists of 3 basic steps which are repeated in the PCR reaction 25 to 30 times. The steps are itemized and described in Tab. 2.14.

Table 2.14: Description of the standard PCR reaction steps.

PCR step	Function	Temperature
Denaturation	Melting of double-stranded DNA.	94-98 °C
Primer annealing	Binding of the two primers to the single-stranded DNA.	50-60 °C
Elongation	DNA polymerase assembles the new DNA strand complementary to the template strand.	72 °C

The exact program depends on the used polymerase, the used primer pair and the length of the DNA stretch to be amplified. It was defined according to the instruction manual of each polymerase. The pipetting instruction of a PCR reaction using the Phusion polymerase is listed in Tab. 2.15.

Table 2.15: Pipetting instructions of a standard PCR reaction using Phusion DNA polymerase.

Component	**Volume [µl]**
Template DNA	1 µl
Polymerase buffer (5 x)	10 µl
dNTPs (10 mM)	1 µl
Primer forward (10 µl)	2.5 µl
Primer reverse (10 µl)	2.5 µl
Phusion High Fidelity Polymerase	0.5 µl
ddH_2O	Add to 50 µl

2.2.2.5 DNA purification after PCR and other enzymatic reactions

Purification of PCR products or DNA which was cut with restriction enzymes is necessary for removal of salts and enzymes which may inhibit downstream reactions like ligation reactions or transformations. For this purpose the NucleoSpin® Gel and PCR Clean-up kit (Macherey-Nagel) was used according to the manufacturer's protocol.

2.2.2.6 Restriction digest of DNA

Restriction enzymes are enzymes which cut double-stranded DNA. They recognize a specific nucleotide sequence of about 4 to 8 nucleotides in length.
A preparative digestion was performed for cloning linear DNA fragments into plasmids. For this application plasmid DNA and linear DNA derived from PCR were used for digestion.

After restriction digest the DNA was purified using the NucleoSpin® Gel and PCR Clean-up (Macherey-Nagel) kit before performing a ligation reaction.
Analytical digestions were performed to check the identity of a plasmid. 1 µl of a plasmid preparation was used for this kind of restriction digest.
All reactions were performed in a total volume of 20 µl. 5 U of each restriction enzyme were used. All reaction mixtures were incubated at 37 °C for 30 -60 min.

2.2.2.7 Dephosphorylation of digested plasmids

Dephosphorylation of digested plasmids before cloning is important for preventing self-ligation of the plasmid. This may happen if the vector is cut with a single restriction enzyme. In this situation the chance for plasmid religation is much higher than for insertion of a DNA fragment cut with the same enzyme.
For the dephosphorylation reaction Shrimp alkaline phosphatase (Thermo Scientific) was used according to the manufacturer's manual. After dephosphorylation, the vector was purified using the NucleoSpin® Gel and PCR Clean-up kit.

2.2.2.8 Ligation

DNA ligases are enzymes which catalyse the joining of two DNA fragments under consumption of ATP. A DNA ligase forms a new phosphodiester bond between the 3´-hydroxyl end of one nucleotide and the 5´-phosphate end of another.
In this work the Rapid ligation Kit was used containing T4-ligase. The ligation reaction was performed according the manufacturer's protocol. The ligation mixture was directly used for transformation of *E. coli* DH5α cells.

2.2.2.9 Transformation of *E. coli*

For each transformation 0.5 µl of purified plasmid DNA or 10 µl of a ligation mixture were used. 50 µl of competent *E. coli* DH5α cells were thawed on ice and carefully mixed with the DNA to be transformed. After incubation on ice for 30 min the transformation mixture was incubated for 30 s at 42 °C for heat shock followed by a 2 min incubation step on ice. Then 950 µl of prewarmed SOC medium were added and the cells were incubated at 37 °C for 1 h. Finally, the cells were spread onto LB plates containing ampicillin. The plates were incubated overnight at 37 °C.

2.2.2.10 Transformation of *S. cerevisiae*

For transformation of plasmids or deletion cassettes into yeast cells, the lithium acetate method was used (Gietz and Woods, 2002). An exponentially growing 50 ml yeast culture was harvested (3000 rpm, 3 min) and washed once with 10 ml ddH_2O. The cells were then resuspended in 1 ml ddH_2O and transferred to a 1.5 ml micro tube. The cells were washed with 1 ml LiAc/TE solution and finally resuspended in 200 µl LiAc/TE solution.
For each transformation reaction 50 µl of competent cells were used. The cells were first mixed with 5 µl pre-boiled and ice-chilled carrier DNA (Heringsperm ssDNA; Roche). Then the DNA to be transformed was added (2 µg of deletion cassettes or 200 ng of purified plasmids). 300 µl of a LiAc/TE/PEG solution were added before incubation at 30 °C for 30 min. Afterwards, the cells were incubated at 42 °C for 15 min. Finally, the cells were washed once with 800 µl ddH_2O, resuspended in 100 µl ddH_20 and spread on corresponding selection plates. The plates were incubated at 30 °C for 3-5 days.

Required solutions:

LiAc/TE: 1 x TE
100 mM Lithium acetate

LiAc/TE/PEG: 1 x TE
100 mm Lithium acetate
40 % (v/v) PEG

2.2.2.11 Deletion of *S. cerevisiae* genes

For deletion of non-essential yeast genes a method based on homologous recombination was used. In a first step a disruption cassette was amplified via a PCR reaction using primers designed according to the instruction published in (Gueldener *et al*, 2002). As template, different plasmids were used dependent on the desired marker gene. A schematic overview of the method is shown in Fig. 2.2.

In a second step 5 µg of each purified disruption cassette were transformed into the corresponding yeast strain using the method described in section 2.2.2.10.

The correct integration of the deletion cassette into the yeast genome was checked via PCR using oligonucleotides which specifically anneal to different regions in the genome, either to flanking regions of the gene to be deleted or to regions in between the ORF or to regions in between the marker gene (Fig. 2.2).

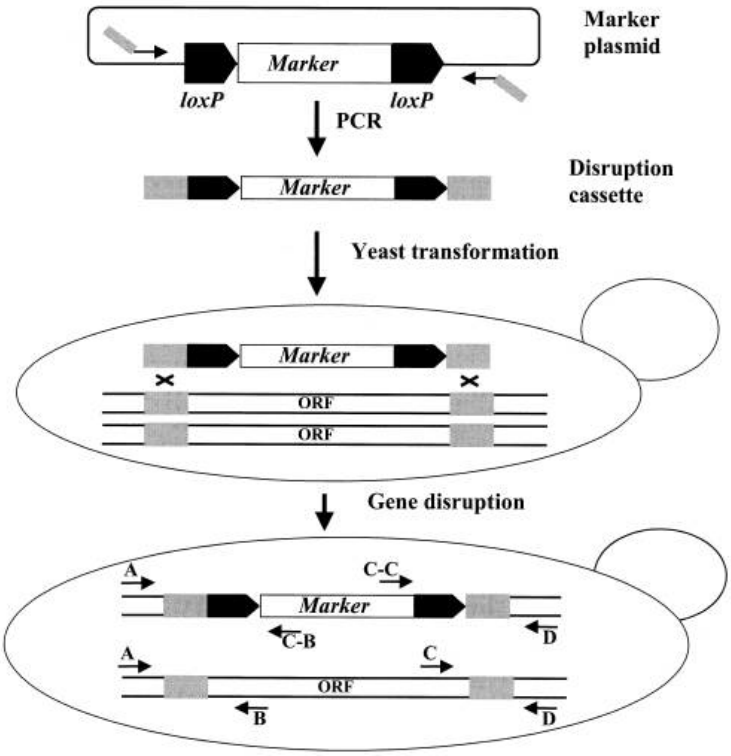

Figure 2.2: Procedure of gene disruption via homologous recombination. In a first step a disruption cassette is generated via a PCR using marker gene-specific plasmids as template and oligonucleotides complementary to both the marker plasmids and to 45 base pairs upstream and downstream of the target gene (ORF). After transformation of the disruption cassette into yeast, transformants are checked for correct cassette integration via colony PCR using primers specific to the gene to be deleted and primers specific to the used marker gene. Figure: (Gueldener *et al*, 2002).

Since the number of marker genes is restricted the marker genes can be removed from the genome for further reuse with help of the Cre recombinase system. The deletion cassettes amplified as shown in Fig. 2.2 also contain *loxP* recognition sites flanking each marker gene (Fig. 2.2). These sites are recognized by the Cre recombinase. This enzyme causes recombination between the *loxP* sites resulting in removal of the marker gene. For marker rescue the plasmids pSH47 or pSH63 were used both encoding the Cre recombinase which is expressed under control of the *GAL1* promoter. After expression of the Cre recombinase using galactose-containing medium, a dilution series of corresponding yeast culture was prepared and afterwards plated out on YPD plates. In order to check the presence of a marker gene in the genome, the YPD plates were replica-plated on corresponding selection plates.

2.2.2.12 Site-directed mutagenesis

This method was used in order to introduce point mutations, deletions ore additional bases into plasmid DNA. In the first step a 5´-phosphorylated primer was designed containing the desired mutation in approximately the middle of the sequence and possessing a melting temperature of more than 75 °C and in addition, one or more C/G bases at the 3´ terminus. Then a PCR reaction was performed using Phusion polymerase. The PCR reaction mixture also contained the heat stable Taq ligase. The Taq ligase in the PCR reaction leads to immediate linkage of the ends of the amplified linear plasmid DNA resulting in a circular DNA molecule. The components used in the mutagenesis PCR were listed in Tab. 2.16.

Table 2.16: Pipetting instructions of a PCR reaction mixture for site-directed mutagenesis.

Component	Volume
Template (plasmid)	1 µl
5 x Polymerase buffer	10 µl
dNTPs (10 mM)	1 µl
Mutagenesis primer (10 µM)	1 µl
NAD^+ (5 mM)	10 µl
Phusion High Fidelity Polymerase	1 µl
Taq Ligase	1 µl
ddH_2O	To 50 µl

In order to remove the non-mutated template plasmid DNA, the reaction mixture was digested with the restriction enzyme DpnI. This enzyme has the property to digest only methylated DNA. This modification does not occur during PCR reactions because of the use of non-methylated dNTPs as DNA building blocks. Therefore, only the template plasmid DNA isolated from *E. coli* DH5α is cleaved. After 2 h of digestion the DNA was purified using the NucleoSpin® Gel and PCR Clean-up (Macherey-Nagel) kit and transformed into *E. coli* DH5α. The next day 5 ml LB (+Amp) cultures of several transformants were prepared. To check for successful mutagenesis the isolated plasmids were sent for sequencing.

2.2.3 Methods in protein biochemistry

2.2.3.1 Lysis of yeast cells

In order to check the expression of proteins in different yeast strains 5 ml overnight cultures were prepared. The next day, 1.5 ml of each yeast culture were harvested in a 1.5 ml micro tube (5000 rpm, 1 min). The supernatant was discarded and the pellet was resuspended in 300 µl of 50 mM KH_2PO_4/K_2HPO_4 buffer. After addition of 100 µl 50 % TCA and subsequent vortexing, each suspension was incubated at – 80 °C for at least 1 h. After lysis and protein precipitation respectively, the pellet was washed once with 100 % acetone and dried at 37 °C. Finally, the pellet was dissolved in 50 µl SDS urea loading buffer containing 1 % β-mercaptoethanol for subsequent SDS-PAGE followed by Western blotting and immunodetection.

2.2.3.2 Sodium dodecyl sulphate polyacrylamide gel electrophoresis (SDS-PAGE)

In biochemistry, SDS-PAGE is used for separation of proteins by size. The gel matrix is composed of polyacrylamide. In addition, the matrix contains the anionic tenside SDS which binds to proteins, causes their linearization and imparts a negatively charge to the proteins. β-mercaptoethanol in the SDS urea loading buffer causes a reduction of disulphide bonds in the protein structure.

In this study, only discontinuous SDS-PAGE was performed which means that the polyacrylamide matrix consists of two different gel types each possessing different pH values. The stacking gel is buffered to a pH of 6.8, and the separation gel to a pH 8.8. This causes a better resolution and sharpness of the protein bands (Laemmli, 1970).

In most of the performed experiments an 8 % separation gel was used. The recipe for the preparation of stacking and separation gels is shown in Tab. 2.17. The polymerization reactions were initiated by addition of APS and TEMED. First, the separation gel was

prepared (Tab. 2.17). After pouring the not yet polymerized separation gel solution in between two glass plates fixed in the SDS gel casting stand each gel was immediately covered with 300 µl isopropanol. After polymerization of the separation gel the isopropanol was discarded and the stacking gel was prepared. After pouring the stacking gel on top of the separation gel (Tab. 2.17) a comb was inserted carefully. After polymerization of the stacking gel the comb was removed and the gel was assembled and placed into a SDS-PAGE chamber before filling up with SDS running buffer. 5 to 20 µl of the protein samples were loaded onto the SDS-PAGE gel. For size estimation of the separated proteins also 1.5 µl of the PageRuler™Prestained Protein ladder (Thermo Scientific) were loaded. For each gel, a constant current of 30 mA was applied. Each SDS-PAGE was run until the bromophenol blue front has reached the bottom of the gel.

Table 2.17: Composition of the stacking gel and separation gel solutions used in SDS-PAGE.

Component	Stacking gel (4 %; 10 ml)	Seperation gel (8 %; 10 ml)
1 M Tris-HCl pH 6.8	1.25 ml	-
1 M Tris-HCl pH 8.8	-	2.5 ml
10 % (m/v) SDS	100 µl	100 µl
DdH_2O	7.35 ml	4.7 ml
30 % (m/v) acrylamide	1.3 ml	2.7 ml
10 % (m/v) APS	100 µl	100 µl
TEMED	10 µl	5 µl

2.2.3.3 Western blot and immunodetection

A Western Blot is defined as the transfer of proteins which were separated before via SDS-PAGE onto the surface of a membrane. The separation pattern of the proteins in the gel remains the same after transfer onto the surface of the membrane.

In this study the wet tank blotting method was used. Here, the blotting process occurs completely immersed in a blotting buffer-containing chamber. For the blotting procedure a "sandwich" has to be assembled like shown in Fig. 2.3.

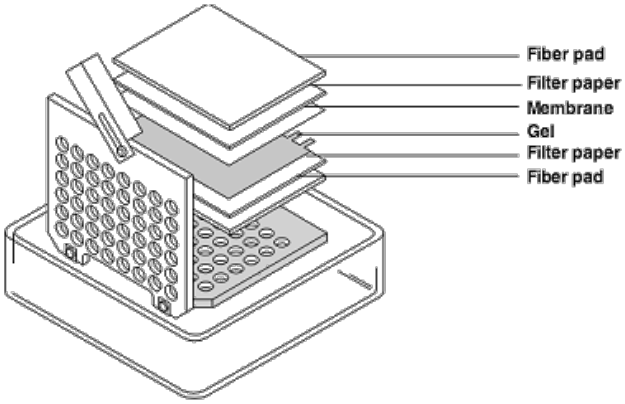

Figure 2.3: Assembly of a blotting sandwich for wet tank blotting. Figure: Bio-Rad Laboratories.

After preparation of the wet tank Western blotting apparatus, a constant current of 300 mA was applied for 2 h. Subsequently, the detection of the proteins fixed on the surface of the membrane was achieved by use of protein-specific antibodies. First, the membrane was incubated for 30 min with 10 % milk solution (in PBS-T buffer) for saturation of free binding sites on the membrane (blocking). Then, the membrane was incubated overnight with a primary antibody specific for the protein of interest. After washing the membrane three times with PBS-T buffer the membrane was incubated with a secondary antibody specific for the constant part of each primary antibody. The secondary antibody is fused to an enzyme which is able to convert a specific substrate under emitance of chemiluminescence. The principle of immunodetection is shown in Fig. 2.4. After washing the membrane three times with PBS-T buffer, the protein detection was performed using the ECL Western blotting substrate kit according to the manufacturer's instructions.

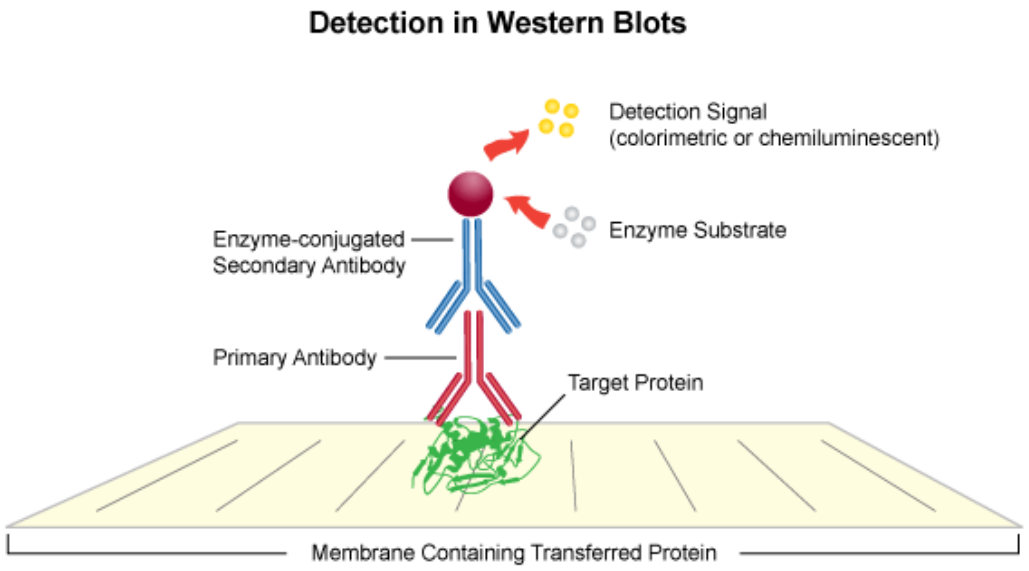

Figure 2.4: Principle of immunodetection of a nitrocellulose membrane-bound protein. The membrane is incubated with a primary antibody specific for the protein of interest. Afterwards, the membrane is incubated with a secondary antibody specific for the constant region of the primary antibody. The secondary antibody is fused to the enzyme horseradish peroxidase (HRP) allowing the final detection of the protein of interest using the ECL Western blotting substrate. Figure: Leinco Technologies.

2.2.3.4 Solubility assay

For determination of the solubility of protein substrates in different yeast strains 20 OD_{600} of yeast cells expressing the substrate of interest were harvested and washed once in 10 ml of cold 30 mM sodium azide solution. Temperature-sensitive strains were shifted to the restrictive temperature for 1 h before harvesting. Afterwards, the cells were resuspended in 1 ml of lysis buffer (0.7 M sorbitol, 50 mM Tris-HCl pH 7.5, 1.46 µM pepstatin A and protease inhibitor cocktail (Roche)). Each cell suspension was then transferred to a 2 ml Eppendorf tube containing glass beads. The cells were lysed by vortexing for 15 min at 4 °C. for preclearing, the crude lysate was centrifuged at 500 g for 5 min. The supernatant represents the total protein fraction (T). 400 µl of the total protein fraction were subjected to TCA precipitation. After precipitation, each pellet was washed once with acetone and solubilized in 60 µl of SDS urea sample buffer by boiling at 95 °C for 5 min. In addition, 400 µl of the total protein fraction were centrifuged at 21,500 g for 15 min. The supernatant represents the soluble fraction (S) and was subjected to TCA precipitation as described above. The pellet

was washed once in sorbitol buffer prior to solubilization in 60 µl of SDS urea sample buffer. This sample represents the pellet fraction (P). All samples were subjected to SDS-PAGE followed by immunoblotting.

2.2.3.5 Cycloheximide chase analysis

Cycloheximide chase experiments were performed in order to monitor protein degradation. Cycloheximide is an antibiotic which inhibits the translation process by binding to the eukaryotic 60 S ribosome subunit.

8 OD_{600} of exponentially growing cells were harvested in a 15 ml falcon tube and resuspended in 2 ml of selection medium. After 30 min of incubation at 30 °C, 50 µl of CHX solution (5 mg/ml) were added to each culture. Immediately, 450 µl of each culture were transferred into a microtube containing 500 µl of cold 30 mM sodium azide solution. Further samples were taken at defined time points.

All the samples were kept on ice. The cells were spun down at 8,000 rpm for 2 min before cell lysis and protein precipitation. For TCA precipitation 300 µl KH_2PO_4/ K_2HPO_4 (pH 7.5) buffer and 100 µl 50 % (m/v) TCA were added to each sample and the samples were incubated at least 1 h at -80 °C. The cells were centrifuged and each pellet was washed once with 500 µl cold 100 % (v/v) acetone. The acetone was discarded and the pellet was dried at 37 °C. Finally each pellet was resuspended in 50 µl of SDS urea loading buffer containing 1.5% (v/v) β-mercaptoethanol and boiled at 95 °C for 5 min. After centrifugation for 1 min at 12,000 rpm the samples were subjected to SDS-PAGE followed by immunoblotting. All cycloheximide chase experiments were performed at least two times.

2.2.3.6 Pulse chase analysis

Pulse chase analysis is another method for monitoring protein degradation. In contrast to cycloheximide chase analysis, the degradation of only newly synthesized proteins is monitored. This method uses radiolabelled methionine (^{35}S methionine) which is incorporated

into all newly synthesized proteins including the protein of interest during a short time scale (Pulse). Afterwards, the incorporation is stopped by adding an excess of unlabelled methionine. The degradation of the radiolabelled proteins can then be monitored using immunoprecipitation and autoradiography.

10 OD_{600} of an exponentially growing yeast culture were harvested and washed three times with labelling medium. Afterwards, the cell pellet was resuspended in 2 ml of labelling medium. The culture was then incubated at 30 °C for 50 min (starvation). Next, 20 µl of ^{35}S-labelled methionine were pipetted into the culture and it was further incubated at 30 °C for 20 min (Pulse). Then 1 ml of prewarmed chase medium was added and 450 µl of the culture were immediately transferred into a 1.5 ml screw cap micro tube containing 50 µl of cold 110 % (m/v) TCA. Further samples were taken at defined time points. All samples were stored at -20 °C. The samples were thawed at room temperature and spun down at 14,000 rpm for 8 min. The supernatants were discarded and the cell pellets washed once with 1 ml of cold acetone. After centrifugation at 14,000 rpm for 5 min the pellets were dried at room temperature. For complete cell lysis about 100 µl of glass beads and 100 µl of BB1 lysis buffer were added to each pellet. Complete cell lysis was achieved by 7 cycles of boiling for one minute at 95 °C and vortexing for one minute. Afterwards, 1 ml IP buffer and 5 µl protease inhibitor cocktail (Roche) were added to each sample. The samples were now vortexed for a few seconds and subjected to centrifugation at 14,000 rpm for 15 min.

For immunoprecipitation of the protein of interest 950 µl of each supernatant were transferred into a new micro tube containing 2-10 µl of the protein-specific antibody. The samples were now incubated at 4 °C for 2 h on a rotator. Afterwards, a suspension consisting of 5 mg protein A sepharose resuspended in 80 µl IP buffer (w/o) Triton X-100 per sample was prepared. 80 µl of the slurry were then added to each sample and the samples were further incubated at 4 °C for 1 h. The protein A sepharose matrix was pelleted at 2,500 rpm for 30 s and each pellet was washed four times with 1 ml of IP buffer. Proteins were eluted from the sepharose matrix by adding 60 µl SDS urea loading buffer containing 1 % β-mercaptoethanol and subsequent boiling at 95 °C for 3 min. After centrifugation at 14,000 rpm for 2 min the samples were subjected to SDS-PAGE. The gel was placed on a Whatman paper and dried for 2 h at 65 °C.

The dried gel was finally fixed in a film cassette and covered with a PhosphorImager screen for 3 to 5 days. The screen was finally scanned using a PhosphorImager (Storm860, Molecular Dynamics) and the data were analysed with the ImageQuant 5.2 Software (GE Healthcare Life Sciences). All pulse chase experiments were performed at least three times.

2.2.3.7 Bradford assay

The Bradford assay is a photometric method for determination of protein concentrations (Bradford, 1976). The method uses the dye Coomassie Brilliant Blue G-250 which irreversibly binds to proteins. After binding to proteins the dye is converted to the unprotonated form which absorbs at 595 nm.
In this study the Bradford assay was used for measuring the protein concentration of yeast cell lysates. First, a straight calibration line was generated for the used batch of Bradford solution. For this purpose, a dilution series of a BSA stock solution (1 mg/ml) was prepared. For setup of each photometric measurement 1 ml of Bradford solution was pipetted into a 1 ml half micro cuvette. Afterwards, 100 µl of each BSA dilution were added. After mixing and 10 min incubation at RT the absorption was measured at 595 nm. For measurement of the protein concentrations of the cell lysates 100 µl of each lysate in an appropriate dilution were used. The unknown concentrations of the lysates were determined by using the calibration line which was generated by measuring the absorption of each BSA dilution and subsequent plotting of the absorption against the concentrations of the different BSA dilutions.

2.2.3.8 Luciferase assay

Luciferases are enzymes belonging to a certain class of oxidative enzymes found in many species. The expression of these enzymes enables the organism to produce light. The process of producing light through a chemical reaction in a living organism is called bioluminescence. The reaction catalysed by luciferases is shown below.

$$\textbf{Luciferin + ATP + } O_2 \rightarrow \textbf{Oxyluciferin + AMP + } PP_i \textbf{ + Light}$$

In this study the assay was used for detection of the steady state levels of model substrates containing the enzyme luciferase from *Photinus Pyralis*. For the assay 10 OD_{600} of luciferase-expressing cells were harvested either in exponential or stationary growth phase and washed once with 10 ml of precooled PBS buffer. Then each cell pellet was resuspended in 500 µl of

lysis buffer (Tab. 2.18). The lysate was now transferred into a 2 ml micro tube containing approximately 500 µl of glass beads. The cells were lysed for 15 min using a cell disruptor. Each crude lysate was transferred into a new 1.5 ml micro tube and subjected to a centrifugation step at 15,000 rpm for 10 min. The cleared lysate was used for a Bradford assay and the luciferase activity measurement. For the measurements of luciferase activity 100 µl of assay buffer containing luciferin and ATP were pipetted into a 96 well plate. Then 20 µl of each lysate were added. Afterwards, the plate was immediately subjected to luciferase activity measurements using a 96 well plate reader (Enspire, PerkinElmer). The compositions of the required solutions and parameters for the measurements are listed in Tab. 2.18 and Tab. 2.19.

Table 2.18: Composition of the solutions needed for the luciferase assay.

Solution	Composition
Lysis buffer	100 mM KH_2PO_4/ K_2HPO_4 buffer pH 7.8 1 % (v/v) Triton X-100 10 % (v/v) glycerol Freshly added: 1 mM DTT 1 x Protease Inhibitor Cocktail (Roche) 1 µg/ml Pepstatin A
Assay buffer	100 mM TRIS-acetate (pH 7.8) 10 mM Magnesium acetate 1 mM EDTA
25 x D-luciferin	25 mM D-Luciferin (sodium salt; in assay buffer)
100 x ATP	0.2 M ATP (in assay buffer)

Table 2.19: Parameters for the measurement of luciferase activity using a 96 well plate reader.

Parameter	Value(s)
Temperature	25 °C
Shaking	5 s; 300 rpm (orbital shaking)
Pause after shaking	5 s
Measuring time	5 s

2.2.3.9 β-galactosidase filter assay

Yeast strains expressing β-galactosidase (β-Gal)-containing proteins were grown two days on corresponding agar plates. Afterwards, a round Whatman filter was placed on the agar plate until the filter was pre-soaked with medium and the yeast cells sticked to the filter surface. The filter was then placed with the colony side up on a new agar plate and incubated again overnight. Next day, the filter with the yeast cells was submerged into liquid nitrogen for 10 seconds and afterwards thawed at room temperature. In a new petri dish a Whatman filter was placed and pre-soaked with a Z buffer/X-Gal solution (5 ml Z buffer, 13.5 µl β-mercaptoethanol, 83.5 µl X-Gal solution). The filter with the attached and lysed yeast cells was placed with colony side up on the pre-soaked filter in the petri dish. The filter was finally incubated at 30 °C for 1 to 3 hours until the yeast cells turned blue.

3. RESULTS

3.1 Protein quality control of the cytoplasmic misfolded model substrate ΔssCPY*Leu2myc (ΔssCL*myc)

3.1.1 The model substrate ΔssCPY*Leu2myc (ΔssCL*myc)

In this work the recognition and degradation of cytoplasmic misfolded proteins in *Saccharomyces cerevisiae* were examined. For this purpose different artificial model substrates were used. ΔssCPY*Leu2myc (ΔssCL*myc) (Eisele and Wolf, 2008), the mainly used model substrate in this study, was derived from carboxypeptidase Y (Prc1 or CPY), a serine carboxypeptidase located in the yeast vacuole. All secretory proteins possess short N-terminally located signal sequences (ss) which are essential for endoplasmic reticulum (ER) import and entry into the secretory pathway (Martoglio and Dobberstein, 1998). The model substrate ΔssCL*myc is based on the ERAD-L substrate CPY* which carries a point mutation (G255R) causing misfolding (Finger *et al*, 1993; Wolf and Fink, 1975). Mutated CPY (CPY*) is recognized in the ER as irreversibly misfolded and is subsequently retrotranslocated out of the ER for proteasomal degradation. Deletion of the signal sequence prevents import into the ER. Therefore ΔssCL*myc remains in the cytosol. The substrate was also C-terminally fused to an enzyme called β-isopropylmalate dehydrogenase (Leu2) which is essential for the synthesis of the amino acid leucine. All the yeast strains used in this study contain a point mutation in the endogenous *LEU2* gene. Therefore they are not able to produce leucine on their own. For this reason the growth medium has to be supplemented with leucine. This allows the use of Leu2 as an auxotrophic marker and testing the stability of the model substrate ΔssCPY*Leu2myc: The higher the steady state level of the model substrate ΔssCPY*Leu2myc, the better is the growth of ΔssCPY*Leu2myc-expressing yeast stains on a medium lacking leucine. Additionally, the substrate is C-terminally tagged with the myc epitope, facilitating the detection of the substrate via immunoblotting. A schematic illustration of the substrate ΔssCPY*Leu2myc is shown in Fig. 3.1 A. The map of the plasmid used for transformation and substrate expression is shown in Fig. 3.1 B.

A

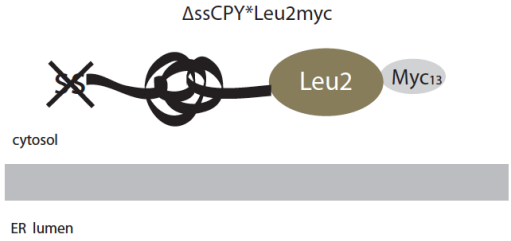

B

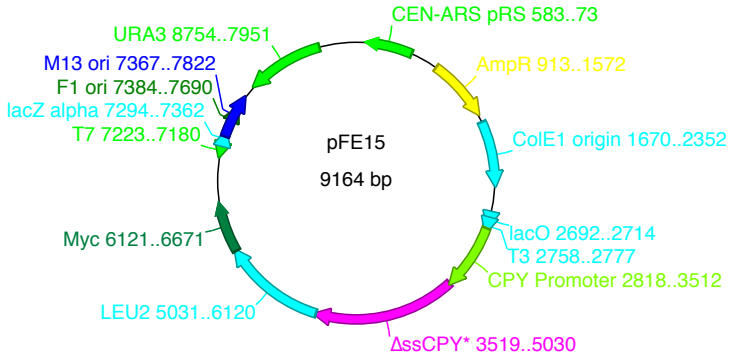

Figure 3.1: The model substrate ΔssCPY*Leu2myc (ΔssCL*myc). A. Topology of the cytoplasmically localized misfolded protein ΔssCPY*Leu2myc (ΔssCL*myc). The signal sequence of CPY G255R (CPY*) responsible for ER import is deleted and the auxotrophic marker Leu2 together with a myc epitope for immunodetection is fused to the C-terminus resulting in a cytosolic misfolded version of CPY serving as a model substrate for cytoplasmic protein quality control. B. Plasmid map of the ΔssCL*myc encoding plasmid pFE15. The expression of the substrate is under control of the native *CPY* promoter. The plasmid also contains the *URA3* marker for plasmid selection.

3.1.2 Dependence of ΔssCL*myc degradation on components of the ubiquitin-proteasome system

In 2008, our lab showed that Ubr1, the E3 ligase of the N-end rule pathway is involved in the degradation of cytoplasmic misfolded proteins using the model substrate ΔssCPY*Leu2myc

(Eisele and Wolf, 2008). In order to confirm the involvement of the ubiquitin-proteasome system, degradation was examined in a strain mutated in the sole ubiquitin-activating enzyme (E1) of yeast, Uba1. Due to the lethality of the *UBA1* deletion in yeast the *uba1-204* allele was used which only expresses a functional E1 enzyme at moderate temperatures up to approximately 30 °C.

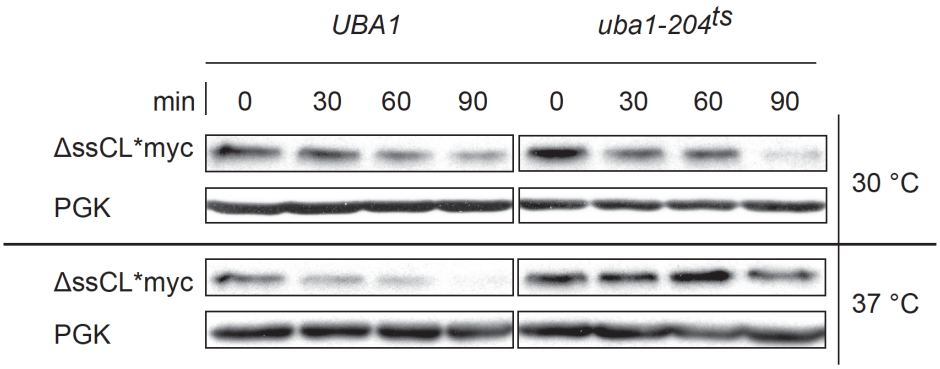

Figure 3.2. Uba1 function is essential for ΔssCL*myc degradation. Cycloheximide chase analysis of yeast strains harbouring either wild type *UBA1* or a mutated allele of *UBA1* (*uba1-204*) resulting in expression of an inactive form of Uba1 at 37 °C. Both strains are transformed with the plasmid pFE15 encoding the substrate ΔssCL*myc. PGK served as a loading control.

As can be seen in Fig. 3.2, at 30 °C, ΔssCL*myc is degraded both in the *UBA1* wild type and the *uba1-204* mutant strain. At 37 °C the substrate is only degraded in the *UBA1* wild type strain showing the importance of functional Uba1 in the degradation process of ΔssCL*myc.
In general, a functional RING domain of RING E3 ligases is essential for ubiquitination of substrates. Therefore a RING mutant of Ubr1 was used for further experiments in order to verify the requirement of an intact RING domain of Ubr1 for targeting the used substrate for degradation. To address the necessity of a functional RING domain for Ubr1 function, growth tests were performed using strains expressing either, wild type Ubr1 or the RING mutant defective in ubiquitination activity (Ubr1C1220S).

A

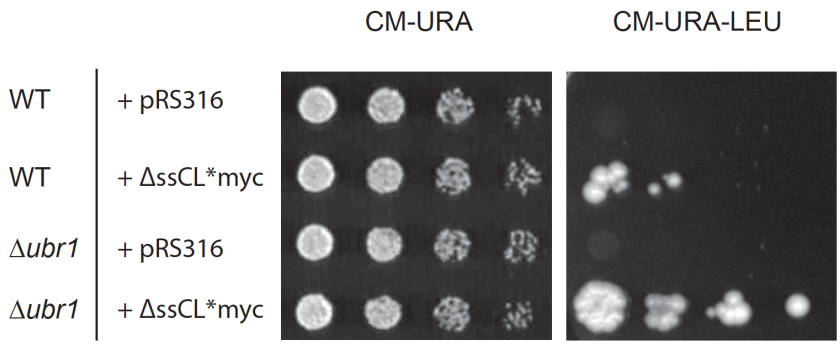

B

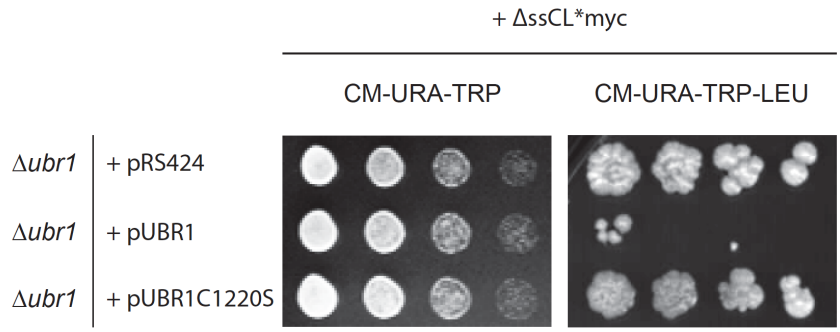

Figure 3.3 Ubr1 is the responsible ubiquitin ligase for ΔssCL*myc degradation. A. Growth tests of wild type and *Δubr1* yeast strains expressing the cytoplasmic misfolded protein ΔssCL*myc from the *URA3* marker-containing plasmid pFE15 were performed. As control, the same strains were transformed with the empty plasmid pRS316. Cells were spotted in a five fold dilution series on plates either selecting only for presence of the plasmids (CM-URA agar plates) or in addition selecting for the substrate ΔssCL*myc making use of the leucine auxotrophy (CM-URA-LEU agar plates). B. Growth tests of the *UBR1* deletion strain expressing ΔssCL*myc from the plasmid pFE15. In addition the Δ*ubr1* strain was transformed either with the empty plasmid pRS424, a Ubr1-expressing plasmid (pUBR1) or a plasmid encoding a RING mutant of Ubr1 (pUBR1C1220S) all containing a tryptophan (*TRP*) marker for plasmid selection.

As can be seen in Fig. 3.3 A all the strains grow equally well on medium lacking uracil (CM-URA), (control) whereas growth of the *Δubr1* strain expressing ΔssCL*myc on CM-URA-LEU plates is increased compared to the corresponding wild type strain confirming the involvement of Ubr1 in the degradation process of ΔssCL*myc. A RING mutant (C1220S) of Ubr1 causes stability of the substrate similar to the *Δubr1* strain expressing the empty plasmid pRS424 (Fig. 3.3 B).

It is known from the N-end rule pathway that Ubr1 ubiquitinates substrates in cooperation with the E2 enzyme Ubc2 (Rad6). To examine the involvement of Ubc2 (Rad6) in the Ubr1-dependent ubiquitination of cytoplasmic misfolded proteins, pulse chase analysis was performed using the *UBC2* (*RAD6*) deletion strain (Fig. 3.4).

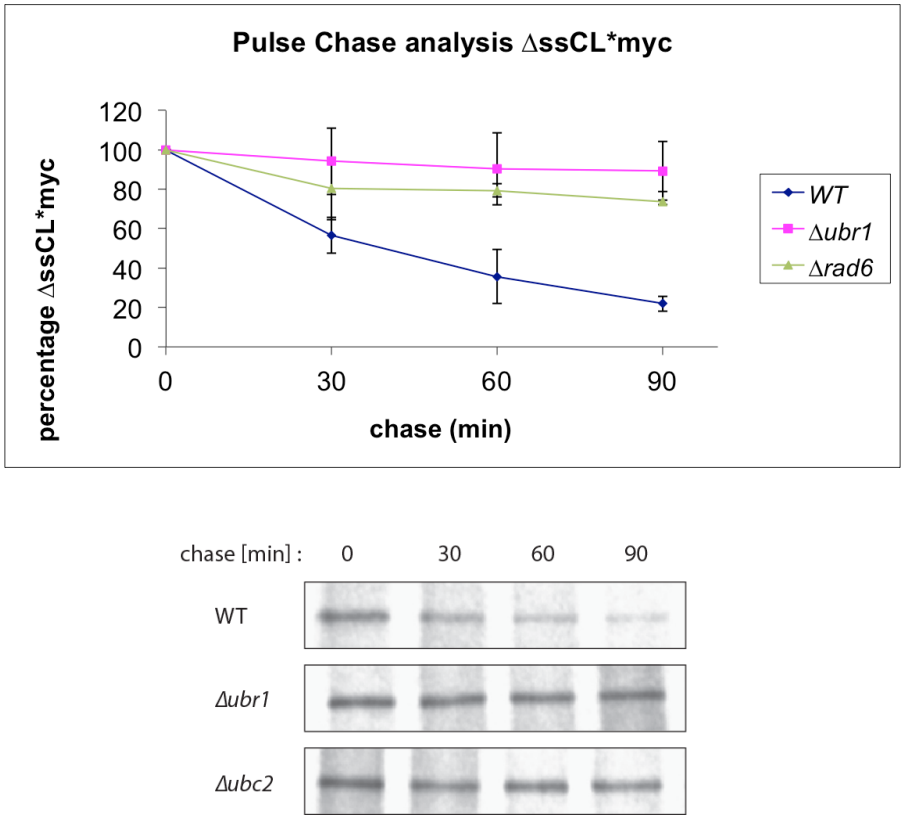

Figure 3.4: Ubr1 and the ubiquitin-conjugating enzyme Ubc2 (Rad6) are involved in the degradation of ΔssCL*myc. Pulse chase analysis using yeast strains expressing ΔssCL*myc. Exponentially growing cells were incubated with radioactive methionine for labelling of newly synthesized proteins. After addition of non-radioactive methionine cells were lysed at the indicated time points. Proteins were immunoprecipitated and separated by size via SDS-PAGE for further analysis using a PhosphorImager. Plotted data represent the mean values of three independent experiments. Error bars indicate the standard error of the mean.

As can be seen in Fig. 3.4 absence of the E2 enzyme Ubc2 (Rad6) causes strong stabilization of the model substrate ΔssCL*myc similar to the stabilization in the *Δubr1* strain. In summary, the ubiquitin-activating enzyme Uba1, the ubiquitin-conjugating enzyme Ubc2

(Rad6) and the ubiquitin ligase Ubr1 are all involved in the ubiquitination process of the cytoplasmic misfolded model substrate ΔssCL*myc.

In order to address the question whether Ubr1 functions in ubiquitinating cytoplasmic misfolded proteins independently of the N-end rule pathway the degradation kinetics of ΔssCL*myc was examined in strains expressing Ubr1 mutants which are defective in degradation of either degrading type 1 (Ubr1 D176E) or type 2 N-end rule substrates (Ubr1 P406S), (Xia *et al*, 2008).

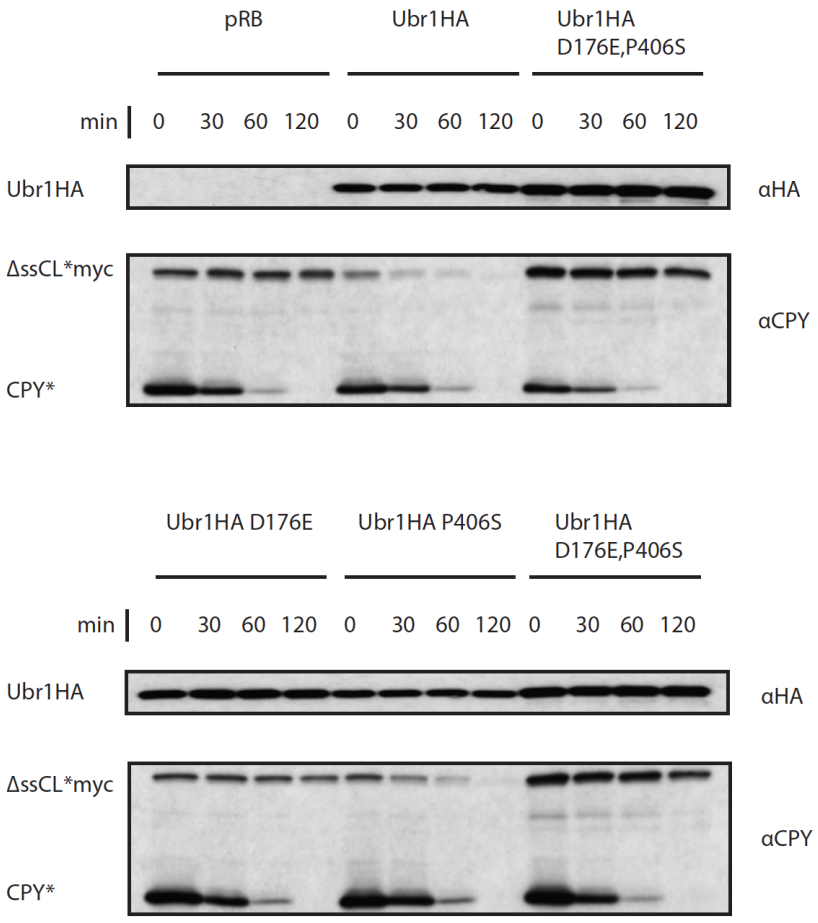

Figure 3.5: The Ubr1 binding site for type 1 N-end rule substrates is required for degradation of ΔssCL*myc. Cycloheximide chase analysis using yeast strains genomically deleted in the gene coding for the E3 ligase Ubr1 transformed with either an empty plasmid (pRB) or plasmids expressing different Ubr1 variants (wild type Ubr1 protein, Ubr1 D176E protein, Ubr1 P406S protein and Ubr1 D176E, P406S protein). All Ubr1 proteins are C-terminally tagged with an HA epitope and expressed under control of the *ADH1* promoter. All the strains were additionally transformed with the plasmid pFE15 encoding the model substrate ΔssCL*myc. Endogenously expressed misfolded carboxypeptidase Y (CPY*) served as a control substrate.

As can be clearly seen in Fig. 3.5 ΔssCL*myc is dramatically stabilized in the strain not expressing any form of Ubr1 (pRB) in contrast to the strain expressing wild type Ubr1 where the substrate is rapidly degraded. Degradation kinetics similar to the wild type Ubr1 expressing strain is observed for the strain expressing a mutant of Ubr1 which is not able to degrade type 2 N-end rule substrates (Ubr1 P406S protein). The strain expressing the Ubr1 variant mutated in the type 1 binding site (Ubr1 D176E protein) is not able to degrade the substrate indicating an involvement of the type 1 binding site in the degradation process. The ERAD substrate CPY* served as a control because its degradation is completely independent of the E3 ligase Ubr1.

To further confirm the stabilization of ΔssCL*myc in the *Δubr1* strain expressing the Ubr1 D176E mutant protein, growth tests were performed.

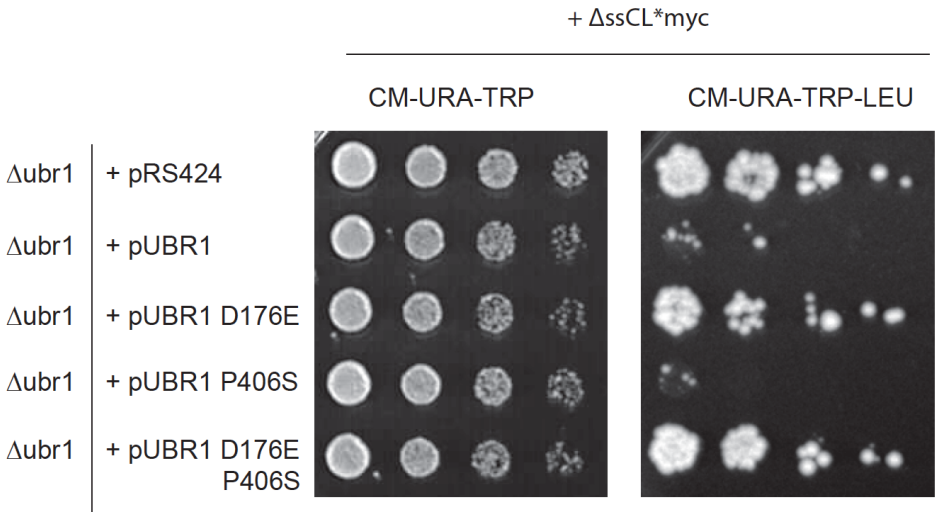

Figure 3.6: Ubr1 mutated in the binding site for type 1 N-end rule substrates causes stabilization of ΔssCL*myc. Growth tests of *Δubr1* yeast strains all expressing cytoplasmic misfolded protein ΔssCL*myc from the *URA3* marker-containing plasmid pFE15. In addition, the strains were transformed with either an empty plasmid (pRS424) or plasmids coding for different Ubr1 variants described above. All the Ubr1-expressing plasmids contain a *TRP1* marker for selection.

As can be seen in Fig. 3.6, on medium without leucine (CM-URA-TRP-LEU) the strains expressing the Ubr1 (D176E) protein grow as well as the *Δubr1* strain expressing the empty plasmid pRS424. Hardly any growth can be observed for the strain expressing wild type Ubr1 or the Ubr1 P406S mutant protein defective in degrading type 2 N-end rule substrates

indicating a fast degradation of the model substrate in these strains. The results perfectly fit to the degradation kinetics shown in Fig. 3.5 indicating that the type 1 binding site of Ubr1 is necessary for degradation of ΔssCL*myc. The growth of all strains on plates lacking both uracil and tryptophan where only the presence of each plasmid pair is monitored is similar.

3.1.3 Involvement of the Ssa subfamily of Hsp70 chaperones in quality control of ΔssCL*myc

Hsp70 chaperones are a very important class of heat shock proteins preventing partially folded and misfolded proteins from aggregation and therefore keeping them in an active or soluble form for further folding steps or delivery to the degradation machinery (see chapter 1.1.2.1). Hsp70 chaperones are found in every compartment of the cell. Since the main focus of this study resided in protein quality control of cytosolic proteins, the involvement of the Ssa chaperone subfamily of Hsp70 (Ssa1, Ssa2, Ssa3, Ssa4) localized in the yeast cytosol was analysed in more detail. To confirm a general requirement of these chaperones for elimination of the model substrate ΔssCL*myc, solubility assays were performed using a strain deleted in the genes coding for three Hsp70 chaperones of the Ssa class (*SSA2, SSA3 and SSA4*) and only expressing a temperature-sensitive allele of *SSA1* (*ssa1-45ts*). While the *ssa1-45*^{ts} allele encodes a mainly active Ssa1 at 25 °C, a temperature shift to 37 °C causes conformational instability of the mutant Ssa1 resulting in loss of its chaperone function. The solubility of ΔssCL*myc expressed in this strain was analysed at 25 °C and at restrictive temperature (37 °C). In a second strain a *UBR1* deletion was introduced in order to examine the influence of the ubiquitin ligase Ubr1 on the solubility of the substrate (Fig. 3.7). Furthermore, solubility of the substrate was examined in the exponential and in the stationary growth phase. In stationary phase a lot of chaperones are expressed to promote survival after consumption of carbon and nitrogen sources. Whereas Ssa1 and Ssa2 are highly expressed during exponential growth phase their expression rapidly drops after diauxic shift. Expression of Ssa3 is only detectable in cells approaching the stationary phase after the diauxic shift (Hasin *et al*, 2014; Werner-Washburne *et al*, 1989).

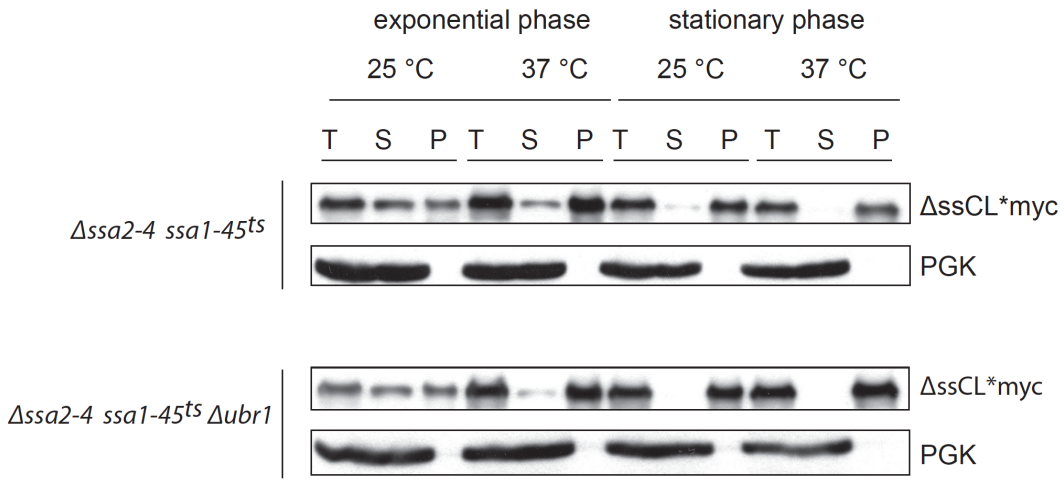

Figure 3.7: The Hsp70 chaperone Ssa1 is important for solubility of ΔssCL*myc. Solubility assays of the substrate ΔssCL*myc expressed in the temperature-sensitive strains *Δssa2Δssa3Δssa4ssa1-45^{ts}* and *Δssa2Δssa3Δssa4ssa1-45^{ts} Δubr1*. Cells were grown at 25 °C, split in two halves and one half shifted to 37 °C for 1h prior to harvesting, lysis and fractionation into soluble (S) and pellet (P) fractions. The total fractions (T) represent the precleared cell lysates prior to fractionation. Exponentially growing cells were harvested after approximately 16 h of growth at an OD_{600} of 1.0 whereas stationary cells were grown 3 days at 25 °C prior to temperature shift and harvesting for fractionation, respectively. PGK served as loading control and reference for a soluble protein.

In exponential growth phase the amounts of substrates in the pellet and soluble fractions at 25 °C are similar. The additional deletion of *UBR1* only slightly increases the amount of substrate in the pellet fraction. At 37 °C most of the substrate is found in the pellet (P) fraction. The *UBR1* deletion additionally decreases the solubility of ΔssCL*myc at 37 °C. At stationary phase, even at 25 °C hardly any substrate signals can be detected in the soluble (S) fractions. At 37 °C all of the substrate is found in the pellet fractions (Fig. 3.7).

To address the question whether the Ssa chaperones are not only needed for keeping substrates soluble but also needed for degradation of the substrate, cycloheximide chase experiments were performed using strains either containing the wild type *SSA1* gene or the temperature sensitive *ssa1-45^{ts}* allele. All strains are additionally deleted in the genes encoding the Ssa chaperones Ssa2, Ssa3 and Ssa4 (Fig. 3.8)

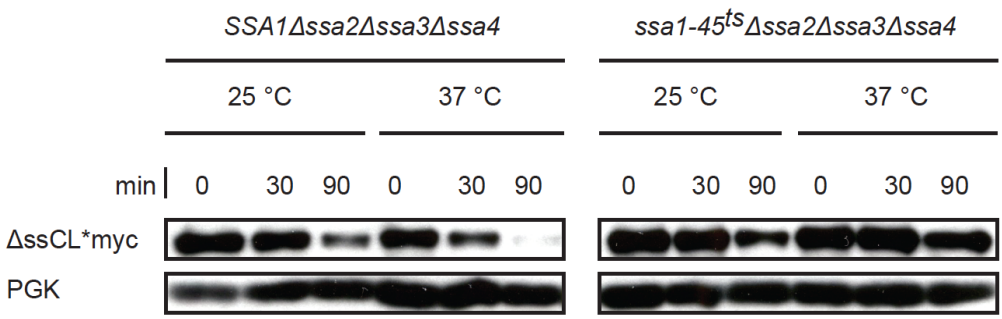

Figure 3.8: The Hsp70 chaperone Ssa1 is necessary for degradation of ΔssCL*myc. Cycloheximide chase analysis of strains deleted in the Hsp70 chaperone genes *SSA2, SSA3, SSA4* expressing either wild type Ssa1 or the temperature-sensitive mutant protein Ssa1-45. Samples were taken after addition of cycloheximide at the indicated time points at 25 °C and 37 °C. PGK served as loading control.

In the strain expressing wild type Ssa1 protein the amount of ΔssCL*myc is clearly reduced after 90 min both at 25 °C and 37 °C. At 37 °C degradation of the substrate is even elevated compared to 25 °C. At 37 °C hardly any substrate signal is visible after 90 min. Using the strain harbouring the temperature-sensitive *ssa1-45*^{ts} allele the cycloheximide chase reveals a drastic stabilization of ΔssCL*myc at 37 °C compared to the strain expressing wild type Ssa1 at the same temperature (Fig. 3.8).

3.1.4 Involvement of chaperones of the Hsp90 family in the quality control of ΔssCL*myc

Chaperones of the Hsp90 family are the most abundant chaperones in eukaryotic cells. The Hsp90 system acts downstream of the Hsp70 proteins and is responsible for refolding of denatured proteins back to their active form and also for the final activation of many signalling molecules like kinases. To address the function of Hsp90 members in degradation of terminally misfolded cytosolic proteins, cycloheximide chase experiments were performed using the specific Hsp90 inhibitor Geldanamycin (Fig. 3.9 A) which binds to the ATP/ADP binding pocket of Hsp90 proteins. The degradation kinetics of the model substrate ΔssCL*myc were determined in yeast strains deleted in the *UBR1* gene expressing either

FLAG-tagged Ubr1 (FLAGUbr1) or the corresponding empty plasmid (pRB) as a control (Fig. 3.9 B).

A

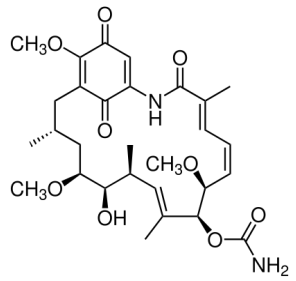

B

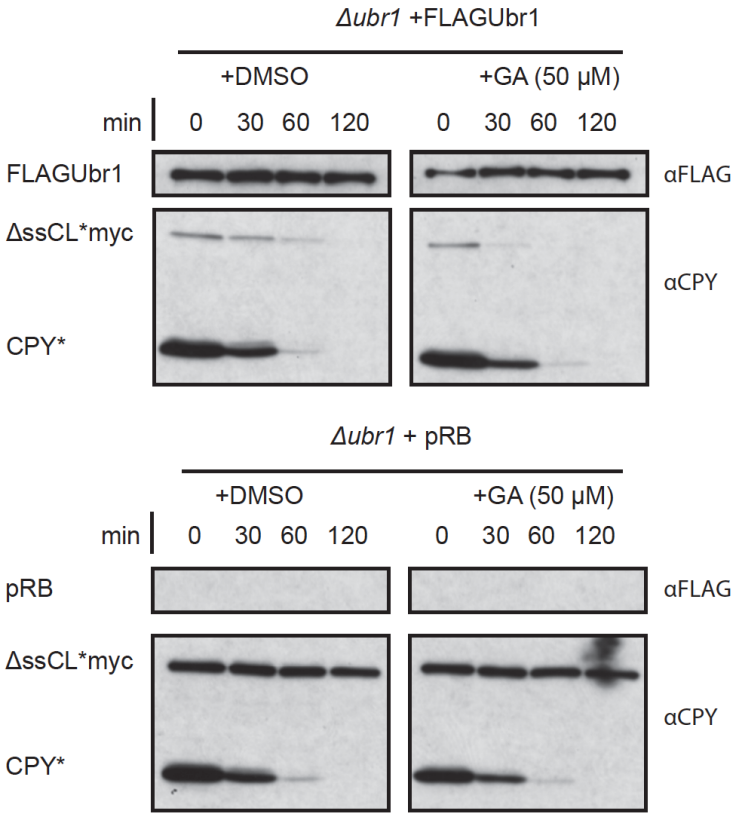

Figure 3.9: Inhibition of Hsp90 causes enhanced degradation of ΔssCL*myc. A. Chemical structure of the specific Hsp90 inhibitor Geldanamycin. B. Cycloheximide chase analysis of a *Δubr1* strain expressing the model substrate ΔssCL*myc from the plasmid pFE15 and FLAG-tagged Ubr1 (FLAGUbr1). A strain lacking Ubr1 (Δubr1 + pRB) served as a control. The cells were additionally incubated with 50 µM Geldanamycin (GA) dissolved in DMSO. Incubation with the solvent DMSO served as negative control. The endogenously expressed ERAD-L substrate CPY* served as substrate control. Ubr1 was detected using FLAG-antibody.

The degradation rate of ΔssCL*myc is increased in cells expressing FLAGUbr1 and treated with Geldanamycin compared to corresponding cells treated only with the solvent DMSO (Fig. 3.9). Absence of Ubr1 causes stabilization of the substrate, confirming previous results. Degradation of the ERAD-L substrate CPY* remains uncompromised independent of Geldanamycin treatment or presence of the ubiquitin ligase Ubr1. FLAG-tagged Ubr1 (FLAGUbr1) remains stable during the time measured (Fig. 3.9).

3.2 Introduction of new luciferase-based model substrates for studying cytoplasmic protein quality control

3.2.1 The new model substrates LucLeu2myc and LucDMLeu2myc

The use of the model substrate ΔssCPY*Leu2myc in studying cytoplasmic protein quality control has great advantages, one of which is the easy performance of growth tests making use of the auxotrophic marker Leu2 which is fused to the cytoplasmically localized carboxypeptidase Y (ΔssCPY*).

A further objective of this work was the establishment of new model substrates based on the enzyme firefly luciferase, which is often used as reporter enzyme for studying i.e. (re)folding kinetics. The aim of this project was to create substrates possessing both advantages of the easy performance of growth tests and the measurement of luciferase activity based on chemiluminescence which can be determined photometrically. Chemiluminescence measurements have many advantages including the low price of reagents needed, the fast procedure of measurement and the suitability for easy use in genome wide screening strategies.

The substrates introduced here were based on the enzyme luciferase of *Photinus pyralis*. The enzyme is localized to the peroxisomes because of the C-terminal sequence motif consisting of the three amino acid containing stretch serine-lysine-leucine (SKL) (Gould *et al*, 1989). When expressed in eukaryotes including yeast the enzyme is bound by the peroxisomal receptor protein Pex5 and subsequently imported into the peroxisome (Kiel *et al*, 2005). For generating model substrates for the cytoplasmic protein quality control system the signal

sequence for peroxisomal import of luciferase had to be deleted. The modified gene coding for luciferase (luc) was afterwards fused to *LEU2myc*. The resulting plasmid (Fig.3.10) expresses the fusion protein LucLeu2myc under control of the *GAL1* promoter.

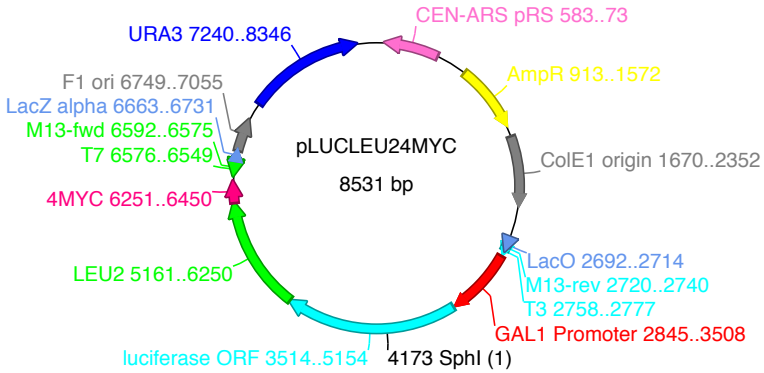

Figure 3.10: Plasmid map of the LucLeu2myc-expressing plasmid (pIA14). The plasmid consists of the *URA3* marker-containing centromeric plasmid pRS316 expressing the model substrate LucLeu2myc under control of the *GAL1* promoter. The plasmid is modified from the original plasmid pLUC provided by (Nillegoda *et al*, 2010).

The luciferase fusion protein expressed from the plasmid pIA14 is tightly folded. To generate a structurally destabilized version of luciferase (LucDMLeu2myc) the DNA coding for luciferase had been mutagenized via site-directed mutagenesis. The corresponding luciferase protein carries the two point mutations R188Q and R261Q described in (Gupta *et al*, 2011).

3.2.2 Ubr1-dependency of degradation of the luciferase substrates

The two generated plasmids encoding the two model substrates LucLeu2myc and LucDMLeu2myc are supposed to be localized in the yeast cytosol because of the absence of the C-terminal sequence motif for peroxisomal import (SKL). To verify the possibility of usage of both substrates in studying cytoplasmic protein quality control the influence of the ubiquitin ligase Ubr1 on the degradation of LucLeu2myc and LucLeu2DMmyc was examined

(Fig.3.11). The corresponding strains were either grown overnight in glucose- or in galactose-containing medium before cycloheximide chase experiments were performed (Fig. 3.11). Using glucose medium only small amounts of the substrates are expressed because of the glucose-repressible *GAL1* promoter. To check whether overexpression of substrate causes alterations in the degradation kinetics the strains were also grown overnight in galactose-containing medium causing overexpression of corresponding substrates.

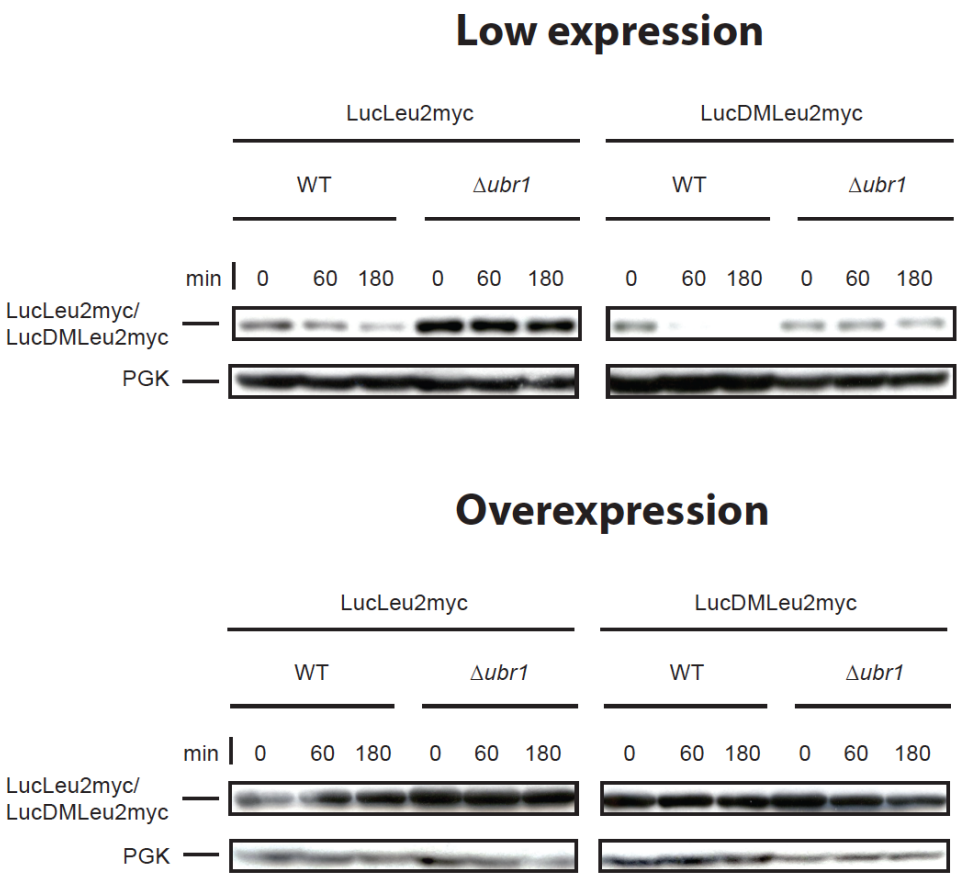

Figure 3.11: Both the substrates LucLeu2myc and LucDMLeu2myc are degraded in a Ubr1-dependent manner when expressed at a low level. Yeast strains are transformed with plasmids either expressing the substrate LucLeu2myc or LucDMLeu2myc both under control of the *GAL1* promoter. Glucose-containing growth medium was used for low expression of the model substrates (upper panel) or galactose-containing medium for high substrate expression (lower panel). Samples were taken at the indicated time points after addition of cycloheximide. PGK served as loading control.

Low expression of the substrates LucLeu2myc and LucDMLeu2myc is caused by the leakiness of the *GAL1* promoter in glucose-containing medium. The degradation of both

substrates in the wild type strain is visible (Fig. 3.11 upper panel). The destabilized version LucDMLeu2myc is degraded more rapidly. Absence of the cytosolic E3 ligase Ubr1 causes a dramatic stabilization of both substrates showing its involvement in the degradation process. Growth of the used yeast strains in galactose-containing medium causes massive expression of the two substrates. Even in the wild type strain no degradation can be observed for both substrates in the measured time period (Fig. 3.11 lower panel).

3.2.3 Detection of the influence of the Hsp70 chaperone Ssa1 on the protein quality control of the substrates LucLeu2myc and LucDMLeu2myc using luciferase assays

An advantage of the substrates LucLeu2myc and LucDMLeu2myc is the easy measurement of their steady state levels via detection of luciferase activity. Luciferase converts the substrate luciferin into oxyluciferin under emission of chemiluminescence. Chemiluminescence can be easily detected by photometric measurements. The involvement of the Hsp70 system in quality control of the two model substrates was examined using luciferase activity measurements. Yeast strains defective in the Hsp70 system and expressing either LucLeu2myc or LucDMLeu2myc were harvested either in exponential or in stationary growth phase and the cells were lysed for subsequent luciferase assays. The strains harbouring the *ssa1-45*^{ts} allele were shifted to 37 °C for 1h prior to harvesting and lysis. As control the strains were grown at 30 °C, conditions where the *ssa1-45*^{ts} allele produces mainly active Ssa1 protein. The strain harbouring the wild type *SSA1* gene served as control strain for the measurements (Fig. 3.12).

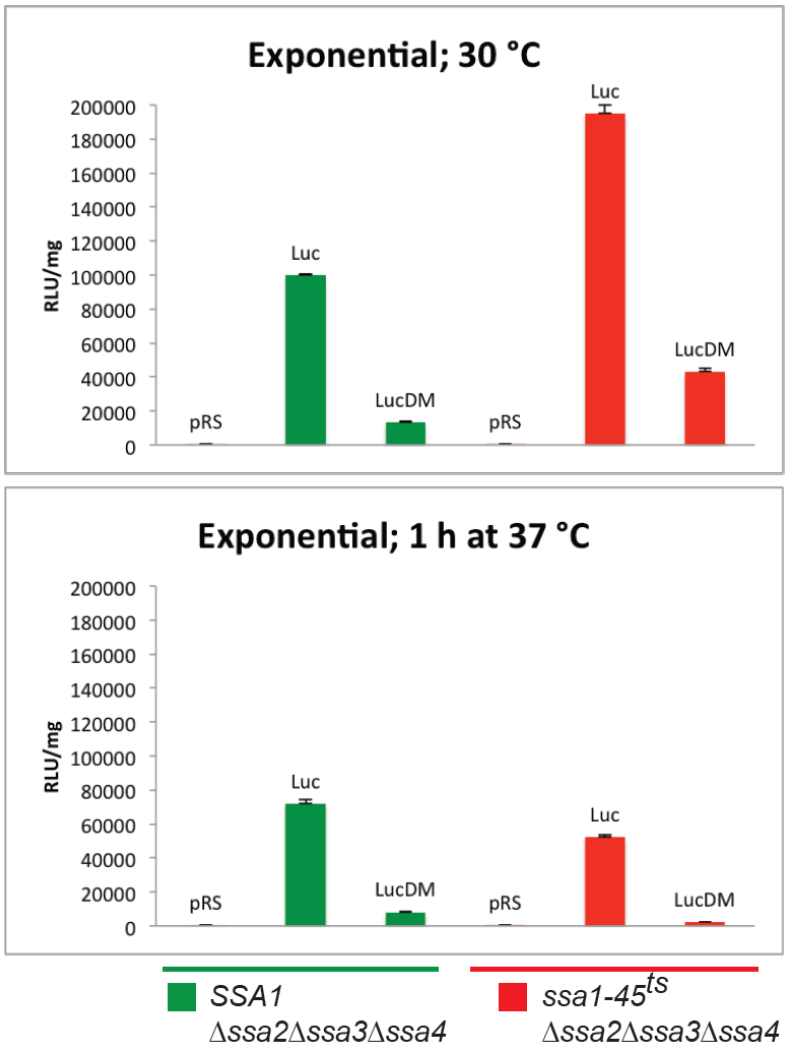

Figure 3.12: In exponential phase loss of Ssa1 function dramatically decreases luciferase activity of the substrate-expressing strains. Both yeast strains harbouring the wild type *SSA1* gene and the temperature-sensitive *ssa1-45*^{ts} allele were transformed either with the plasmids pIA14 or pIA15 coding for the substrates LucLeu2myc (Luc), LucLeu2DMmyc (LucDM) or the corresponding empty plasmid pRS316 (pRS). Cells were harvested in exponential growth phase at an OD_{600} of 1.0 prior to cell lysis and luciferase measurements. The temperature-sensitive *ssa1-45*^{ts} strain was shifted to 37 °C prior to harvesting. The relative light units (RLU) were normalized to the total protein concentration of each cell lysate (specific activity). Plotted data represent the mean of three luciferase measurements. Error bars indicate the standard deviation of the mean.

Under both permissive (30 °C) and restrictive (37 °C) conditions lysates of both yeast strains expressing the luciferase-containing substrates exhibit luciferase activity (Fig. 3.12). Strains expressing the destabilized version of luciferase (LucDM) always show lower activities. As expected, control strains transformed with empty plasmid (pRS) do not show any luciferase

activity. The activity of lysates obtained from *ssa1-45*^{ts} strains at 30 °C show higher activities than lysates of *SSA1* wild type strains both expressing the luciferase substrates (Fig. 3.12 upper panel). At restrictive temperature the lysates of the *ssa1-45*^{ts} strain show a dramatically decreased luciferase activity whereas in the wild type *SSA1* situation the activities only moderately decrease after shift to 37 °C (Fig. 3.12 lower panel).

Next, the same assays were performed but using cultures grown for three days at 30 °C. One part of the cultures were shifted to 37 °C for 1 hour prior to lysis and luciferase assays (Fig. 3.13).

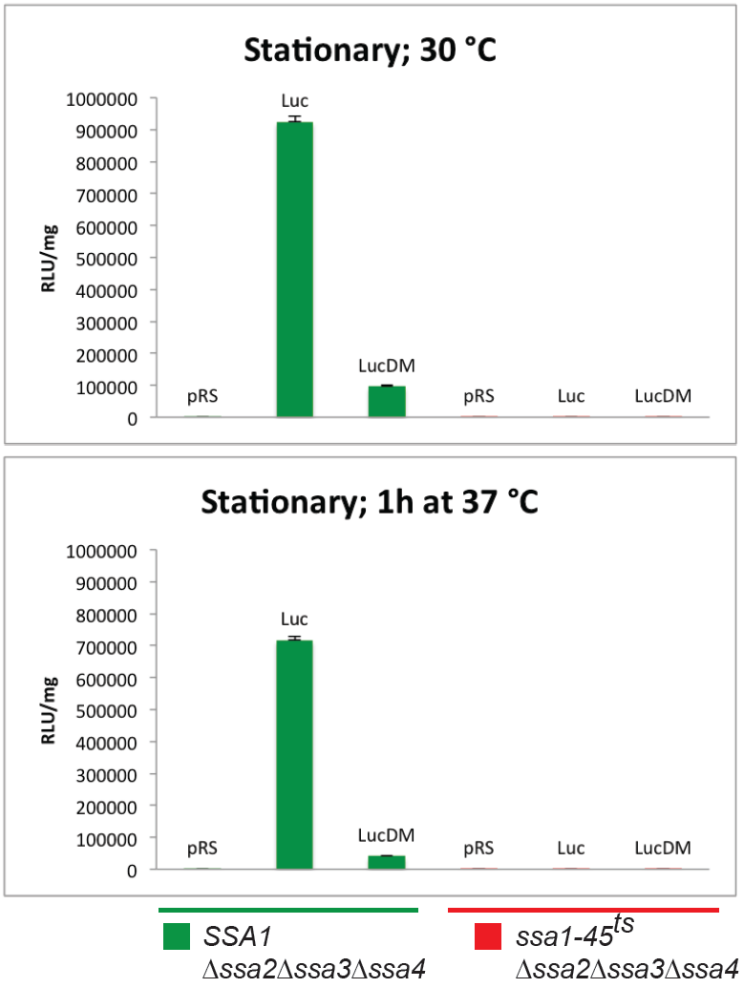

Figure 3.13: In stationary phase the mutated Ssa1 protein expressed from the *ssa1-45*^{ts} allele even at permissive temperature cannot retain luciferase activity. The same yeast strains and plasmids were used as described in the legends to Fig.3.12. The cells were harvested after three days of growth prior to lysis and luciferase measurements. The temperature-sensitive *ssa1-45*^{ts} strain was shifted to 37 °C prior to harvesting. The relative light units (RLU) were normalized to the total protein concentration of each cell lysate. Plotted data represent the mean of three luciferase measurements. Error bars indicate the standard deviation of the mean.

When grown to stationary phase the lysates of strains harbouring the temperature-sensitive *ssa1-45*^{ts} allele and expressing the luciferase-containing substrates do not exhibit any luciferase activity even at 30 °C. Only for the wild type *SSA1* strains expressing the luciferase substrates luciferase activity can be detected which decreased after shift to 37 °C in a similar modest way like in exponential phase (Fig. 3.13). As mentioned previously in chapter 3.1.3, Ssa1 and Ssa2 are only expressed during exponential growth until diauxic shift. In contrast, Ssa3 is not detectable under exponential conditions but strongly expressed in stationary phase (Hasin *et al*, 2014; Werner-Washburne *et al*, 1989). This difference in expression of the Ssa chaperones might also explain the results in the stationary growth phase seen in Fig. 3.13 because the used strains are deleted in the *SSA3* gene.

3.3 San1-dependency of degradation of cytoplasmic misfolded proteins

3.3.1 Ubr1 and San1 as the E3 ligases of the cytoplasmic protein quality control

In 2008 it was shown for the first time that the cytosolic ubiquitin ligase (E3 ligase) Ubr1 which is known to target N-end rule substrates for proteasomal degradation is also involved in degradation of misfolded cytosolic proteins (Eisele and Wolf, 2008). Further studies using different cytosolic model substrates revealed also an involvement of the nuclear RING ubiquitin ligase, San1 (Dasgupta *et al*, 2004), in the degradation process of cytosolic misfolded proteins (Heck *et al*, 2010; Khosrow-Khavar *et al*, 2012; Prasad *et al*, 2010). San1 is a nuclear E3 ligase known to target aberrant nuclear proteins for proteasomal degradation (Gardner *et al*, 2005). San1 is nuclear-localized due to a bipartite nuclear localization signal (NLS). In contrast to Ubr1, San1 contains a high amount of intrinsically disordered regions allowing San1 to adopt multiple conformations for direct interaction with client proteins (Fredrickson *et al*, 2011; Rosenbaum *et al*, 2011).

Obviously, some cytoplasmic misfolded substrates can be shuttled into the nucleus. Shuttling of cytoplasmic misfolded proteins into the nucleus for San1-dependent degradation is

dependent of the Hsp70 machinery including the Hsp40 chaperone Sis1 and the Hsp110 chaperone Sse1 (Heck *et al*, 2010; Park *et al*, 2013; Prasad *et al*, 2010). Why some cytosolic substrates are shuttled into the nucleus and some of them reside in the cytosol is mainly unclear. A list of some model substrates used by different work groups for studying cytoplasmic protein quality control including their molecular mass is listed in Tab. 3.1. Also the dependency of their degradation on San1 is indicated.

Table 3.1: San1-dependency of degradation of several cytoplasmic protein quality control substrates.

Substrate	Molecular mass [kDa]	Influence of San1 on substrate degradation	Reference/Source
Δ2GFP	26	+++	(Prasad *et al*, 2010)
ΔssPrA	40	+++	(Prasad *et al*, 2010)
ΔssCPY*	60	++	Frederik Eisele; this study
ΔssCPY*GFP	85	+	(Heck *et al*, 2010)
ΔssCPY*Leu2myc	116	-	(Eisele and Wolf, 2008); this study
Orphan Fas2	207	-	(Scazzari, 2013); this study

The different substrates listed in Tab. 3.1 used for studying cytoplasmic protein quality control strongly differ in molecular mass from 26 kDa up to 207 kDa. Interestingly, degradation of the two substrates with the highest molecular mass, ΔssCPY*Leu2myc and orphan Fas2, seems not to be dependent on the nuclear E3 ligase San1. The smaller substrates can be still degraded in a strain deleted in *UBR1* but not in the double deletion strains deleted in both the *SAN1* and *UBR1* genes implying a nuclear import mechanism for those substrates (References see Tab. 3.1).

3.3.2 San1 localized to the cytosol can target cytosolic misfolded substrates for degradation

The E3 ligase San1 contains a bipartite NLS sequence essential for its nuclear localization. Since San1 is able to target some cytosolic substrates for degradation (Tab. 3.1) but does not seem to be able to target the substrate ΔssCL*myc for degradation it was examined if San1 can target ΔssCL*myc for degradation when its localization is changed to the yeast cytosol. Therefore, the bipartite NLS sequence of San1 was mutated and the corresponding mutated San1 expressed in a strain absent of the cytosolic E3 ligase Ubr1. Degradation kinetics were determined using cycloheximide chase experiments (Fig. 3.14).

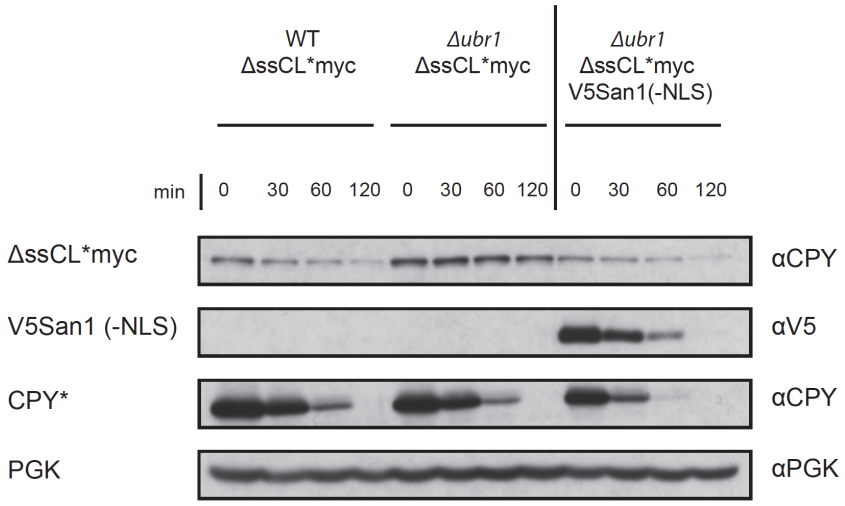

Figure 3.14: Cytosol-localized San1 can restore degradation of ΔssCL*myc in the absence of Ubr1. Cycloheximide chase experiments were performed using strains expressing the substrate ΔssCL*myc from the plasmid pIA1. In addition, all the strains were transformed with the plasmid pIA16 coding for V5-tagged San1 (-NLS) under control of the *GAL1* promoter and mutated in the NLS sequence. V5San1 (-NLS) expression was either repressed by using glucose-containing medium or induced by use of galactose-containing medium. Samples were taken at the indicated time points. PGK served as loading control. The endogenously expressed ERAD-L substrate CPY* served as control substrate. The San1 protein was detected using V5 antibody.

In the wild type strain the substrate ΔssCL*myc is degraded whereas in the strain lacking Ubr1 the substrate is stabilized. Expressing cytosol-localized San1 in the *Δubr1* strain restores the degradation of ΔssCL*myc. Degradation of the ERAD-L substrate CPY* endogenously expressed from the *prc1-1* allele is uncompromised in all the used strains. The San1 protein itself is degraded but still abundant in such high levels to exhibit E3 ligase function.

To check whether San1 instability is caused by autoubiquitination cycloheximide chase experiments were performed using a yeast strain expressing a San1 protein mutated in the RING domain (C257S). This point mutation abolishes San1 E3 ligase activity.

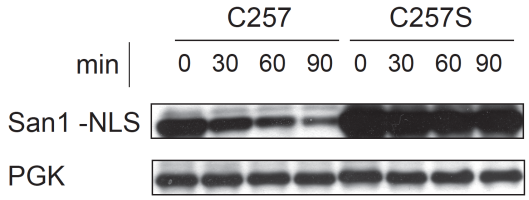

Figure 3.15: V5-tagged San1 (-NLS) used in this study is unstable. Cycloheximide chase experiments were performed using a *Δubr1* strain expressing either San1 (-NLS) or the point mutant of San1 defective in ubiquitination activity (San1 (-NLS) C257S). Samples were taken at the indicated time points. PGK served as loading control. The San1 constructs were detected using V5 antibody.

As can be seen in Fig. 3.15 cytosolic San1 containing a functional RING domain is degraded. In contrast, the mutated San1 protein containing a point mutation in the essential cysteine residue at position 257 is stable. This indicates a ubiquitination process of the V5-tagged San1 (-NLS) in cis or in trans by another San1 protein.

Since the substrate ΔssCL*myc contains the auxotrophic marker Leu2 growth tests were performed using strains either expressing nuclear or cytosol-localized San1 (Fig. 3.16).

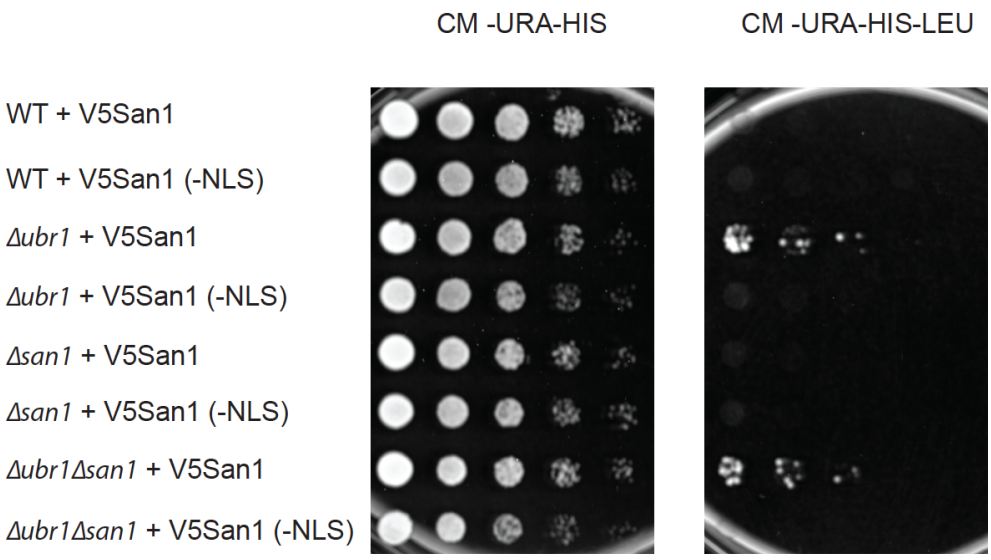

Figure 3.16: Cytosolic San1 rescues the *Δubr1* phenotype regarding steady state level of ΔssCL*myc. Growth tests were performed as described earlier using yeast strains expressing ΔssCL*myc from the *HIS5* marker-containing plasmid pIA1 and either expressing non-mutated San1 or cytosol-localized San1 encoded by the plasmids pSK146 or pIA16 both containing a *URA3* marker. The medium contained galactose for induction of expression of the San1 proteins. Medium lacking uracil and histidine was used for plasmid selection and served as control.

The growth tests imply that ΔssCL*myc is degraded independently of the coexpressed San1 construct seen by the absence of growth on plates lacking leucine (Fig. 3.16). The strain lacking the cytosolic E3 ligase Ubr1 and expressing functional San1 containing an NLS sequence for nuclear import is able to grow on medium lacking leucine indicating stabilization of the substrate ΔssCL*myc. As expected, the *Δsan1* strains expressing Ubr1 do not show any growth comparable to the wild type strain. The double deletion strain both lacking Ubr1 and San1 show similar growth when either expressing cytosolic or nuclear San1 indicating again for a non-San1-dependent degradation of the substrate ΔssCL*myc.

Further growth tests were performed for checking the influence of a functional RING domain of San1 on the steady state level of ΔssCL*myc in a *UBR1*-deficient yeast strain (Fig. 3.17).

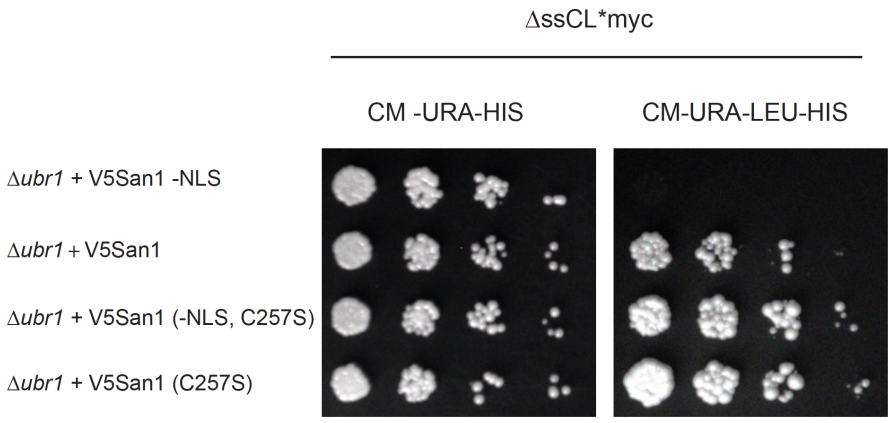

Figure 3.17: Cytosolic San1 deficient in a functional RING domain cannot rescue the *Δubr1* phenotype. Growth tests were performed as described before using a *Δubr1* strain expressing the substrate ΔssCL*myc from the histidine (*HIS5*) marker-containing plasmid pIA1 and either wild type San1 (V5San1) or functional San1 localized in the cytosol (V5San1-NLS) both mutated and non-mutated in the RING domain (C257S). The plasmids encoding the different San1 proteins contain a uracil (*URA3*) marker for plasmid selection.

Similar results could be observed as in the growth test in Fig. 3.16 using the *Δubr1* strains expressing either nuclear San1 (V5San1) or cytosolic San1 which is mutated in the NLS sequence (V5San1-NLS). Expression of cytosolic San1 rescues the *Δubr1* phenotype regarding steady state level of ΔssCL*myc (Fig. 3.17). When expressing non-functional cytosolic San1, growth on medium lacking leucine is visible corresponding to a high steady state level of ΔssCL*myc and lack of degradation respectively. As expected, similar growth can be observed when expressing mutated nuclear San1 again indicating no influence of the nuclear ubiquitin ligase San1 on ΔssCL*myc degradation. In addition, the growth of the *Δubr1* strain expressing functional nuclear localized San1 is increased compared to the strain expressing cytosolic San1. This result indicates again the dependency of substrate degradation on cytosolic components of the degradation machinery and the cytosolic localization of ΔssCL*myc. However, the growth of the strain expressing functional nuclear San1 on medium lacking leucine is slightly reduced compared to the non-functional San1-expressing strain.

In further experiments I examined the impact of a directed import of the substrate ΔssCL*myc into the nucleus on its degradation. In previous experiments it was shown that the steady state level and the stability of the substrate ΔssCL*myc is dependent on the cytosolic E3 ligase Ubr1. The substrate was now N-terminally fused to the nuclear localization signal (NLS) of the SV40 large T antigen consisting of the basic amino acid

stretch Pro-Lys-Lys-Lys-Arg-Lys-Val. As control, ΔssCL*myc was fused to a nuclear export signal (NES) consisting of the hydrophobic amino acid stretch Asn-Ile-Asn-Glu-Leu-Ala-Leu-Lys-Phe-Ala-Gly-Leu-Asp-Leu. In order to prevent a change of the substrates' fate according to the N-end rule the first two N-terminal amino acids of ΔssCL*myc are unchanged (Met-Ile). The steady state levels of the substrates were monitored using growth tests (Fig. 3.18).

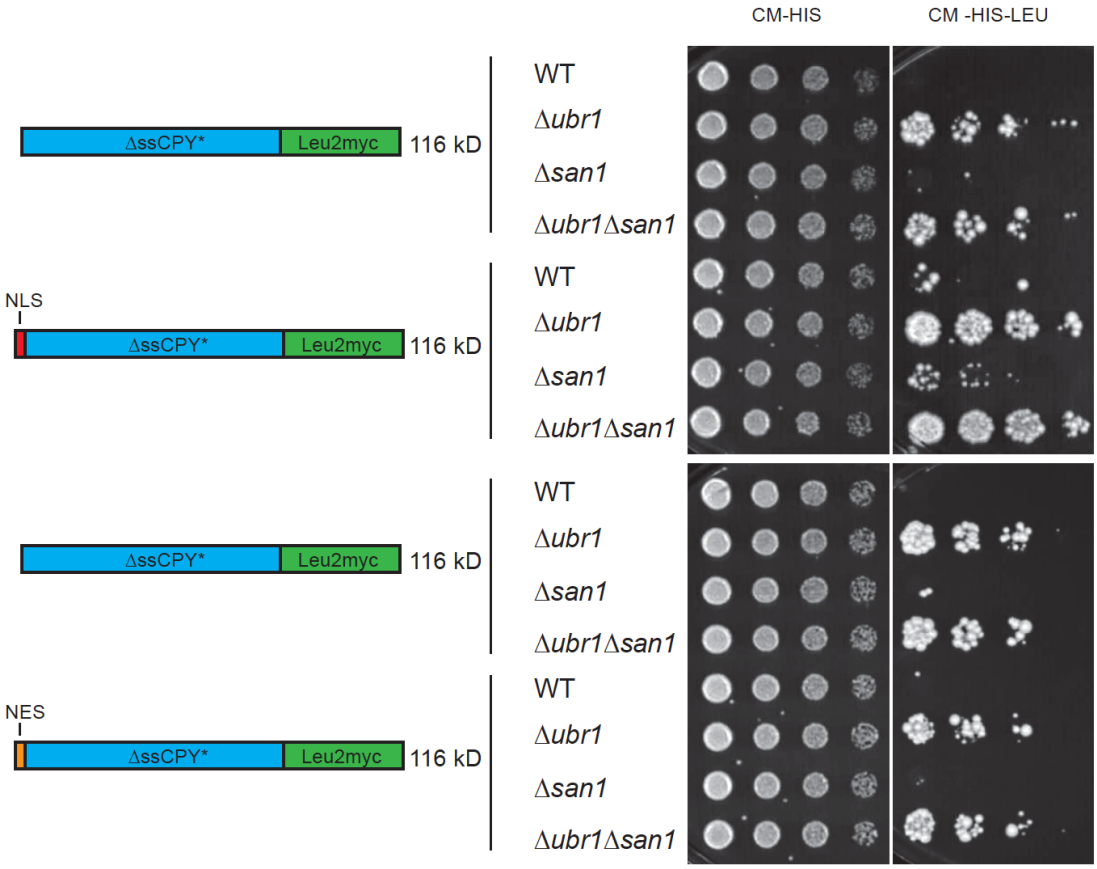

Figure 3.18: Fusion of an NLS sequence to the substrate ΔssCL*myc only slightly enhances the influence of San1 on substrate steady state level. Growth tests were performed using different yeast strains expressing either ΔssCL*myc or the NLS and NES-fused versions of ΔssCL*myc from pRS313-based plasmids containing a histidine marker. The steady state levels of the substrates were monitored using medium lacking leucine. Plates lacking only histidine served as controls, selecting for presence of the substrate-containing plasmids.

As expected from previous experiments the steady state levels of the substrate ΔssCL*myc seems to be similar in both the *Δubr1* and the *Δubr1Δsan1* strains seen by similar growth on

plates lacking leucine (Fig. 3.18). Fusion of an NLS sequence to the N-terminus of ΔssCL*myc causes a slight enhancement of growth of the strain only lacking San1 compared to the original substrate ΔssCL*myc indicating some nuclear import of the substrate NLSΔssCL*myc. In contrast, the growth phenotypes on medium lacking leucine of the substrates ΔssCL*myc and NESΔssCL*myc do not differ confirming the independency of the steady state level of ΔssCl*myc on the nuclear E3 ligase San1.

3.3.3 New model substrates for studying the influence of San1 in cytoplasmic protein quality control

In Tab. 3.1 it was indicated that substrate degradation of substrates with a high molecular mass like ΔssCL*myc or orphan Fas2 is not dependent on nuclear San1. To evaluate the influence of substrate size on the selection of either Ubr1 or San1 as ubiquitin ligase for further degradation a new set of model substrates was designed which are all derivatives of the cytosol-localized substrate ΔssCPY*Leu2myc (ΔssCL*myc). The two newly generated substrates contain shortened versions of the ΔssCPY* part either lacking the amino acids 16-204 (F1ΔssCL*myc) or the amino acids 16-398 (F2ΔssCL*myc), (Fig. 3.19). The N-termini were not changed in order to prevent a change in substrate stability according to the N-end rule. In both substrates the Leu2myc part is still active allowing the performance of growth tests using medium lacking leucine.

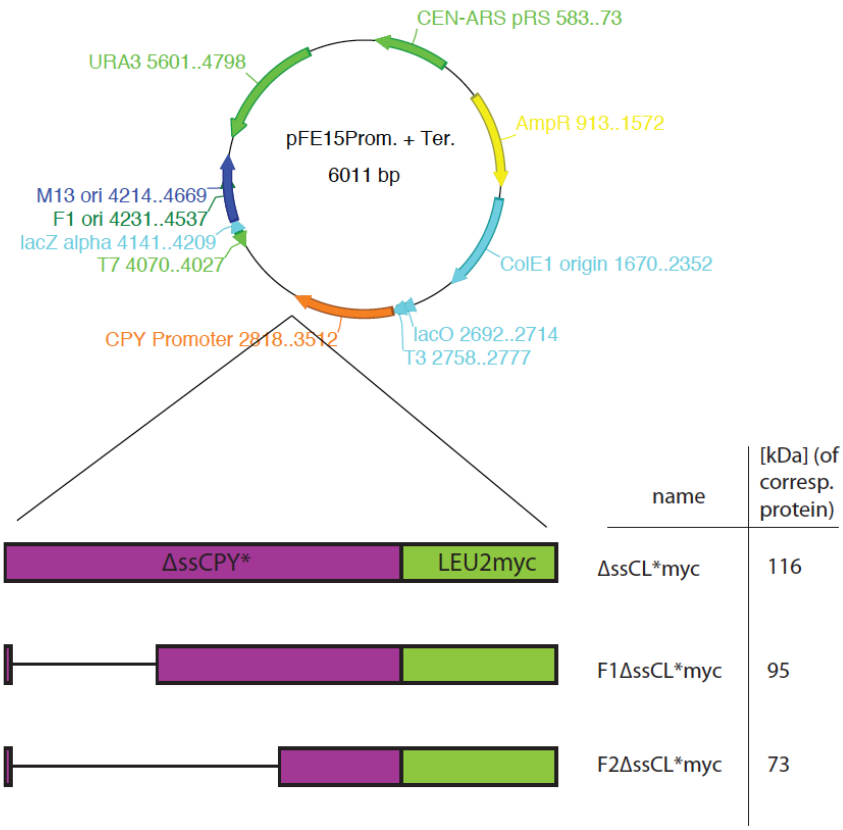

Figure 3.19: General map of the plasmids coding for the shortened versions of ΔssCL*myc. The two plasmids expressing the shortened versions of ΔssCL*myc (pIA2, pIA3) were derived from the plasmid pFE15. The N-termini of the two shortened model substrates are unchanged.

Since the two new model substrates F1ΔssCL*myc and F2ΔssCL*myc both contain the Leu2 protein growth tests were performed comparing the steady state levels of the two substrates with the original ΔssCL*myc substrate in strains either lacking the E3 ligases Ubr1 or both Ubr1 and San1 (Fig. 3.20).

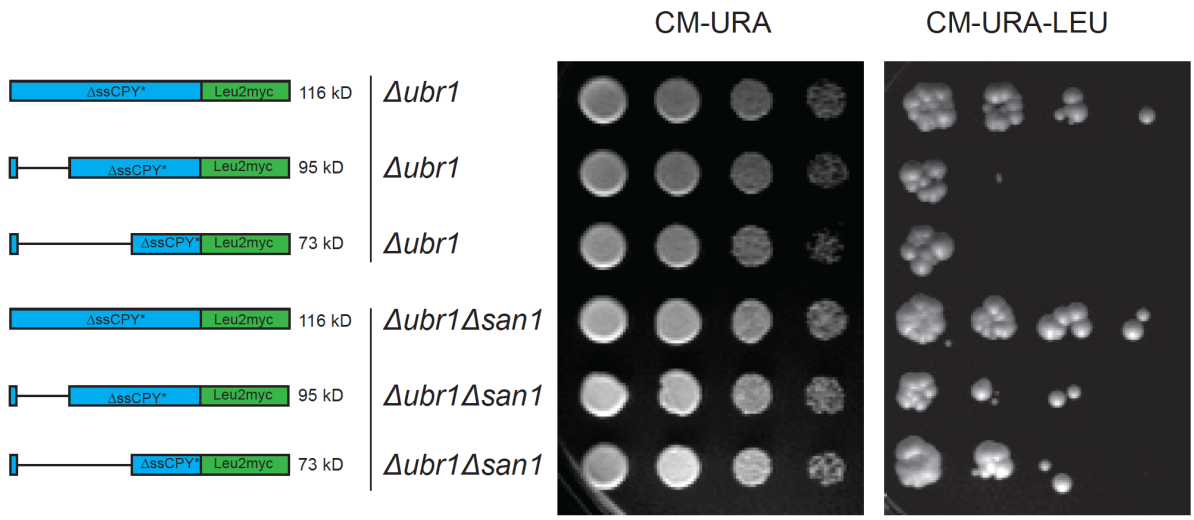

Figure 3.20: The steady state levels of the model substrates F1ΔssCL*myc and F2ΔssCL*myc show increased dependency on the nuclear E3 ligase San1. Growth tests were performed as described above using the *Δubr1* and *Δubr1Δsan1* yeast strains each expressing three different substrates all containing the Leu2 marker protein. The steady state levels of the three different substrates were monitored using agar plates lacking leucine. Plates only lacking uracil served as controls selecting only for presence of the three substrate-expressing plasmids.

As can be seen in Fig. 3.20 the steady state levels of the full-length substrate ΔssCL*myc do not differ between the *Δubr1* single deletion and the *Δubr1Δsan1* double deletion strain confirming the results of the growth test shown in Fig. 3.18. The steady state levels of the two truncated versions of ΔssCL*myc are considerably increased in the double deletion mutant *Δubr1Δsan1* strain compared to the *Δubr1* single deletion strain indicating an influence of San1 on the steady state level of the two truncated substrates. The influence of San1 on F2ΔssCL*myc protein level is even somewhat stronger than on the bigger version F1ΔssCL*myc.

Next, I was interested in the influence of the fusion of NLS and NES sequences to the N-termini of the substrate F2ΔssCL*myc on the San1-dependency of its steady state level as had been done for the full-length substrate ΔssCL*myc seen in Fig. 3.18.

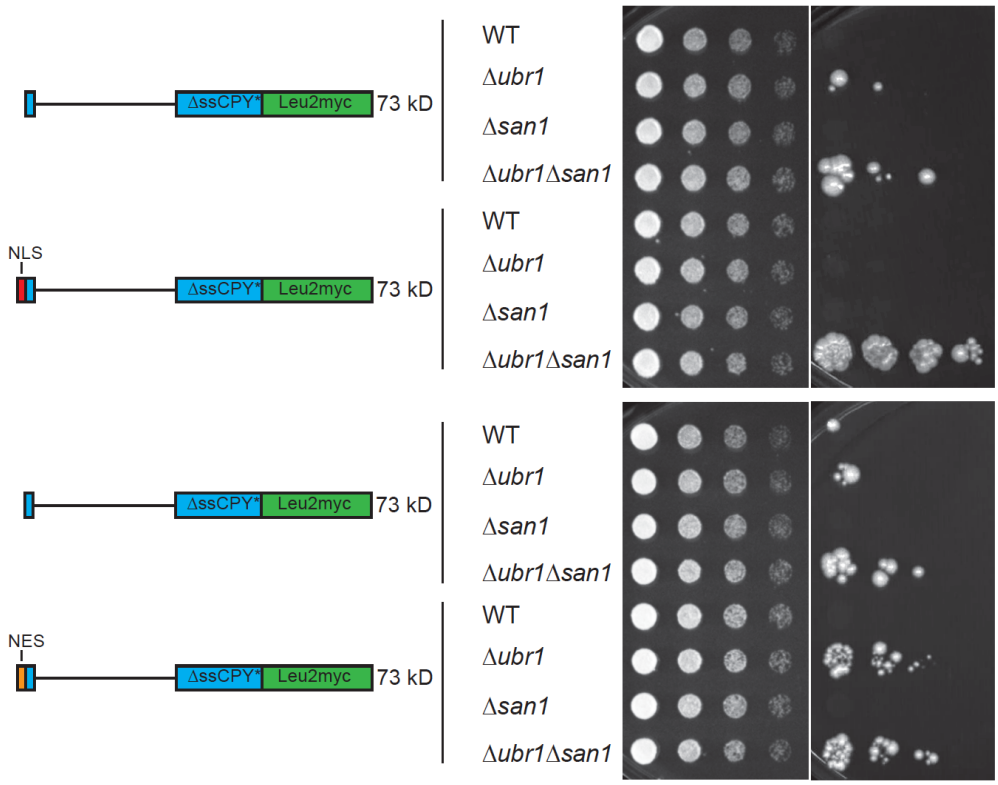

Figure 3.21: Fusion of an NLS sequence to the N-terminus of the substrate F2ΔssCL*myc causes an increase of substrate steady state level only in the *Δubr1Δsan1* strain. Growth tests were performed using different yeast strains expressing F2ΔssCL*myc or the NLS and NES-fused versions of F2ΔssCL*myc from pRS313-based plasmids containing a histidine marker. The steady state levels of the substrates were monitored using agar plates lacking leucine. Plates only lacking histidine served as controls selecting only for presence of the substrate-expressing plasmids.

As shown previously in Fig. 3.18, the steady state level of the full-length substrate ΔssCL*myc fused to an NLS sequence hardly differs between the *Δubr1* single deletion and the *Δubr1Δsan1* double deletion strain. Interestingly, strains expressing the 73 kDa protein F2ΔssCL*myc fused to an NLS sequence behave quite different concerning growth on medium lacking leucine (Fig. 3.21). Neither a strain defective in Ubr1 nor in San1 shows growth, indicating degradation of the substrate NLS-F2ΔssCL*myc. However, a *Δubr1Δsan1* double deletion strain shows considerable growth, indicating Ubr1 and San1 as being responsible for elimination of 73 kDa NLS-F2ΔssCL*myc. As control, an NES sequence was fused to the N-terminus of F2ΔssCL*myc. As can be seen for the substrate NES-ΔssCL*myc (Fig. 3.18) no differences in growth on medium lacking leucine can be observed between the *Δubr1* and the *Δubr1Δsan1* double deletion strains (Fig. 3.21).

3.3.4 Solubility of the truncated model substrate F2ΔssCL*myc

In a recent study, Fredrickson *et al*. found that San1 targets exposed hydrophobicity of aberrant nuclear proteins for subsequent proteasomal degradation (Fredrickson *et al*, 2013b). As exposed hydrophobicity often correlates with aggregation tendency I wanted to check whether a difference in solubility of the two substrates might be the reason for increased San1-dependency of the steady state level of 73 kDa F2ΔssCL*myc compared to the 116 kDa substrate ΔssCL*myc. To address this question solubility assays were performed (Fig. 3.22).

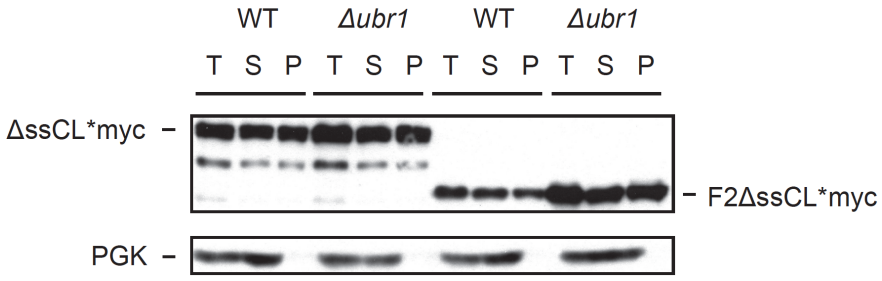

Figure 3.22: Both substrates ΔssCL*myc and F2ΔssCL*myc show similar solubility. For solubility assays exponentially growing cells expressing either ΔssCL*myc or F2ΔssCL*myc were harvested at an OD_{600} of 1.0, lysed and subjected to fractionation into soluble (S) and pellet (P) fractions. The total fractions (T) represent the precleared cell lysates prior to fractionation. PGK served as loading control and reference for a soluble protein.

When comparing the solubility of F2ΔssCL*myc with the solubility of the full length substrate ΔssCL*myc similar amounts of both substrates are found in the pellet (P) and soluble (S) fractions (Fig. 3.22). This indicates that the truncation of the misfolded ΔssCPY* part of the substrate F2ΔssCL*myc does not change the substrate's aggregation tendency.

3.3.5 Degradation of the new model substrates based on misfolded cytosolic ΔssCPY*

For further investigation of the San1-dependeny of substrate degradation a new set of model substrates were constructed consisting of one up to three misfolded cytosolic CPY versions. In addition, the new substrates do not contain an auxotrophic marker like Leu2 (Fig. 3.23).

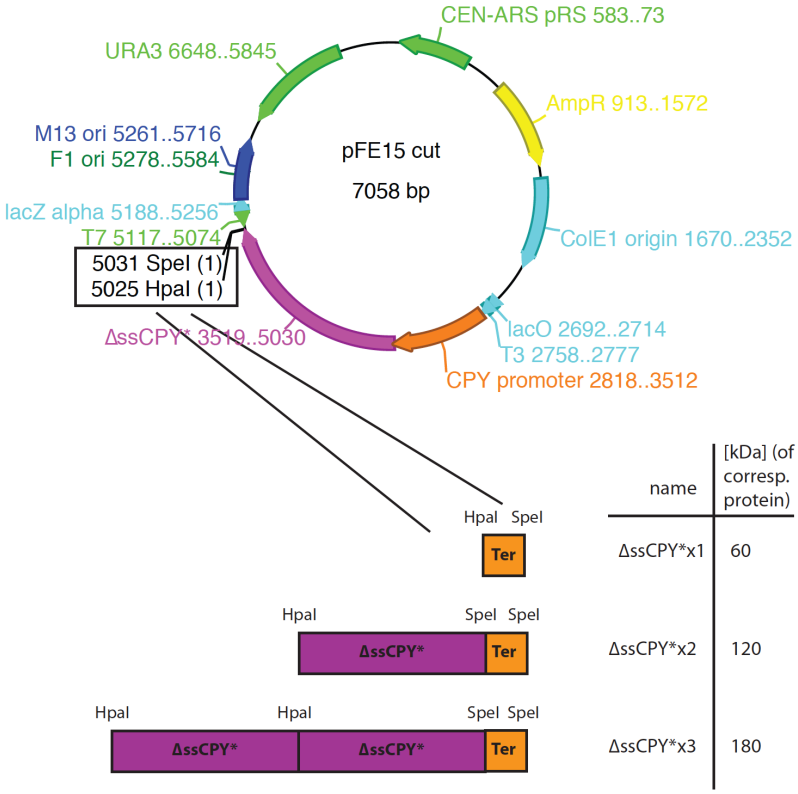

Figure 3.23: General plasmid map of the plasmids coding for the substrates consisting of one up to three repeats of cytoplasmic misfolded CPY* (ΔssCPY*). The three plasmids were derived from the plasmid pFE15. All three substrates are expressed under control of the *CPY* promoter. The size of corresponding substrates varies from 60 kDa corresponding to a single ΔssCPY* protein up to 180 kDa corresponding to a substrate consisting of three sequent ΔssCPY* proteins.

The three newly generated substrates do not contain any auxotrophic marker protein. Therfore, these substrates are not suitable for the performance of growth tests for determination of substrate steady state levels. Instead, cycloheximide chase experiments were performed in order to monitor substrate stability (Fig. 3.24).

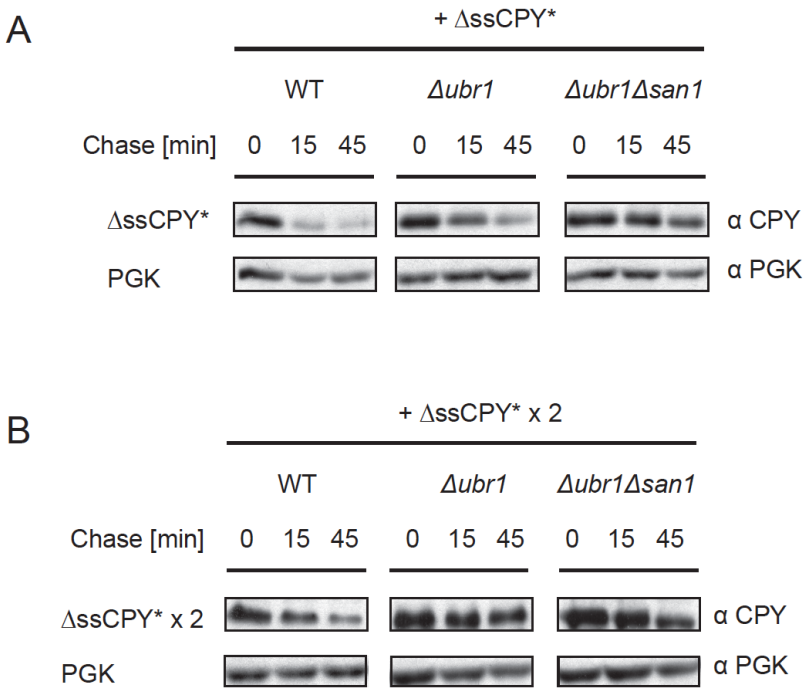

Figure 3.24: Doubling the molecular mass of ΔssCPY* by fusion with one extra ΔssCPY* protein abolishes the San1-dependency of degradation. Cycloheximide chase experiments were performed using yeast strains expressing either the substrate ΔssCPY* (A) or ΔssCPY*x2 (B) from the *URA3* marker-containing plasmids pIA19 and pIA20. Samples were taken at the indicated time points. PGK served as loading control.

As can be seen in Fig. 3.24 A the substrate ΔssCPY* is degraded in the wild type strain. In the strain lacking Ubr1 the substrate is still degraded but with an extended half-life. In the strain absent in both the E3 ligases Ubr1 and San1 the substrate is almost completely stable after 30 min indicating that ΔssCPY* can be imported into the nucleus for San1-dependent degradation. In contrast, the substrate ΔssCPY* x 2 shows similar degradation kinetics both in the *Δubr1* and *Δubr1Δsan1* strains indicating that this substrate with doubled molecular mass (120 kDa) remains in the cytosol for Ubr1-dependent degradation (Fig. 3.24 B). Preliminary results of the degradation kinetics of the substrate ΔssCPY* x 3 also exist (not

shown). The degradation of this substrate behaves like the degradation of the substrate ΔssCPY* x 2.

3.4. The previously unknown function of the Hsp31 chaperone family in cytoplasmic protein quality control

3.4.1 The deletion of genes encoding the Hsp31 chaperones causes an increased protein level of ΔssCL*myc

The Hsp31 chaperone family consists of the 4 members of cytoplasmically localized small chaperones Hsp31, Hsp32, Hsp33 and Hsp34. They belong to the DJ-1/ThiJ/PfpI superfamily which also includes as the most prominent member, the human protein DJ-1, which is involved in Parkinson's disease (Abou-Sleiman *et al*, 2003; Bonifati *et al*, 2003; Hague *et al*, 2003). In the *Saccharomyces cerevisiae* strain W303 used in this study the Hsp34 chaperone cannot be detected in the genome. The members of this chaperone family share high sequence homology (Fig. 3.25 A) caused by gene duplication events of the evolutionary parental Hsp31 gene. Because of the involvement of the human homologue DJ-1 in the neurodegenerative Parkinson's disease and also the discovery of a genetic interaction between one member of the Hsp31 family, Hsp34, and the ubiquitin ligase Ubr1 in yeast (Costanzo *et al*, 2010), the Hsp31 family members are promising candidates for studying their influence on the protein quality control of cytoplasmic proteins.

Growth tests were performed as described earlier using the misfolded cytoplasmic model substrate ΔssCL*myc expressed in yeast strains lacking chaperones of the Hsp31 family (Fig. 3.25 B).

A

```
Hsp32          MTPKRALISLTSYHGPFYKDGAKTGVFVVEILRSFDIFEKHGFEVDFVSETGGFGWDEHY 60
Hsp33          MTPKRALISLTSYHGPFYKDGAKTGVFVVEILRSFDIFEKHGFEVDFVSETGGFGWDEHY 60
Hsp31          MAPKKVLLALTSYNDVFYSDGAKTGVFVVEALHPFNTFRKEGFEVDFVSETGKFGWDEHS 60
               *:**:.*::****:. **.*********** *:.*:**.*.*********** ******

Hsp32          LPKSFIGGEDKMNFETKNSAFNKALARIKTANEVNASDYKIFFASAGHGALFDYPKAKNL 120
Hsp33          LPKSFIGGEDKMNFETKNSAFNKALARIKTANEVNASDYKVFFASAGHGALFDYPKAKNL 120
Hsp31          LAKDFLNGQDETDFKNKDSDFNKTLAKIKTPKEVNADDYQIFFASAGHGTLFDYPKAKDL 120
               *.*.*:.*:*: :*:.*:* ***:**:***.:****.**::********:********:*

Hsp32          QDIASKIYANGGVIAAICHGPLLFDGLIDIKTTRPLIEGKAITGFPLEGEIALGVDDILR 180
Hsp33          QDIASKIYANGGVIAAICHGPLLFDGLIDIKTTRPLIEGKAITGFPLEGEIALGVDDILR 180
Hsp31          QDIASEIYANGGVVAAVCHGPAIFDGLTDKKTGRPLIEGKSITGFTDVGETILGVDSILK 180
               *****:*******:**:**** :**** * ** *******:****.  **  ****.**:

Hsp32          SRKLTTVERVANKNGAKYLAPIHPWDDYSITDGKLVTGVNANSSYSTTIRAINALYS 237
Hsp33          SRKLTTVERVANKNGAKYLAPIHPWDDYSITDGKLVTGVNANSSYSTTIRAINALYS 237
Hsp31          AKNLATVEDVAKKYGAKYLAPVGPWDDYSITDGRLVTGVNPASAHSTAVRSIDALKN 237
               :::*:*** **:* *******: **********:******. *::**::*:*:** .
```

B

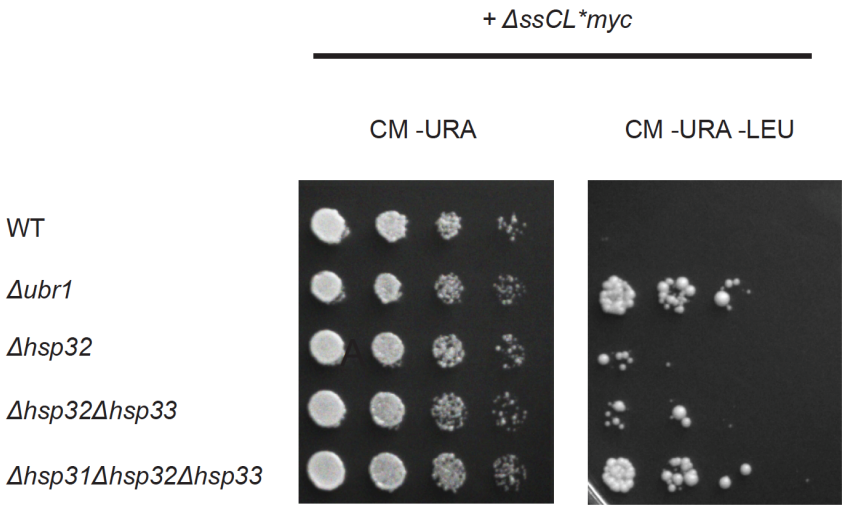

Figure 3.25: Absence of the three members of the Hsp31 chaperone family causes a growth phenotype similar to lack of the E3 ligase Ubr1. A. Sequence alignment of the three members of the Hsp31 chaperone family in *Saccharomyces cerevisiae* W303 show a sequence homology of 99 % between Hsp32 and Hsp33 and both compared to Hsp31 a homology of about 70 %. B. Growth tests of strains absent either in members of the Hsp31 family or the ubiquitin ligase Ubr1 all expressing the cytoplasmic misfolded protein ΔssCL*myc under control of the *CPY* promoter (plasmid pFE15). The growth tests were performed as described earlier.

The growth tests based on the substrate ΔssCPY*Leu2myc (ΔssCL*myc) which contains the auxotrophic marker protein Leu2 reveal an influence of the Hsp31 chaperone family on the steady state level of the substrate. Growth of the *Δhsp31Δhsp32Δhsp33 (Δhsp31-33)* strain on

medium lacking leucine is comparable to the growth of the *Δubr1* strain. The wild type strain hardly shows any growth on medium lacking leucine because of fast substrate degradation. On plates only lacking uracil the presence of the plasmid expressing ΔssCL*myc is monitored. All strains show similar growth. Former experiments already showed Ubr1 as being involved in the degradation process of misfolded ΔssCL*myc (Fig. 3.3).
In order to show that the misfolded part of the used model substrate is responsible for both the growth effects seen for the *Δubr1* and *Δhsp31Δhsp32Δhsp33* deletion strains the strains were transformed with a plasmid encoding the protein Leu2myc. Growth tests were performed as described for the strains expressing ΔssCL*myc (Fig. 3.26).

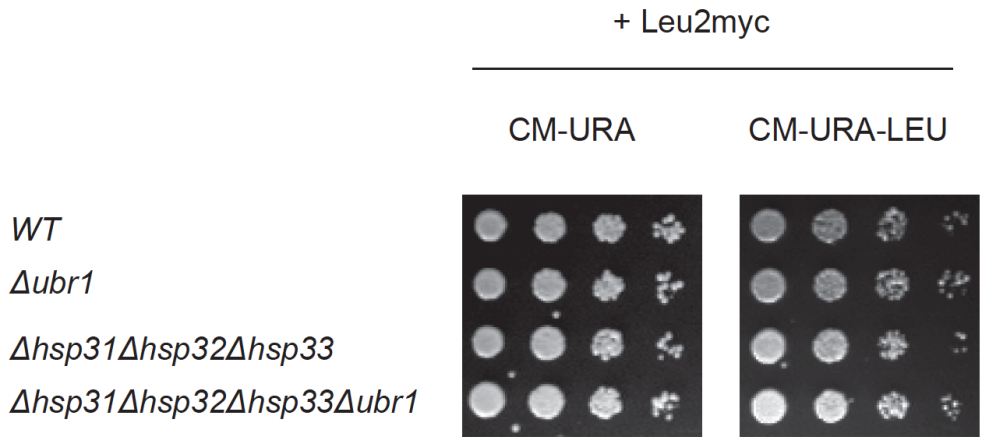

Figure 3.26: The protein Leu2myc, - part of the model substrate ΔssCL*myc -, is stable. Growth tests were performed using Leu2myc as substrate. The Leu2myc-expressing plasmid (pIA13) is derived from the plasmid pFE15. Leu2myc is expressed under control of the *CPY* promoter.

As can be seen in Fig. 3.26 the substrate Leu2myc consisting of functional myc-tagged β-isopropylmalate dehydrogenase (Leu2) is stable. Even in the wild type strain a high steady state level of Leu2myc can be observed. Deletion of either the E3 ligase Ubr1 or the genes encoding the Hsp31 chaperones does not further increase the steady state level of Leu2myc. This result indicates that the dependency of the steady state level of ΔssCL*myc on the Hsp31 chaperone family and Ubr1 is not dependent on the Leu2myc part of the model substrate but resides in the misfolded character of ΔssCPY* part of the substrate ΔssCL*myc.

3.4.2 Absence of the Hsp31 chaperone family forces a delayed entry of strains into diauxic shift

It was shown that members of the Hsp31 chaperones are strongly upregulated during the diauxic shift (Miller-Fleming *et al*, 2014). At diauxic shift nutrients become limiting resulting in the reduction of growth rate. Cells entering the diauxic shift are stressed due to lack of nutrients and accumulation of toxic molecules caused by increased oxidative stress. Therefore stress response pathways are induced including upregulation of several heat shock proteins. To investigate effects of the deletion of genes coding for the Hsp31 chaperones on cell growth, growth of different yeast strains was monitored using photometric measurement at 600 nm (OD_{600}), (Fig. 3.27).

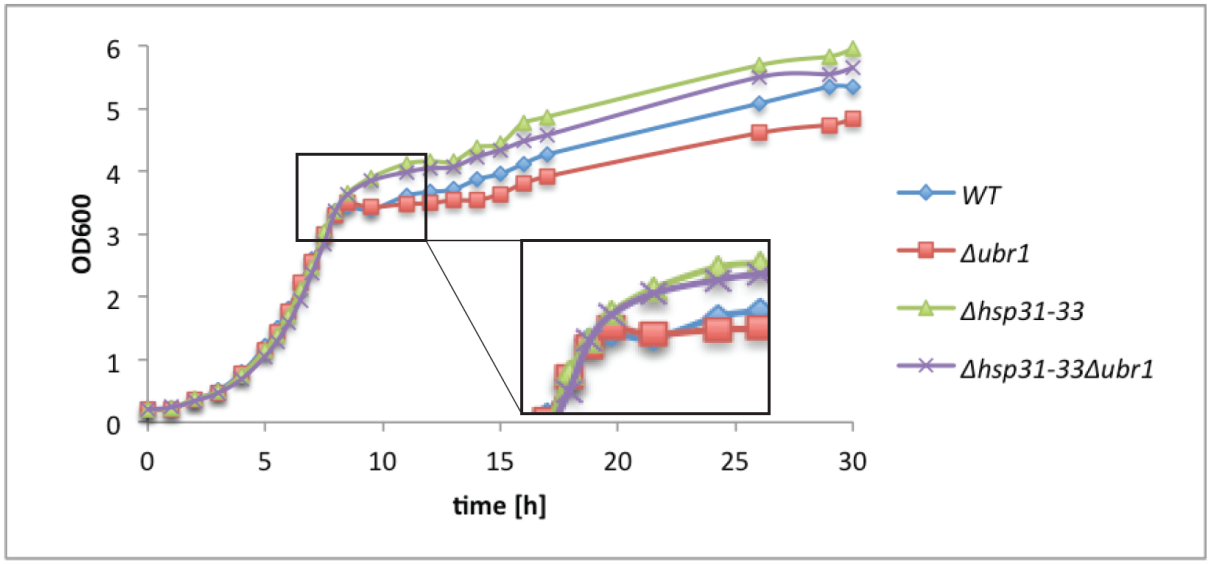

Figure 3.27: Strains deleted in the genes coding for the Hsp31 chaperones show delayed entry into diauxic shift. Overnight yeast cultures of selected strains were diluted with YPD medium to an OD_{600} of 0.2 and further incubated at 30 °C. At indicated time points the optical density was measured at 600 nm. The absorption values were plotted against the incubation time in order to generate growth curves.

As can be seen in Fig. 3.27 growth of the four strains is indistinguishable during the first 8 hours representing the exponential growth phase. In the wild type and *Δubr1* strains growth is

reduced after 8 hours representing the time point where nutrients become limiting (diauxic shift). The strains deleted in the genes coding for the Hsp31 chaperone family remain longer in the exponential phase. Then, 1 hour later the growth rates decrease in the *Δhsp31-33* and *Δhsp31-33Δubr1* strains. From that point the strains grow further with similar growth rates. The *Δubr1* strain shows reduced growth after exit from the exponential phase compared to the wild type strain. The negative growth effect of the *UBR1* deletion can be also seen in the *Δhsp31-33Δubr1* strain which shows reduced growth after diauxic shift compared to the *Δhsp31-33* strain.

3.4.3 The Hsp31 family acts in a pathway overlapping with Ubr1-mediated degradation

In order to address the question whether the Hsp31 chaperone family is involved in the same protein quality control pathway as the ubiquitin ligase Ubr1, an epistasis analysis was performed comparing both the *Δubr1* deletion and the *Δhsp31Δhsp32Δhsp33* deletion strains with a strain defective in both the E3 ligase Ubr1 and the Hsp31 chaperone family regarding the steady state level of ΔssCL*myc (Fig. 3.28).

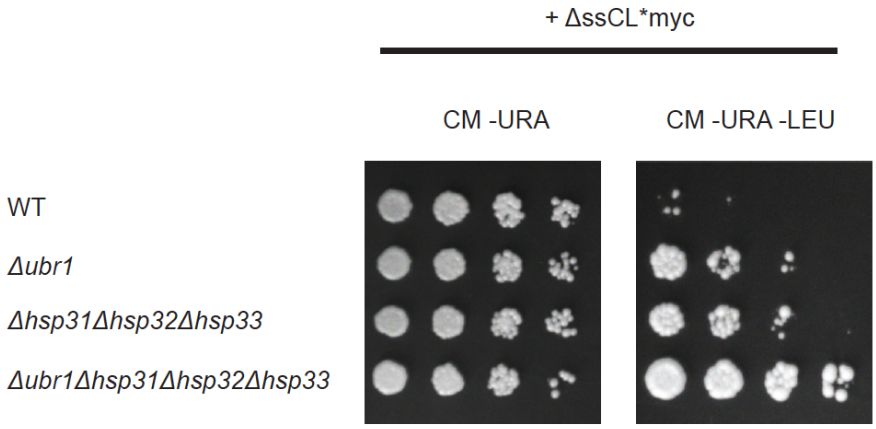

Figure 3.28: Ubr1 and the Hsp31 chaperone family have overlapping functions in regulating the steady state level of ΔssCL*myc. Growth tests were performed as described above comparing the strains absent in either the E3 ligase Ubr1 or the members of the Hsp31 chaperone family and the strain combining all the deletions.

As can be seen in Fig. 3.28 the strain combining the *UBR1* deletion with the deletion of the genes encoding the Hsp31 chaperones shows strongest growth on medium lacking leucine. This effect indicates that both Ubr1 and the Hsp31 chaperones are involved in two different pathways regulating the steady state level of ΔssCL*myc. To further confirm the existence of two different pathways plasmids were transformed into the four used yeast strains either overexpressing Ubr1 or the inactive Ubr1 RING mutant. Again, growth tests were performed with the corresponding strains all expressing the substrate ΔssCL*myc (Fig. 3.29).

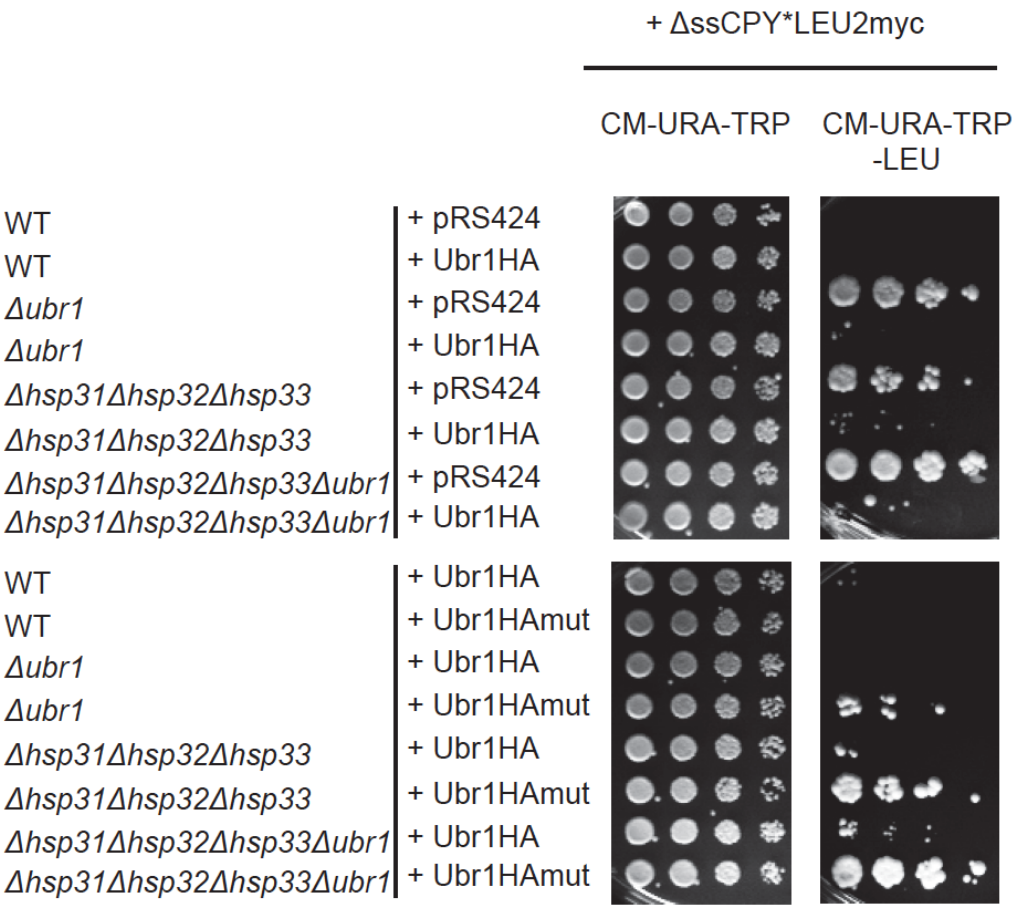

Figure 3.29: Expression of plasmid-encoded Ubr1 rescues the *Δhsp31-33* growth phenotype. Plasmids coding for either HA-tagged Ubr1 or the inactive Ubr1 RING-mutant or, as control, the corresponding empty plasmid (pRS424) were transformed into the used yeast strains. Ubr1HA and Ubr1HAmut were expressed under control of the *ADH1* promoter. The plasmids contain a tryptophan marker. All the used strains were additionally transformed with the substrate ΔssCL*myc encoding plasmid pFE15.

Overexpression of functional Ubr1, but not the RING mutant of Ubr1 which is defective in substrate ubiquitination, compensate the lack of the chaperones of the Hsp31 family (Fig. 3.29). The *Δhsp31-33Δubr1* strain transformed with either the plasmid coding for the Ubr1 RING mutant or the corresponding empty plasmid (pRS424) show strongest growth on medium without leucine corresponding to the highest steady state levels of ΔssCL*myc in these strains. Wild type strains hardly show any growth on CM-URA-TRP-LEU plates independent of the transformed Ubr1 plasmids. All the strains show similar growth on plates lacking both tryptophan and uracil selecting only for the presence of each plasmid pair.

A corresponding experiment was performed using an Hsp31-expressing plasmid transformed into the 4 different deletion strains which were also used in the experiment above. Hsp31 is expressed like Ubr1 before from a high copy plasmid (pRS426). The Hsp31-expressing plasmid carries a *URA3* marker for selection. The substrate ΔssCL*myc is expressed from a plasmid containing a *HIS3* marker (pIA1), (Fig. 3.30).

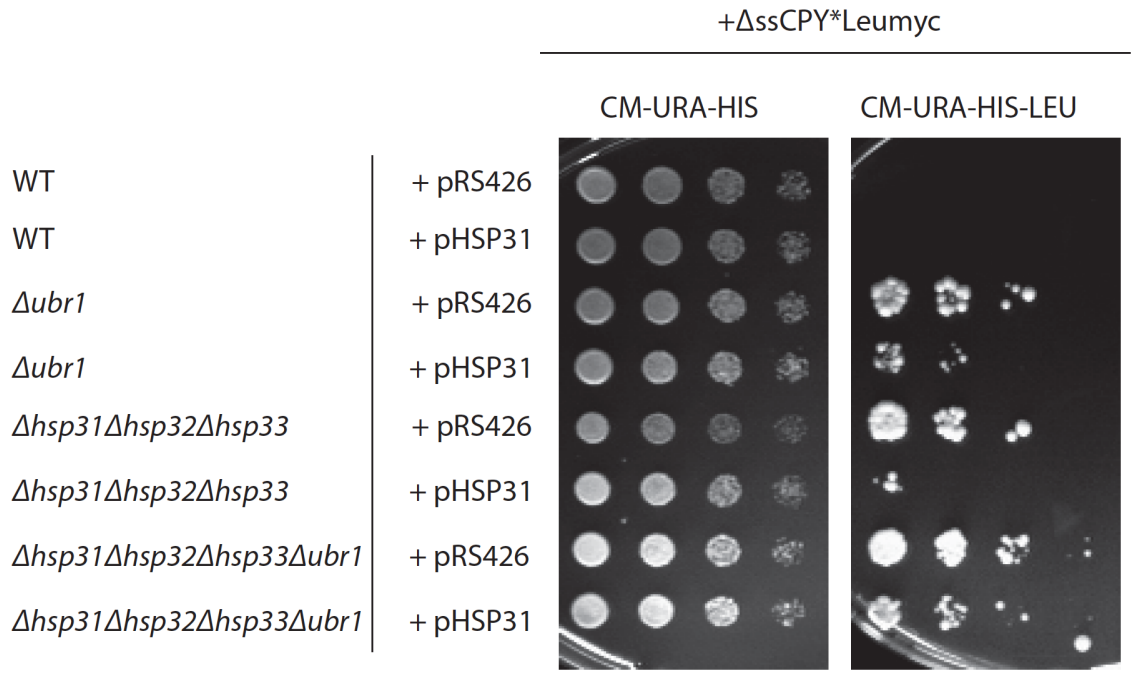

Figure 3.30: Expression of plasmid-encoded Hsp31 can partially rescue the *Δubr1* growth phenotype. A high-copy plasmid encoding Hsp31 under control of its native promoter and the corresponding empty plasmid (pRS426) were transformed into the used yeast strains. These plasmids carry a *URA3* marker gene for selection. In addition, all the transformed strains express the substrate ΔssCL*myc from a *HIS3* marker-containing plasmid (pIA1).

As can be seen in Fig. 3.30 the ΔssCL*myc-expressing strain deleted in both *UBR1* and genes coding for the Hsp31 chaperone family shows strongest growth on medium without leucine when additionally transformed with the empty plasmid pRS426. Expression of Hsp31 in the quadruple deletion strain and *Δubr1* strain can partially compensate the lack of Ubr1 as reasoned by the reduced growth of the corresponding strains on medium without leucine when compared to the strains transformed only with the empty plasmid pRS426. The wild type strain does not show any difference in growth when either transformed with the Hsp31-encoding plasmid or the corresponding empty vector. Growth on plates lacking uracil and histidine was used for monitoring the presence of each plasmid pair.

3.4.4 The influence of the Hsp31 chaperone family on substrate steady state level is stationary phase-dependent

As it is known from former publications, members of the Hsp31 chaperone family are expressed after diauxic shift under conditions of nutrient limitation (Miller-Fleming *et al*, 2014; Skoneczna *et al*, 2007). In order to analyse whether the influence of the Hsp31 chaperones on the steady state level of ΔssCL*myc is indeed restricted to late growth phases equal amounts of cells were harvested both in exponential and stationary growth phase, lysed and subjected to SDS-PAGE and immunoblotting.

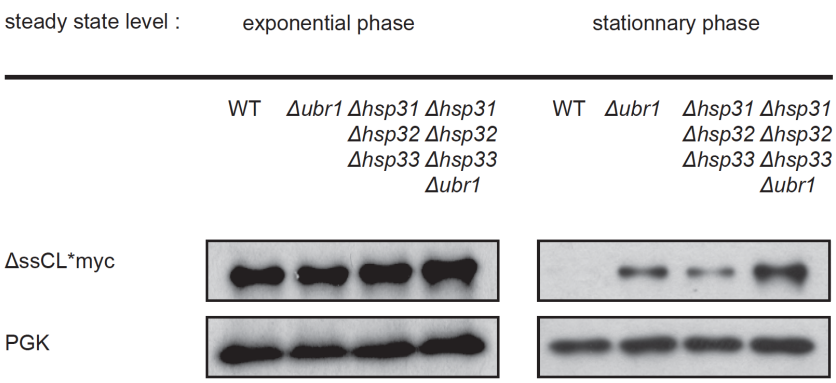

Figure 3.31: The influence of the Hsp31 chaperone family on the steady state level of ΔssCL*myc is stationary phase-dependent. In exponential growth phase and in stationary phase three OD_{600} of cells were harvested, lysed and subjected to TCA precipitation before resolubilization in SDS urea sample buffer. The samples were loaded on SDS gels prior to Western blot and immunodetection. The substrate ΔssCL*myc was detected using c-Myc antibody. PGK served as reference protein.

The steady state levels of the substrate ΔssCL*myc in exponential growth phase are similar in all used strains and are not influenced by the absence of either the E3 ligase Ubr1 or the members of the Hsp31 chaperone family (Fig. 3.31). The protein levels of the housekeeping protein 3-phosphoglycerate kinase (PGK) also show no differences in the different deletion strains. In contrast, in stationary phase, hardly any substrate is detectable in the wild type strain whereas in the *Δubr1* and *Δhsp31Δhsp32Δhsp33* strains an increase of the steady state levels of ΔssCL* can be detected. The highest substrate level is visible in the quadruple deletion strain combining deletions of *UBR1* and of the genes coding for the members of the Hsp31 chaperone family. Again, the protein levels of PGK in stationary phase show no differences in the used yeast strains. The results fit to the results of the growth tests seen in Fig. 3.28.

3.4.5 Influence of the Hsp31 chaperone family on the degradation kinetics of ΔssCL*myc

It was already shown in Fig. 3.4 that the E3 ligase Ubr1 is essential for degradation of the substrate ΔssCL*myc. In order to check whether also the Hsp31 chaperone family influences the degradation kinetics of ΔssCL*myc pulse chase experiments were performed. For efficient radioactive labelling of the substrate exponentially growing cells had to be used (Fig. 3.32).

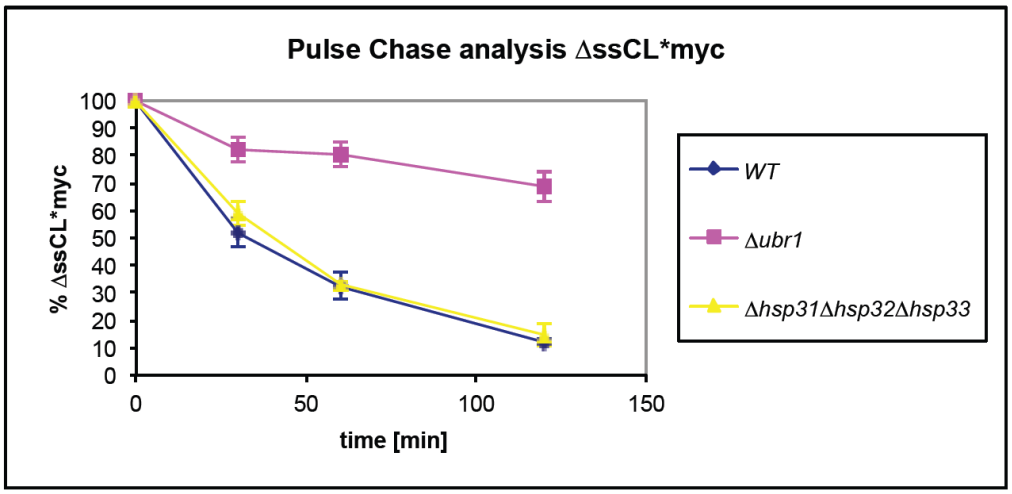

Figure 3.32: The degradation kinetics of ΔssCL*myc is not altered in exponentially growing cells in absence of the Hsp31 chaperone family. Pulse chase experiments were done with exponentially growing yeast cells expressing ΔssCL*myc. Cells were labelled with radioactive methionine before addition of non-labelled methionine to the medium. Cells were lysed at the indicated time points. Proteins were immunoprecipitated and separated by SDS-PAGE for further analysis using a PhosphorImager (Storm 860, Molecular Dynamics). Plotted data represent the mean values of three independent experiments. Error bars indicate the standard error of the mean.

In the wild type situation the substrate is degraded very fast whereas in the strain lacking the E3 ligase Ubr1 the substrate ΔssCL*myc is dramatically stabilized confirming previous results. Deletion of genes coding for the Hsp31 family members shows no decrease in degradation. The degradation kinetics looks similar to the wild type strain (Fig. 3.32). In

retrospect, this is not surprising as the Hsp31 family is strongly upregulated upon diauxic shift.

3.4.6 Influence of the Hsp31 chaperones on yeast N-end rule substrates

Before the discovery of Ubr1 as the E3 ligase involved in ubiquitination of misfolded cytosolic proteins (Eisele and Wolf, 2008; Heck *et al*, 2010; Nillegoda *et al*, 2010) Ubr1 was only known as the E3 ligase of the N-end rule pathway responsible for ubiquitination of proteins according to the identity of the N-terminal amino acid residue of the respective protein (Bachmair *et al*, 1986; Varshavsky, 2011). To address the question whether Ubr1 and the Hsp31 chaperone family have also overlapping functions on the stability and steady state levels of N-end rule substrates the steady state levels of the classical N-end rule substrates Arg-βGal and Arg-Ura3 were monitored. These two substrates are initially expressed as N-terminal fusion proteins with ubiquitin (Ub) but then cotranslationally deubiquitinated resulting in the N-terminal exposure of the first amino acid after the ubiquitin amino acid sequence, in this case arginine. Proteins with arginine at their N-termini are classified as type 1 N-end rule substrates. The substrate Arg-Ura3 is a functional Ura3 enzyme essential for uracil biosynthesis, therefore allowing the performance of growth tests on medium lacking uracil (Fig. 3.33 A). The corresponding plasmid contains a tryptophan marker. The substrate Arg-βGal consists of the functional enzyme β-galactosidase allowing the performance of activity tests using the substrate X-Gal which is converted via β-galactosidase into a blue dye (Fig. 3.33 B).

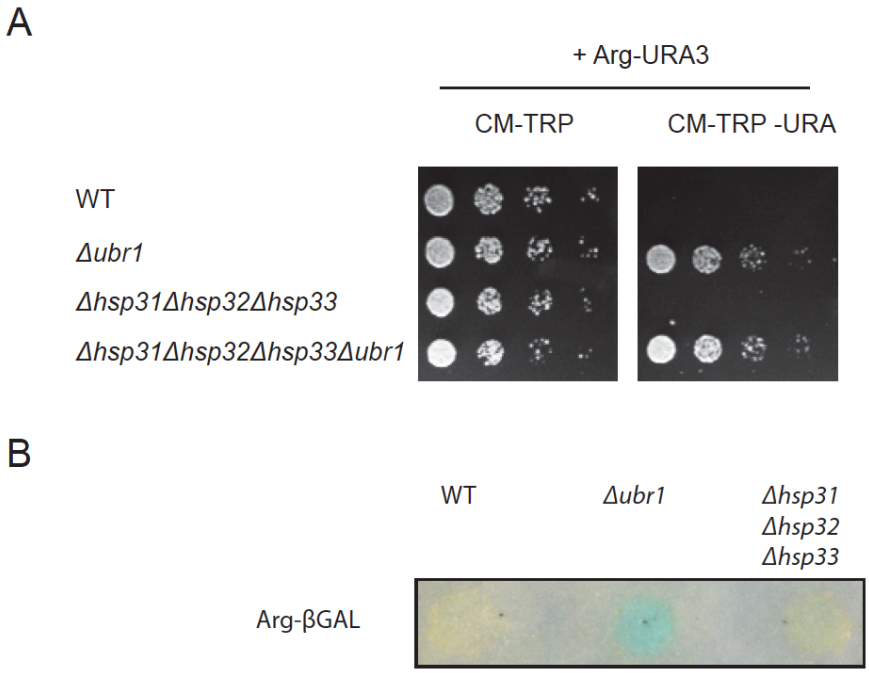

Figure 3.33: The Hsp31 chaperone family does not influence the steady state levels of classical type 1 N-end rule substrates. A. Growth tests were performed with the type 1 N-end rule substrate Arg-Ura3 initially expressed as fusion protein DHFR-HA-Ub-Arg-URA3HA and then released as Arg-Ura3HA after cotranslational deubiquitination. Steady state levels of Arg-Ura3 were monitored using agar plates lacking uracil. B. A β-galactosidase filter lift assay was performed with strains transformed with a plasmid expressing the type 1 N-end rule substrate Arg-βGal. Initially, the substrate is expressed as a fusion protein Ub-ArgβGal which is cotranslationally deubiquitinated. βGal (β-galactosidase) is an enzyme converting the substrate X-Gal into a blue dye.

Fig. 3.33 A shows that there is no visible difference in growth between the wild type strain and the *Δhsp31Δhsp32Δhsp33* strain expressing the substrate Arg-Ura3. This is in contrast to the growth tests performed with the same strains but expressing the misfolded model substrate ΔssCL*myc. When expressing ΔssCL*myc the *HSP31-33* deletions cause an enhancement of growth on medium lacking leucine (Fig. 3.25 B). The β-galactosidase activity assay also shows no difference between the Arg-βgal-expressing wild type and *Δhsp31-33* strains. Therefore, the Hsp31 chaperone family does not seem to influence the steady state levels of both model type 1 N-end rule substrates.

3.4.7 Influence of N-degrons on the steady state level of ΔssCL*myc

The substrate ΔssCL*myc does not contain a classical N-degron because of the methionine encoded by the start codon ATG at position one. Methionine does not represent a type 1 or type 2 destabilizing residue. Since the N-end rule substrates used in the experiments described above do not contain misfolded domains I was interested in the question whether an N-degron at the N-terminus of ΔssCL*myc can abolish the influence of the Hsp31 chaperone family on the steady state level of the misfolded substrate. For this purpose two substrates based on ΔssCL*myc were generated either exposing arginine as type 1 destabilizing residue or isoleucine as type 2 destabilizing residue at the N-terminus of ΔssCL*myc. This was achieved by N-terminal fusion of ΔssCL*myc with ubiquitin followed by arginine or isoleucine. As mentioned above, ubiquitin is cotranslationally cleaved off and therefore either arginine or isoleucine are exposed at position one of corresponding substrates. The generated substrates were used for growth tests as described above (Fig. 3.34).

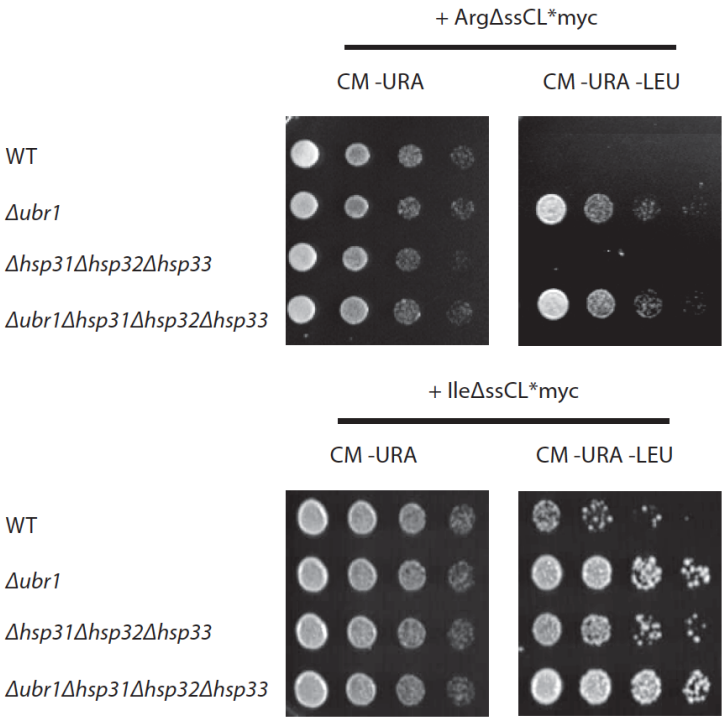

Figure 3.34: N-degrons alter the steady state level of the substrate ΔssCL*myc in strains lacking the Hsp31 chaperones. Growth tests were performed using ΔssCL*myc which is N-terminally fused to either Ub-Arg generating an type 1 N-degron or Ub-Ile generating a type 2 N-degron. The growth tests were performed as described above.

The growth tests performed with strains expressing the substrate ArgΔssCL*myc do not show differences in growth between the wild type and the *Δhsp31-33* strains in medium lacking leucine (Fig. 3.34). Also growth of the *UBR1* deletion strain and the quadruple deletion strain is identical indicating that the Hsp31 chaperone family has no influence on the steady state level of ΔssCL*myc fused to the type 1 N-degron arginine. In contrast, fusion of the type 2 N-degron isoleucine to ΔssCL*myc leads to an enhanced steady state level of the corresponding substrate when expressed in the *Δhsp31-33* deletion strain compared to the wild type strain.

3.4.8 Influence of the Hsp31 chaperones on the ERAD-L substrate CTL*myc

Next, the influence of the Hsp31 chaperones on the steady state levels of misfolded proteins of the secretory pathway was analysed. For this purpose, the ER membrane-localized substrate CTL*myc was used which consists of ER-lumenal misfolded carboxypeptidase Y (CPY*), a transmembrane domain of yeast Pdr5 protein and a cytosolic Leu2 domain (Fig. 3.35) allowing the performance of growth tests comparable to cytosolic misfolded substrate ΔssCL*myc (Medicherla *et al*, 2004). It is known that ERAD-L substrates like CTL*myc are ubiquitinated by the E3 ligase Der3/Hrd1 (Bordallo *et al*, 1998). Therefore, the *Δder3/hrd1* strain served as control strain.

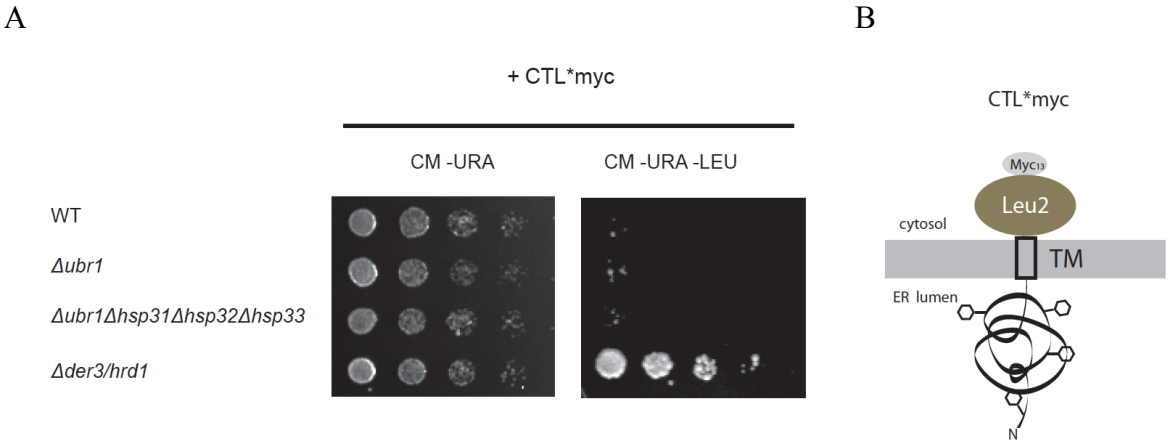

Figure 3.35: The steady state level of the ERAD-L substrate CTL*myc is not influenced by the Hsp31 chaperones. A. Topology of the misfolded ERAD-L substrate CTL*myc. The substrate is composed of misfolded carboxypeptidase Y (CPY*) residing in the ER lumen, a transmembrane domain of yeast Pdr5 and the Leu2 protein localized in the cytosol. B. Growth tests were performed using yeast strains transformed with the *URA3*-marker containing plasmid pBM10 expressing the ERAD-L substrate CTL*myc under control of the *GAL4* promoter. Growth on CM-URA medium served as control.

In Fig. 3.35 the known influence of the Der3/Hrd1 E3 ligase on CTL*myc stability can be clearly confirmed. The *Δder3/hrd1* strain transformed with the plasmid encoding CTL*myc shows enhanced growth on medium lacking leucine compared to the wild type strain where hardly any growth can be detected. The cytosolic E3 ligase Ubr1 as well as the Hsp31 chaperones seem not to be involved in the quality control pathway of CTL*myc indicated by the wild type-like phenotype.

3.4.9 Involvement of the Hsp31 chaperones on misfolded cytosolic substrates which are delivered into the nucleus for degradation

As shown previously, the substrate ΔssCL*myc is degraded in a Ubr1-dependent manner (Fig. 3.4). Furthermore, it was shown that the stability of the truncated version of the model substrate ΔssCL*myc (F2ΔssCL*myc) is partly dependent on nuclear San1 implying a nuclear import process prior to its degradation (Figs. 3.20, 3.21). The Hsp31 chaperones reside in the yeast cytosol. Therefore it was interesting to compare, as control of the cytosolic

localization of the Hsp31 chaperones, the steady state levels of both ΔssCL*myc and the truncated substrate F2ΔssCL*myc in yeast strains deficient in the Hsp31 chaperone family (Fig. 3.36).

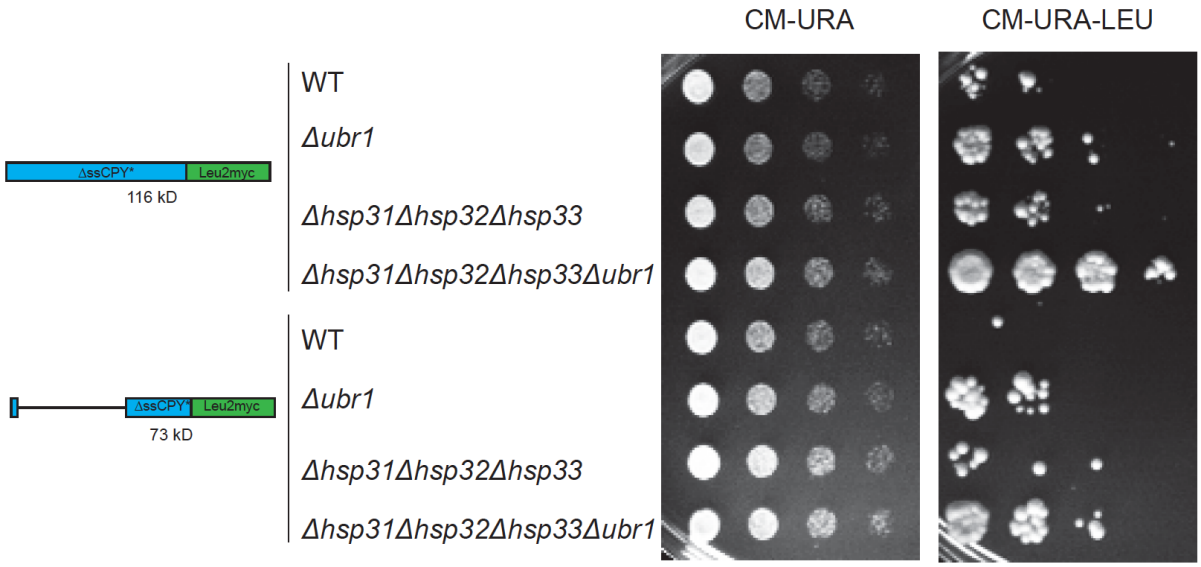

Figure 3.36: The Hsp31 chaperones have a somewhat decreased influence on the steady state level of misfolded cytosolic substrates capable of entering the nucleus for degradation. Growth tests were performed as described above. Each strain was transformed with plasmids either encoding ΔssCL*myc (pFE15) or a truncated form of the substrate F2ΔssCL*myc deleted in the amino acids 16 to 398 (pIA3) resulting in a reduction of molecular mass of 42 kDa. The N-terminus is unchanged. All the plasmids carry a *URA3* selection marker.

Previous results have already shown that the steady state level of the substrate ΔssCL*myc in the *Δubr1* strain is comparable to that of the strain deleted in the genes coding for the Hsp31 chaperones (Fig. 3.28). The same results are observable in Fig. 3.36. The quadruple deletion strain combining the deletions of *HSP31-33* and *UBR1* shows enhanced growth compared to the *Δubr1* or *Δhsp31-33* strains. Strains expressing a truncated version of ΔssCL*myc (F2dssCL*myc) which is deleted in the amino acids 16 to 398 show decreased dependency of the steady state level on the Hsp31 chaperones. This can be deducted from the decreased growth of the *Δhsp31-33* strain when compared to the *Δubr1* strain, both expressing the truncated substrate F2ΔssCL*myc (Fig. 3 36). Also, the steady state level of the substrate

F2ΔssCL*myc in the quadruple deletion strain *Δhsp31-33Δubr1* is only slightly increased as compared to the *Δubr1* strain.

3.4.10 Influence of the Hsp31 chaperones on the solubility of ΔssCL*myc

As shown in Fig. 3.7 the Hsp70 chaperones of the Ssa type are important for keeping misfolded cytoplasmic proteins in a soluble state for subsequent degradation via the ubiquitin-proteasome system. To check whether the Hsp31 chaperones influence the solubility of ΔssCL*myc solubility assays were performed using yeast cells from both growth phases, exponential and stationary phase.

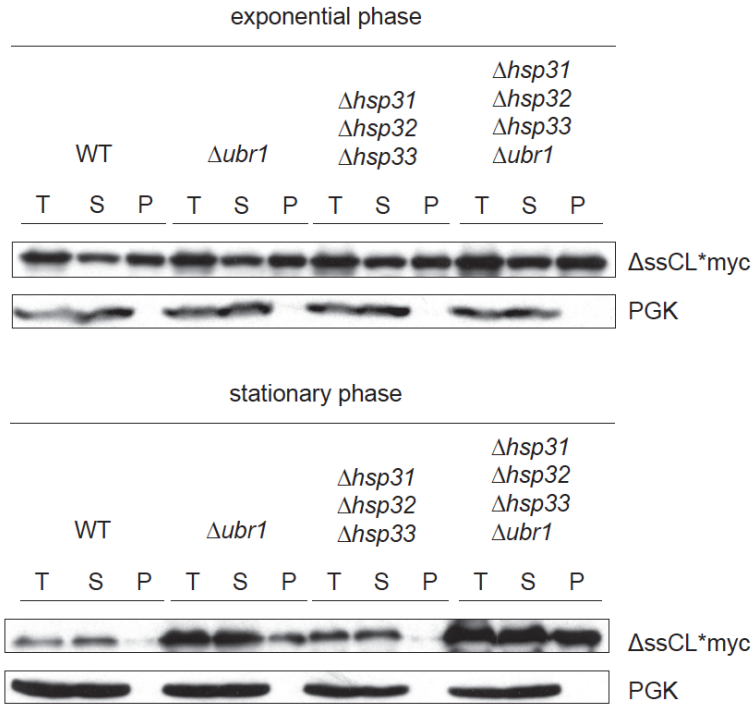

Figure 3.37: Absence of the Hsp31 chaperone family does not influence the solubility of ΔssCL*myc when Ubr1 is present. For the solubility assays either exponentially or stationary growing cells were harvested, lysed and subjected to fractionation into soluble (S) and pellet (P) fractions. The total fractions (T) represent the precleared cell lysates prior to fractionation. PGK served as loading control and reference for a soluble protein.

The solubility of the substrate ΔssCL*myc in exponential growth phase is not influenced by deletion of either *UBR1* or the genes encoding the Hsp31 chaperone family (Fig. 3.37). For all the tested strains similar substrate amounts are found in the pellet (P) and soluble fractions (S). In contrast, in stationary phase cells in the wild type strain more substrate is found in the soluble fraction as compared to exponential phase. This is probably due to a higher concentration of Hsp70 chaperones of the Ssa type in stationary phase cells. The substrate signal in the total protein fractions (T) is strongest for the *Δhsp31-33Δubr1* strain. This observation fits to the results shown in Fig. 3.31. In the strain defective in the Hsp31 chaperones and the wild type strain the solubility of the substrate is similar indicating that the Hsp31 chaperones are neither involved directly nor indirectly in keeping ΔssCL*myc soluble when Ubr1 is present. In the strain absent in both Ubr1 and the Hsp31 chaperones the ratio between the amount of ΔssCL*myc in the soluble and in the pellet fractions is shifted towards the pellet fraction (P). This indicates that the Hsp31 chaperones influences the solubility of ΔssCL*myc in stationary growth phase when Ubr1-dependent degradation is absent.

3.4.11 Influence of the vacuole on the Hsp31 chaperone-mediated quality control pathway

The vacuolar pathway represents the second cellular proteolytic pathway beside the ubiquitin-proteasome system. In order to figure out the influence of the vacuole on the protein quality control pathway concerning the model substrate ΔssCL*myc yeast strains were produced lacking the vacuolar protein Pep4. Pep4 is the vacuolar aspartyl protease called proteinase A responsible for maturation of vacuolar proteinases as well as general protein degradation in the vacuole (Ammerer *et al*, 1986).

Growth tests were performed comparing yeast strains harbouring the *PEP4* gene with strains deleted in *PEP4* (Fig. 3.38). All strains used express the model substrate ΔssCL*myc.

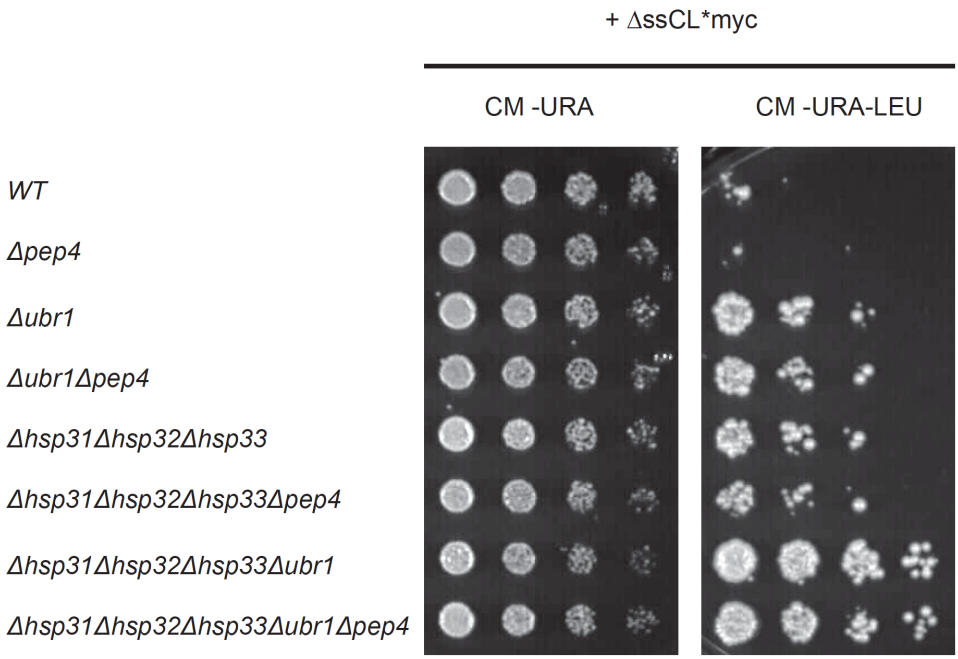

Figure 3.38: The vacuole is not involved in either the Ubr1-dependent degradation pathway or the Hsp31 chaperone-mediated quality control. Growth tests were performed as described above using yeast strains carrying a *PEP4* deletion. All strains were transformed with the plasmid pFE15 encoding the model substrate ΔssCL*myc. Medium lacking uracil served as control selecting only for the presence of the plasmid.

As can be seen in Fig. 3.38 an additional *PEP4* deletion has no influence on the growth of corresponding yeast strains on medium lacking leucine indicating that the vacuolar pathway is not involved in the quality control of ΔssCL*myc.

3.4.12 Influence of the Hsp31 chaperone family on rapamycin-induced inhibition of TOR signalling

The TOR signalling pathway is a central, conserved signalling pathway in eukaryotic cell responsible for controlling cell growth and proliferation dependent on nutrient availability (Rohde *et al*, 2001; Schmelzle and Hall, 2000; Thomas and Hall, 1997). Under nutrient-rich conditions TOR-signalling is active where it activates translation initiation and cell cycle progression in G1 phase (Barbet *et al*, 1996). At diauxic shift the nutrient limitation induces inhibition of the TOR pathway which results in a general down-regulation of translation

(Barbet *et al*, 1996; Berset *et al*, 1998). In addition, the TOR pathway is involved in cell growth under stress conditions like oxidative stress or heat stress. In non-stressed cells TOR prevents nuclear localization of the transcription factors Msn2/Msn4 (Beck and Hall, 1999). Msn2/Msn4 affect transcription of hundreds of genes after nuclear import in response to general stress conditions. It has also been shown that Hsp32 and Hsp33 expression is Msn2/4-dependent (Venters *et al*, 2011). Autophagy is also induced when cells are starved or treated with rapamycin, respectively (Noda and Ohsumi, 1998), whereas in cells growing in nutrient-rich conditions autophagy is blocked (Kamada *et al*, 2000).

Addition of rapamycin to growing cells inhibits the TOR pathway thus inhibiting cell cycle progression and autophagy. Since members of the Hsp31 chaperone family are expressed under conditions of nutrient limitation the influence of the Hsp31 chaperones on rapamycin tolerance/ sensitivity of corresponding yeast strains was examined.

For examining the rapamycin sensitivity of yeast strains deleted in the Hsp31 chaperones, the Ubr1 E3 ligase or the vacuolar proteinase A (Pep4), the yeast strains were grown overnight and plated out on YPD plates containing 100 nM rapamycin. The plates were incubated at 30 °C for approximately one week. In addition, the same strains were grown overnight on YPD plates containing the solvent DMSO either at 30 °C or for investigating of the heat sensitivity of the used strains at 37 °C (Fig. 3.39).

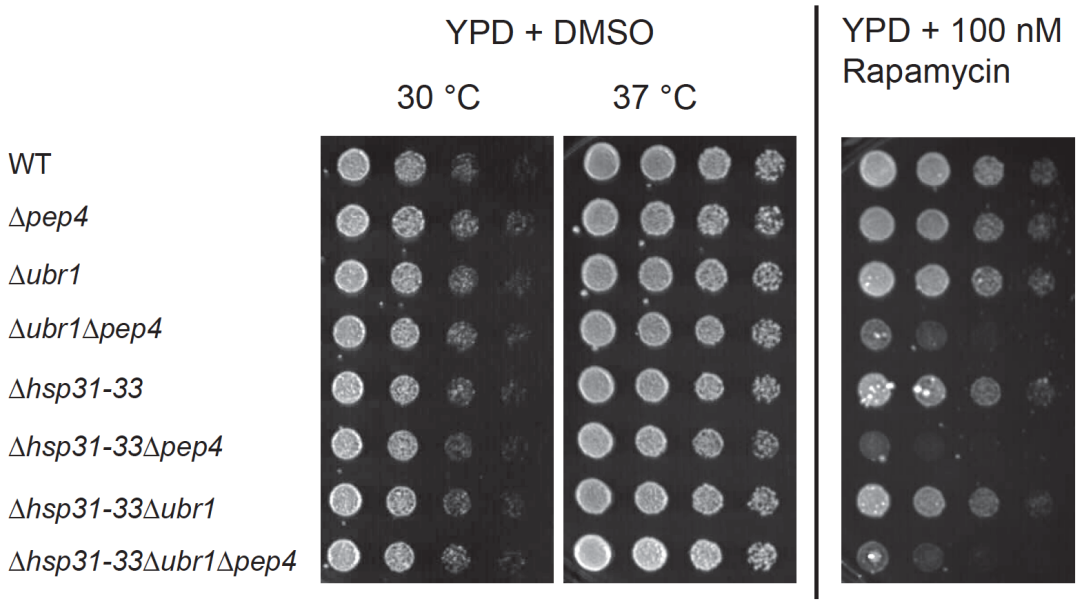

Figure 3.39: Absence of either Ubr1 or the Hsp31 family in combination with the *PEP4* deletion increases rapamycin sensitivity of corresponding yeast strains. Growth tests were performed using yeast strains either absent in the E3 ligase Ubr1 and/ or members of the Hsp31 family. Rapamycin sensitivity was compared between these strains and corresponding strains with an additional deletion of the *PEP4* gene. Growth on YPD plates for one day containing the solvent DMSO either at 30 °C or 37 °C served as control.

As can be seen in Fig. 3.39 growth of the eight yeast strains on medium containing only the solvent DMSO does not differ, both at 30 °C and 37 °C. At 37 °C all strains grow faster than at 30 °C. On rapamycin-containing YPD plates growth of the wild type strain is comparable to strains lacking the E3 ligase Ubr1, the vacuolar proteinase A (Pep4), the Hsp31 chaperones or the strain lacking both Ubr1 and the Hsp31 chaperones. Deletion of the *PEP4* gene in strains already lacking in the E3 ligase Ubr1 and/ or the Hsp31 chaperone family members causes a severe growth defect and therefore an increased rapamycin sensitivity of these strains.

3.4.13 The function of the Hsp31 chaperones in quality control of ΔssCL*myc is independent of their function in the oxidative stress response

It was published that Hsp31 expression is induced under conditions of oxidative stress in a *YAP1*-dependent manner (Skoneczna *et al*, 2007). *YAP1* codes for a transcription factor essential for oxidative stress tolerance (Kuge *et al*, 1997). Therefore, it was interesting to find out whether the growth effects on leucine-lacking medium seen for the *HSP31-33* deletion strain transformed with a ΔssCL*myc-encoding plasmid were due to a defective oxidative stress response. Strains lacking genes encoding the E3 ligase Ubr1 or the Hsp31 chaperone family were additionally deleted in *YAP1*. In addition, all the strains express the substrate ΔssCL*myc. Growth tests were performed making use of the auxotrophic marker leucine of the substrate. Plates containing hydrogen peroxide were used for confirming the presence of the *YAP1* deletion (Fig. 3.40).

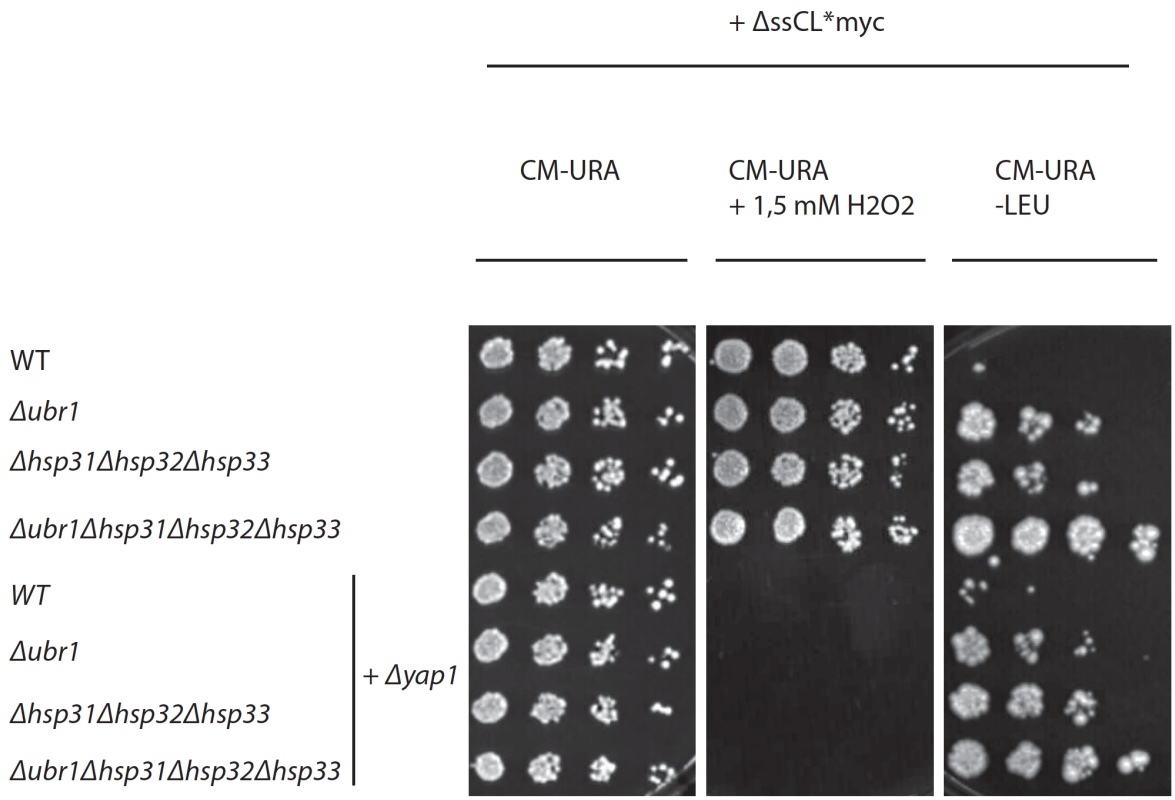

Figure 3.40: The oxidative stress response is not involved in Hsp31 chaperone-mediated quality control of ΔssCL*myc. Yeast strains transformed with the plasmid pFE15 encoding ΔssCL*myc were used for the growth tests performed as described earlier. Yeast strains possessing the *YAP1* gene were compared with *YAP1* deletion strains. Plates containing 1.5 mM hydrogen peroxide served as verification for the absence of Yap1. Medium lacking uracil served as control only selecting for the presence of the plasmid pFE15.

The plate containing hydrogen peroxide does not show any growth of strains containing the *YAP1* deletion confirming the identity of the yeast strains since Yap1 is the major player in oxidative stress response. Yap1 is therefore essential for survival of yeast strains treated with 1.5 mM hydrogen peroxide (Fig. 3.40). Only a slight enhancement of growth of the strain lacking the Hsp31 chaperone members compared to the *Δubr1* strain can be observed on plates lacking leucine when in addition Yap1 is missing. Generally, the growth phenotypes observed for the Yap1-expressing strains regarding growth on leucine-lacking plates is comparable to growth of corresponding strains lacking Yap1. In summary, these results indicate a main function of the Hsp31 chaperone family in quality control of ΔssCL*myc which is independent of the oxidative stress response.

3.4.14 Influence of the Hsp31 chaperone family on the quality control of the substrates LucLeu2myc and LucDMLeu2myc

In cycloheximide chase experiments it has been shown that the luciferase-based model substrates LucLeu2myc and LucDMLeu2myc are degraded in a Ubr1-dependent manner (Fig. 3.11). In order to confirm these results growth tests were performed making use of the auxotrophic marker Leu2 of the two luciferase-based substrates. In addition, growth tests were performed using strains lacking the members of the Hsp31 chaperone family in order to analyse the influence of the chaperones on the steady state levels of the two luciferase-containing substrates (Fig. 3.41).

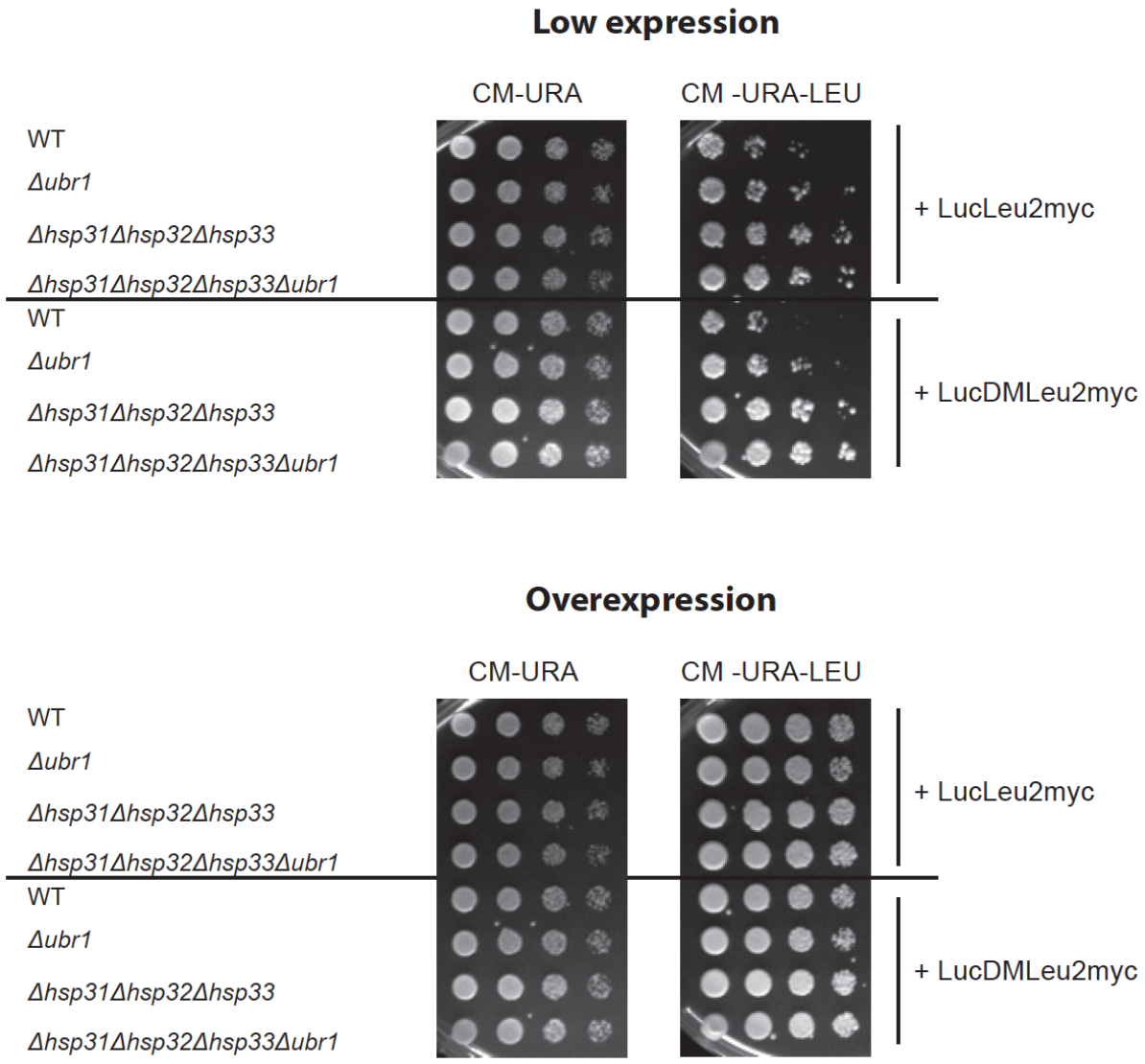

Figure 3.41: The steady state levels of LucLeu2myc and LucDMLeu2myc are influenced by the E3 ligase Ubr1 and the Hsp31 chaperone family. Growth tests were performed with yeast strains transformed with either the plasmid pIA14 or pIA15 coding for the substrates LucLeu2myc or LucDMLeu2myc respectively. Substrate levels were monitored using medium lacking leucine whereas medium only lacking uracil monitors the presence of the used plasmids. Low expression was achieved in glucose-containing medium (upper panel) whereas galactose-containing medium caused high induction of substrate expression due to the *GAL1* promoter (lower panel).

Low expression of the two substrates LucLeu2myc and LucDMLeu2myc upon use of glucose-containing medium results in visible growth differences of the used yeast strains on plates lacking leucine. The wild type strains exhibit the weakest growth on medium lacking

leucine corresponding to the lowest substrate steady state levels (Fig. 3.41 upper panel). Similar to the *Δubr1* strain expressing the misfolded substrate ΔssCL*myc, *Δubr1* cells containing the luciferase-based substrates show increased growth on medium lacking leucine indicating an involvement of Ubr1 in the degradation process. Using yeast strains lacking the Hsp31 chaperone family only small effects can be detected when expressing the substrate LucLeu2myc. Also the strain lacking both Ubr1 and the Hsp31 chaperones shows similar growth compared to the *Δhsp31-33* strain. The effect of Ubr1 was stronger when the steady state level of the mutated version of luciferase, LucDMLeu2myc, is monitored. Also the influence of the Hsp31 chaperone family on the steady state level of LucDMLeu2myc is enhanced as indicated by a clear increase of growth of the *Δhsp31-33* deletion strain compared to wild type. Overexpression of the substrates causes similar growth of all used yeast strains (Fig. 3.41 lower panel). Due to the high substrate protein concentration even in the wild type strain a high level of growth can be observed on plates lacking leucine. These results fit to the cycloheximide chase experiments where no differences in substrate degradation among the used strains can be observed when the substrates are overexpressed (Fig. 3.11).

The same strains expressing both the substrates LucLeu2myc or LucDMLeu2myc were used for luciferase activity assays. The assays were performed using cell lysates obtained either from exponential growing cells or stationary cells in glucose-containing medium.

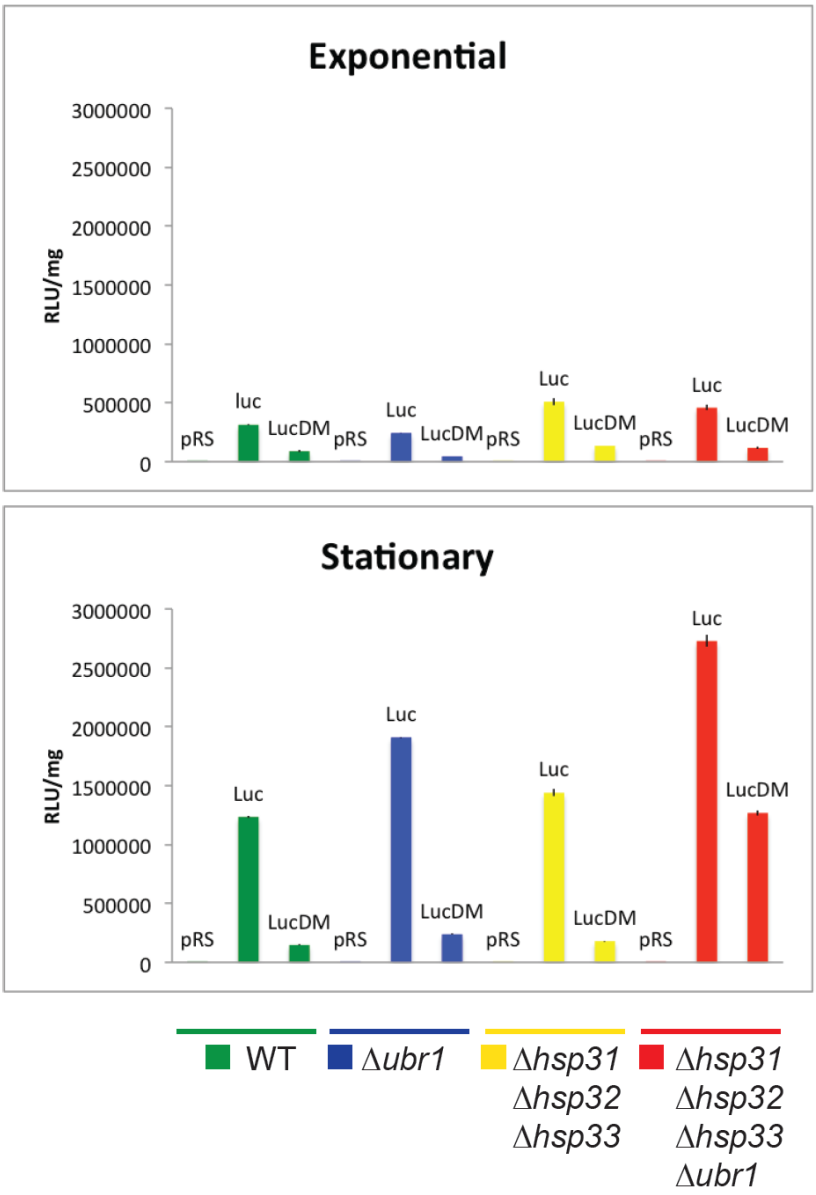

Figure 3.42: The cell lysate of a LucDMLeu2myc-expressing strain absent in both Ubr1 and the Hsp31 chaperones exhibits a dramatic increase of luciferase activity when grown to stationary phase. 10 OD_{600} of cells were harvested either in exponential phase at an OD_{600} of approximately 1.0 or after 72 h of growth at 30 °C prior to cell lysis and luciferase activity measurements. The relative light units (RLU) were normalized to the total protein concentration of each cell lysate by dividing by the protein concentration of each cell lysate. Plotted data represent the mean of three luciferase measurements. Error bars indicate the standard error of the mean.

In Fig. 3.42 it can be observed that the specific luciferase activity of the destabilized luciferase substrate LucDMLeu2myc (LucDM) is clearly decreased in all strains compared to the relative tightly folded LucLeu2myc substrate (Luc). As expected, cell lysates obtained from strains not expressing any Luciferase substrate (pRS) only display background luciferase

activity. In exponential phase the luciferase activities differ between the used strains in a way that is difficult to interpret. Therefore, the data obtained from exponential and stationary phase were used for generating Fig. 3.43 showing the change of luciferase activity after growth from exponential to stationary growth phase. In exponential growth phase the *Δubr1* strain shows the lowest luciferase activity for both substrates (Fig. 3.42 upper panel) whereas in cells grown to stationary phase a clear influence of Ubr1 on luciferase activity can be observed compared to the wild type strain. The influence of Ubr1 on luciferase activity is expected confirming previous results showing stabilization of LucLeu2myc and LucDMLeu2myc in strains lacking Ubr1 whereas degradation can be observed in corresponding wild type strains (Fig. 3.11). The stabilization of both substrates in the *Δubr1* strain is also visible in Fig. 3.43 where the change of luciferase activity after 72 h of growth is displayed. A clear difference in luciferase activity between exponential and stationary phase can be observed for the quadruple deletion strain *Δhsp31-33Δubr1*. When expressing the destabilized substrate LucDMLeu2myc the luciferase signal in exponential phase is relatively low whereas in stationary phase cells the signal dramatically increased in the *Δhsp31-33Δubr1* strain (Fig. 3.42).

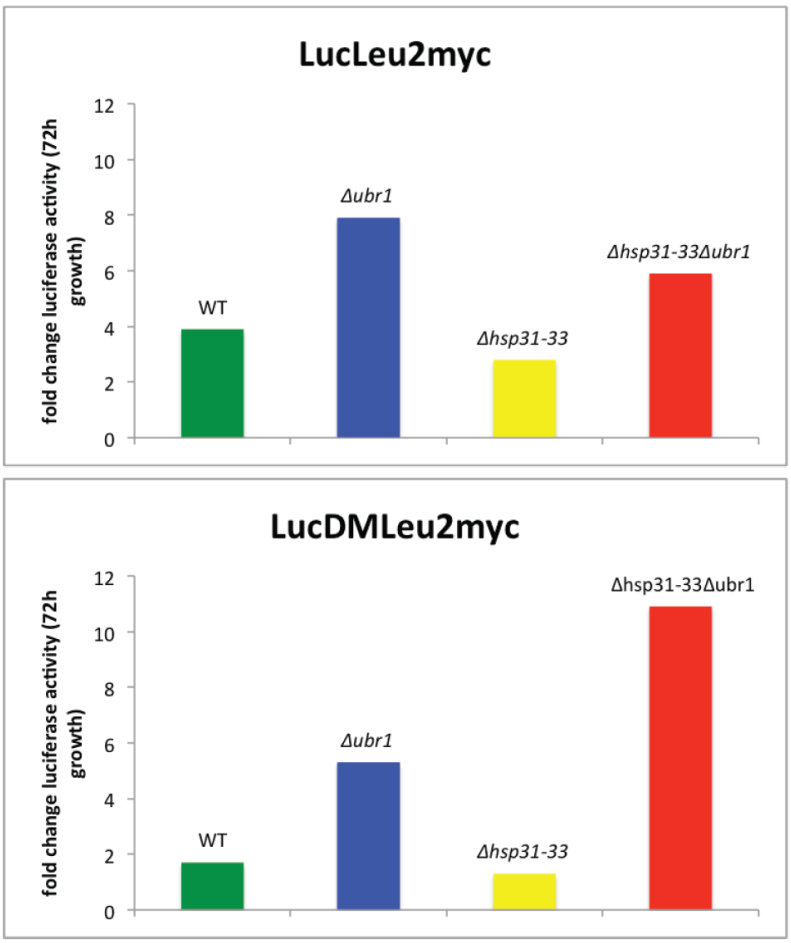

Figure 3.43: Cell growth from exponential to stationary phase (72 h growth) causes a strong increase of luciferase activity in the cell lysate obtained from the *Δhsp31-33Δubr1* strain expressing the mutated luciferase substrate LucDMLeu2myc. The data shown in Fig. 3.42 were used for generating this figure. The RLU/mg values obtained from stationary phase (Fig. 3.42) were divided by the corresponding values of the exponential phase. The resulting factor describes the change of luciferase activity after 72 h growth of corresponding yeast strains expressing either LucLeu2myc (upper panel) or the destabilized luciferase substrate LucDMLeu2myc (lower panel).

In Fig. 3.43 one can observe that in the wild type, *Δubr1* and *Δhsp31-33* strains the luciferase activity of the destabilized version LucDMLeu2myc increase only to a less extent compared to LucLeu2myc. This is probably due to increased degradation of LucDMLeu2myc compared to LucLeu2myc. This can also be observed in degradation kinetics displayed in Fig. 3.11. Also from growth tests one may conduct that the steady state levels of LucLeu2myc in the *Δubr1* and wild type strains are more similar than those of the LucDMLeu2myc substrate. Here, growth of the *Δubr1* strain expressing LucDMLeu2myc is stronger on medium lacking leucine compared to the wild type strain (Fig. 3.41). The results for the strains lacking the

Hsp31 chaperones are surprising. Whereas the ratio of increase in luciferase activity after 72 hours of growth among the wild type, *Δubr1* and *Δhsp31-33* strains is similar for both luciferase substrates it is not the case for the quadruple deletion strain *Δhsp31-33Δubr1*. For this strain expressing LucLeu2myc it can be observed that the change of luciferase activity after entry into stationary phase is in between the *Δubr1* and *Δhsp31-33* strain. In contrast, for the LucDMLeu2myc-expressing *Δhsp31-33Δubr1* strain the luciferase activity increases more than ten fold. This indicates a great influence of the Hsp31 chaperones on the steady state level of instable or misfolded proteins when the ubiquitin ligase Ubr1 is missing.

3.5 Protein quality control of the cytoplasmic fatty acid synthase complex (FAS)

3.5.1 Orphan fatty acid synthase subunit 2 (Fas2) as a new Ubr1 substrate

Proteins in cells are often organized in complexes containing different polypeptides expressed from different genes. These different proteins are linked in a distinct stoichiometry via non-covalent protein-protein interactions. Protein complexes are often characterized by multiple catalytic activities. In case of enzyme complexes the proximity of the different catalytic subunits enhance the efficiency of substrate turnover and prevent possible side-reactions due to product diffusion into the environment. The FAS-complex (fatty acid synthase complex) is a 2.6 MDa barrel-shaped complex composed of two different subunits, Fas1 (β) and Fas2 (α). The complex contains 6 protomers of each, Fas2 and Fas1, resulting in an $\alpha_6\beta_6$ structure (Lomakin *et al*, 2007), Fig. 3.44.

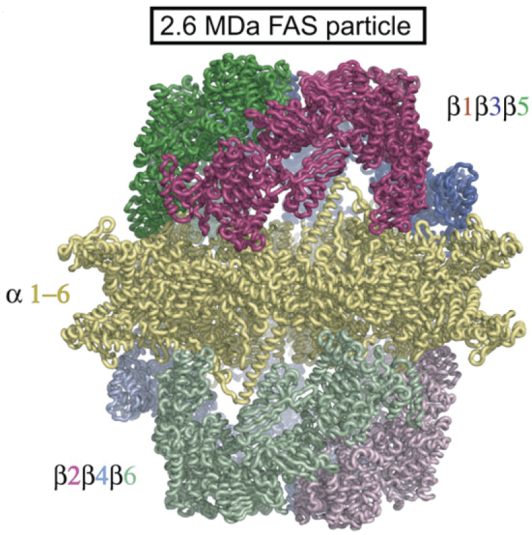

Figure 3.44: Overall structure of the 2.6 MDa barrel-shaped FAS-complex. The hexameric Fas2-ring has a wheel-like structure and is shown in yellow. The Fas2-ring is located in between two Fas1 trimers shown in pink, green and blue. Figure: Modified from (Lomakin *et al*, 2007).

Fatty acid synthase catalyses the synthesis of long chain fatty acids from acetyl-CoA and malonyl-CoA. Since the genes encoding the two subunits are unlinked, the correct stoichiometry of both subunits has to be regulated, preventing a surplus of Fas1 or Fas2 subunits. The expression of both subunits is therefore regulated by several transcription factors and also Fas1-dependent autoregulation of Fas2 (Burkl *et al*, 1972; Schweizer and Hofmann, 2004; Siebenlist *et al*, 1990). Furthermore, it has been shown that the Fas subunits are subjected to proteolysis (Egner *et al*, 1993). In this study, the proteolytic degradation of the Fas2 subunit in absence of its partner Fas1 was further investigated.

The studies were done together with Mario Scazzari. Most of the results shown in this chapter were published in (Scazzari *et al*, 2015).

3.5.2 Experimental setup for studying Fas2 stability

In order to study the post-translational control of complex subunits via proteolysis, the FAS complex was used as experimental system (Fig. 3.45).

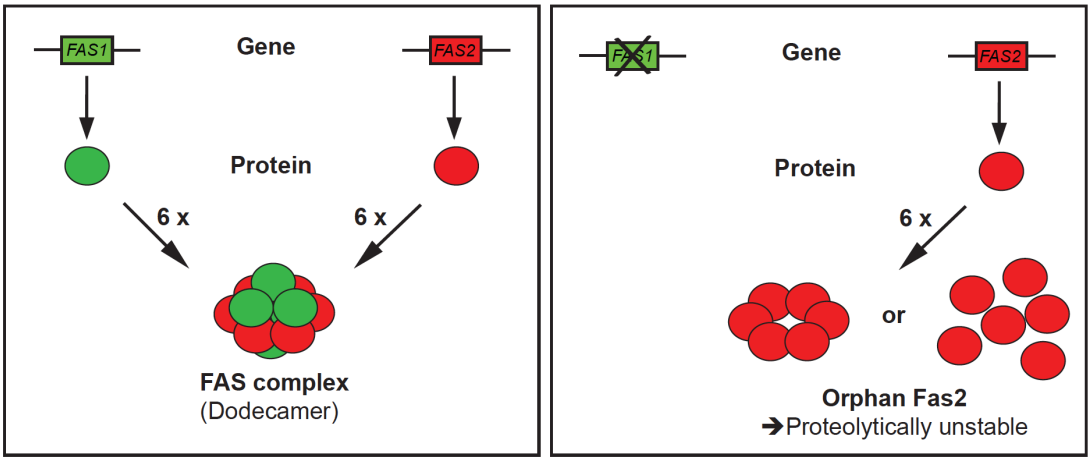

Figre 3.45: Experimental setup for investigation of quality control of orphan Fas2. The wild type situation where both FAS-subunits Fas1 and Fas2 are expressed (left panel) is compared with conditions where the *FAS1* gene is deleted (right panel).

For studying the stability of orphan Fas2 a strain deleted in the gene coding for the β-subunit of the FAS complex *FAS1* was used. The corresponding strain is not able to produce long chain fatty acids any more. Therefore the growth medium has to be supplemented with the saturated C14 fatty acid myristic acid which can also be incorporated into cell membranes, by this providing viability to *Δfas1* cells.

3.5.3 Orphan Fas2 is mainly organized in an oligomeric complex

The FAS complex is organized as a dodecamer consisting of a central hexameric Fas2 ring and two Fas1 trimers bound on the top and bottom of the hexameric Fas2 ring (Fig. 3.45). In

the absence of Fas1 the hexameric organization of the Fas2 subunits may persist or get lost resulting in Fas2 monomers. To check the organization of orphan Fas2 both, wild type and *Δfas1* cells were lysed under native conditions and the extracts were subjected to a glycerol density centrifugation (Fig. 3.46).

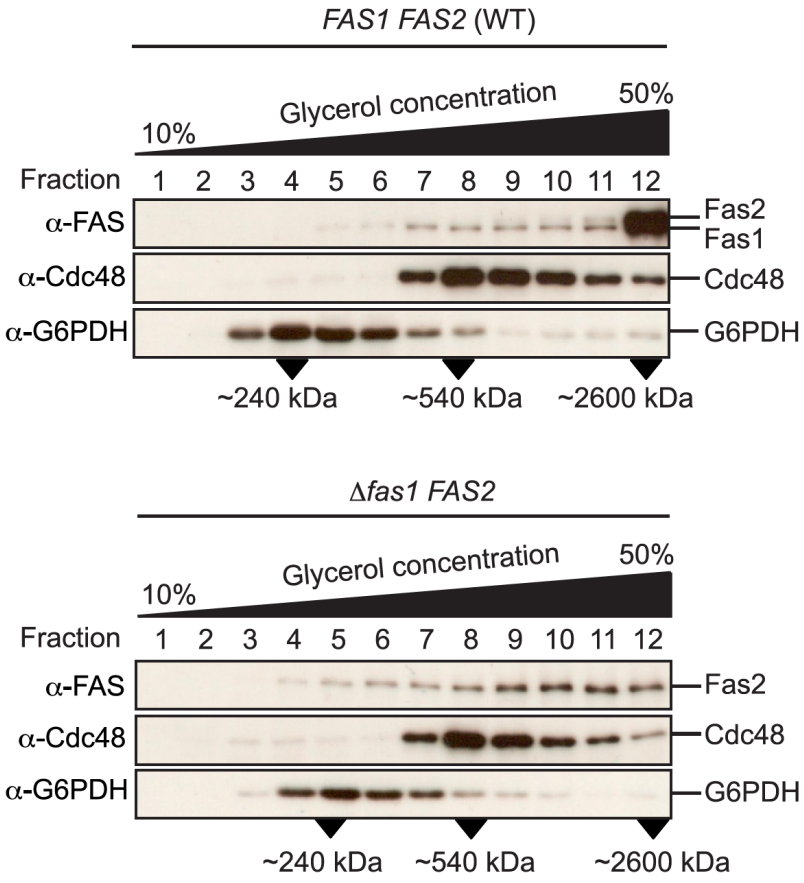

Figure 3.46: Orphan Fas2 is mainly organized in Fas-assembly intermediates. Both exponential wild type and *Δfas1* yeast cells were harvested, lysed and the extracts loaded on a glycerol gradient consisting of 10 to 50 % glycerol solutions. After centrifugation at 55,000 rpm for 4 h, 12 fractions were collected. The fractions were subjected to TCA precipitation prior to SDS-PAGE and immunobloting. Endogenously expressed proteins served as molecular mass markers: Cdc48 is organized as a hexamer (540 kDa), glucose-6-phosphate dehydrogenase (G6PDH) as tetramer (240 kDa) and the FAS complex as a dodecamer (2.6 MDa). Figure: (Scazzari, 2013).

As can be seen in Fig. 3.46 in the wild type situation (upper panel) the FAS complex is detected in fraction #12 corresponding to a molecular mass of 2.6 MDa. Cdc48 and glucose-6-phosphate dehydrogenase (G6PDH) served as molecular mass marker proteins. The strongest Cdc48 signal is detected in fraction #8. Cdc48 forms a hexameric complex with a

molecular mass of 540 kDa. The G6PDH is organized as a tetramer with a molecular mass of 240 kda. The maximum of the G6PDH signal is detected in fraction #4.

In the *FAS1* deletion strain (Fig. 3.46, lower panel) the molecular mass of the two marker proteins Cdc48 and G6PDH is unchanged compared to the wild type strain. A single Fas2 subunit has a molecular mass of 207 kDa and should therefore be detected in the fractions #2 - #4. However, the strongest Fas2 signals in *Δfas1* cells are detected in the fractions #9 - #11. This indicates in Fas1-lacking cells the formation of a complex, most likely the Fas2 hexameric ring which serves as the platform for Fas1 docking.

3.5.4 Orphan Fas2 is proteolytically unstable

In vitro, orphan Fas2 was shown to be proteolytically susceptible to proteases like trypsin, in contrast to the wild type $(Fas1)_6(Fas2)_6$ complex, where proteases cannot attack Fas2 (Scazzari *et al*, 2015). It was important to confirm this result *in vivo* by monitoring the degradation kinetics of Fas2 in a wild type strain expressing also Fas1 and in a *Δfas1* strain (Fig. 3.47). Fas2 was expressed as a C-terminal TAP fusion protein. The TAP tag does not alter its catalytic activity (not shown).

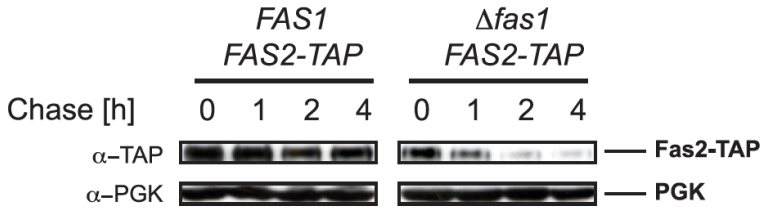

Figre 3.47: Orphan Fas2 is proteolytically unstable *in vivo*. Cycloheximide chase experiments were performed using yeast strains expressing a TAP-tagged version of Fas2. Cells were harvested after addition of cycloheximide at the indicated time points. Fas2 was detected using TAP antibody. PGK served as loading control.

As can be seen in Fig. 3.47 in the wild type strain where both Fas1 and Fas2 are expressed Fas2-TAP is rather stable within 4 hours. In contrast, the absence of Fas1 causes rapid degradation of orphan Fas2-TAP.

3.5.5 Proteasomal degradation of orphan Fas2

As can be seen in Fig. 3.47 orphan Fas2 is proteolytically unstable and degraded. Yeast possesses two proteolytic systems, the ubiquitin-proteasome system and the vacuole (lysosome). In order to find out whether orphan Fas2 is degraded in a proteasome-dependent manner cycloheximide chase experiments were performed using a yeast strain expressing a temperature-sensitive mutant of Cim3 (Rpt6), (Ghislain *et al*, 1993), an ATPase subunit of the 19 S regulatory particle of the proteasome essential for its function (Fig. 3.48).

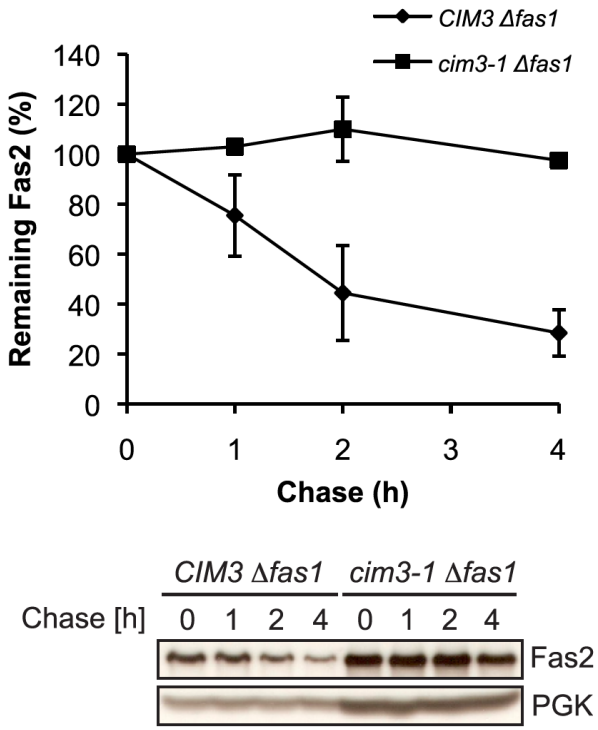

Figure 3.48. Degradation of orphan Fas2 depends on the proteasome. Cycloheximide chase experiments were performed using yeast strains expressing either wild type Cim3 (Rpt6), an ATPase of the 19S proteasome or a mutant version encoded by the allele *cim3-1*. At 37 °C, *cim3-1* expresses an inactive form of Cim3 inhibiting proteasome function. Samples were taken at the indicated time points after addition of cycloheximide. PGK served as loading control. The data represent the mean of three independent experiments. Error bars indicate the standard deviation of the mean. Figure: (Scazzari, 2013).

Mutation of Cim3 (Rpt6) renders the proteasome inactive and causes stabilization of orphan Fas2, showing the proteasome as being responsible for its proteolysis. In contrast, in the

CIM3 wild type situation orphan Fas2 is degraded. This clearly shows the proteasome as being prominently involved in degradation of orphan Fas2.

3.5.6 Orphan Fas2 is ubiquitinated if not complexed with Fas1

Since orphan Fas2 is degraded via the proteasome, ubiquitin conjugation of Fas2 is supposed to occur prior to recognition by the proteasome. Therefore a ubiquitination assay was performed to detect ubiquitinated Fas2 in a *FAS1*-deficient strain (Fig. 3.49).

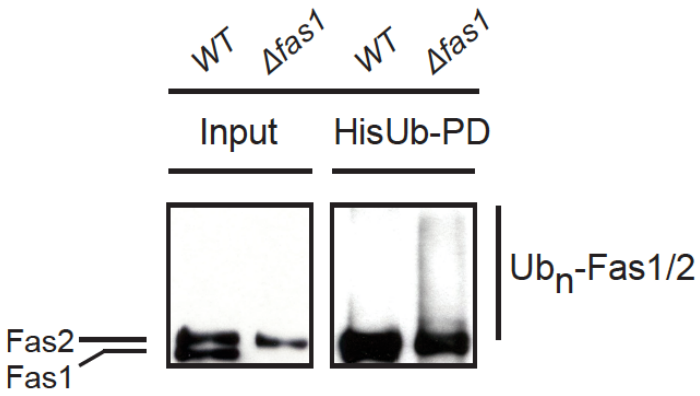

Figure 3.49: Fas2 is ubiquitinated when not complexed with Fas1. For detection of ubiquitinated Fas2 both wild type and *Δfas1* yeast strains were transformed with a plasmid encoding histidine-tagged ubiquitin (pJD421). Equal amounts of cells were used for lysis. Equal lysate amounts were loaded on an SDS-gel serving as input controls. Ubiquitinated material was precipitated using Ni-NTA-agarose beads. After elution of ubiquitinated material the samples were subjected to SDS-PAGE followed by immunoblotting using Fas antibody.

In the lysate of the wild type strain both subunits of the FAS complex can be detected using Fas antibody. In the pulldown fractions (HisUb-PD) ubiquitin-conjugated Fas2 can be prominently detected in the *Δfas1* strain whereas hardly any high-molecular mass ubiquitin conjugates can be detected in the wild type. This indicates that orphan Fas2 is ubiquitinated prior to degradation by the proteasome (Fig. 3.49).

3.5.7 Involvement of Ubr1 in orphan Fas2 degradation

Since the ubiquitin ligase Ubr1 is the major E3 enzyme for ubiquitinating cytoplasmic misfolded proteins for subsequent proteasomal degradation, the influence of Ubr1 in the ubiquitination and degradation process of orphan Fas2 was examined.
The first hint for the involvement of Ubr1 in degradation of orphan Fas2 could be obtained by steady state analysis of Fas2 (Fig. 3.50).

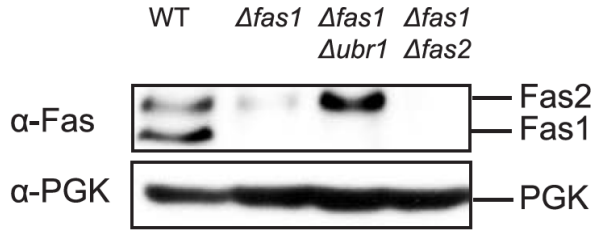

Figure 3.50: The steady state level of orphan Fas2 is dramatically increased if Ubr1 is absent. Steady state analysis was performed with exponentially growing cells. 3 OD cells were harvested, lysed and subjected to TCA precipitation prior to SDS-PAGE and immunoblotting using Fas antibody. PGK served as loading control. The strain *Δfas1Δfas2* served as antibody control.

In the wild type strain both subunits of the FAS complex Fas1 and Fas2 can be detected with the Fas antibody. Deletion of *FAS1* causes a decrease in the Fas2 steady state level due to the proteolytic instability of orphan Fas2. An additional deletion of *UBR1* encoding the cytosolic E3 ligase Ubr1 dramatically increases the steady state level of orphan Fas2 indicating that Ubr1 is involved in the degradation process (Fig. 3.50).
To further confirm the involvement of Ubr1 in the degradation process of orphan Fas2 pulse chase experiments were performed in order to monitor the degradation kinetics of orphan Fas2 in a *Δubr1* strain (Fig. 3.51).

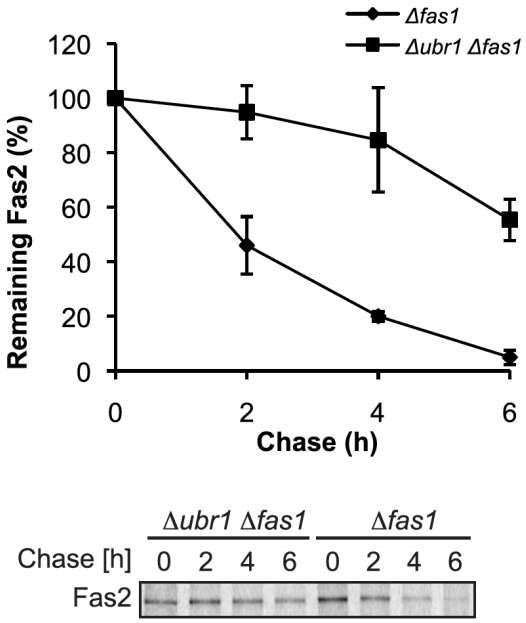

Figure 3.51: Ubr1 is involved in the degradation of orphan Fas2. Pulse chase experiments were performed in order to monitor the degradation kinetics of orphan Fas2 using yeast strains *Δfas1* and *Δfas1Δubr1*. Samples were taken at the indicated time points. Data represent the mean of three independent experiments. Error bars indicate the standard deviation of the mean. Figure: (Scazzari, 2013).

In the *Δfas1* strain about 80 % of orphan Fas2 is degraded after 4 hours. In the strain lacking the E3 ligase Ubr1 90 % of Fas2 is still detectable after 4 hours indicating that Ubr1 is the major E3 ligase responsible for ubiquitination of orphan Fas2. After 4 hours some amount of orphan Fas2 is degraded also in absence of Ubr1 indicating an additional mechanism in charge to further eliminate orphan Fas2 (Fig. 3.51).

To confirm the involvement of Ubr1 in ubiquitination of orphan Fas2 a ubiquitination assay was performed to actually prove the absence of Fas2 ubiquitination in a Ubr1 deficient strain (Fig. 3.52).

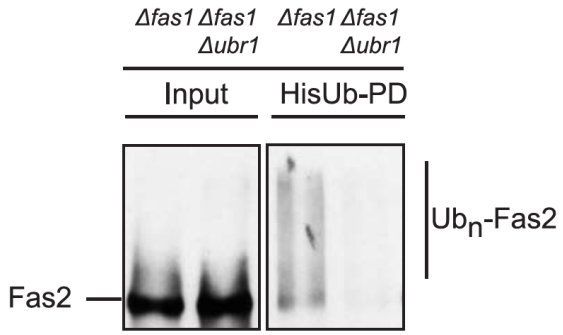

Figure 3.52: Ubr1 is involved in ubiquitination of orphan Fas2. A ubiquitination assay was performed comparing the amounts of ubiquitin-conjugated Fas2 in *Δfas1* and *Δfas1Δubr1* strains. Both strains were transformed with a plasmid coding for histidine-tagged ubiquitin (pJD421). A Ni-NTA-agarose based pulldown assay was performed as described in the legends to Fig.3.13.

As can be seen in Fig. 3.52 orphan Fas2 is ubiquitinated in a Fas1-deficient strain whereas hardly any ubiquitin conjugates of Fas2 can be detected in a strain lacking the E3-ligase Ubr1. This confirms the importance of Ubr1 in orphan Fas2 ubiquitination and subsequent proteolytic clearance.
In further experiments it was also shown that orphan Fas2 physically interacts with Ubr1 (Scazzari, 2013).

3.5.8 Function of Hsp70 chaperones of the Ssa class in the degradation process of orphan Fas2

In previous experiments it was shown that the Hsp70 chaperones of the Ssa class are important for keeping cytosolic misfolded proteins soluble for subsequent degradation. To analyse whether the solubility of orphan Fas2 is also influenced by the Ssa chaperones, solubility assays were performed using a strain deficient in functional Ssa chaperones (Fig. 3.53).

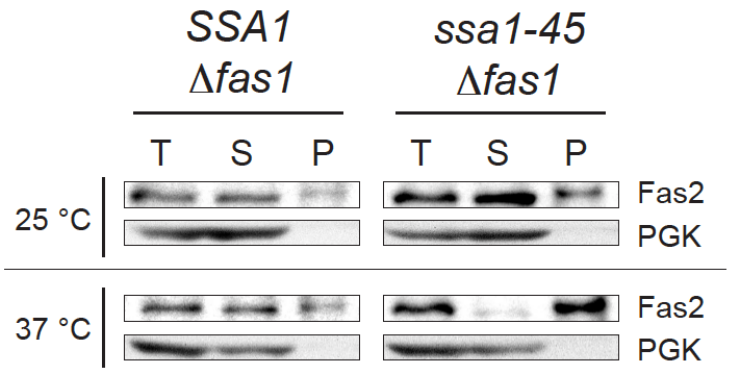

Figure 3.53: Ssa1 is important for keeping orphan Fas2 soluble. For the solubility assay of orphan Fas2 equal amounts of cells containing either the wild type *SSA1* gene or the temperature-sensitive *ssa1-45*^{ts} allele, both strains deleted in *SSA2*, *SSA3* and *SSA4* were harvested prior to or after shift to restrictive temperature (37 °C) and lysed with glass beads. After preclearing by centrifugation at 500 g the supernatants represented the total protein fractions (T). Afterwards, the total protein fractions were subjected to fractionation at 21,500 g for 15 min into soluble (S) and pellet fractions (P). The total (T) and soluble fractions (S) were subjected to TCA precipitation prior to SDS-PAGE and immunoblotting. The pellet fractions (P) were solubilized in SDS urea sample buffer prior to SDS-PAGE and immunoblotting. PGK served as loading control.

In the yeast strain expressing the wild type *SSA1* gene the major portion of orphan Fas2 is detected in the soluble (S) fractions at both temperatures, 30 °C and 37 °C. At 37 °C a slight shift of Fas2 material towards the pellet fraction is observed (Fig. 3.53). Also in the temperature-sensitive strain, at permissive temperature, where *ssa1-45*^{ts} expresses a functional Ssa1 protein, more Fas2 substrate is detected in the soluble than in the pellet fraction. However, after shift to 37 °C almost all Fas2 substrate is now found in the pellet fraction indicating that loss of function of the Ssa1-45 protein causes aggregation of orphan Fas2. The PGK protein represents a soluble cytosolic protein and is therefore only detected in the total (T) and soluble (S) protein fractions.

In order to analyse whether Ssa1 function is essential for ubiquitination of orphan Fas2 a ubiquitination assay was performed in order to detect orphan Fas2 ubiquitination in the *ssa1-45*^{ts} and the *SSA1* strain at restrictive temperature (Fig. 3.54).

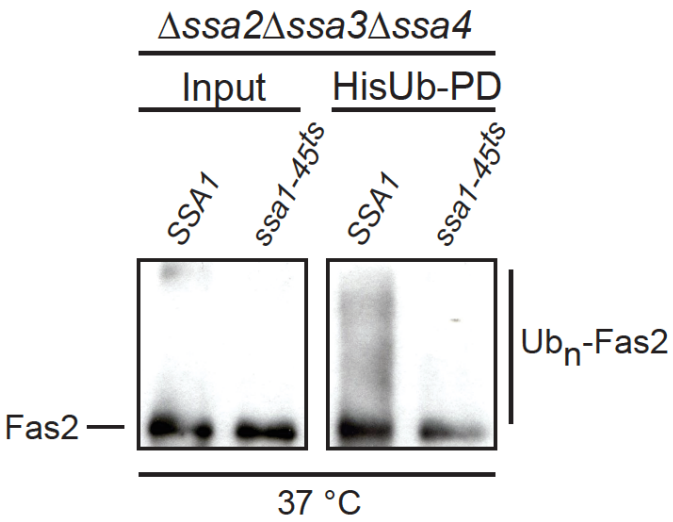

Figure 3.54: Functional Ssa1 is essential for ubiquitination of orphan Fas2. A Ubiquitination assay was performed using yeast strains containing either wild type *SSA1* or the temperature-sensitive *ssa1-45*^{ts} allele both expressing histidine-tagged ubiquitin from the plasmid pIA18. After shift to 37 °C for 1 h equal amounts of cells were harvested and subjected to Ni-NTA agarose based pulldown as decribed above. Both input samples and pulldown samples (HisUb-PD) were subjected to SDS-PAGE and immunoblotting using Fas antibody.

The strain expressing the wild type *SSA1* gene at 37 °C can still ubiquitinate orphan Fas2 whereas the temperature-sensitive *ssa1-45*^{ts} strain is not able to ubiquitinate Fas2 anymore (Fig. 3.54). This indicates an essential role of the Ssa1 protein in the ubiquitination process of orphan Fas2.

3.5.9 Involvement of the Cdc48 machinery in orphan Fas2 degradation

The Cdc48 machinery is involved in many disaggregation and disassembly processes in cells. It obtains its energy for these processes by ATP hydrolysis (Stolz *et al*, 2011). Since orphan Fas2 is still organized in oligomeric states it was interesting to examine the involvement of Cdc48 in the degradation process of orphan Fas2 (Fig. 3.55).

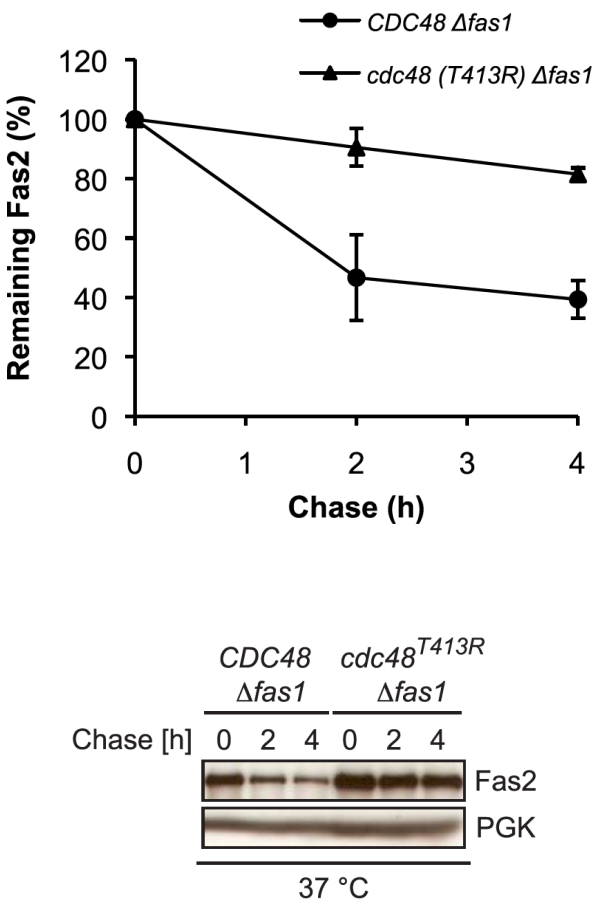

Figure 3.55: Functional Cdc48 is essential for degradation of orphan Fas2. Cycloheximide chase experiments were performed using either a *Δfas1* strain containing wild type *CDC48* or a temperature-sensitive *cdc48* allele. After shift to 37 °C for 1 h cycloheximide was added and samples were taken at the indicated time points and subjected to SDS-PAGE and immunoblotting using Fas and PGK antibodies. Data represent the mean of three independent experiments. PGK served as loading control. Error bars indicate the standard deviation of the mean. Figure: (Scazzari, 2013).

In the *Δfas1* strain containing wild type *CDC48* orphan Fas2 is degraded at 37 °C. In contrast, orphan Fas2 is stabilized in the strain containing the temperature-sensitive *cdc48* allele which expresses inactive Cdc48 (Cdc48 T413R) at 37 °C (Fig. 3.55). Obviously, the Cdc48 machinery is important for degradation of orphan Fas2.

In order to examine whether the Cdc48 machinery is also important for the Ubr1-dependent ubiquitination of Fas2, a ubiquitination assay was performed (Fig. 3.56).

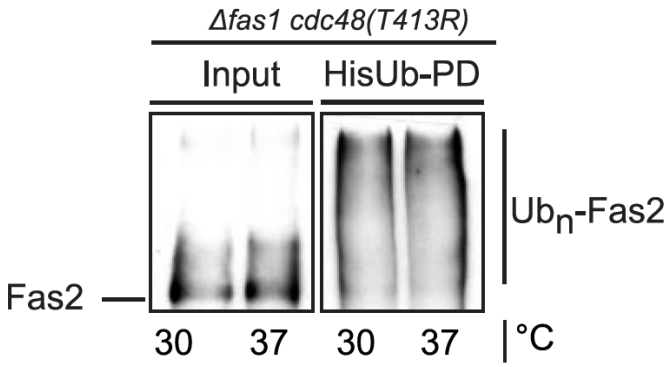

Figure 3.56: Cdc48 is not involved in ubiquitination of orphan Fas2. A ubiquitination assay was performed using a yeast strain containing a temperature-sensitive *cdc48* allele resulting in an inactive Cdc48 protein at 37 °C. In addition, the strain expresses histidine-tagged ubiquitin from the plasmid pJD421. The strain was grown either at 30 °C or shifted to 37 °C for 1 h before harvesting and subsequent Ni-NTA agarose based pulldown assay as described earlier. Both input and pulldown samples were subjected to SDS-PAGE and immunoblotting using Fas antibody.

As can be seen in Fig. 3.56 orphan Fas2 is ubiquitinated at permissive and restrictive temperatures indicating that Cdc48 function is not required for ubiquitination. Therefore Cdc48 seems to act after ubiquitination of the oligomeric orphan Fas2.

4. DISCUSSION

4.1 Protein quality control of the cytoplasmic misfolded model substrate ΔssCPY*Leu2myc (ΔssCL*myc)

Misfolded proteins are constantly produced in living cells. Therefore, protein quality control mechanisms have to be present for surveillance of the folding status of each protein, and in case of terminally misfolding, specific recognition and removal of the misfolded proteins from the cellular environment has to occur. Failure of this protein quality control due to mutations or enhanced cellular stress conditions can cause severe diseases like Parkinson's or Alzheimer's disease, diabetes or cancer (Lima *et al*, 2014; Ross and Poirier, 2004). The endoplasmic reticulum-associated degradation pathway (ERAD) was extensively studied during the last two decades. In the ERAD pathway misfolded secretory proteins which cannot be folded properly in the endoplasmic reticulum (ER) are retrotranslocated out of the ER with help of the Cdc48 machinery and further ubiquitinated before proteasomal degradation (Hiller *et al*, 1996; Kostova and Wolf, 2003; Stolz *et al*, 2011). The model substrates used for studying ERAD in our lab are based on the protein carboxypeptidase Y (CPY) which enters the secretory pathway for folding and further transport into the vacuole, its organelle of action. Insertion of the point mutation G255R causes misfolding and retention of the protein, called CPY*, in the ER for further retrotranslocation into the cytosol and proteasomal degradation (Hiller *et al*, 1996; Kostova and Wolf, 2003; Stolz *et al*, 2011). In 2007, the question arose how misfolded proteins of the cytosol are recognized and degraded. For solving this question misfolded CPY* deleted in the signal sequence for ER import was constructed (Park *et al*, 2007). Using the derivative of the then cytosol-localized CPY*, ΔssCPY*Leu2myc (ΔssCL*myc), expressed in a yeast deletion strain library of non-essential genes, the ubiquitin ligase Ubr1 was discovered as being involved in the degradation process of ΔssCL*myc (Eisele and Wolf, 2008). Since Ubr1 was initially discovered as the ubiquitin ligase of the N-end rule pathway the question arose whether ΔssCL*myc represents a classical N-end rule substrate. In a recent study it was shown that ΔssCL*myc can be targeted to Ubr1 via its N-terminal degron Met-Ile, which represents the first two N-terminal amino acids of the substrate (Kim *et al*, 2014). These kinds of degrons consist of methionine followed by a hydrophobic amino acid (Met-Φ). For the Met-Φ model substrate ML-GST it

was shown in pulldown assays that these degrons can be recognized by the type 2 binding site of Ubr1, known to target proteins containing type II destabilizing residues at the N-terminus (Trp, Phe, Tyr, Leu, Ile) (Xia *et al*, 2008). However, in former experiments performed by Frederik Eisele, as well as in this study it was shown that only mutants of Ubr1, defective in binding type 1 N-end rule substrates stabilize ΔssCL*myc *in vivo*. A strain expressing Ubr1 defective in the type 2 N-end rule substrate recognition site (Ubr1 P406S) shows wild type behaviour. The same result was obtained when the substrate orphan Fas2 which does not contain a Met-Φ degron but Met-Lys as first amino acids, was tested (Scazzari, 2013). Even though the second amino acid, lysine, of orphan Fas2 represents a type 1 destabilizing residue, according to the Sherman rule the methionine cannot be cut off due to the large size of lysine (Sherman *et al*, 1985). These unexpected results may be explained as follows: For mapping the Ubr1 binding site of substrates containing Met-Φ degrons Kim *et al*. used a GST (glutathione S-transferase) version as substrate (Kim *et al*, 2014). However, this protein does not exhibit typical features of a misfolded cytosolic protein because it is functional. It is therefore dangerous to generalize the found type 2 binding site harbouring Met-Φ proteins as also being involved in recognition of misfolded proteins containing a Met-Φ degron. An additional difference between ΔssCL*myc and ML-GST is the size. It may be possible that small substrates like ML-GST can be easily bound by Ubr1 without help of other factors or additional binding sites in Ubr1. These data either indicate the presence of additional factors present in the cell which are required for *in vivo* processing of the misfolded substrate to yield a type 1 N-end rule substrate or an overlapping function of the type 1 binding site in Ubr1. There might be in addition a binding site in Ubr1 present which recognizes hydrophobic patches in the misfolded proteins tested and which cooperates with the type 1 binding site. In previous studies it has been shown that Ubr1 mutated in both the type 1 and type 2 binding sites is still able to bind either ΔssCl*myc and orphan Fas2, indicating for more than one Ubr1 binding site for misfolded substrates (Diploma thesis Ingo Amm, 2009, Diploma thesis Kathrin Deuschle, 2010, (Scazzari, 2013)). For further characterization of the degron of ΔssCL*myc or orphan Fas2 recognized by Ubr1 Edman degradation for sequencing of the N-terminus of ΔssCL*myc in wild type cell lysates should be performed.

It was shown for the cytosolic model substrate ΔssCPY*GFP (ΔssCG*) that the Hsp70 chaperones of the Ssa type are essential for keeping the substrate soluble and for proteasomal degradation to occur (Park *et al*, 2007). As can be seen in Fig. 3.7 and Fig. 3.8, this is also the case for the similarly constructed substrate ΔssCPY*Leu2myc (ΔssCL*myc). In exponential growth phase almost 50 percent of the ΔssCL*myc substrate is found in a soluble state when

Ssa1 function is uncompromised. Abolishing Ssa1 function causes a dramatic decrease in substrate solubility. Interestingly, in stationary growth phase even at 25 °C where Ssa1 is functional, almost all substrate is found in an insoluble state, similar to the situation when Ssa1 is non-functional. At 37 °C no substrate can be detected in the soluble fraction (Fig. 3.7). A possible explanation for this phenomenon might reside in the different expression profiles of the four Ssa chaperones. It had been discovered that Ssa1 and Ssa2 expression is considerably downregulated after diauxic shift. In contrast, Ssa3 levels are not detectable in exponential growth phase but dramatically rise after diauxic shift and in stationary phase (Hasin *et al*, 2014; Werner-Washburne *et al*, 1989). All strains used in the solubility assays carry deletions in the *SSA2*, *SSA3* and *SSA4* genes (Fig. 3.7). Therefore, they only possess the gene encoding Ssa1. Obviously, in exponential phase Ssa1 is sufficient for keeping approximately 50 % of ΔssCL*myc in a soluble state. This solubility value is also reached in a strain possessing all four *SSA* genes (Fig. 3.37). In stationary phase cells, hardly any Ssa1 is present (Hasin *et al*, 2014; Werner-Washburne *et al*, 1989). This might be the reason for the very small difference in substrate solubility in these cells between 25 °C and the restrictive temperature where the Ssa1-45 protein is inactive (Fig. 3.7). It can be also observed that an additional deletion of *UBR1* both in exponential and stationary phase causes a decrease in substrate solubility (Fig. 3.7). As Ubr1 is essential for degradation of the substrate ΔssCL*myc, a stabilization of substrate causes a severe accumulation during growth to stationary phase. Therefore, available Ssa chaperones might get titrated away leaving not enough Ssa1 anymore present for the substrate.

Nillegoda *et al*, 2010 used in their studies on cytoplasmic protein degradation the kinase Tpk2 as model substrate which is a stable protein in wild type cells. After inhibition of the Hsp90 system by the drug Geldanamycin, Tpk2 is degraded in a Ubr1-dependent manner. This is explained by the involvement of the Hsp90 system in the final maturation of Tpk2. In the absence of Hsp90 Tpk2 shows characteristics of a misfolded protein. Therefore it is degraded in a Ubr1-dependent manner. The terminally misfolded protein ΔssCL*myc is already degraded in Hsp90 wild type cells due to its permanent misfolding. However, after inhibition of Hsp90 it is degraded even faster. This might be explained by binding of Hsp90 to ΔssCL*myc. This binding may delay the recruitment of components of the Ubr1-dependent degradation machinery and subsequent degradation.

4.2 Introduction of new Luciferase-based model substrates for studying cytoplasmic protein quality control

The cytosolic model substrate ΔssCL*myc was initially created for conducting a genomic screen to identify new components of cytoplasmic protein quality control. For this, the steady state level of the substrate was determined by conducting growth tests on agar plates lacking leucine. One disadvantage of growth tests lies in the time of growth until good results are available. Therefore, additional model substrates were established in this study for investigation of cytoplasmic protein quality control. The new substrates were based on firefly luciferase. This enzyme is localized in peroxisomes. To make use of this enzyme in cytoplasmic protein quality control a mutant enzyme deficient in peroxisomal import was constructed. As luciferase is a relative stable protein two mutations were introduced rendering the protein unstable. In addition, the luciferase variants were also C-terminally fused to the Leu2 protein which also allows the performance of growth tests. For measuring luciferase activity cell lysates of luciferase-expressing yeast strains were prepared. 96 well plates were used for the measurements. For the chemiluminescence measurements a 96 well plate reader was used. Therefore the luciferase activity of 96 strains can be measured at once generating a big advantage for high throughput screening experiments. Somewhat more difficult is the interpretation of the output values. Since cell lysis is never 100 % efficient and the efficiency may differ among the different yeast strains tested, the chemiluminescence signals have to be normalized against the protein concentrations of the cell lysates. The chemiluminescence signals do also not necessarily correspond to the amounts of the luciferase substrates in the cell. If the signal is very weak there are three possible interpretations of the result: (1) The degradation of the luciferase substrate is very fast, (2) folding of the luciferase substrate is impaired, (3) increased luciferase aggregation occurs leading to luciferase inactivity. To address these questions in future experiments the luciferase activity signals should also be normalized against the substrate amount obtained from Western blotting. For example, if the luciferase signal for one luciferase-expressing strain is very weak and the corresponding protein signal in the Western blot strong, then the folding of the substrate is impaired or the substrate is present in an aggregated form. This conflict can be observed in Fig. 3.12 and Fig. 3.13. Here, luciferase activity measurements were performed using strains deficient of active Hsp70 chaperones of the Ssa type. In exponential phase, it can be seen that the luciferase signals in the *ssa1-45*^{ts} strain at 30 °C are higher than those detected in the *SSA1* strain. In a

previous experiment, it was shown that degradation of the susbtrate ΔssCL*myc is decreased even at 25 °C in the *ssa1-45^{ts}* strain compared to the *SSA1* strain (Fig. 3.8). This might be due to less functionality of the temperature-sensitive Ssa1 protein encoded by the *ssa1-45^{ts}* allele as compared to the wild type Ssa1 protein. The increased luciferase activity observed for the *ssa1-45^{ts}* strain (Fig. 3.12) could therefore be due to a higher steady state level of the two luciferase substrates caused by a decreased degradation rate.

At 37 °C, the activity of both luciferase substrates is decreased in the temperature-sensitive *ssa1-45^{ts}* strain. Luciferase activity is almost absent in case of the substrate LucDMLeu2myc. This result makes sense because this mutated luciferase-substrate is unstable and therefore more prone to misfolding and aggregation at 37 °C than the substrate LucLeu2myc. Therefore, functional Ssa1 seems to be very important for maintaining substrate solubility and activity, respectively. The luciferase activity of both substrates is also somewhat lower in the *SSA1* strain at 37 °C. This can be explained by the higher temperature where both luciferase substrates do not show full activity any more due to denaturation or aggregation. In stationary phase (Fig. 3.13), even at 30 °C no visible luciferase signals can be detected any more in the *ssa1-45^{ts}* strain. This might be due to increased cell stress in this growth phase. Chaperones are very important in stationary phase. Due to absence of Ssa2, Ssa3 and Ssa4 and expression of a mutated Ssa1 protein from the *ssa1-45^{ts}* allele the capacity of this mutated Ssa1 protein is not high enough, - even at 30 °C-, for guaranteeing functionality of the luciferase substrates.

As mentioned above, the substrate protein levels should also be determined via Western blot. The luciferase signals (RLU) normalized to the protein concentrations of corresponding cell lysates (specific activity) should be normalized in addition to the substrate steady state levels obtained by Western blot. The obtained values would now give insights into the folding status of the luciferase substrates. A low specific activity value of a lysate in combination with a strong signal in the Western blot indicates a high amount of inactive or aggregated luciferase substrate which is expected for the luciferase-expressing *ssa1-45^{ts}* strain at restrictive temperature.

4.3 San1-dependency of degradation of cytosolic misfolded proteins

In several publications dealing with cytoplasmic protein quality control it has been observed that the proteasomal degradation of some cytosolic substrates not only depends on the

cytosolic ubiquitin ligase Ubr1 but also on the nuclear ubiquitin ligase San1 (Heck *et al*, 2010; Khosrow-Khavar *et al*, 2012; Prasad *et al*, 2010). The dependence of the degradation of cytoplasmic misfolded proteins on the nuclear ubiquitin ligase San1 is probably not surprising because about 80 % of the proteasomes are found in the nucleus throughout the cell cycle (Russell *et al*, 1999). Therefore, the additional nuclear import of cytoplasmic substrates may ensure an effective and faster clearance of misfolded substrates. In previous studies, the involvement of the Hsp70 chaperone system in the shuttling process into the nucleus, including the Hsp40 co-chaperone Sis1 and the Hsp110 chaperone Sse1 has been uncovered (Heck *et al*, 2010; Park *et al*, 2013; Prasad *et al*, 2010). Since the Hsp70 chaperone Ssa1 is localized both in cytosol and nucleus (Shulga *et al*, 1996) it might be possible that cytoplasmic misfolded proteins are shuttled into the nucleus in an Ssa1-bound state. Such a model could also explain why cytoplasmic folded proteins are prevented from nuclear import and degradation: Completely folded proteins are normally not associated with Ssa chaperones. Only folded proteins containing a nuclear localization signal (NLS) would be imported into the nucleus as such. It was shown that the NLS sequence carries the information for nuclear transport when fused to a non-nuclear protein (Goldfarb *et al*, 1986). Even functional cytosolic proteins which are not associated to other proteins can be targeted to the nucleus via fusion to a NLS sequence. The NLS sequence binds to shuttle factors called karyopherins or importins which dock to the cytoplasmic part of the nuclear pore complex prior to translocation (Gorlich *et al*, 1994; Lusk *et al*, 2007; Patel *et al*, 2007). For entering the nucleus, all cargo molecules have to pass the highly selective, bidirectional nuclear pore complex (NPC). Several studies showed that the NPC shows high permeability for small molecules like metal ions, metabolites or proteins which are smaller than 40 KDa in molecular mass (Feldherr and Akin, 1997; Keminer and Peters, 1999; Popken *et al*, 2015). To enter the nucleus, larger macromolecules have to interact directly with the NPC or additional shuttle proteins for nuclear import.

Degradation of the cytoplasmic misfolded protein ΔssCL*myc (size 116 kDa) seems not to be dependent on the nuclear ubiquitin ligase San1 as observed in both, degradation kinetics experiments and growth tests performed in this study: In growth tests no difference in the steady state level of ΔssCL*myc can be observed between the *Δubr1* and the double deletion strain *Δubr1Δsan1* (Fig. 3.18, Fig. 3.20). Pulse chase experiments and cycloheximide chase experiments show almost complete stabilization of ΔssCL*myc in the *Δubr1* strain (Fig. 3.4, Fig. 3.5). In principle, San1 is able to ubiquitinate cytosol-localized ΔssCL*myc. This was tested by expression of San1 mutated in its NLS-sequence in a *Δubr1* strain. Expression of

this San1 version can compensate the lack of Ubr1 concerning degradation of ΔssCL*myc (Fig. 3.14, Fig. 3.16). Interestingly, the V5-tagged San1 construct is degraded itself as can be seen in the cycloheximide chase experiments in Fig. 3.14 and Fig. 3.15. This is probably due to a cis-autoubiquitination process by V5-tagged San1 (Fredrickson *et al*, 2013a). Untagged San1 does not contain lysine residues at the N- and C-terminus. Fusion of the V5 tag (G**K**PIPNPLLGLDST) to the C-terminus introduces an unstructured V5 oligopeptide at the N-terminus containing one lysine residue which can be ubiquitinated by San1 in cis. Abolishing San1 function by mutation of the RING domain stabilizes V5-tagged San1 (Fig. 3.16) confirming this model.

When comparing the substrates used in several studies dealing with cytoplasmic quality control it was observed that some substrates are degraded in a more San1-dependent manner than others (Tab. 3.1). Interestingly, the two largest substrates listed here, ΔssCL*myc (116 kDa) and orphan Fas2 (207 kDa) are degraded in a San1-independent manner. The different substrates listed in Tab. 3.1 are very dissimilar proteins and differ in their cellular origin. Therefore, in this study smaller variants of ΔssCL*myc were generated to investigate a possible size-dependency of San1-dependent protein degradation of cytoplasmic misfolded proteins. As measured by cell growth, the steady state level of the truncated version of ΔssCL*myc called F2ΔssCL*myc is increased in the strain deleted in both genes encoding the E3 ligases *UBR1* and *SAN1* compared to the *UBR1* single deletion strain (Fig. 3.20, Fig. 3.21). To rule out that that differences in San1-dependency of the steady state level is caused by an altered N-terminus which might change the fate of the substrate due to the N-end rule the truncated versions F2ΔssCL*myc contain the same N-terminus as the original ΔssCL*myc substrate. The observed differences in San1-dependency of the substrates' steady state levels indicate an involvement of San1 in the degradation process of F2ΔssCL*myc. Fredrickson *et al*. observed that San1 prefers substrates with a high amount of exposed hydrophobicity and therefore possessing a preference for aggregation and insolubility (Fredrickson *et al*, 2013b). Therefore, I wanted to rule out whether there are any differences between the two substrates ΔssCL*myc and F2ΔssCL*myc concerning insolubility by performing a solubility assay. Both substrates show similar tendencies towards aggregation (Fig. 3.22). Therefore, the dependency of the steady state level of the substrate F2ΔssCL*myc on San1 does not seem to be reasoned in the exposed hydrophobicity. Furthermore, the misfolded part of the substrate is even smaller in the shortened substrate F2ΔssCL*myc. As controls, the substrates ΔssCL*myc and F2ΔssCL*myc were N-terminally fused to either NLS or NES sequences in order to find out whether the NLS-guided nuclear import

influences the fate of ΔssCL*myc towards San1-dependency of degradation. Fusion of ΔssCL*myc to an NLS sequence causes enhanced growth in a *SAN1* single deletion strain compared to wild type, but the influence of Ubr1 on the steady state level of NLS ΔssCL*myc is still strongly dominating (Fig. 3.18). This can be explained by the relative high molecular mass of ΔssCL*myc. This substrate might enter the nucleus rather slowly despite the NLS sequence. The steady state level of the truncated version F2ΔssCL*myc fused to an NLS sequence does not show any dependency on either Ubr1 or San1 when deleted individually (Fig. 3.21). Double deletion caused a dramatic increase in growth on medium lacking leucine. This can be explained by the fact that in absence of Ubr1 the substrate can be easily imported into the nucleus in a very short time scale for subsequent San1-dependent degradation. Surprisingly, the *SAN1* deletion strain shows as the *Δubr1* strain no growth on medium lacking leucine. This can be explained by an enhanced shuttling of NLSF2ΔssCL*myc between cytosol and the nucleus facilitated by the decreased substrate size. Even though San1 is missing, the substrate might be imported into the nucleus as expected. Because of the lack of nuclear degradation due to the *SAN1* deletion the substrate can be easily exported out of the nucleus and degraded in a Ubr1-dependent manner. Therefore, only deletion of both *UBR1* and *SAN1* causes an increase of the steady state level of F2ΔssCL*myc. The fusion of F2ΔssCL*myc to an NES sequence results in similar growth of the NES-F2ΔssCL*myc-expressing *Δubr1* and *Δubr1Δsan1* strains on medium lacking leucine. This indicates that the NES sequence totally abolishes nuclear import of the truncated version F2ΔssCL*myc which showed San1-dependence when not fused to a NES sequence. Another aspect important to discuss is the location of leucine biosynthesis and the suitability of corresponding substrates for studying intranuclear protein degradation deducted from growth experiments. In the wild type yeast strain β-isopropylmalate dehydrogenase is located in the cytosol. In former studies it has been discovered that small metabolites like 3-isopropylmalate converted by the Leu2 enzyme and the product 3-carboxy-4-methyl-2-oxopentanoate can both enter and exit the nucleus without limitations or expenditure of time (Feldherr and Akin, 1997; Keminer and Peters, 1999). Therefore, the Leu2-containing substrates can be used for studying nuclear protein stability on the basis of growth tests.

For further experiments cytosolic substrates were generated consisting of one up to three ΔssCPY* proteins. The substrate ΔssCPY* of 60 kDa molecular mass shows only a slight dependency on the cytosolic ubiquitin ligase Ubr1 whereas a drastic stabilization can be observed in the double deletion strain *Δubr1Δsan1* (Fig. 3.24) indicating considerable elimination of the protein by the action of nuclear San1. The degradation of a fusion protein

containing two (120 kda) ΔssCPY* entities shows no differences in degradation kinetics between the *Δubr1* and the *Δubr1Δsan1* strains (Fig. 3.24). This confirms the suspicion that molecular mass influences nuclear import and thus San1-dependency of degradation. Direct localization studies via immunofluorescence under proteasome inhibition should be able to give further evidence for import of the smaller substrates into the nucleus and the exclusion of substrates with high molecular mass from the nucleus.

4.4 The previously unknown involvement of chaperones of the Hsp31 family involved in quality control of ΔssCL*myc

In 2008, Ubr1 was discovered as being involved in degradation of the cytosolic model substrate ΔssCL*myc (Eisele and Wolf, 2008). It was the aim of this study to uncover further factors involved in clearance of cytoplasmic misfolded proteins. In a genome-wide genetic interaction study it was found that one member of the Hsp31 chaperone family shows a genetic interaction with the ubiquitin ligase Ubr1 (Costanzo *et al*, 2010). Epistasis analysis by the use of growth tests performed in this study could confirm this result (Fig. 3.28, Fig. 3.31). The steady state level of ΔssCL*myc is increased in both, *Δubr1* strain and the strain deficient in the *Δhsp31* chaperones (Fig. 3.25). Combining these deletions further increases the steady state level of ΔssCL*myc (Fig. 3.28). This result shows that the Hsp31 chaperones have overlapping functions with respect to the Ubr1-mediated degradation pathway. This is also consistent with the result that an excess of Ubr1 can rescue the growth phenotype of the *Δhsp31-33* strain (Fig. 3.29). Vice versa, additional expression of Hsp31 in a *Δubr1* strain can partially compensate the *Δubr1* phenotype (Fig. 3.30). In localization studies it has been proposed that the Hsp31 chaperones are localized in yeast cytosol under nutrient-limitated conditions (Miller-Fleming *et al*, 2014; Skoneczna *et al*, 2007). Therefore the influence of the Hsp31 chaperones on the steady state level of the ERAD-L substrate CTL*myc which enters the ER was examined. Deletion of the genes encoding the Hsp31 chaperones and Ubr1 did not increase the steady state level of CTL*myc (Fig. 3.35). It was discovered that the steady state level of the truncated version of the cytosolic model substrate ΔssCL*myc, F2ΔssCL*myc is partly dependent on the nuclear ubiquitin ligase San1 (Fig. 3.20, Fig. 3.21). Therefore, it was expected that the influence of the cytosol-located Hsp31 chaperones on the steady state level of F2ΔssCL*myc is decreased as compared to the steady state level of ΔssCL*myc. Indeed,

growth tests revealed that the steady state level of F2ΔssCL*myc is increased to some extent in *Δhsp31-33* and *Δhsp31-33Δubr1* strains compared to the full-length ΔssCL*myc (Fig. 3.36). Ubr1 was initially discovered as being involved in the ubiquitination of N-end rule substrates (Bartel *et al*, 1990). To test whether the classical type 1 N-end rule substrates Arg-βGal and Arg-URA3, which are not misfolded per se, show increased steady state levels in absence of the Hsp31 chaperones, growth tests and β-galactosidase activity assays were performed. No influence of the Hsp31 chaperones on the steady state level of these N-end rule substrates was detected (Fig. 3.33). Possible explanations for these observations could be that Ubr1 can directly bind to the two N-end rule substrates via the type 1 binding site which is located in the N-terminal region of Ubr1 domain without any help of other factors or other Ubr1 binding sites. Also the strength of binding and ubiquitinating activity might be dramatically increased if N-degrons are exposed in these substrates. Therefore, other degradation pathways might get dispensable. The most comprehensible explanation is that both Arg-βGal and Arg-Ura3 are not misfolded per se. Chaperones therefore might not be required either for keeping these substrates soluble or for shuttling them to the degradation machinery. The question was, what happens if a type 1 degron (Arg) is fused to the N-terminus of the misfolded model substrate ΔssCL*myc? Does the N-degron abolish the dependency of the steady state level of the substrate on the Hsp31 chaperones despite the misfolded character of ArgΔssCL*myc? Indeed, no influence of the Hsp31 chaperones on the steady state level of ArgΔssCL*myc can be observed any more (Fig. 3.34, upper panel). The type 1 N-degron seems to be the hierarchically highest degron for Ubr1-triggered degradation independent of the nature of the subsequent protein part. Fusion of a type 2 N-degron to the N-terminus of ΔssCL*myc (IleΔssCL*myc) has different effects on substrate steady state level: A general observation is that even in a wild type strain the steady state level of IleΔssCL*myc is enhanced as observed by good growth on medium lacking leucine (Fig. 3.34, lower panel). This result fits to the data obtained in a study measuring half-lives of different N-end rule substrates based on β-galactosidase (Bachmair *et al*, 1986). Bachmair *et al*. showed that the substrate Arg-βGal has a half-life of 2 min whereas Ile-βGal has a half-life of 30 min in wild type cells. One can conclude that IleΔssCL*myc has also a longer half-life, therefore its steady state level is enhanced compared to ArgΔssCL*myc. Interestingly, the steady state level of IleΔssCL*myc is slightly dependent on the Hsp31 chaperones seen by enhanced growth of the *Δhsp31-33* strain on medium lacking leucine compared to the wild type strain. Therefore, one can assume that the extended half-life of the IleΔssCL*myc as compared to ArgΔssCL*myc makes it a target for the Hsp31 chaperone family.

In general, the growth phase of yeast strains growing on agar plates is difficult to monitor. The performed growth tests on plates lacking leucine for detection of the steady state levels of Leu2-containing substrates were analysed after three to 5 days of growth. After this time almost all cells should be in stationary growth phase. Pulse chase analysis was performed with exponentially growing cells to assess whether the degradation of ΔssCL*myc is influenced by deletion of the genes encoding the Hsp31 chaperones. The results show that the substrate is degraded in the *Δhsp31-33* strain as in a wild type under these conditions. This discrepancy of pulse chase analysis and growth tests first indicates that the Hsp31 chaperones have no influence on ΔssCL*myc degradation in exponentially growing yeast cells. Indeed, previous studies on Hsp31 chaperone expression confirmed this suspicion. It has been shown that the Hsp31 chaperones are expressed under conditions of glucose limitation at diauxic shift or stationary phase (Miller-Fleming *et al*, 2014; Skoneczna *et al*, 2007). In order to further elucidate the differences between the steady state levels of ΔssCL*myc in exponential and stationary phase, a steady state analysis was performed in the two growth phases. As can be seen in Fig. 3.31 the steady state levels of ΔssCL*myc in exponential phase do not differ considerably between the wild type and the *Δhsp31-33* strain. In contrast, in stationary phase considerably more substrate can be detected in the strain lacking the Hsp31 chaperones. In stationary phase, most of the substrate is detected in the quadruple deletion strain where both the E3 ligase Ubr1 and the Hsp31 chaperone family are absent. These results nicely fit the performed growth test with the substrate ΔssCL*myc using medium lacking leucine (Fig. 3.28). These results further confirm the influence of the Hsp31 chaperones on the steady state level of ΔssCL*myc only in stationary phase. It was shown in this study that the Hsp70 chaperones of the Ssa type are essential for solubility of ΔssCL*myc (Fig. 3.7). To check whether also the Hsp31 chaperones influence the solubility of ΔssCL*myc, both, in exponential and stationary growth phase, analogous solubility assays were performed. In exponential phase, no differences in solubility of ΔssCL*myc in the four strains can be observed. In stationary phase, the substrate solubility is similar both in wild type and *Δhsp31-33* strains indicating that the Hsp31 chaperones are not involved in keeping the substrates soluble (Fig. 3.37). The steady state level of ΔssCL*myc is higher in the *Δubr1* strain compared to the wild type strain due to lack of degradation. The substrate signal ratio between the soluble and pellet fractions is only slightly shifted towards the pellet fraction compared to wild type strain. Combining the *UBR1* deletion with deletion of the genes encoding the Hsp31 chaperones causes even more substrate aggregation. The ratio of amount of ΔssCL*myc between pellet and soluble fraction seems to shift towards pellet fraction. This might be due to

decreased expression of chaperones important for guaranteeing protein solubility in stationary phase. Since in the quadruple deletion (*Δhsp31-33Δubr1*) strain also the Ubr1-dependent degradation of misfolded cytoplasmic proteins is absent, the residual amounts of chaperones in the cell might not be sufficient any more for keeping the increased substrate amounts soluble which is in contrast to the *Δhsp31-33* strain where degradation via Ubr1 still can occur. This will be further discussed below.

In order to further characterize the Hsp31 chaperone-dependent cytoplasmic protein quality control pathway an epistasis analysis was performed to check whether vacuolar degradation is somehow involved in the process. It is known that vacuolar degradation becomes more and more predominant in stationary cells towards proteasomal degradation (Dunn, 1990; Takeshige *et al*, 1992). Interestingly, in growth tests no difference of the strain deleted in the vacuolar protease gene *PEP4,* the genes encoding the Hsp31 chaperone family and the wild type strain can be observed on medium lacking leucine (Fig. 3.38). This indicates that the vacuole is not involved in the clearance of ΔssCL*myc. In epistasis experiments the growth on plates lacking leucine of wild type, *Δubr1, Δhsp31-33* and *Δhsp31-33Δubr1* strains expressing ΔssCL*myc with or without additional deletion of the *PEP4* gene was compared. No influence of the additional *PEP4* deletion on cell growth on medium lacking leucine can be observed (Fig. 3.38). Therefore, the Hsp31 chaperones seem to act in a vacuole-independent pathway with respect to the steady state level regulation of the substrate ΔssCl*myc.

The TOR signalling pathway is very important for regulation of the entry of cells into stationary growth phase. Treatment of cells with the immunosuppressant rapamycin mimics the nutrient starvation response even under nutrient-rich conditions (Crespo and Hall, 2002). The autophagic pathway is also induced upon rapamycin treatment (Noda and Ohsumi, 1998). In expression studies it was shown that inhibition of the TOR pathway induces expression of the vacuolar protease Pep4 (Hardwick *et al*, 1999). Using the same strains as used for the growth tests shown in Fig. 3.38 their sensitivity against rapamycin-induced inhibition of the TOR pathway was examined by growth tests on YPD plates containing 100 nM rapamycin. Surprisingly, the deletion of the *PEP4* gene does not alter the sensitivity of cells against rapamycin. The *Δpep4* strain shows similar growth as the wild type strain (Fig. 3.39). An explanation might come from a recent study (Marrakchi *et al*, 2013). They proposed that upon rapamycin treatment the helicase Sgs1 which is important for genomic stability (Versini *et al*, 2003) is rapidly degraded by autophagy. Deletion of *PEP4* therefore causes stabilization of Sgs1 and also other key proteins in the rapamycin response pathway. In their opinion, this

might be the reason for the missing growth defect of rapamycin-treated *Δpep4* cells. Also the strains deleted in *UBR1* and/ or the *HSP31-33* genes showed no increased sensitivity against rapamycin. However, the combination of these deletions together with the *PEP4* deletion causes inhibition of growth of cells on rapamycin-containing YPD plates. This indicates that the vacuolar pathway is only dispensable in stationary phase if both the Hsp31 chaperones and the Ubr1-mediated degradation pathway are active.

Miller-Fleming *et al*. showed that the Hsp31 chaperones are involved in the assembly of stress granules (SG) and processing (P)-bodies and that Hsp31 and Hsp32 colocalize with both structures (Miller-Fleming *et al*, 2014). Stress granules are structures important for storage of non-translating RNAs after translational inhibition during diverse stress responses. P-bodies are similar but contain enzymes for mRNA degradation (Buchan *et al*, 2008; Buchan and Parker, 2009). Therefore in future studies it has to be ruled out whether the effect of the Hsp31 chaperones on the steady state level of misfolded cytoplasmic substrates is due to mRNA stability. However, the question arises here how misfolding of a substrate should be detected on mRNA level? The influence of the Hsp31 chaperone family on the steady state levels of substrates seems to depend on the degree of misfolding of the protein as seen in the luciferase-experiments (Fig. 3.43). In this study it was shown that the absence of the Hsp31 chaperones in a *Δubr1* strain causes dramatic increase of the luciferase activity of the highly unstable substrate LucDMLeu2myc whereas such an influence on the relative stable substrate LucLeu2myc is small (Fig. 3.43). Once antibodies get available, direct interaction between Hsp31 family members and substrates can be tested in pulldown experiments.

Expression data revealed that several genes are down-regulated in absence of the Hsp31 chaperone family. These genes include gluconeogenic genes, genes involved in trehalose and glycogen synthesis and also chaperones like the Hsp70 family member Ssa3, all expressed in wild type cells at diauxic shift (Boorstein and Craig, 1990; Miller-Fleming *et al*, 2014). Therefore, it seems that expression of stationary phase proteins is disturbed when members of the Hsp31 chaperone family are absent. It is also known from expression data that the ubiquitin-conjugating enzymes Ubc1 and Ubc5 (Seufert and Jentsch, 1990; Seufert *et al*, 1990) and the ubiquitin-encoding gene Ubi4 are induced in stationary-phase cells (Finley *et al*, 1987) as is the small chaperone Hsp26 (Susek and Lindquist, 1990). Thus the possibility exists that the increased steady state level of ΔssCL*myc might be due to down-regulation of these genes caused by absence of the Hsp31 chaperone family. In future experiments overexpression of these genes in a *Δhsp31-33* strain could be tested for checking whether the ΔssCL*myc-expressing *Δhsp31-33* strain phenotype concerning growth on media lacking

leucine can be rescued. Another study dealing with a yeast model of Parkinson's disease showed that α-synuclein expressed in yeast induces apoptosis and that Ssa3 expression can protect cells from α-synuclein toxicity (Flower *et al*, 2005). It is known that human DJ-1 which is the homologue of the yeast Hsp31-33 proteins is a chaperone possessing neuroprotecive functions. Loss of DJ-1 function causes familial Parkinson' disease by loss of dopaminergic neurons (Abou-Sleiman *et al*, 2003; Bonifati *et al*, 2003; Hague *et al*, 2003). The reason of the loss of neuronal cells might be the downregulation of Ssa3 and therefore increased α-synuclein toxicity followed by apoptosis of dopaminergic neurons.

A direct function of Hsp31 chaperones in the elimination of misfolded proteins in an own proteolytic pathway has also been discussed. The structure of Hsp31 family members in yeast has been resolved (Graille *et al*, 2004; Guo *et al*, 2010; Wilson *et al*, 2004). It has been found that they possess a putative Cys-His-Glu catalytic triad. They are structurally similar to the *E. coli* Hsp31. It has been shown that *E. coli* Hsp31 possesses both, chaperone and aminopeptidase activity (Malki *et al*, 2005; Mujacic *et al*, 2004). Therefore mutational analysis performed in future experiments could unravel a potential influence of the putative catalytic triad on Hsp31 chaperone family function.

4.5 Protein quality control of the cytoplasmic FAS protein complex

Most protein complexes are built up by non-covalent protein-protein interactions between the different subunits in a fixed stoichiometry. An imbalance of subunit stoichiometry resulting in non-complexed subunit species can be dangerous for the cell because unwanted interactions with other proteins could occur. This study uses the fatty acid synthase (FAS) complex as model protein complex for investigating the fate of an orphan subunit, Fas2, when its complex partner Fas1 is missing. This situation mimics a stoichiometric imbalance of complex subunit protein levels. As known for misfolded cytoplasmic proteins like ΔssCl*myc also used in this study, orphan Fas2 is degraded in an Ubr1-dependent manner (Scazzari, 2013). It was shown in this study that Ubr1 labels orphan Fas2 with ubiquitin chains and that Fas2, if complexed with Fas1, is not ubiquitinated and is therefore stable. This implies that the degradation signal in orphan Fas2 essential for Ubr1 recognition is shielded in the functional FAS complex. Ubr1 was first discovered as the E3 ligase of the N-end rule pathway. Therefore, the question arose whether orphan Fas2 exposes an N-degron which is recognized by Ubr1. The N-

terminus of Fas2 consists of the amino acids methionine followed by the basic amino acid lysine. According to the Sherman rule (Sherman *et al*, 1985) methionine in front of lysine cannot be cleaved off by methionine amino peptidases. Methionine as N-terminal amino acid is classified as a stabilizing residue not recognized by Ubr1 according the N-end rule (Varshavsky, 2011) except when methionine is followed by hydrophobic residues (Kim *et al*, 2014). It was shown that acetylation of N-terminal methionine can also cause ubiquitination and degradation of corresponding substrates (Kim *et al*, 2014; Starheim *et al*, 2012). However, acetyltransferases hardly acetylate N-termini of proteins possessing lysine on the second position. Therefore, Fas2 does not represent an N-end rule substrate. Since intermolecular protein interactions among complex subunits are mainly hydrophobic it might be that Fas2, if Fas1 is absent, exposes hydrophobic patches on its protein surface for further recognition by chaperones or components of the proteasomal degradation machinery. The most misfolded proteins are characterized by high surface hydrophobicity which might explain the dependency of both, orphan Fas2 and misfolded cytosolic proteins like ΔssCL*myc on the cytoplasmic protein quality control components Ubr1 and Hsp70 chaperones of the Ssa type. Absence of functional Ssa chaperones causes both aggregation of ΔssCL*myc and orphan Fas2 (Fig. 3.7, Fig. 3.53). Further experiments are needed to uncover the degron in orphan Fas2 recognized by the degradation machinery. Site-direct mutagenesis of amino acids present in the Fas1-interacting region of Fas2 should give an answer.

Interestingly, the misfolded cytosolic model substrates tested are degraded with a half-life of about half an hour (Fig. 3.4). In contrast, orphan Fas2 is degraded with a rather long half-life of 2 hours (Fig. 3.48). This might be explained by the observation that orphan Fas2 is not organized as monomers but as oligomeric complexes (Fig. 3.46). Probably the wheel-like hexameric Fas2 rings are formed which are the docking sites for the Fas1 subunits. Therefore, the time-consuming step responsible for this long half-life could be the initial dissociation of the Fas2 ring into Fas2 monomers prior to proteasomal degradation. The Cdc48 machinery is known to be involved in many dissociation processes like the extraction of ERAD substrates from the ER membrane. The force for these processes is generated by ATP hydrolysis exerted by Cdc48 (Stolz *et al*, 2011). In this study, it was shown that non-functional Cdc48 does not inhibit Ubr1-dependent ubiquitination of orphan Fas2 but its degradation (Fig. 3.55, Fig. 3.56). Orphan Fas2 is ubiquitinated by Ubr1 despite organization in oligomeric states prior to its dissociation into monomeric ubiquitinated Fas2 via the Cdc48 machinery. This step is essential for subsequent proteasomal degradation. This sequential mode of steps required for

orphan Fas2 degradation is similar to the catabolite degradation of the enzyme fructose-1,6 bisphosphatase (FBPase): Under glycolytic conditions the homotetrameric FBPase complex binds to the GID (glucose induced degradation deficient) ligase complex and is ubiquitinated (Barbin *et al*, 2010; Santt *et al*, 2008). Afterwards ubiquitinated FBPase is separated and extracted from the GID complex by the action of the Cdc48 machine prior to proteasomal degradation.

The Hsp70 chaperone Ssa1 is also essential for the degradation of orphan Fas2. In contrast to Cdc48, ubiquitination of orphan Fas2 is abolished if a functional Ssa1 chaperone is missing (Fig. 3.54). This result indicates that Ssa1 functions upstream of Ubr1-mediated ubiquitination of orphan Fas2. In this study, it was also shown that ΔssCL*myc is an aggregation-prone protein and that Ssa1 is needed for keeping ΔssCL*myc in a soluble state for further degradation (Fig. 3.7, Fig. 3.8). Interestingly, this is also the case for orphan Fas2 (Fig. 3.53). Absence of Fas1 probably causes exposure of hydrophobic patches on Fas2 which might be necessary in the wild type situation for mediating protein interactions with its partner Fas1. In this study, orphan Fas2 was shown to aggregate in absence of functional Ssa chaperones (Fig. 3.53). Therefore, Ssa function probably resides in keeping orphan Fas2 soluble for subsequent recognition by the Ubr1-dependent degradation machinery. The proposed model for protein quality control of orphan Fas2 is illustrated in Fig. 4.1.

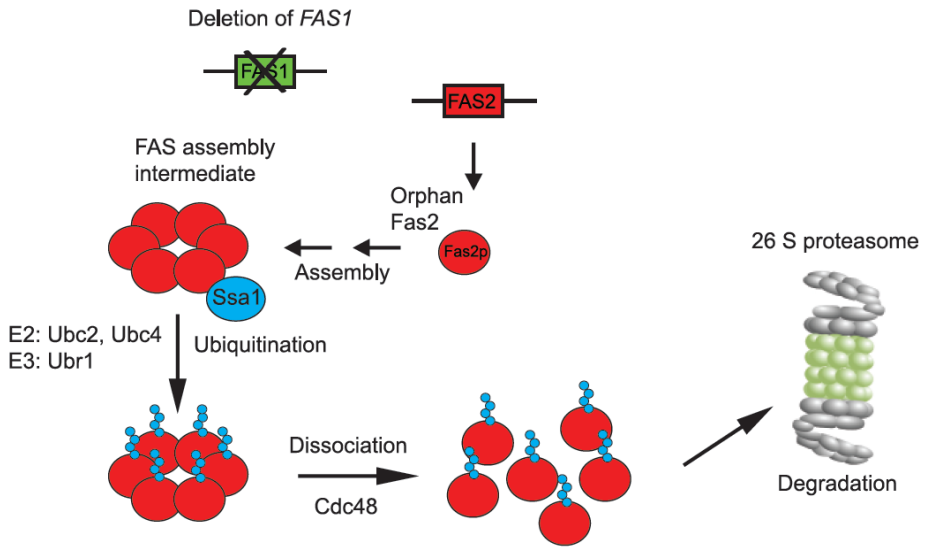

Figure 4.1: Proposed model of protein quality control of orphan Fas2. In the absence of Fas1, Fas2 which is organized in oligomeric (probably hexameric) complexes is recognized by the ubiquitin ligase Ubr1. The ubiquitin-conjugating enzymes Ubc2 and Ubc4 serve as ubiquitin-conjugating enzymes (Scazzari, 2013). Ubiquitinated orphan Fas2 is disassembled by the action of the Cdc48 machinery before final degradation by the proteasome. The degradation of orphan Fas2 also requires the Hsp70 chaperone Ssa1 which keeps orphan Fas2 in a soluble state essential for ubiquitination and degradation by the Ubr1-mediated degradation machinery.

Degradation of orphan Fas2 is almost blocked if Ubr1 is missing as shown in Fig. 3.51. After 4 hours still a certain degree of degradation in the *Δubr1* strain can be observed. Therefore, other proteolytic systems might complement the Ubr1-mediated degradation pathway. In future experiments the influence of other degradation components should be tested. It is very surprising that orphan Fas2 is mainly degraded by the proteasome whereas orphan Fas1 is predominantly degraded by the vacuole (Egner *et al*, 1993). This challenging phenomenon also awaits further elucidation.

5. REFERENCES

Abou-Sleiman PM, Healy DG, Quinn N, Lees AJ, Wood NW (2003) The role of pathogenic DJ-1 mutations in Parkinson's disease. *Ann Neurol* **54:** 283-286

Achstetter T, Emter O, Ehmann C, Wolf DH (1984) Proteolysis in eukaryotic cells. Identification of multiple proteolytic enzymes in yeast. *J Biol Chem* **259:** 13334-13343

Aebi M, Bernasconi R, Clerc S, Molinari M (2010) N-glycan structures: recognition and processing in the ER. *Trends Biochem Sci* **35:** 74-82

Akimitsu N (2008) Messenger RNA surveillance systems monitoring proper translation termination. *J Biochem* **143:** 1-8

Alamgir M, Erukova V, Jessulat M, Azizi A, Golshani A (2010) Chemical-genetic profile analysis of five inhibitory compounds in yeast. *BMC Chem Biol* **10:** 6

Alberti S, Esser C, Hohfeld J (2003) BAG-1--a nucleotide exchange factor of Hsc70 with multiple cellular functions. *Cell Stress Chaperones* **8:** 225-231

Ali MM, Roe SM, Vaughan CK, Meyer P, Panaretou B, Piper PW, Prodromou C, Pearl LH (2006) Crystal structure of an Hsp90-nucleotide-p23/Sba1 closed chaperone complex. *Nature* **440:** 1013-1017

Amerik A, Swaminathan S, Krantz BA, Wilkinson KD, Hochstrasser M (1997) In vivo disassembly of free polyubiquitin chains by yeast Ubp14 modulates rates of protein degradation by the proteasome. *EMBO J* **16:** 4826-4838

Amm I, Sommer T, Wolf DH (2014) Protein quality control and elimination of protein waste: The role of the ubiquitin-proteasome system. *Biochim Biophys Acta* **1843:** 182-196

Ammerer G, Hunter CP, Rothman JH, Saari GC, Valls LA, Stevens TH (1986) PEP4 gene of Saccharomyces cerevisiae encodes proteinase A, a vacuolar enzyme required for processing of vacuolar precursors. *Mol Cell Biol* **6:** 2490-2499

Anfinsen CB (1973) Principles that govern the folding of protein chains. *Science* **181:** 223-230

Anfinsen CB, Haber E, Sela M, White FH, Jr. (1961) The kinetics of formation of native ribonuclease during oxidation of the reduced polypeptide chain. *Proc Natl Acad Sci U S A* **47:** 1309-1314

Araki K, Nagata K (2011) Protein folding and quality control in the ER. *Cold Spring Harb Perspect Biol* **3:** a015438

Aviram S, Kornitzer D (2010) The ubiquitin ligase Hul5 promotes proteasomal processivity. *Mol Cell Biol* **30:** 985-994

Bachmair A, Finley D, Varshavsky A (1986) In vivo half-life of a protein is a function of its amino-terminal residue. *Science* **234:** 179-186

Barbet NC, Schneider U, Helliwell SB, Stansfield I, Tuite MF, Hall MN (1996) TOR controls translation initiation and early G1 progression in yeast. *Mol Biol Cell* **7:** 25-42

Barbin L, Eisele F, Santt O, Wolf DH (2010) The Cdc48-Ufd1-Npl4 complex is central in ubiquitin-proteasome triggered catabolite degradation of fructose-1,6-bisphosphatase. *Biochem Biophys Res Commun* **394:** 335-341

Barriere H, Nemes C, Du K, Lukacs GL (2007) Plasticity of polyubiquitin recognition as lysosomal targeting signals by the endosomal sorting machinery. *Mol Biol Cell* **18:** 3952-3965

Bartel B, Wunning I, Varshavsky A (1990) The recognition component of the N-end rule pathway. *EMBO J* **9:** 3179-3189

Bays NW, Wilhovsky SK, Goradia A, Hodgkiss-Harlow K, Hampton RY (2001) HRD4/NPL4 is required for the proteasomal processing of ubiquitinated ER proteins. *Mol Biol Cell* **12:** 4114-4128

Beck T, Hall MN (1999) The TOR signalling pathway controls nuclear localization of nutrient-regulated transcription factors. *Nature* **402:** 689-692

Becker J, Walter W, Yan W, Craig EA (1996) Functional interaction of cytosolic hsp70 and a DnaJ-related protein, Ydj1p, in protein translocation in vivo. *Mol Cell Biol* **16:** 4378-4386

Berset C, Trachsel H, Altmann M (1998) The TOR (target of rapamycin) signal transduction pathway regulates the stability of translation initiation factor eIF4G in the yeast Saccharomyces cerevisiae. *Proc Natl Acad Sci U S A* **95:** 4264-4269

Bonifati V, Rizzu P, van Baren MJ, Schaap O, Breedveld GJ, Krieger E, Dekker MC, Squitieri F, Ibanez P, Joosse M, van Dongen JW, Vanacore N, van Swieten JC, Brice A, Meco G, van Duijn CM, Oostra BA, Heutink P (2003) Mutations in the DJ-1 gene associated with autosomal recessive early-onset parkinsonism. *Science* **299:** 256-259

Boorstein WR, Craig EA (1990) Transcriptional regulation of SSA3, an HSP70 gene from Saccharomyces cerevisiae. *Mol Cell Biol* **10:** 3262-3267

Bordallo J, Plemper RK, Finger A, Wolf DH (1998) Der3p/Hrd1p is required for endoplasmic reticulum-associated degradation of misfolded lumenal and integral membrane proteins. *Mol Biol Cell* **9:** 209-222

Bradford MM (1976) A rapid and sensitive method for the quantitation of microgram quantities of protein utilizing the principle of protein-dye binding. *Analytical biochemistry* **72:** 248-254

Brandman O, Stewart-Ornstein J, Wong D, Larson A, Williams CC, Li GW, Zhou S, King D, Shen PS, Weibezahn J, Dunn JG, Rouskin S, Inada T, Frost A, Weissman JS (2012) A ribosome-bound quality control complex triggers degradation of nascent peptides and signals translation stress. *Cell* **151:** 1042-1054

Braun MA, Costa PJ, Crisucci EM, Arndt KM (2007) Identification of Rkr1, a nuclear RING domain protein with functional connections to chromatin modification in Saccharomyces cerevisiae. *Mol Cell Biol* **27:** 2800-2811

Buchan JR, Muhlrad D, Parker R (2008) P bodies promote stress granule assembly in Saccharomyces cerevisiae. *J Cell Biol* **183:** 441-455

Buchan JR, Parker R (2009) Eukaryotic stress granules: the ins and outs of translation. *Mol Cell* **36:** 932-941

Bukau B, Weissman J, Horwich A (2006) Molecular chaperones and protein quality control. *Cell* **125:** 443-451

Burkl G, Castorph H, Schweizer E (1972) Mapping of a complex gene locus coding for part of the Saccharomyces cerevisiae fatty acid synthetase multienzyme complex. *Mol Gen Genet* **119:** 315-322

Byrd C, Turner GC, Varshavsky A (1998) The N-end rule pathway controls the import of peptides through degradation of a transcriptional repressor. *EMBO J* **17:** 269-277

Camasses A, Bogdanova A, Shevchenko A, Zachariae W (2003) The CCT chaperonin promotes activation of the anaphase-promoting complex through the generation of functional Cdc20. *Mol Cell* **12:** 87-100

Carvalho P, Goder V, Rapoport TA (2006) Distinct ubiquitin-ligase complexes define convergent pathways for the degradation of ER proteins. *Cell* **126:** 361-373

Cashikar AG, Duennwald M, Lindquist SL (2005) A chaperone pathway in protein disaggregation. Hsp26 alters the nature of protein aggregates to facilitate reactivation by Hsp104. *J Biol Chem* **280:** 23869-23875

Chandler D (2005) Interfaces and the driving force of hydrophobic assembly. *Nature* **437:** 640-647

Chau V, Tobias JW, Bachmair A, Marriott D, Ecker DJ, Gonda DK, Varshavsky A (1989) A multiubiquitin chain is confined to specific lysine in a targeted short-lived protein. *Science* **243:** 1576-1583

Chen B, Retzlaff M, Roos T, Frydman J (2011) Cellular strategies of protein quality control. *Cold Spring Harb Perspect Biol* **3:** a004374

Chen S, Smith DF (1998) Hop as an adaptor in the heat shock protein 70 (Hsp70) and hsp90 chaperone machinery. *J Biol Chem* **273:** 35194-35200

Chiang HL, Schekman R (1991) Regulated import and degradation of a cytosolic protein in the yeast vacuole. *Nature* **350:** 313-318

Choi WS, Jeong BC, Joo YJ, Lee MR, Kim J, Eck MJ, Song HK (2010) Structural basis for the recognition of N-end rule substrates by the UBR box of ubiquitin ligases. *Nat Struct Mol Biol* **17:** 1175-1181

Christianson TW, Sikorski RS, Dante M, Shero JH, Hieter P (1992) Multifunctional yeast high-copy-number shuttle vectors. *Gene* **110:** 119-122

Ciechanover A, Stanhill A (2014) The complexity of recognition of ubiquitinated substrates by the 26S proteasome. *Biochim Biophys Acta* **1843:** 86-96

Clerc S, Hirsch C, Oggier DM, Deprez P, Jakob C, Sommer T, Aebi M (2009) Htm1 protein generates the N-glycan signal for glycoprotein degradation in the endoplasmic reticulum. *J Cell Biol* **184:** 159-172

Coffino P (2001) Regulation of cellular polyamines by antizyme. *Nat Rev Mol Cell Biol* **2:** 188-194

Conz C, Otto H, Peisker K, Gautschi M, Wolfle T, Mayer MP, Rospert S (2007) Functional characterization of the atypical Hsp70 subunit of yeast ribosome-associated complex. *J Biol Chem* **282:** 33977-33984

Costanzo M, Baryshnikova A, Bellay J, Kim Y, Spear ED, Sevier CS, Ding H, Koh JL, Toufighi K, Mostafavi S, Prinz J, St Onge RP, VanderSluis B, Makhnevych T, Vizeacoumar FJ, Alizadeh S, Bahr S, Brost RL, Chen Y, Cokol M, Deshpande R, Li Z, Lin ZY, Liang W, Marback M, Paw J, San Luis BJ, Shuteriqi E, Tong AH, van Dyk N, Wallace IM, Whitney JA, Weirauch MT, Zhong G, Zhu H, Houry WA, Brudno M, Ragibizadeh S, Papp B, Pal C, Roth FP, Giaever G, Nislow C, Troyanskaya OG, Bussey H, Bader GD, Gingras AC, Morris QD, Kim PM, Kaiser CA, Myers CL, Andrews BJ, Boone C (2010) The genetic landscape of a cell. *Science* **327:** 425-431

Craig EA, Eisenman HC, Hundley HA (2003) Ribosome-tethered molecular chaperones: the first line of defense against protein misfolding? *Curr Opin Microbiol* **6:** 157-162

Crespo JL, Hall MN (2002) Elucidating TOR signaling and rapamycin action: lessons from Saccharomyces cerevisiae. *Microbiol Mol Biol Rev* **66:** 579-591, table of contents

Cuervo AM (2004) Autophagy: in sickness and in health. *Trends Cell Biol* **14:** 70-77

Dasgupta A, Ramsey KL, Smith JS, Auble DT (2004) Sir Antagonist 1 (San1) is a ubiquitin ligase. *J Biol Chem* **279:** 26830-26838

Davies KJ (2001) Degradation of oxidized proteins by the 20S proteasome. *Biochimie* **83:** 301-310

Deak PM, Wolf DH (2001) Membrane topology and function of Der3/Hrd1p as a ubiquitin-protein ligase (E3) involved in endoplasmic reticulum degradation. *J Biol Chem* **276:** 10663-10669

Deshaies RJ, Joazeiro CA (2009) RING domain E3 ubiquitin ligases. *Annu Rev Biochem* **78:** 399-434

Deveraux Q, Ustrell V, Pickart C, Rechsteiner M (1994) A 26 S protease subunit that binds ubiquitin conjugates. *J Biol Chem* **269:** 7059-7061

Diamant S, Ben-Zvi AP, Bukau B, Goloubinoff P (2000) Size-dependent disaggregation of stable protein aggregates by the DnaK chaperone machinery. *J Biol Chem* **275:** 21107-21113

Dill KA, Chan HS (1997) From Levinthal to pathways to funnels. *Nat Struct Biol* **4:** 10-19

Dimitrova LN, Kuroha K, Tatematsu T, Inada T (2009) Nascent peptide-dependent translation arrest leads to Not4p-mediated protein degradation by the proteasome. *J Biol Chem* **284:** 10343-10352

Dobson CM, Sali A, Kaplus M (1998) Protein Folding: A Perspective from Theory and Experiment. *Angew Chem Int Ed Engl* **37:** 868-893

Dohmen RJ, Stappen R, McGrath JP, Forrova H, Kolarov J, Goffeau A, Varshavsky A (1995) An essential yeast gene encoding a homolog of ubiquitin-activating enzyme. *J Biol Chem* **270:** 18099-18109

Dollins DE, Warren JJ, Immormino RM, Gewirth DT (2007) Structures of GRP94-nucleotide complexes reveal mechanistic differences between the hsp90 chaperones. *Mol Cell* **28:** 41-56

Douglas NR, Reissmann S, Zhang J, Chen B, Jakana J, Kumar R, Chiu W, Frydman J (2011) Dual action of ATP hydrolysis couples lid closure to substrate release into the group II chaperonin chamber. *Cell* **144:** 240-252

Doyle SM, Wickner S (2009) Hsp104 and ClpB: protein disaggregating machines. *Trends Biochem Sci* **34:** 40-48

Dunn WA, Jr. (1990) Studies on the mechanisms of autophagy: formation of the autophagic vacuole. *J Cell Biol* **110:** 1923-1933

Dunn WA, Jr., Cregg JM, Kiel JA, van der Klei IJ, Oku M, Sakai Y, Sibirny AA, Stasyk OV, Veenhuis M (2005) Pexophagy: the selective autophagy of peroxisomes. *Autophagy* **1:** 75-83

Egner R, Thumm M, Straub M, Simeon A, Schuller HJ, Wolf DH (1993) Tracing intracellular proteolytic pathways. Proteolysis of fatty acid synthase and other cytoplasmic proteins in the yeast Saccharomyces cerevisiae. *J Biol Chem* **268:** 27269-27276

Eisele F, Wolf DH (2008) Degradation of misfolded protein in the cytoplasm is mediated by the ubiquitin ligase Ubr1. *FEBS Lett* **582:** 4143-4146

Ellis RJ (2001) Macromolecular crowding: obvious but underappreciated. *Trends Biochem Sci* **26:** 597-604

Ellis RJ, Minton AP (2006) Protein aggregation in crowded environments. *Biol Chem* **387:** 485-497

Elsasser S, Chandler-Militello D, Muller B, Hanna J, Finley D (2004) Rad23 and Rpn10 serve as alternative ubiquitin receptors for the proteasome. *J Biol Chem* **279:** 26817-26822

Elsasser S, Gali RR, Schwickart M, Larsen CN, Leggett DS, Muller B, Feng MT, Tubing F, Dittmar GA, Finley D (2002) Proteasome subunit Rpn1 binds ubiquitin-like protein domains. *Nat Cell Biol* **4:** 725-730

Erales J, Coffino P (2014) Ubiquitin-independent proteasomal degradation. *Biochim Biophys Acta* **1843:** 216-221

Feldherr CM, Akin D (1997) The location of the transport gate in the nuclear pore complex. *J Cell Sci* **110 (Pt 24):** 3065-3070

Feldman DE, Thulasiraman V, Ferreyra RG, Frydman J (1999) Formation of the VHL-elongin BC tumor suppressor complex is mediated by the chaperonin TRiC. *Mol Cell* **4:** 1051-1061

Finger A, Knop M, Wolf DH (1993) Analysis of two mutated vacuolar proteins reveals a degradation pathway in the endoplasmic reticulum or a related compartment of yeast. *Eur J Biochem* **218:** 565-574

Finley D, Ozkaynak E, Varshavsky A (1987) The yeast polyubiquitin gene is essential for resistance to high temperatures, starvation, and other stresses. *Cell* **48:** 1035-1046

Flower TR, Chesnokova LS, Froelich CA, Dixon C, Witt SN (2005) Heat shock prevents alpha-synuclein-induced apoptosis in a yeast model of Parkinson's disease. *J Mol Biol* **351:** 1081-1100

Fredrickson EK, Clowes Candadai SV, Tam CH, Gardner RG (2013a) Means of self-preservation: how an intrinsically disordered ubiquitin-protein ligase averts self-destruction. *Mol Biol Cell* **24:** 1041-1052

Fredrickson EK, Gallagher PS, Clowes Candadai SV, Gardner RG (2013b) Substrate recognition in nuclear protein quality control degradation is governed by exposed hydrophobicity that correlates with aggregation and insolubility. *J Biol Chem* **288:** 6130-6139

Fredrickson EK, Rosenbaum JC, Locke MN, Milac TI, Gardner RG (2011) Exposed hydrophobicity is a key determinant of nuclear quality control degradation. *Mol Biol Cell* **22:** 2384-2395

Freedman RB, Hirst TR, Tuite MF (1994) Protein disulphide isomerase: building bridges in protein folding. *Trends Biochem Sci* **19:** 331-336

Frydman J (2001) Folding of newly translated proteins in vivo: the role of molecular chaperones. *Annu Rev Biochem* **70:** 603-647

Frydman J, Nimmesgern E, Ohtsuka K, Hartl FU (1994) Folding of nascent polypeptide chains in a high molecular mass assembly with molecular chaperones. *Nature* **370:** 111-117

Gao Y, Thomas JO, Chow RL, Lee GH, Cowan NJ (1992) A cytoplasmic chaperonin that catalyzes beta-actin folding. *Cell* **69:** 1043-1050

Gao Y, Vainberg IE, Chow RL, Cowan NJ (1993) Two cofactors and cytoplasmic chaperonin are required for the folding of alpha- and beta-tubulin. *Mol Cell Biol* **13:** 2478-2485

Gardner RG, Nelson ZW, Gottschling DE (2005) Degradation-mediated protein quality control in the nucleus. *Cell* **120:** 803-815

Gauss R, Kanehara K, Carvalho P, Ng DT, Aebi M (2011) A complex of Pdi1p and the mannosidase Htm1p initiates clearance of unfolded glycoproteins from the endoplasmic reticulum. *Mol Cell* **42:** 782-793

Ghaboosi N, Deshaies RJ (2007) A conditional yeast E1 mutant blocks the ubiquitin-proteasome pathway and reveals a role for ubiquitin conjugates in targeting Rad23 to the proteasome. *Mol Biol Cell* **18:** 1953-1963

Ghislain M, Udvardy A, Mann C (1993) S. cerevisiae 26S protease mutants arrest cell division in G2/metaphase. *Nature* **366:** 358-362

Gietz RD, Sugino A (1988) New yeast-Escherichia coli shuttle vectors constructed with in vitro mutagenized yeast genes lacking six-base pair restriction sites. *Gene* **74:** 527-534

Gietz RD, Woods RA (2002) Transformation of yeast by lithium acetate/single-stranded carrier DNA/polyethylene glycol method. *Methods Enzymol* **350:** 87-96

Gilon T, Chomsky O, Kulka RG (1998) Degradation signals for ubiquitin system proteolysis in Saccharomyces cerevisiae. *EMBO J* **17:** 2759-2766

Gilon T, Chomsky O, Kulka RG (2000) Degradation signals recognized by the Ubc6p-Ubc7p ubiquitin-conjugating enzyme pair. *Mol Cell Biol* **20:** 7214-7219

Glickman MH, Ciechanover A (2002) The ubiquitin-proteasome proteolytic pathway: destruction for the sake of construction. *Physiol Rev* **82:** 373-428

Glover JR, Lindquist S (1998) Hsp104, Hsp70, and Hsp40: a novel chaperone system that rescues previously aggregated proteins. *Cell* **94:** 73-82

Goldfarb DS, Gariepy J, Schoolnik G, Kornberg RD (1986) Synthetic peptides as nuclear localization signals. *Nature* **322:** 641-644

Goloubinoff P, Mogk A, Zvi AP, Tomoyasu T, Bukau B (1999) Sequential mechanism of solubilization and refolding of stable protein aggregates by a bichaperone network. *Proc Natl Acad Sci U S A* **96:** 13732-13737

Gomez-Puertas P, Martin-Benito J, Carrascosa JL, Willison KR, Valpuesta JM (2004) The substrate recognition mechanisms in chaperonins. *J Mol Recognit* **17:** 85-94

Gorlich D, Prehn S, Laskey RA, Hartmann E (1994) Isolation of a protein that is essential for the first step of nuclear protein import. *Cell* **79:** 767-778

Gould SJ, Keller GA, Hosken N, Wilkinson J, Subramani S (1989) A conserved tripeptide sorts proteins to peroxisomes. *J Cell Biol* **108:** 1657-1664

Graille M, Quevillon-Cheruel S, Leulliot N, Zhou CZ, Li de la Sierra Gallay I, Jacquamet L, Ferrer JL, Liger D, Poupon A, Janin J, van Tilbeurgh H (2004) Crystal structure of the YDR533c S. cerevisiae protein, a class II member of the Hsp31 family. *Structure* **12:** 839-847

Gueldener U, Heinisch J, Koehler GJ, Voss D, Hegemann JH (2002) A second set of loxP marker cassettes for Cre-mediated multiple gene knockouts in budding yeast. *Nucleic Acids Res* **30:** e23

Guo PC, Zhou YY, Ma XX, Li WF (2010) Structure of Hsp33/YOR391Cp from the yeast Saccharomyces cerevisiae. *Acta Crystallogr Sect F Struct Biol Cryst Commun* **66:** 1557-1561

Gupta R, Kasturi P, Bracher A, Loew C, Zheng M, Villella A, Garza D, Hartl FU, Raychaudhuri S (2011) Firefly luciferase mutants as sensors of proteome stress. *Nat Methods* **8:** 879-884

Hague S, Rogaeva E, Hernandez D, Gulick C, Singleton A, Hanson M, Johnson J, Weiser R, Gallardo M, Ravina B, Gwinn-Hardy K, Crawley A, St George-Hyslop PH, Lang AE, Heutink P, Bonifati V, Hardy J (2003) Early-onset Parkinson's disease caused by a compound heterozygous DJ-1 mutation. *Ann Neurol* **54:** 271-274

Haigh NG, Johnson AE (2002) Protein Sorting at the Membrane of the Endoplasmic Reticulum. In *Protein Targeting, Transport, and Translocation*, Dalbey R, Von Heijne G (eds), pp 74-106. London: Academic Press

Hampton RY, Sommer T (2012) Finding the will and the way of ERAD substrate retrotranslocation. *Curr Opin Cell Biol* **24:** 460-466

Hardwick JS, Kuruvilla FG, Tong JK, Shamji AF, Schreiber SL (1999) Rapamycin-modulated transcription defines the subset of nutrient-sensitive signaling pathways directly controlled by the Tor proteins. *Proc Natl Acad Sci U S A* **96:** 14866-14870

Harris SF, Shiau AK, Agard DA (2004) The crystal structure of the carboxy-terminal dimerization domain of htpG, the Escherichia coli Hsp90, reveals a potential substrate binding site. *Structure* **12:** 1087-1097

Hartl FU, Bracher A, Hayer-Hartl M (2011) Molecular chaperones in protein folding and proteostasis. *Nature* **475:** 324-332

Hartl FU, Hayer-Hartl M (2002) Molecular chaperones in the cytosol: from nascent chain to folded protein. *Science* **295:** 1852-1858

Hartl FU, Hayer-Hartl M (2009) Converging concepts of protein folding in vitro and in vivo. *Nat Struct Mol Biol* **16:** 574-581

Hartmann-Petersen R, Gordon C (2004a) Integral UBL domain proteins: a family of proteasome interacting proteins. *Semin Cell Dev Biol* **15:** 247-259

Hartmann-Petersen R, Gordon C (2004b) Protein degradation: recognition of ubiquitinylated substrates. *Curr Biol* **14:** R754-756

Hartmann-Petersen R, Gordon C (2004c) Proteins interacting with the 26S proteasome. *Cell Mol Life Sci* **61:** 1589-1595

Hartmann-Petersen R, Seeger M, Gordon C (2003) Transferring substrates to the 26S proteasome. *Trends Biochem Sci* **28:** 26-31

Hasin N, Cusack SA, Ali SS, Fitzpatrick DA, Jones GW (2014) Global transcript and phenotypic analysis of yeast cells expressing Ssa1, Ssa2, Ssa3 or Ssa4 as sole source of cytosolic Hsp70-Ssa chaperone activity. *BMC Genomics* **15:** 1-12

Haslbeck M, Braun N, Stromer T, Richter B, Model N, Weinkauf S, Buchner J (2004) Hsp42 is the general small heat shock protein in the cytosol of Saccharomyces cerevisiae. *EMBO J* **23:** 638-649

Haslbeck M, Miess A, Stromer T, Walter S, Buchner J (2005) Disassembling protein aggregates in the yeast cytosol. The cooperation of Hsp26 with Ssa1 and Hsp104. *J Biol Chem* **280:** 23861-23868

Haslberger T, Weibezahn J, Zahn R, Lee S, Tsai FT, Bukau B, Mogk A (2007) M domains couple the ClpB threading motor with the DnaK chaperone activity. *Mol Cell* **25:** 247-260

Haslberger T, Zdanowicz A, Brand I, Kirstein J, Turgay K, Mogk A, Bukau B (2008) Protein disaggregation by the AAA+ chaperone ClpB involves partial threading of looped polypeptide segments. *Nat Struct Mol Biol* **15:** 641-650

Hattendorf DA, Lindquist SL (2002) Cooperative kinetics of both Hsp104 ATPase domains and interdomain communication revealed by AAA sensor-1 mutants. *EMBO J* **21:** 12-21

He C, Klionsky DJ (2009) Regulation mechanisms and signaling pathways of autophagy. *Annu Rev Genet* **43:** 67-93

Heck JW, Cheung SK, Hampton RY (2010) Cytoplasmic protein quality control degradation mediated by parallel actions of the E3 ubiquitin ligases Ubr1 and San1. *Proc Natl Acad Sci U S A* **107:** 1106-1111

Hennessy F, Nicoll WS, Zimmermann R, Cheetham ME, Blatch GL (2005) Not all J domains are created equal: implications for the specificity of Hsp40-Hsp70 interactions. *Protein Sci* **14:** 1697-1709

Hershko A, Ciechanover A, Rose IA (1979) Resolution of the ATP-dependent proteolytic system from reticulocytes: a component that interacts with ATP. *Proc Natl Acad Sci U S A* **76:** 3107-3110

Hershko A, Heller H, Elias S, Ciechanover A (1983) Components of ubiquitin-protein ligase system. Resolution, affinity purification, and role in protein breakdown. *J Biol Chem* **258:** 8206-8214

Hiller MM, Finger A, Schweiger M, Wolf DH (1996) ER degradation of a misfolded luminal protein by the cytosolic ubiquitin-proteasome pathway. *Science* **273:** 1725-1728

Horwich AL, Fenton WA, Chapman E, Farr GW (2007) Two families of chaperonin: physiology and mechanism. *Annu Rev Cell Dev Biol* **23:** 115-145

Huang P, Gautschi M, Walter W, Rospert S, Craig EA (2005) The Hsp70 Ssz1 modulates the function of the ribosome-associated J-protein Zuo1. *Nat Struct Mol Biol* **12:** 497-504

Huibregtse JM, Scheffner M, Beaudenon S, Howley PM (1995) A family of proteins structurally and functionally related to the E6-AP ubiquitin-protein ligase. *Proc Natl Acad Sci U S A* **92:** 2563-2567

Husnjak K, Elsasser S, Zhang N, Chen X, Randles L, Shi Y, Hofmann K, Walters KJ, Finley D, Dikic I (2008) Proteasome subunit Rpn13 is a novel ubiquitin receptor. *Nature* **453:** 481-488

Huyer G, Piluek WF, Fansler Z, Kreft SG, Hochstrasser M, Brodsky JL, Michaelis S (2004) Distinct machinery is required in Saccharomyces cerevisiae for the endoplasmic reticulum-associated degradation of a multispanning membrane protein and a soluble luminal protein. *J Biol Chem* **279:** 38369-38378

Ikeda F, Dikic I (2008) Atypical ubiquitin chains: new molecular signals. 'Protein Modifications: Beyond the Usual Suspects' review series. *EMBO Rep* **9:** 536-542

Ito-Harashima S, Kuroha K, Tatematsu T, Inada T (2007) Translation of the poly(A) tail plays crucial roles in nonstop mRNA surveillance via translation repression and protein destabilization by proteasome in yeast. *Genes Dev* **21:** 519-524

Iwata A, Riley BE, Johnston JA, Kopito RR (2005) HDAC6 and microtubules are required for autophagic degradation of aggregated huntingtin. *J Biol Chem* **280:** 40282-40292

Jahn TR, Radford SE (2005) The Yin and Yang of protein folding. *FEBS J* **272:** 5962-5970

Jakob CA, Burda P, Roth J, Aebi M (1998) Degradation of misfolded endoplasmic reticulum glycoproteins in Saccharomyces cerevisiae is determined by a specific oligosaccharide structure. *J Cell Biol* **142:** 1223-1233

Jakob U, Gaestel M, Engel K, Buchner J (1993) Small heat shock proteins are molecular chaperones. *J Biol Chem* **268:** 1517-1520

Jaya N, Garcia V, Vierling E (2009) Substrate binding site flexibility of the small heat shock protein molecular chaperones. *Proc Natl Acad Sci U S A* **106:** 15604-15609

Jiang J, Maes EG, Taylor AB, Wang L, Hinck AP, Lafer EM, Sousa R (2007) Structural basis of J cochaperone binding and regulation of Hsp70. *Mol Cell* **28:** 422-433

Johnson BD, Schumacher RJ, Ross ED, Toft DO (1998) Hop modulates Hsp70/Hsp90 interactions in protein folding. *J Biol Chem* **273:** 3679-3686

Kaganovich D, Kopito R, Frydman J (2008) Misfolded proteins partition between two distinct quality control compartments. *Nature* **454:** 1088-1095

Kalisman N, Adams CM, Levitt M (2012) Subunit order of eukaryotic TRiC/CCT chaperonin by cross-linking, mass spectrometry, and combinatorial homology modeling. *Proc Natl Acad Sci U S A* **109:** 2884-2889

Kamada Y, Funakoshi T, Shintani T, Nagano K, Ohsumi M, Ohsumi Y (2000) Tor-mediated induction of autophagy via an Apg1 protein kinase complex. *J Cell Biol* **150:** 1507-1513

Kampinga HH, Craig EA (2010) The HSP70 chaperone machinery: J proteins as drivers of functional specificity. *Nat Rev Mol Cell Biol* **11:** 579-592

Kastle M, Reeg S, Rogowska-Wrzesinska A, Grune T (2012) Chaperones, but not oxidized proteins, are ubiquitinated after oxidative stress. *Free Radic Biol Med* **53:** 1468-1477

Keminer O, Peters R (1999) Permeability of single nuclear pores. *Biophys J* **77:** 217-228

Khosrow-Khavar F, Fang NN, Ng AH, Winget JM, Comyn SA, Mayor T (2012) The yeast ubr1 ubiquitin ligase participates in a prominent pathway that targets cytosolic thermosensitive mutants for degradation. *G3 (Bethesda)* **2:** 619-628

Kiel JA, Emmrich K, Meyer HE, Kunau WH (2005) Ubiquitination of the peroxisomal targeting signal type 1 receptor, Pex5p, suggests the presence of a quality control mechanism during peroxisomal matrix protein import. *J Biol Chem* **280:** 1921-1930

Kim HK, Kim RR, Oh JH, Cho H, Varshavsky A, Hwang CS (2014) The N-terminal methionine of cellular proteins as a degradation signal. *Cell* **156:** 158-169

Kim YE, Hipp MS, Bracher A, Hayer-Hartl M, Hartl FU (2013) Molecular chaperone functions in protein folding and proteostasis. *Annu Rev Biochem* **82:** 323-355

Kimmig P, Diaz M, Zheng J, Williams CC, Lang A, Aragon T, Li H, Walter P (2012) The unfolded protein response in fission yeast modulates stability of select mRNAs to maintain protein homeostasis. *Elife* **1:** e00048

Kirkin V, McEwan DG, Novak I, Dikic I (2009) A role for ubiquitin in selective autophagy. *Mol Cell* **34:** 259-269

Knop M, Finger A, Braun T, Hellmuth K, Wolf DH (1996a) Der1, a novel protein specifically required for endoplasmic reticulum degradation in yeast. *EMBO J* **15:** 753-763

Knop M, Hauser N, Wolf DH (1996b) N-Glycosylation affects endoplasmic reticulum degradation of a mutated derivative of carboxypeptidase yscY in yeast. *Yeast* **12:** 1229-1238

Koegl M, Hoppe T, Schlenker S, Ulrich HD, Mayer TU, Jentsch S (1999) A novel ubiquitination factor, E4, is involved in multiubiquitin chain assembly. *Cell* **96:** 635-644

Koepp DM, Harper JW, Elledge SJ (1999) How the cyclin became a cyclin: regulated proteolysis in the cell cycle. *Cell* **97:** 431-434

Kohlmann S, Schafer A, Wolf DH (2008) Ubiquitin ligase Hul5 is required for fragment-specific substrate degradation in endoplasmic reticulum-associated degradation. *J Biol Chem* **283:** 16374-16383

Korennykh A, Walter P (2012) Structural basis of the unfolded protein response. *Annu Rev Cell Dev Biol* **28:** 251-277

Kostova Z, Wolf DH (2003) For whom the bell tolls: protein quality control of the endoplasmic reticulum and the ubiquitin-proteasome connection. *EMBO J* **22:** 2309-2317

Kravtsova-Ivantsiv Y, Sommer T, Ciechanover A (2013) The lysine48-based polyubiquitin chain proteasomal signal: not a single child anymore. *Angew Chem Int Ed Engl* **52:** 192-198

Krukenberg KA, Forster F, Rice LM, Sali A, Agard DA (2008) Multiple conformations of E. coli Hsp90 in solution: insights into the conformational dynamics of Hsp90. *Structure* **16:** 755-765

Kuge S, Jones N, Nomoto A (1997) Regulation of yAP-1 nuclear localization in response to oxidative stress. *EMBO J* **16:** 1710-1720

Kuma A, Matsui M, Mizushima N (2007) LC3, an autophagosome marker, can be incorporated into protein aggregates independent of autophagy: caution in the interpretation of LC3 localization. *Autophagy* **3:** 323-328

Kundu M, Thompson CB (2005) Macroautophagy versus mitochondrial autophagy: a question of fate? *Cell Death Differ* **12 Suppl 2:** 1484-1489

Laemmli UK (1970) Cleavage of structural proteins during the assembly of the head of bacteriophage T4. *Nature* **227:** 680-685

Lander GC, Martin A, Nogales E (2013) The proteasome under the microscope: the regulatory particle in focus. *Curr Opin Struct Biol* **23:** 243-251

Leao-Helder AN, Krikken AM, Gellissen G, van der Klei IJ, Veenhuis M, Kiel JA (2004) Atg21p is essential for macropexophagy and microautophagy in the yeast Hansenula polymorpha. *FEBS Lett* **577:** 491-495

Leitner A, Joachimiak LA, Bracher A, Monkemeyer L, Walzthoeni T, Chen B, Pechmann S, Holmes S, Cong Y, Ma B, Ludtke S, Chiu W, Hartl FU, Aebersold R, Frydman J (2012) The molecular architecture of the eukaryotic chaperonin TRiC/CCT. *Structure* **20:** 814-825

Li J, Soroka J, Buchner J (2012) The Hsp90 chaperone machinery: conformational dynamics and regulation by co-chaperones. *Biochim Biophys Acta* **1823:** 624-635

Lima MM, Targa AD, Noseda AC, Rodrigues LS, Delattre AM, dos Santos FV, Fortes MH, Maturana MJ, Ferraz AC (2014) Does Parkinson's disease and type-2 diabetes mellitus present common pathophysiological mechanisms and treatments? *CNS Neurol Disord Drug Targets* **13:** 418-428

Lindquist S, Kim G (1996) Heat-shock protein 104 expression is sufficient for thermotolerance in yeast. *Proc Natl Acad Sci U S A* **93:** 5301-5306

Lomakin IB, Xiong Y, Steitz TA (2007) The crystal structure of yeast fatty acid synthase, a cellular machine with eight active sites working together. *Cell* **129:** 319-332

Lum R, Tkach JM, Vierling E, Glover JR (2004) Evidence for an unfolding/threading mechanism for protein disaggregation by Saccharomyces cerevisiae Hsp104. *J Biol Chem* **279:** 29139-29146

Lund PA (2001) Microbial molecular chaperones. *Adv Microb Physiol* **44:** 93-140

Lusk CP, Blobel G, King MC (2007) Highway to the inner nuclear membrane: rules for the road. *Nat Rev Mol Cell Biol* **8:** 414-420

Malki A, Caldas T, Abdallah J, Kern R, Eckey V, Kim SJ, Cha SS, Mori H, Richarme G (2005) Peptidase activity of the Escherichia coli Hsp31 chaperone. *J Biol Chem* **280:** 14420-14426

Marrakchi R, Chouchani C, Poschmann J, Andreev E, Cherif M, Ramotar D (2013) A functional autophagy pathway is required for rapamycin-induced degradation of the Sgs1 helicase in Saccharomyces cerevisiae. *Biochem Cell Biol* **91:** 123-130

Martoglio B, Dobberstein B (1998) Signal sequences: more than just greasy peptides. *Trends Cell Biol* **8:** 410-415

Mayer MP, Brehmer D, Gassler CS, Bukau B (2001) Hsp70 chaperone machines. *Adv Protein Chem* **59:** 1-44

Mayer MP, Bukau B (2005) Hsp70 chaperones: cellular functions and molecular mechanism. *Cell Mol Life Sci* **62:** 670-684

McClellan AJ, Scott MD, Frydman J (2005) Folding and quality control of the VHL tumor suppressor proceed through distinct chaperone pathways. *Cell* **121:** 739-748

Medicherla B, Kostova Z, Schaefer A, Wolf DH (2004) A genomic screen identifies Dsk2p and Rad23p as essential components of ER-associated degradation. *EMBO Rep* **5:** 692-697

Melville MW, McClellan AJ, Meyer AS, Darveau A, Frydman J (2003) The Hsp70 and TRiC/CCT chaperone systems cooperate in vivo to assemble the von Hippel-Lindau tumor suppressor complex. *Mol Cell Biol* **23:** 3141-3151

Metzger MB, Maurer MJ, Dancy BM, Michaelis S (2008) Degradation of a cytosolic protein requires endoplasmic reticulum-associated degradation machinery. *J Biol Chem* **283:** 32302-32316

Metzger MB, Pruneda JN, Klevit RE, Weissman AM (2014) RING-type E3 ligases: master manipulators of E2 ubiquitin-conjugating enzymes and ubiquitination. *Biochim Biophys Acta* **1843:** 47-60

Meyer AS, Gillespie JR, Walther D, Millet IS, Doniach S, Frydman J (2003) Closing the folding chamber of the eukaryotic chaperonin requires the transition state of ATP hydrolysis. *Cell* **113:** 369-381

Miller SB, Ho CT, Winkler J, Khokhrina M, Neuner A, Mohamed MY, Guilbride DL, Richter K, Lisby M, Schiebel E, Mogk A, Bukau B (2015a) Compartment-specific aggregases direct distinct nuclear and cytoplasmic aggregate deposition. *EMBO J* **34:** 778-797

Miller SB, Mogk A, Bukau B (2015b) Spatially Organized Aggregation of Misfolded Proteins as Cellular Stress Defense Strategy. *J Mol Biol* **427:** 1564-1574

Miller-Fleming L, Antas P, Pais TF, Smalley JL, Giorgini F, Outeiro TF (2014) Yeast DJ-1 superfamily members are required for diauxic-shift reprogramming and cell survival in stationary phase. *Proc Natl Acad Sci U S A* **111:** 7012-7017

Mujacic M, Bader MW, Baneyx F (2004) Escherichia coli Hsp31 functions as a holding chaperone that cooperates with the DnaK-DnaJ-GrpE system in the management of protein misfolding under severe stress conditions. *Mol Microbiol* **51:** 849-859

Nakatogawa H, Suzuki K, Kamada Y, Ohsumi Y (2009) Dynamics and diversity in autophagy mechanisms: lessons from yeast. *Nat Rev Mol Cell Biol* **10:** 458-467

Nakatsukasa K, Huyer G, Michaelis S, Brodsky JL (2008) Dissecting the ER-associated degradation of a misfolded polytopic membrane protein. *Cell* **132:** 101-112

Neuber O, Jarosch E, Volkwein C, Walter J, Sommer T (2005) Ubx2 links the Cdc48 complex to ER-associated protein degradation. *Nat Cell Biol* **7:** 993-998

Nillegoda NB, Theodoraki MA, Mandal AK, Mayo KJ, Ren HY, Sultana R, Wu K, Johnson J, Cyr DM, Caplan AJ (2010) Ubr1 and Ubr2 function in a quality control pathway for degradation of unfolded cytosolic proteins. *Mol Biol Cell* **21:** 2102-2116

Noda T, Ohsumi Y (1998) Tor, a phosphatidylinositol kinase homologue, controls autophagy in yeast. *J Biol Chem* **273:** 3963-3966

Ogura T, Wilkinson AJ (2001) AAA+ superfamily ATPases: common structure--diverse function. *Genes Cells* **6:** 575-597

Onuchic JN, Wolynes PG (2004) Theory of protein folding. *Curr Opin Struct Biol* **14:** 70-75

Panaretou B, Siligardi G, Meyer P, Maloney A, Sullivan JK, Singh S, Millson SH, Clarke PA, Naaby-Hansen S, Stein R, Cramer R, Mollapour M, Workman P, Piper PW, Pearl LH, Prodromou C (2002) Activation of the ATPase activity of hsp90 by the stress-regulated cochaperone aha1. *Mol Cell* **10:** 1307-1318

Park KC, Woo SK, Yoo YJ, Wyndham AM, Baker RT, Chung CH (1997) Purification and characterization of UBP6, a new ubiquitin-specific protease in Saccharomyces cerevisiae. *Arch Biochem Biophys* **347:** 78-84

Park SH, Bolender N, Eisele F, Kostova Z, Takeuchi J, Coffino P, Wolf DH (2007) The cytoplasmic Hsp70 chaperone machinery subjects misfolded and endoplasmic reticulum import-incompetent proteins to degradation via the ubiquitin-proteasome system. *Mol Biol Cell* **18:** 153-165

Park SH, Kukushkin Y, Gupta R, Chen T, Konagai A, Hipp MS, Hayer-Hartl M, Hartl FU (2013) PolyQ proteins interfere with nuclear degradation of cytosolic proteins by sequestering the Sis1p chaperone. *Cell* **154:** 134-145

Patel SS, Belmont BJ, Sante JM, Rexach MF (2007) Natively unfolded nucleoporins gate protein diffusion across the nuclear pore complex. *Cell* **129:** 83-96

Pearse BR, Hebert DN (2010) Lectin chaperones help direct the maturation of glycoproteins in the endoplasmic reticulum. *Biochim Biophys Acta* **1803:** 684-693

Picard D (2002) Heat-shock protein 90, a chaperone for folding and regulation. *Cell Mol Life Sci* **59:** 1640-1648

Pickering AM, Koop AL, Teoh CY, Ermak G, Grune T, Davies KJ (2010) The immunoproteasome, the 20S proteasome and the PA28alphabeta proteasome regulator are oxidative-stress-adaptive proteolytic complexes. *Biochem J* **432:** 585-594

Plemper RK, Deak PM, Otto RT, Wolf DH (1999) Re-entering the translocon from the lumenal side of the endoplasmic reticulum. Studies on mutated carboxypeptidase yscY species. *FEBS Lett* **443:** 241-245

Popken P, Ghavami A, Onck PR, Poolman B, Veenhoff LM (2015) Size-dependent leak of soluble and membrane proteins through the yeast nuclear pore complex. *Mol Biol Cell* **26:** 1386-1394

Prasad R, Kawaguchi S, Ng DT (2010) A nucleus-based quality control mechanism for cytosolic proteins. *Mol Biol Cell* **21:** 2117-2127

Preissler S, Deuerling E (2012) Ribosome-associated chaperones as key players in proteostasis. *Trends Biochem Sci* **37:** 274-283

Quan EM, Kamiya Y, Kamiya D, Denic V, Weibezahn J, Kato K, Weissman JS (2008) Defining the glycan destruction signal for endoplasmic reticulum-associated degradation. *Mol Cell* **32:** 870-877

Raasi S, Wolf DH (2007) Ubiquitin receptors and ERAD: a network of pathways to the proteasome. *Semin Cell Dev Biol* **18:** 780-791

Rapoport TA (2007) Protein translocation across the eukaryotic endoplasmic reticulum and bacterial plasma membranes. *Nature* **450:** 663-669

Richly H, Rape M, Braun S, Rumpf S, Hoege C, Jentsch S (2005) A series of ubiquitin binding factors connects CDC48/p97 to substrate multiubiquitylation and proteasomal targeting. *Cell* **120:** 73-84

Richter K, Walter S, Buchner J (2004) The Co-chaperone Sba1 connects the ATPase reaction of Hsp90 to the progression of the chaperone cycle. *J Mol Biol* **342:** 1403-1413

Roe SM, Ali MM, Meyer P, Vaughan CK, Panaretou B, Piper PW, Prodromou C, Pearl LH (2004) The Mechanism of Hsp90 regulation by the protein kinase-specific cochaperone p50(cdc37). *Cell* **116:** 87-98

Rohde J, Heitman J, Cardenas ME (2001) The TOR kinases link nutrient sensing to cell growth. *J Biol Chem* **276:** 9583-9586

Rosenbaum JC, Fredrickson EK, Oeser ML, Garrett-Engele CM, Locke MN, Richardson LA, Nelson ZW, Hetrick ED, Milac TI, Gottschling DE, Gardner RG (2011) Disorder targets misorder in nuclear quality control degradation: a disordered ubiquitin ligase directly recognizes its misfolded substrates. *Mol Cell* **41:** 93-106

Rospert S, Dubaquie Y, Gautschi M (2002) Nascent-polypeptide-associated complex. *Cell Mol Life Sci* **59:** 1632-1639

Ross CA, Poirier MA (2004) Protein aggregation and neurodegenerative disease. *Nat Med* **10 Suppl:** S10-17

Rubinsztein DC (2006) The roles of intracellular protein-degradation pathways in neurodegeneration. *Nature* **443:** 780-786

Russell SJ, Steger KA, Johnston SA (1999) Subcellular localization, stoichiometry, and protein levels of 26 S proteasome subunits in yeast. *J Biol Chem* **274:** 21943-21952
Santt O, Pfirrmann T, Braun B, Juretschke J, Kimmig P, Scheel H, Hofmann K, Thumm M, Wolf DH (2008) The yeast GID complex, a novel ubiquitin ligase (E3) involved in the regulation of carbohydrate metabolism. *Mol Biol Cell* **19:** 3323-3333

Saric T, Graef CI, Goldberg AL (2004) Pathway for degradation of peptides generated by proteasomes: a key role for thimet oligopeptidase and other metallopeptidases. *J Biol Chem* **279:** 46723-46732

Scazzari M. (2013) Cytosolic protein quality control of the orphan protein Fas2, a novel physiological substrate of the E3 ligase Ubr1. Thesis, University of Stuttgart.

Scazzari M, Amm I, Wolf DH (2015) Quality control of a cytoplasmic protein complex: Chaperone motors and the ubiquitin-proteasome system govern the fate of orphan fatty acid synthase subunit Fas2 of yeast. *J Biol Chem* **290:** 4677-4687

Scheffner M, Kumar S (2014) Mammalian HECT ubiquitin-protein ligases: biological and pathophysiological aspects. *Biochim Biophys Acta* **1843:** 61-74

Scheffner M, Nuber U, Huibregtse JM (1995) Protein ubiquitination involving an E1-E2-E3 enzyme ubiquitin thioester cascade. *Nature* **373:** 81-83

Scheufler C, Brinker A, Bourenkov G, Pegoraro S, Moroder L, Bartunik H, Hartl FU, Moarefi I (2000) Structure of TPR domain-peptide complexes: critical elements in the assembly of the Hsp70-Hsp90 multichaperone machine. *Cell* **101:** 199-210

Schlieker C, Weibezahn J, Patzelt H, Tessarz P, Strub C, Zeth K, Erbse A, Schneider-Mergener J, Chin JW, Schultz PG, Bukau B, Mogk A (2004) Substrate recognition by the AAA+ chaperone ClpB. *Nat Struct Mol Biol* **11:** 607-615

Schmelzle T, Hall MN (2000) TOR, a central controller of cell growth. *Cell* **103:** 253-262

Schork SM, Bee G, Thumm M, Wolf DH (1994) Catabolite inactivation of fructose-1,6-bisphosphatase in yeast is mediated by the proteasome. *FEBS Lett* **349:** 270-274

Schuberth C, Buchberger A (2005) Membrane-bound Ubx2 recruits Cdc48 to ubiquitin ligases and their substrates to ensure efficient ER-associated protein degradation. *Nat Cell Biol* **7:** 999-1006

Schweizer E, Hofmann J (2004) Microbial type I fatty acid synthases (FAS): major players in a network of cellular FAS systems. *Microbiol Mol Biol Rev* **68:** 501-517

Seufert W, Jentsch S (1990) Ubiquitin-conjugating enzymes UBC4 and UBC5 mediate selective degradation of short-lived and abnormal proteins. *EMBO J* **9:** 543-550

Seufert W, McGrath JP, Jentsch S (1990) UBC1 encodes a novel member of an essential subfamily of yeast ubiquitin-conjugating enzymes involved in protein degradation. *EMBO J* **9:** 4535-4541

Sherman F, Stewart JW, Tsunasawa S (1985) Methionine or not methionine at the beginning of a protein. *BioEssays : news and reviews in molecular, cellular and developmental biology* **3:** 27-31

Shorter J, Lindquist S (2006) Destruction or potentiation of different prions catalyzed by similar Hsp104 remodeling activities. *Mol Cell* **23:** 425-438

Shulga N, Roberts P, Gu Z, Spitz L, Tabb MM, Nomura M, Goldfarb DS (1996) In vivo nuclear transport kinetics in Saccharomyces cerevisiae: a role for heat shock protein 70 during targeting and translocation. *J Cell Biol* **135:** 329-339

Siebenlist U, Nix J, Schweizer M, Jager D, Schweizer E (1990) Mapping of the trifunctional fatty acid synthetase gene FAS2 on chromosome XVI of Saccharomyces cerevisiae. *Yeast* **6:** 411-415

Siegers K, Bolter B, Schwarz JP, Bottcher UM, Guha S, Hartl FU (2003) TRiC/CCT cooperates with different upstream chaperones in the folding of distinct protein classes. *EMBO J* **22:** 5230-5240

Sikorski RS, Hieter P (1989) A system of shuttle vectors and yeast host strains designed for efficient manipulation of DNA in Saccharomyces cerevisiae. *Genetics* **122:** 19-27

Skoneczna A, Micialkiewicz A, Skoneczny M (2007) Saccharomyces cerevisiae Hsp31p, a stress response protein conferring protection against reactive oxygen species. *Free Radic Biol Med* **42:** 1409-1420

Specht S, Miller SB, Mogk A, Bukau B (2011) Hsp42 is required for sequestration of protein aggregates into deposition sites in Saccharomyces cerevisiae. *J Cell Biol* **195:** 617-629

Spiess C, Meyer AS, Reissmann S, Frydman J (2004) Mechanism of the eukaryotic chaperonin: protein folding in the chamber of secrets. *Trends Cell Biol* **14:** 598-604

Starheim KK, Gevaert K, Arnesen T (2012) Protein N-terminal acetyltransferases: when the start matters. *Trends Biochem Sci* **37:** 152-161

Stoldt V, Rademacher F, Kehren V, Ernst JF, Pearce DA, Sherman F (1996) Review: the Cct eukaryotic chaperonin subunits of Saccharomyces cerevisiae and other yeasts. *Yeast* **12:** 523-529

Stolz A, Besser S, Hottmann H, Wolf DH (2013) Previously unknown role for the ubiquitin ligase Ubr1 in endoplasmic reticulum-associated protein degradation. *Proc Natl Acad Sci U S A* **110:** 15271-15276

Stolz A, Ernst A, Dikic I (2014) Cargo recognition and trafficking in selective autophagy. *Nat Cell Biol* **16:** 495-501

Stolz A, Hilt W, Buchberger A, Wolf DH (2011) Cdc48: a power machine in protein degradation. *Trends Biochem Sci* **36:** 515-523

Stryer L, Berg JM, Tymoczko JL (2013) *Biochemistry*, 7th edn. New York: W. H. Freeman.

Susek RE, Lindquist S (1990) Transcriptional derepression of the Saccharomyces cerevisiae HSP26 gene during heat shock. *Mol Cell Biol* **10:** 6362-6373

Swanson R, Locher M, Hochstrasser M (2001) A conserved ubiquitin ligase of the nuclear envelope/endoplasmic reticulum that functions in both ER-associated and Matalpha2 repressor degradation. *Genes Dev* **15:** 2660-2674

Takeshige K, Baba M, Tsuboi S, Noda T, Ohsumi Y (1992) Autophagy in yeast demonstrated with proteinase-deficient mutants and conditions for its induction. *J Cell Biol* **119:** 301-311

Taxis C, Hitt R, Park SH, Deak PM, Kostova Z, Wolf DH (2003) Use of modular substrates demonstrates mechanistic diversity and reveals differences in chaperone requirement of ERAD. *J Biol Chem* **278:** 35903-35913

Thomas G, Hall MN (1997) TOR signalling and control of cell growth. *Curr Opin Cell Biol* **9:** 782-787

Thrower JS, Hoffman L, Rechsteiner M, Pickart CM (2000) Recognition of the polyubiquitin proteolytic signal. *EMBO J* **19:** 94-102

Tomko RJ, Jr., Hochstrasser M (2013) Molecular architecture and assembly of the eukaryotic proteasome. *Annu Rev Biochem* **82:** 415-445

Trepel J, Mollapour M, Giaccone G, Neckers L (2010) Targeting the dynamic HSP90 complex in cancer. *Nat Rev Cancer* **10:** 537-549

Tyedmers J, Mogk A, Bukau B (2010) Cellular strategies for controlling protein aggregation. *Nat Rev Mol Cell Biol* **11:** 777-788

van Anken E, Braakman I (2005) Versatility of the endoplasmic reticulum protein folding factory. *Crit Rev Biochem Mol Biol* **40:** 191-228

van den Berg B, Ellis RJ, Dobson CM (1999) Effects of macromolecular crowding on protein folding and aggregation. *EMBO J* **18:** 6927-6933

van den Berg B, Wain R, Dobson CM, Ellis RJ (2000) Macromolecular crowding perturbs protein refolding kinetics: implications for folding inside the cell. *EMBO J* **19:** 3870-3875

Varshavsky A (2011) The N-end rule pathway and regulation by proteolysis. *Protein Sci* **20:** 1298-1345

Vashist S, Ng DT (2004) Misfolded proteins are sorted by a sequential checkpoint mechanism of ER quality control. *J Cell Biol* **165:** 41-52

Vaughan CK, Gohlke U, Sobott F, Good VM, Ali MM, Prodromou C, Robinson CV, Saibil HR, Pearl LH (2006) Structure of an Hsp90-Cdc37-Cdk4 complex. *Mol Cell* **23:** 697-707

Venters BJ, Wachi S, Mavrich TN, Andersen BE, Jena P, Sinnamon AJ, Jain P, Rolleri NS, Jiang C, Hemeryck-Walsh C, Pugh BF (2011) A comprehensive genomic binding map of gene and chromatin regulatory proteins in Saccharomyces. *Mol Cell* **41:** 480-492

Versini G, Comet I, Wu M, Hoopes L, Schwob E, Pasero P (2003) The yeast Sgs1 helicase is differentially required for genomic and ribosomal DNA replication. *EMBO J* **22:** 1939-1949

Walter P, Ron D (2011) The unfolded protein response: from stress pathway to homeostatic regulation. *Science* **334:** 1081-1086

Wandinger SK, Richter K, Buchner J (2008) The Hsp90 chaperone machinery. *J Biol Chem* **283:** 18473-18477

Wang J, Maldonado MA (2006) The ubiquitin-proteasome system and its role in inflammatory and autoimmune diseases. *Cell Mol Immunol* **3:** 255-261

Webb JL, Ravikumar B, Atkins J, Skepper JN, Rubinsztein DC (2003) Alpha-Synuclein is degraded by both autophagy and the proteasome. *J Biol Chem* **278:** 25009-25013

Werner-Washburne M, Becker J, Kosic-Smithers J, Craig EA (1989) Yeast Hsp70 RNA levels vary in response to the physiological status of the cell. *J Bacteriol* **171:** 2680-2688

Whitesell L, Lindquist SL (2005) HSP90 and the chaperoning of cancer. *Nat Rev Cancer* **5:** 761-772

Wilson MA, St Amour CV, Collins JL, Ringe D, Petsko GA (2004) The 1.8-A resolution crystal structure of YDR533Cp from Saccharomyces cerevisiae: a member of the DJ-1/ThiJ/PfpI superfamily. *Proc Natl Acad Sci U S A* **101:** 1531-1536

Winkler J, Tyedmers J, Bukau B, Mogk A (2012) Hsp70 targets Hsp100 chaperones to substrates for protein disaggregation and prion fragmentation. *J Cell Biol* **198:** 387-404

Wojcik C (2002) Regulation of apoptosis by the ubiquitin and proteasome pathway. *J Cell Mol Med* **6:** 25-48

Wolf DH, Fink GR (1975) Proteinase C (carboxypeptidase Y) mutant of yeast. *J Bacteriol* **123:** 1150-1156

Wolf DH, Hilt W (2004) The proteasome: a proteolytic nanomachine of cell regulation and waste disposal. *Biochim Biophys Acta* **1695:** 19-31

Wolf DH, Stolz A (2012) The Cdc48 machine in endoplasmic reticulum associated protein degradation. *Biochim Biophys Acta* **1823:** 117-124

Xia Z, Webster A, Du F, Piatkov K, Ghislain M, Varshavsky A (2008) Substrate-binding sites of UBR1, the ubiquitin ligase of the N-end rule pathway. *J Biol Chem* **283:** 24011-24028

Yaffe MB, Farr GW, Miklos D, Horwich AL, Sternlicht ML, Sternlicht H (1992) TCP1 complex is a molecular chaperone in tubulin biogenesis. *Nature* **358:** 245-248

Yorimitsu T, Klionsky DJ (2005) Autophagy: molecular machinery for self-eating. *Cell Death Differ* **12 Suppl 2:** 1542-1552

Zeng X, Kinsella TJ (2011) Impact of Autophagy on Chemotherapy and Radiotherapy Mediated Tumor Cytotoxicity: "To Live or not to Live". *Front Oncol* **1:** 30

6. ACKNOWLEDGEMENTS

First, I want to thank Prof. Dr. Dieter H. Wolf for giving me the possibility to work in his lab on very interesting projects. He had always time for discussions and also let me a lot freedom in the lab which both contributed to a great atmosphere.

I also want to thank Priv. Doz. Dr. Hans Rudolph for a lot of great scientific discussions.

I am grateful to all my former and current lab members for a great atmosphere, a lot of cakes and also great moments and activities beyond the daily job routine.

A special thank goes to my mother without her my academic education would not have been possible.

Last but not least I want to thank my girl friend Nicole who supported me in every way. She always motivated me and managed to make me smile even when I came home after a lab working day full of failed experiments.